PRESENT AND PAST COCCOLITHS IN THE SOUTHERN INDIAN OCEAN AND THEIR PALEOENVIRONMENTAL APPLICABILITY

A Thesis submitted in partial fulfillment for the degree of

DOCTOR OF PHILOSOPHY

in the School of Earth, Ocean and Atmospheric Sciences

Goa University

By

PALLAVI P. CHOUDHARI

National Centre for Polar and Ocean Research,
Headland Sada, Vasco-da-Gama,
Goa, India-403804, India

January 2024

DECLARATION

I, Pallavi P. Choudhari hereby declare that this thesis entitled "PRESENT AND PAST COCCOLITHS IN THE SOUTHERN INDIAN OCEAN AND THEIR PALEOENVIRONMENTAL APPLICABILITY" represents work which has been carried out by me and it has not been submitted, either in part or full, to any other University or Institution for the award of any research degree.

Place: Taleigao Plateau Pallavi P. Choudhari

Date:

CERTIFICATE

I hereby certify that the above declaration of the candidate, Ms. Pallavi P. Choudhari is true and the work was carried out under my supervision

Dr. Rahul Mohan (Scientist F)
Research Guide
National Centre for Polar and Ocean Research
Vasco-da-Gama, 403804, Goa, India

Acknowledgement

I am very grateful to have reached this point; I thank each and every person who supported me throughout my research work and learning process, who not sparked my interest but also kept it alive at breaking points and helped me to keep going and continue towards the completion of my Ph.D. thesis. I am very grateful to my supervisor Dr. Rahul Mohan for his guidance and assistance throughout my study period, I am very thankful to him for looking out for me, providing opportunities to go on expeditions, and encouraging me to participate in national and international conferences, ensuring my overall development as a researcher.

I acknowledge the National Centre for Polar and Ocean Research for providing academic and administrative support to me throughout the course of my work, and I am also thankful to the Director of NCPOR, Dr. Thamban Meloth. I would like to convey my gratitude to Dr. M. Ravichandran, Secretary, Ministry of Earth Sciences (MoES), Govt. of India.

I would also like to acknowledge Dr. Sushant Naik and Prof. C. U. Rivonker for duly assessing the progress of my work and providing valuable suggestions as well as the Faculty Research Committee members for examining my research progress.

I sincerely thank Dr. Shramik Patil for providing me the opportunity to work in the DST-INSPIRE (DST/INSPIRE/04/2015/001969) project. I am grateful to him for teaching me everything about coccolithophores, microscopes, and also would like to acknowledge all the advice and help I received from him during laboratory work and manuscript writing. I would also like to thank Syed A. Jafar for his insights into coccoliths and life lessons from his tremendous experience.

I would especially like to express my gratitude to Dr. Abhilash Nair for sharing his insights into paleoceanography, and for the invaluable help he provided throughout the process of writing and making the completion of this thesis possible.

I want to thank Sahina and Vailancy for supporting, training and assisting me with scanning electron microscope analysis and also for always looking out for me. I would like to thank Ms. Melena A. Soares and Dr. Michelle Fernandes for providing nutrient data for the samples of 10th Southern Ocean Expedition. I am also grateful to Dr. Sabu Prabhakaran who shared the physical parameter data from the 10th Southern Ocean Expedition. I would like to thank Ms. Juhi Yadav and Anandu S.V. for assisting with the extraction of satellite data. I would like to specially express my gratitude to Dr. Ravidas K. Naik for always watching my back, and advising me in both the better and tough times.

I would like to thank Dr. Mahesh Badanal, Dr. Syed Mohammad Saalim, and Dr. Cheryl A. Noronha E. D'Mello, for teaching, helping with questions related to paleoceanography, and being there to discuss any doubts related to science and other things about life. I especially thank my roommates Nibedita Sahoo, Dr. Padmasini Bhera, and Dr. Pooja Ghadi, for discussions in and out of science. A special thanks to Pooja for her constant support and help with all the administrative procedures related to DRCs and this Ph.D. I would also like to thank Dr. Femi Anna Thomas for her helpful suggestions, and Hari Krishnan for always taking my mind off worries and engaging in interesting discussions.

I would like to thank Dr. Alok Kumar Sinha, Kalpana Dhiman, Dr. Mohammad Nuruzzama, Priyesh Prabhat, Rahul Dey, Sunil Oulkar, Dr. Shabnam Choudhary, Dr. Swati Nagar, and a special thanks to Sweta Morje and Ankita Satoskar for helping me. I would also like to thank Dr. Ansari for his assistance with Hindi language translations. A special thanks to Bikram Reddy, Prachi Marathe, Sai Elangovan, and Shil Abhyankar.

Special gratitude to my late Nani and Uncle who played a major role in my life. Finally, I am eternally grateful to my parents and my sister, and my in-laws for their support, love, faith, and encouragement during all these years. I am immensely grateful to my husband for being by my side at every moment and considering my commitments as his own helping me in every way

possible. Lastly, I am thankful to my daughter Siya whose arrival has motivated and given me the strength required for the completion of this thesis.

DEDICATED TO MY FAMILY AND FRIENDS

Contents

List of Tables

List of Figures

PREFACE

The present study is intended to explore the extant and fossil coccolithophores in the Southern Indian Ocean and Southern Ocean. Coccolithophore response to associated prevalent environmental conditions affecting their production and preservation during the present and immediate past is discussed. Additionally, their application as a proxy to reconstruct paleoenvironmental conditions is investigated. The introduction chapter elaborates on the importance and significance of the proposed work with respect to coccolithophore biogeography, distribution, and ecology in the Southern Ocean and their paleoenvironmental applications. Further, a brief introduction of the Southern Indian Ocean and the regional setting of this study is described in the Methodology section, followed by a description of the procedures followed to obtain and analyze the samples is described. In the next chapter, key coccolithophore species recorded in the Southern Indian Ocean, their identification characters, and their preference for environmental parameters such as temperature, salinity, nutrients, and associated frontal zones are described. Chapter 4 provides a detailed picture of the latitudinal distribution of coccolithophore species in the surface waters in association with the oceanic fronts of the Southern Indian Ocean. Temperature and nutrients play a vital role in the diversity and abundance of coccolithophores. Further, based on similarity indices different coccolithophore assemblages were highlighted and differences in the distribution of a few species in comparison to other sectors of the Southern Ocean are described. In Chapter 5, the distribution pattern, and factors affecting the preservation and carbonate contribution of coccolithophores in the surface sediments of the Southern Indian Ocean are discussed. The highest abundance and diversity was observed in sediments taken from the STZ and SAZ, which is similar to the trends observed in the surface waters. However, mismatches in the abundances of a few species were recorded, which may be due to different mechanisms such as differential dissolution between species, carbonate saturation of the water column and/or

transport via oceanic currents. Chapter 6 highlights the paleoceanographic changes in the Indian sector of the Southern Ocean over the past 41,500 years (41.5 ka BP). This study is based on the coccoliths and $CaCO_3$ records from marine sediment core SK200/22a. Reduced carbonate burial/preservation in the glacial sediments is recorded owing to the shallowing of North Atlantic Deep Waters which is complimented by the size variation in *Coccolithus pelagicus* subsp. *braarudii.* The coccolith records also captured the changes in the strength of the Agulhas Return Current (ARC) through the shifts in the abundance of tropical-subtropical coccolithophore assemblages and suggest a glacial enhancement of the ARC transport.

Chapter 1

Introduction

1.1. Background and rationale

The growing concentration of greenhouse gases such as carbon dioxide and methane in the atmosphere has raised average temperatures around the world, leading to global warming and a rise in ocean acidification (Rost and Riebesell, 2004; IPCC, 2013). Though the earth has undergone warming periods in its history (Masson-Delmotte et al., 2013), the current anthropogenic-induced unprecedented warming has occurred rapidly. The ocean acts as a buffer, absorbing 90% of the excess heat generated by greenhouse gases such as carbon dioxide (IPCC, 2019). Furthermore, due to the ever-rising atmospheric concentration of greenhouse gases, the world's oceans are warming at a faster rate than ever and significant changes in oceanographic parameters have been reported at higher latitudes (Swart et al., 2018). Since 2006, an estimated 60%–90% of changes in global ocean heat content associated with global warming have occurred in the Southern Ocean (Sallée, 2018). The brunt of these changes can be observed in the circumpolar Southern Ocean as it is not bound by land and is a link that connects the atmosphere to the ocean depths. The diverse environmental array of the Southern Ocean exposes phytoplankton to the environmental factors that regulate their composition, distribution, and production (Deppeler and Davidson, 2017). It has also been suggested that this will have a major bearing on calcifying organisms such as corals, pteropods, planktonic foraminifera, and coccolithophores, affecting their rate of calcification under the circumstances of the present and future ocean acidification (Bijma et al., 2002; Langdon and Atkinson, 2005; Orr et al., 2005; Bach et al., 2015; Meyer and Riebesell, 2015). These effects will ultimately influence assemblage composition, necessitating adaptations to their changing environments, which in turn affect nutrient bioavailability and other biogeochemical parameters. Simultaneously, phytoplankton themselves influence the climate with their responses to environmental changes (Käse and Geuer, 2018). The present study focuses on understanding

the biogeographic distribution of coccolithophores, a calcifying group of phytoplankton, in the Southern Ocean and their importance in deciphering the paleoceanographic changes.

1.2. The Southern Ocean

The Southern Ocean is defined as the southern portions of the Pacific, Atlantic, and Indian oceans and their tributary seas surrounding Antarctica. The Antarctic treaty and the United States Board on Geographic Names delimit the Southern Ocean from the Antarctic coast up to a latitude of 60°S. However, as per the National Ocean and Atmospheric Administration, not all the countries agree on the proposed location of the Southern Ocean and this is yet to be ratified by the International Hydrographic Organisation. In addition, the Southern Ocean is considered as the area from the 70°S up to 40°S as the Southern Ocean (Bodas-Salcedo et al., 2014). The Southern Ocean influences the earth's climate via the storage of heat and carbon dioxide (CO_2), air-sea exchange of heat and gasses, and ocean circulation. The Southern Ocean is documented to have influenced past climate by sequestering CO_2 during glacial periods and possibly outgassing during the interglacial periods (Sigman and Boyle, 2000; Choudhury et al., 2022).

The Southern Ocean is distinct from other oceans in being a large circumpolar body of water encircling the Antarctic continent with no meridional boundary (Olbers et al., 2004), allowing the Antarctic Circumpolar Current (ACC) to exist (Whitworth, 1983). The ACC flows eastward and is driven by westerly winds (Gille, 1994). It plays several key roles in overturning circulations—it connects the ocean basins and allows a global circulation pattern that serves as a path to transmit climatic signals between the major oceans (Gille, 2002). The Southern Ocean is important due to its unique setting, water masses, water circulation patterns, and vital role in modulating global climate.

The ACC shifts and splits into the Atlantic and Indian sectors of the Southern Ocean and forms different current systems (e.g., Agulhas Return Current, Falkland Current). In the Southeast Atlantic, due to the shear interaction with the ACC, Agulhas Current retroflects, (with a small part being transported into South Atlantic to form the 'Agulhas leakage') and forms the Agulhas Return Current (ARC); which exhibits sea surface temperatures (SST) of 17–19 °C (Holliday and Read 1998). The ARC flows towards the east along the Subtropical Front (STF; SST of 11–17 °C) at the surface (Holliday and Read, 1998) and sheds cold and warm eddies in the Subtropical Zone, increasing biological productivity (Lutjeharms et al., 2004).

The Southern Ocean comprises different oceanic frontal zones such as STZ, Subantarctic Zone (SAZ), and Polar Frontal Zone (PFZ). The Subantarctic Zone (SAZ) is bound by STF to the north and the Subantarctic Front (SAF), having SST of 6–11°C, to the south (Orsi et al., 1995; Anilkumar et al., 2006). The Polar Frontal Zone (PFZ) is restricted by SAF to the north and the Antarctic Polar Front; 4–5 °C SST; (Orsi et al., 1995; Anilkumar et al., 2006; Sokolov and Rintoul, 2009b) to the south. The PFZ is a high nutrient low chlorophyll (HNLC) zone as a consequence of iron limitation (Boyd et al., 2000; Boyd et al., 2007; De Baar et al., 2005).

In addition to the oceanic fronts, the Southern Ocean also comprises various water masses such as (1) the Subantarctic Surface Waters (SASW; <34 PSU; ~9 ℃ temperature) located at ~43°S; (2) the Antarctic Surface Waters (AASW; <34 PSU; <5 ℃) positioned between 44 and56°S; (3) the Antarctic Intermediate Water (AAIW; ~34.42 PSU; ~4.4 ℃); (4) the Circumpolar Deep Water (CDW; 34.62–34.73 PSU; 1–2 ℃), (5) the North Atlantic Deep Water (NADW; 34.77–34.88 PSU) and (6) the Antarctic Bottom Water (AABW; ~34.66 PSU; -0.165℃) (Park et al., 1993; Emery, 2001, Anilkumar et al., 2006).

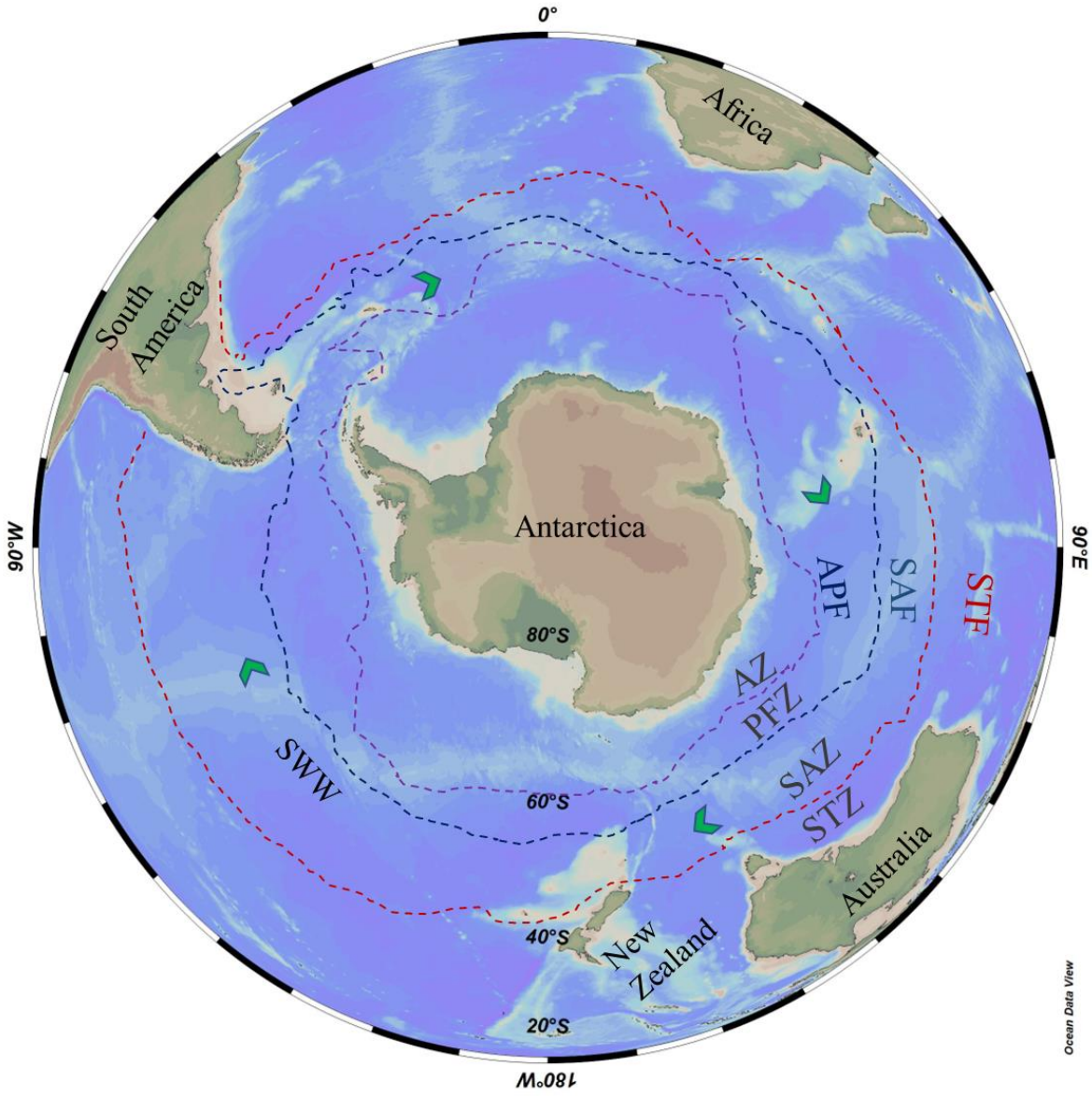

Figure 1. Location of oceanographic fronts in the Southern Ocean (modified after Orsi et al., 1995). APF, Antarctic Polar Front; PFZ, Polar Frontal Zone; SAF, Subantarctic Front; SAZ, Subantarctic Zone; STF, Subtropical Front; STZ, Subtropical Zone.

1.3. Coccolithophores and coccoliths

Coccolithophores are unicellular (2.0–75.0 μm in cell diameter), eukaryotic phytoplankton that makes up a significant fraction of oceanic primary producers and consequently, are of great interdisciplinary interest. Coccolithophores are characterized by the

calcareous plates (coccoliths) that form an extracellular covering around the living cell, termed the coccosphere (Winter and Siesser, 1994; Young, 1994). In the geological record, coccolithophores appeared in the Late Triassic about ~230 million years ago (Jafar, 1983; Bralower, et al., 1991). Today more than 250 coccolithophore species flourish in the global oceans, highlighting their presence from coastal to open ocean waters and indicating dominance in the subtropical and subpolar regions (Balch et al., 2019).

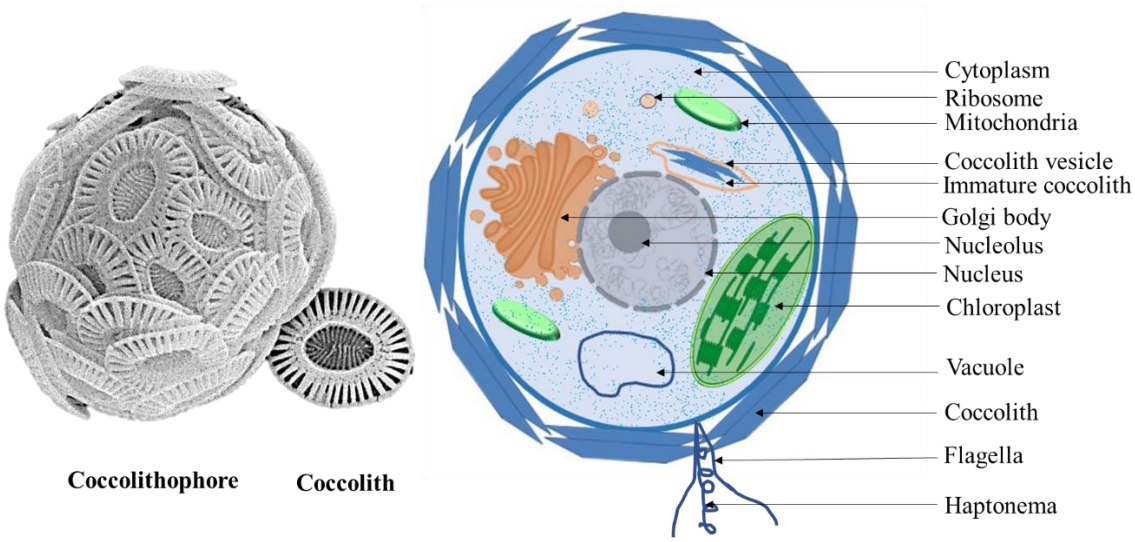

Figure 2. Coccosphere and schematic representation of the cell structures of coccolithophore, (modified after Billard & Inouye, 2004e)

1.4. Biology of coccolithophores

Coccolithophores are grouped under the division Haptophyta and class Prymnesiophyceae (Edvardsen et al., 2000). They are identified by the organelle similar to the flagellar apparatus known as haptonema, present along with a pair of flagella. In most coccolithophores species, the haptonema is rudimentary. In contrast to other haptophyte groups, where the haptonema plays a role in adhering and predation, in coccolithophores, it appears to serve as more of an obstacle-sensing device (Billard and Inouye, 2004). However, certain coccolithophores that live in extreme oligotrophic conditions and prolonged darkness show

indications of potential mixotrophy and phagotrophy and consist of distinct coiled haptonema (Billard and Inouye, 2004). Coccolithophores photosynthesize through pigments such as chlorophyll a+c in their paired golden-brown chloroplasts. In certain holococcolithophores of Calyptrosphaera spp., species of Prymnesiophytes, and genera like Pavlovphyceae, a solitary chloroplast is observed (Billard and Inouye, 2004). According to the hypothesis of endosymbiotic evolution, the arrangement of the thylakoids and the absence of a girdle or peripheral lamella reflect the secondary origin of coccolithophore chloroplasts (Billard and Inouye, 2004) suggesting that the coccolithophores evolved from heterotrophs/mixotrophs to autotrophs (DeVargas et al., 2007). Other cell structures and organelles such as cell membranes and Golgi bodies form coccoliths (Brownlee and Taylor, 2004). In a single coccosphere (which mineralizes during both stages of the life cycle), the type of coccolith is defined by the distinct phases of the life cycle. Generally, coccolithophores reproduce asexually by mitotic division followed by meiotic division with redistribution of coccoliths to the daughter cells. However, many species exhibit complicated life cycles with two stages, viz. ‘haploid phase’ and ‘diploid phase’ (Geisen et al., 2002). The haploid phase bearing holococcoliths is made up of only one type of numerous crystallites of equal shape and size, whereas the diploid phase bears heterococcoliths, which are formed from crystal units of variable shapes and size (Fig. 3) (Young et al., 1997).

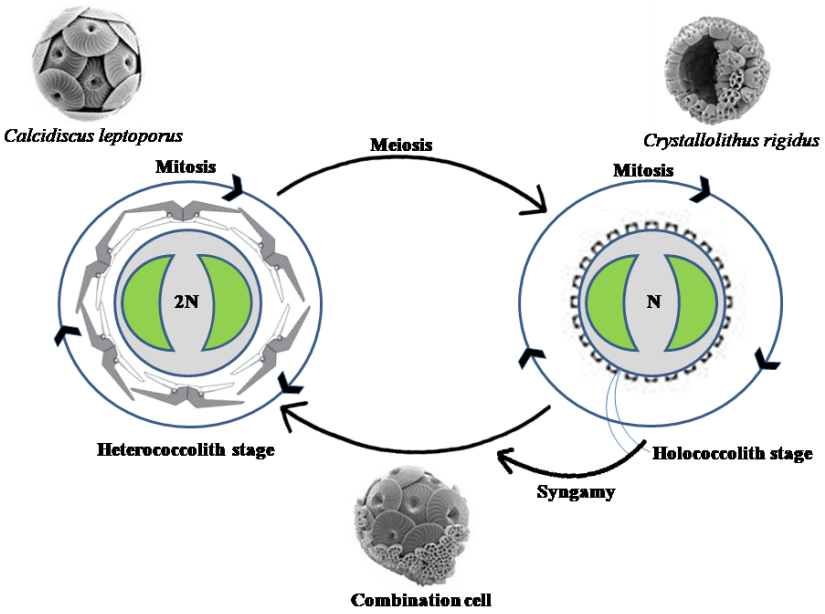

Figure 3. Life cycle of coccolithophore (eg., *Calcidiscus leptoporus*, modified after Geisen et al., 2002)

1.5. Ecology and distribution

Coccolithophores inhabit the photic zone of the ocean where they are influenced by light availability, latitude, ocean currents, water masses, nutrients, salinity, temperature, trace elements, and vitamins. These are the most abundant calcifying phytoplankton in the world's oceans, with an extremely fast turnover rate (Winter and Siesser, 1994; Bown, 1998) and they play a pivotal role in the functioning of marine ecosystems and the biogeochemical cycle (Fig. 4). Coccolithophores are ubiquitous and generally form an important component of the phytoplankton community from the tropics to subpolar waters, (Balch et al., 2007; Poulton et al., 2007; Thierstein and Young, 2013). They are prevalent along the Great Calcite Belt (40–60°S), whereas the region beyond 60°S is dominated by another group of phytoplankton known as diatoms (Balch et al., 2016; Nissen et al., 2018). Coccolithophores contribute 17% to the annually integrated net primary productivity south of 30°S. Coccolithophore biomass reaches a peak north of 50°S during the late austral summer, due to high light levels and the inhibition of diatom growth resulting from low silicic acid levels (Nissen et al., 2018). Coccolithophores

thrive in stratified, nutrient-poor waters and are also adapted to high irradiance making them resistant to photoinhibition (Nanninga and Tyrrell, 1996; Cavender-Bares et al., 2001; Haidar and Thierstein, 2001).

Distinct coccolith types dominate specific oceanic environments and are indicators of water mass characteristics (Young, 1994; Flores and Sierro, 2007). For example, placolith bearing species dominate upwelling areas and high latitudes, umbelliform-bearing species dominate the oligotrophic mid-ocean environment, and floriform species dominate the deep photic zone assemblage in the stable water column. Though coccolithophores are generally associated with oligotrophic conditions (e.g., McIntyre and Bé, 1967; Winter and Siesser, 1994; Ziveri et al., 2004), their productivity is regulated by regional settings such as island masses, bottom topography, coastal currents, gyres, eddies, upwelling, and river runoffs (Cachão and Moita, 2000; Ziveri et al., 2004).

Coccolithophore species exhibit latitudinal distribution in accordance with the optimum range of tolerance towards varying parameters, particularly temperature ranges and nutrient concentrations (Melinte, 2004). The general pattern of coccolithophore distribution in plankton and surface sediment of the Southern Ocean has been documented in prior studies, conducted in the South Atlantic and Pacific, elucidating latitudinal and poleward temperature limits. (Hasle 1969; McIntyre and Bé, 1967; McIntyre et al., 1970; Nishida, 1986; Hiramatsu and De Dekker, 1996). In recent years, studies targeting the species-specific distribution of coccolithophores along latitudinal gradients in different sectors of the Southern Ocean and affinity to frontal systems have been carried out in the Australian sector (Findlay and Giraudeau, 2000). The vertical and lateral variations in the coccolithophore community structure were documented across the subtropical frontal zone in the South Atlantic Ocean (Böeckel and Baumann, 2008), and the Pacific sector of the Southern Ocean. The SAZ close to STF was characterized by higher diversity and abundance of coccolithophores relative to the

PFZ (Saavedra-Pellitero et al., 2014; Saavedra-Pellitero and Baumann, 2015). Malinverno et al. (2015) documented coccolithophore species composition in the surface waters along the fronts of the ACC in a North-South transect from New Zealand to the Ross Sea. The distribution and preservation of coccolith assemblages in the surface sediment across the Drake Passage were studied by Vollmar et al. (2021). Balch et al. (2016) confirmed the presence of coccolithophores and associated optical scattering, primarily in the region of subtropical, Agulhas, and subantarctic frontal regions in the Atlantic and Indian sectors of the Southern Ocean. In the Indian sector of the Southern Ocean, three major zones concerning coccolithophore assemblages were recognized. Coccolithophore assemblages of the Agulhas Retroflection Frontal Zone (ARFZ) and STZ are characterized by high coccolithophore diversity. The SAZ is characterized by low diversity and a high abundance of coccolithophores, whereas the PFZ exhibits a monospecific assemblage of *E. huxleyi* (Mohan et al., 2008; Patil et al., 2017). Though temperature plays a crucial role in the distribution of coccolithophores in the higher latitudes, at the regional level other factors such as positioning of the fronts, nutrient/trophic level, and austral seasons affect the distribution (Baumann et al., 2008; Gravalosa et al., 2008).

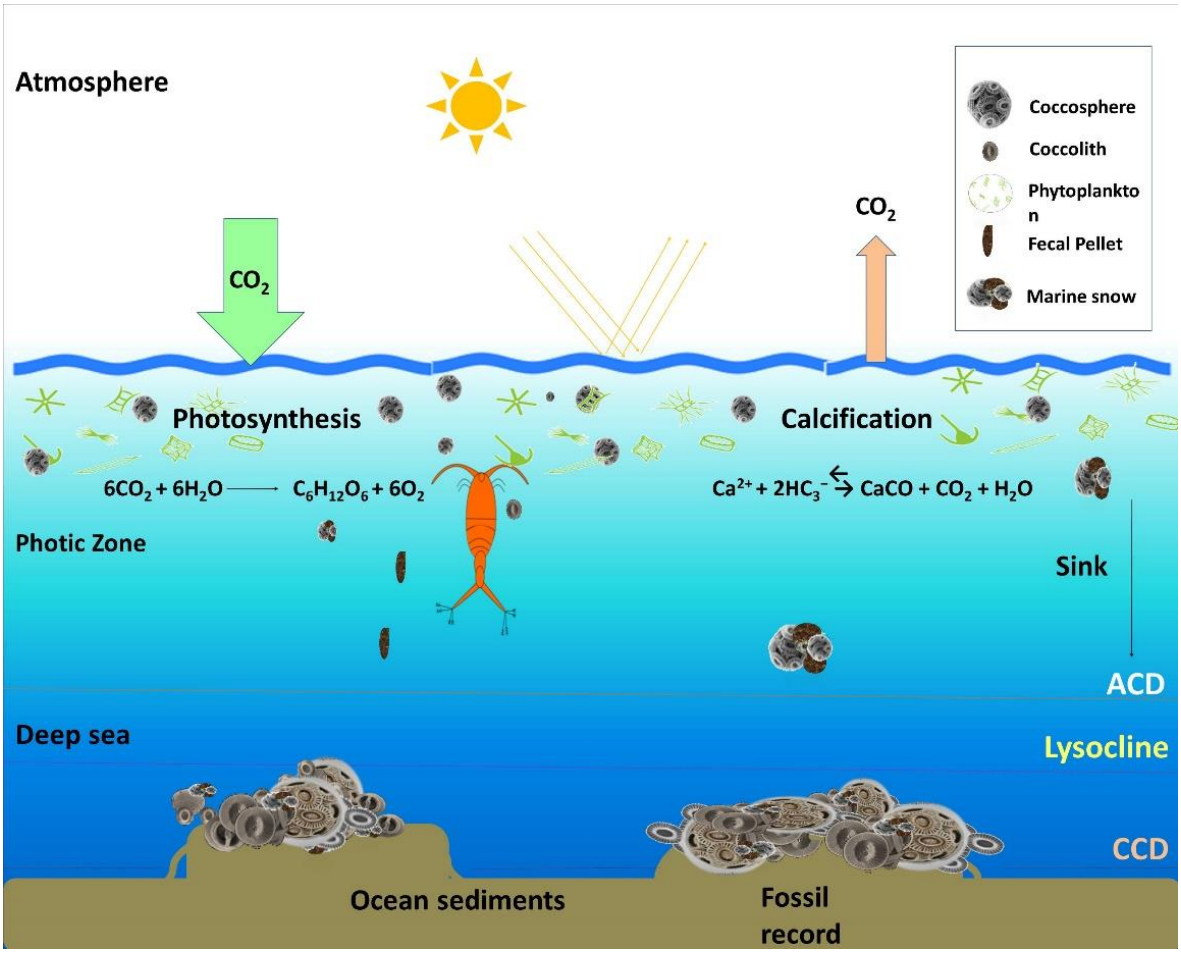

Figure 4. Role of coccolithophores in the biogeochemical cycles. (ACD: Aragonite Compensation Depth; CCD: Calcite Compensation Depth) (image modified after Rost and Riebesell, 2004)

1.6. Coccolith preservation and paleoceanographic implications

In the present oceans, coccolithophores are recognized as one of the largest calcium carbonate producers, affecting the carbon cycle through the carbonate and biological pumps. They are also known to alter the upper ocean alkalinity, and directly affect the CO_2 exchange between air and sea (Rost and Riebesell, 2004). Through the process of calcification, the coccolithophores utilize bicarbonate (HCO_3^-) and calcium ions to form calcium carbonate ($CaCO_3$), with the release of CO_2 as a byproduct (Fig. 4). However, during photosynthesis, coccolithophores convert surface water CO_2 to organic matter and a fraction of the fixed CO_2 is redistributed into the deep ocean and the seafloor (Westbroek et al., 1993; Le Moigne, 2019). On the other hand, $CaCO_3$ may function as a "ballast" mineral that increases the sinking speed

of coccolith/particulate organic carbon from the surface waters to the deep sea (Armstrong et al., 2001). Recent studies indicate that coccolithophore productivity, distribution, and calcification are sensitive to ocean acidification and thermal stratification caused by rising atmospheric CO_2 concentrations (Gattuso et al., 1998; Wolf-Gladrow et al., 1999; Riebesell et al., 2000a; Zondervan et al., 2001). Climate-induced changes might initially increase $CaCO_3$ production and lead to the expansion of the distribution of coccolithophore species to higher latitudes. On the other hand, continuously increasing atmospheric CO_2 concentrations will increase productivity, but impaired calcification may also result in the diminishing of the subantarctic coccolithophore population (Krumhardt et al., 2019; Rigual Hernández et al., 2019).

Studies on extant coccolithophores in the water column provide evidence of climatic and oceanographic alterations based on the abundance, distribution, morphometric variation, and physiological adaptations of coccolithophores (Bown, 1998; Mohan et al., 2008). The inorganic components of coccolithophores, the coccoliths – constitute the most important component of the deep-sea oozes/sediments and preserve the general composition of the overlying photic zone communities (McIntyre and Bé, 1967; Okada and Honjo, 1973; Baumann et al., 1999; Baumann et al., 2005). Consequently, sediment assemblages provide good proxy records of the 1) environmental conditions that control the distribution and production of coccolithophores in the surface waters and 2) the dissolution of the calcite remains on the seafloor (Roth, 1994). Several studies of Late Quaternary sediments indicate fluctuations of frontal positions, variability of current systems (Okada and Wells, 1997; Flores et al., 1999), changes in productivity or nutricline and thermocline dynamics (Jordan et al., 1996; Kinkel et al., 2000; Saavedra-Pellitero et al., 2011). The paleotemperature reconstruction using morphometric measurements of *Gephyrocapsa* spp., relative abundances of different *Gephyrocapsa* spp. (Bollmann, 1997; Bollmann et al 1998), Mg/Ca of bulk coccoliths and

unsaturated alkenones (Sikes et al., 1991; Chapman et al., 1996; Mix et al., 2001) have been conducted to understand the surface ocean changes. Meer et al. (2007) reconstructed past variations in the sea surface salinity (SSS) using alkenones and combined this data with the relative past SSS generated using organic walled dinocyst distribution data. Unlike paleotemperature, paleosalinity is difficult to reconstruct using geological archives with the same accuracy and reliability as temperature (Rohling et al., 1998). The proposed study will aim for insights regarding extant coccolithophores in the Southern Indian Ocean to decipher how coccolithophores respond based on the local/ prevalent environmental conditions. It is also hypothesized that coccolith assemblages in the immediate past reflect the characteristics of the overlying surface waters of the Southern Indian Ocean. The reliability of coccolithophores as a proxy depends largely on the dissolution and production affected by local environmental settings, which alter the preservation of coccoliths in the ocean sediments.

1.7. Objectives

1) Ecology and biogeography of extant coccolithophores in the Southern Indian Ocean.
2) Distribution of coccoliths in the surface sediments of the Southern Indian Ocean: biogeography, preservation and carbonate contribution
3) Reconstruction of paleoenvironmental changes using coccolith assemblages and their morphometric variation.

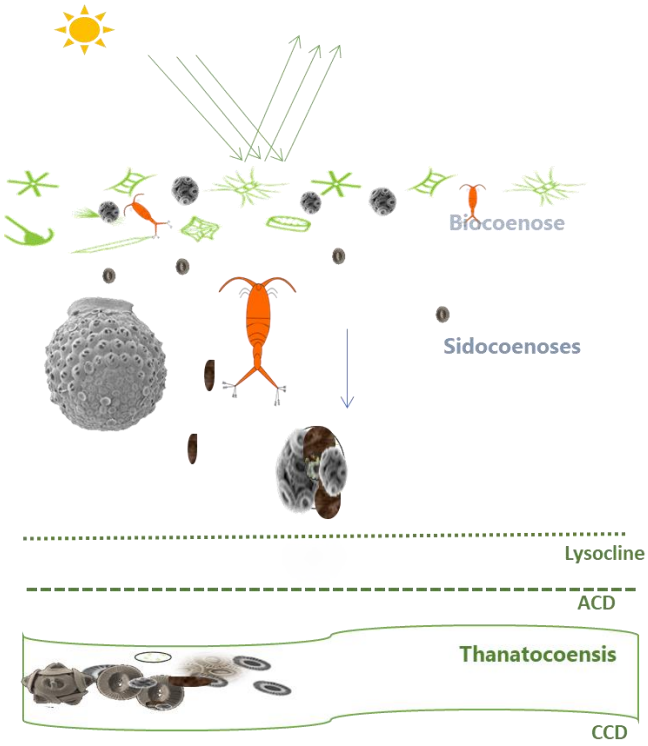

Figure 5. Representation of the journey of coccolithophores from living community to fossil record

Chapter 2

Materials and methods

2.1. Study area: Southern Indian Ocean

To accomplish the objectives mentioned, water samples, surface sediments, and downcore samples from the southern Indian Ocean were analysed (Fig. 1). The proposed study area consists of unique oceanographic settings and living ecosystems that alter as a response to changes in the environment and climate. The Southern Indian Ocean has complex zonal frontal systems. The individual branches of these fronts often merge and diverge in response to variations in bathymetry (Del Caño Rise and Conrad Rise)and the subantarctic islands such as the Crozet Islands, Merion Island, Kerguelen Island, and Prince Edward islands(Pollard and Read, 2001; Pollard et al., 2007; Sokolov and Rintoul, 2007, 2009). These fronts extend through the water column since the Antarctic circumpolar current (ACC) is a deep-reaching barotropic current (Firing et al., 2011). The ACC is driven by Southern Hemispheric westerly winds (Rintoul et al., 2001) that flow eastward around Antarctica consisting of fronts characterized by different temperatures, Salinity, density, and nutrient concentrations (Table 1)(Belkin and Gordon, 1996; Lutjeharms, 2006). Different fronts, frontal zones, and oceanic water masses can be observed in the west of the Southern Indian Ocean from north to south, namely, the Agulhas Front (AF) associated with Agulhas Current; the Agulhas Retroflection Frontal Zone (ARFZ); the Agulhas Return Current (ARC) associated with Agulhas Retroflection; the Subantarctic Zone (SAZ); the Subantarctic Front (SAF); the Polar Frontal Zone (PFZ); the Polar Front (PF); and the Antarctic Zone (AZ) (Orsi et al., 1995).

Pollard et al. (2007a, b) specified that the SAF, one of the major branches of the ACC, flows anticyclonically around the Del Caño Rise (west of the Crozet Plateau) forming an S-shaped bend in the front, before turning back eastward and combining with the ARC and the STF. This S-bend in the SAF is a permanent feature, controlled by the regional bathymetry (Pollard and Read, 2001), and consists of weak circulation fed mainly by the meanders from the SAF. Due to weak circulation accumulation of dissolved iron from the Crozet plateau and

islands in the PFZ between the north of Crozet Island and SAF leads to the annual phytoplankton blooms, which are higher than in the HNLC region, south of Crozet. Thus, the sporadic nature of the productivity and distribution of phytoplankton in this region is due to the complexity of the fronts (Pollard et al., 2007).

The vertical water masses in the Southern Indian Ocean consist of Antarctic Bottom Water (AABW), North Atlantic Deep Waters (NADW), Circumpolar Deep Water (CDW) and the Antarctic Intermediate Water (AAIW), Subantarctic Mode Water (SAMW). The North Atlantic Deep Water (NADW), identified by its high salinity, originates in the North Atlantic, where the surface waters cool and descend at deeper depths through convection and spread as the NADW through thermohaline circulation (Park et al., 1993; Talley, 2013). The NADW combines with CDW in the South Atlantic and exits by flowing into the southwest Indian Ocean (Mantyla and Reid, 1995; Talley, 2013). In the SAF region, a significant volume of the NADW is transformed into the CDW, suggesting that the SAF is the source of CDW (You, 2000). In the northern Indian Ocean, the CDW layer overturns and enters indigenous intermediate waters to form the Indian Deep Water (IDW) flowing toward the Southern Ocean, eventually contributing to the formation of the AAIW/ SAMW and the CDW water masses (Talley, 2013). Within the ACC, CDW and the AABW largely influence sediment transport (Dezileau et al., 2000).

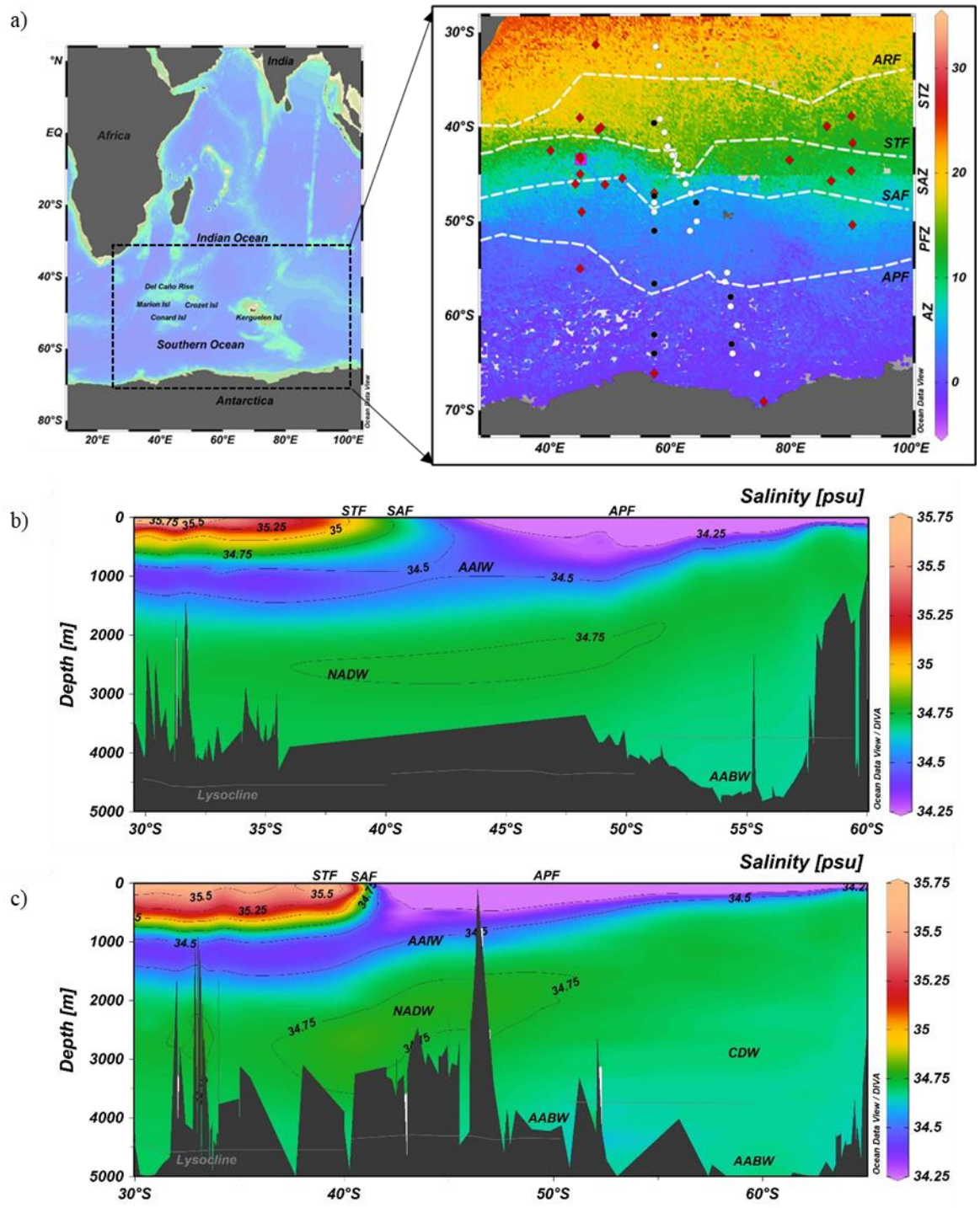

Figure 1. Study area, (a) background map of annual mean sea surface temperature derived from World Ocean Atlas 2018 (Garcia et al., 2019) and gridded with Ocean Data View V4.7.10 (Schlitzer, 2016), location of water samples (profile samples are denoted by black dots, surface samples are denoted by white dots), surface sediments (red diamonds), and sediment core SK200/22a (pink square), (b) Latitudinal section (30–60°S) at 40–60°E longitude hydrographic section of annual mean salinity (Garcia et al., 2019), and (c) Latitudinal section (30–65°S) at 75–90°E longitude hydrographic section of annual mean salinity (Garcia et al., 2019).

Table 1. Oceanographic Settings

Fronts and water masses	Abbreviation	Temperature	Salinity	References
Northern Subtropical Front	NSTF	21–22 °C at surface	~35.5 PSU	Belkin and Gordon (1996); Holliday and Read (1998)
Agulhas Return Front	ARF	17–19 °C at surface; 10 °C isotherm from 300 to 800 m	35.39–35.54 PSU at surface; 34.90–35.57 PSU at 200 m depth	Holliday and Read (1998); Belkin and Gordon (1996); Sparrow et al. (1996); Kostianoy et al. (2004
Southern Subtropical Front	STF	11–17 °C at surface, 10–12 °C at 100 m	34.04–35.35 PSU at surface; 34.6–35 PSU at 100 m; 34.42–34.92 PSU at 200 m	Holliday and Read (1998); Belkin and Gordon (1996); Sparrow et al. (1996); Kostianoy et al. (2004)
Subantarctic Front	SAF	9–10 °C at surface; 4–8.4 °C at 200 m	33.85–34.0 PSU at surface; 34.11–34.40 PSU at 200 m	Holliday and Read (1998); Belkin and Gordon (1996); Sparrow et al. (1996); Kostianoy et al. (2004); Park et al. (1993)

Antarctic Polar Front	APF	4–5 °C at the surface, northern limit of the 2 °C isotherm below 200 m, 2–3 °C at the southern limit	33.8–33.9 PSU at the surface	Holliday and Read (1998); Belkin and Gordon (1996); Sparrow et al. (1996); Kostianoy et al. (2004)
Subantarctic Surface Waters	SASW	~9 °C (~43°S)	<34 PSU	Park et al., 1993; Emery, 2001, Anilkumar et al., 2006).
Antarctic Surface Waters	AASW	<5 °C	<34 PSU	Park et al., 1993; Emery, 2001, Anilkumar et al., 2006).
Antarctic Intermediate Water	AAIW	~4.4 °C	~34.42 PSU	
Circumpolar Deep Water	CDW	1–2 °C	34.62–34.73 PSU	
North Atlantic Deep Water	NADW	1.5–4.0°C	34.77–34.88 PSU	
Antarctic Bottom Water	AABW	0.165 °C	~34.66 PSU	

2.2. Water and sediment sample details and processing

2.2.1. Water samples

Water sampling was carried out during the 10th Southern Ocean Expedition (December 2017–February 2018), between latitude 31°S–66°S and along longitude 57°E–75°E, from Mauritius to Prydz Bay and back (Fig. 1, Table 2). The surface and profile water samples (with average values of depths: 0 m, 10 m, 30 m, 50 m, 75 m, and 100 m) were collected at one-degree intervals using the onboard conductivity temperature depth (CTD) rosette with a 24-bottle capacity. The coccolithophore samples were analysed using a scanning electron microscopic (SEM), and physical parameters of seawater such as pH and nutrients, namely, nitrate (NO_3), nitrite (NO_2), phosphate (PO_4), and silicate (SiO_4) were determined using an autoanalyser. The temperature and salinity profiles were obtained using sensors attached to a CTD rig.

For the coccolithophore study, 0.5–2.5 L of water was collected in a prewashed plastic bottle and filtered through 0.8 μm pore size Whatman Nuclepore Track-Etched membrane filters of 47 mm diameter using Pall (TM) manifold unit at low vacuum. The filter papers with the samples were dried and kept in the Millipore sterile Petri dish until further analysis using a SEM.

For scanning electron microscope (SEM) analysis, a 5 mm^2 piece of filter paper was attached on double-sided carbon tape, which was fixed to a 1 cm diameter aluminium stub and sputter coated with platinum. The SEM analysis was conducted using a JEOLJSM 6360LV scanning electron microscope using 3–15 kV accelerating voltage and 3,000 × to 20,000 × magnification. Around 500–3,000 fields of view were observed and a total of ~400 coccospheres were counted for each sample. The coccolithophores were identified up to the species level following the taxonomic description by Young et al. (2003), the revised

classification by Jordan et al. (2004), and the Nannotax3 online guide to the biodiversity and taxonomy of coccolithophores (https://www.mikrotax.org/Nannotax3/). To understand the factors influencing coccolithophore productivity and distribution, nutrient analysis was carried out using a Seal Analytical Model AA3-segmented flow analyser (Seal Analytical, UK). For analysis, 60 ml of seawater subsamples were collected from the Niskin bottles and preserved at -20 °C until nutrient analysis (nitrate, nitrite, phosphate, silicate). The samples were thawed and analysed at room temperature prior to analysis,. The seawater samples were analysed based on standard colorimetry principle as described by Grasshoff et al. (1983). Standards were used to calibrate the autoanalyser (accepted r ≤0.999 for all calibration curves). Frequent baseline checks were carried out using Milli-Q water and drift checks using standards (calibration standard) at regular intervals during the sample analysis run. Seawater samples were analysed in duplicate. The standard deviation for all nutrients analysed was ±1%.

Table 2. Water and sediment sample stations

Water samples				**Sediment samples**			
Station	**Depth (m)**	**Latitude (°S)**	**Longitude (°E)**	**Station**	**Depth (m)**	**Latitude (°S)**	**Longitude (°E)**
Surface 50	0	-31.5	57.56	ABP S6	4065	-31.3	47.58
Surface 4	0	-33.51	58.09	MD94-08BC	3491	-38.86	90.12
Surface 44	0	-39.17	58.27	Sk 200/17	4022	-39.03	44.97
Profile 1	0-100	-39.59	57.29	MD97-2102	3440	-39.92	86.01
Surface 10	0	-40.55	59.02	ABP S4	4065	-40.03	48.44
Surface 11	0	-42.06	59.57	ABP S3	3635	-40.29	48
Surface 12	0	-43	60.35	MD94-07BC	2768	-41.71	90.28
Surface 13	0	-44	61.23	ABP S1	3182	-42.5	40.08

Surface 14	0	-45.03	62.09	Sk 200/21	3210	-43.15	44.98
Surface 15	0	-46.04	62.55	Sk20022a	2723	-43.42	45.04
Profile 21	0-100	-47.3	57.3	MD94-102	3205	-43.5	79.83
Surface 16	0	-47.02	63.41	MD97-2101G	-	-43.50	79.84
Surface 37	0	-48	57.3	MD94-06BC	-	-44.66	90.06
Profile 2	0-100	-48	64.28	MD94-109	-	-44.67	90.06
Surface 36	0	-49	57.3	Sk 200/23	1423	-45	45.01
Surface 17	0	-50	64.37	MD19-3579	2720-2760	-45.43	52.01
Profile 20	0-100	-51	57.3	MD00-2375G	-	-45.72	86.75
Surface 18	0	-51	63.22	MD19-3575	2400	-46.03	44.22
Surface 22	0	-55.42	69.45	MD19-3577	800	-46.11	49.11
Profile 19	0-100	-56.59	57.32	SN2	4400	-47	57.3
Surface 23	0	-56.4	69.06	MD94-04BC		-50.38	90.25
Profile 4	0-100	-58	70.04	Sk200/27	4377	-49	45.22
Surface 24	0	-59	70.04	Sk200/33	4185	-55.01	45.01
Surface 26	0	-61.02	71.08	St 1	-	-66.1	57.31
Profile 18	0-100	-62	57.3	ANT 1	-	-69.09	75.53
Profile 5	0-100	-63	70.19	-	-	-	-
Profile 17	0-50	-64	57.3	-	-	-	-
Surface 28	0	-64	70.35	-	-	-	-
Surface 30	0	-66.15	74.43	-	-	-	-

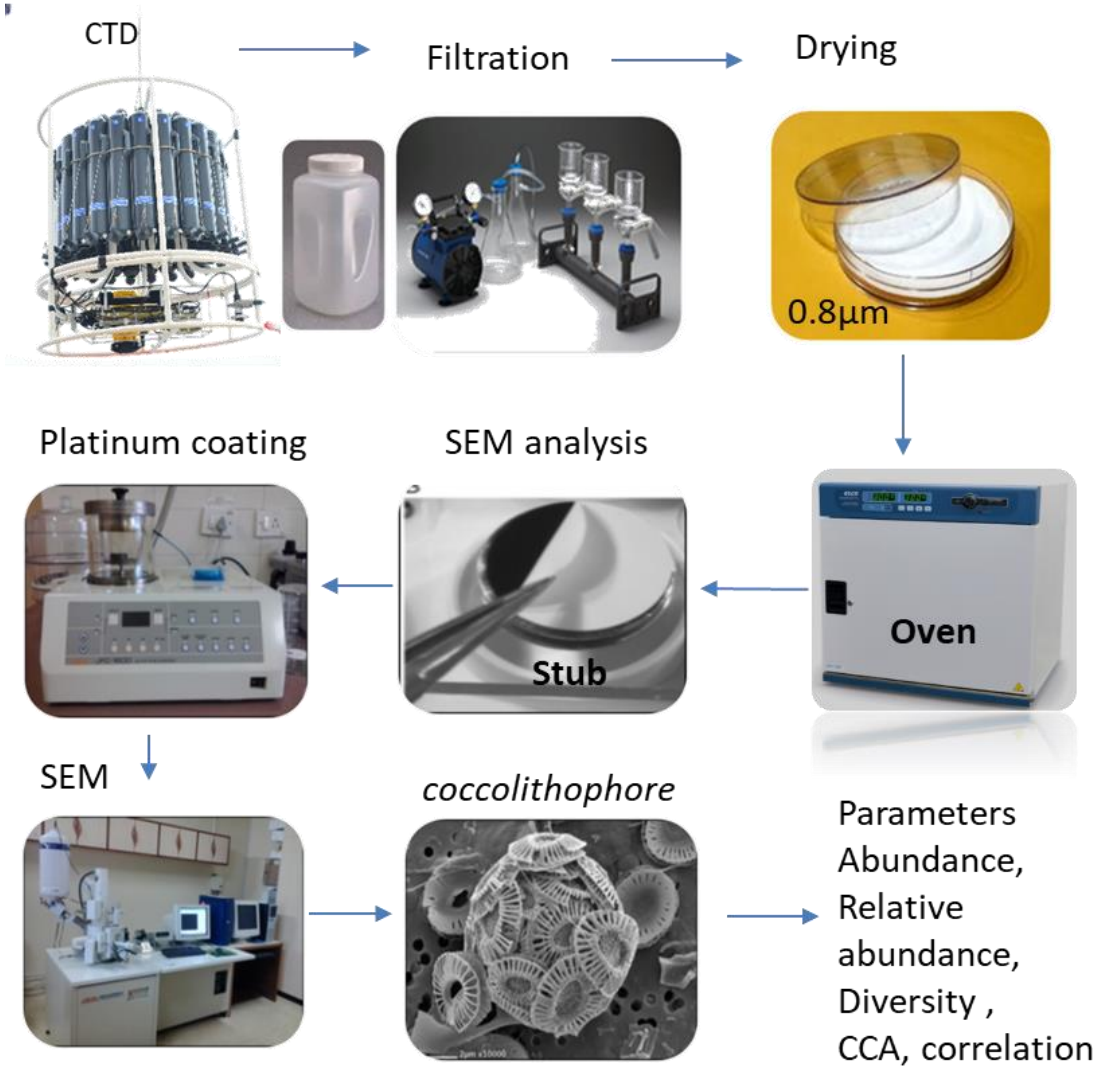

Figure 2. Water sample collection and analysis

2.2.2. Surface sediments

Surface sediment samples: 25 core-top samples (Table 2) from the archives of NCPOR and the University of Bordeaux collected during various Southern Indian Ocean expeditions from 1994–2019 along the latitude 30°S–70°S and longitude 30°E–100°E were used in this study. The temporal resolution of most sediment samples is assumed to be of recent age (Anand et al., 2019). The physicochemical parameter data has been extracted from the European Commission's Copernicus Marine Environment Monitoring Service. These data were collected by SENTINEL-1, a land and ocean services satellite. Average values of the physical parameters

(temperature and salinity) for the last 50 years and nutrient parameters (nitrate and phosphate) were extracted for each location of the surface sediments using Python.

2.2.3. Sediment core

A marine sediment core, SK200/22a, of 7.54 m length was recovered onboard ORV Sagar Kanya from north of the Del Caño Rise, just south of SAF (43°42ˈS, 45°04ˈE; 2730 m water depth) in the Indian Sector of SO during the 2004 Indian Southern Ocean Expedition (Fig. 1a).

The chronology of the sediment core was determined by Accelerator Mass Spectrometry (AMS) ^{14}C dating of handpicked tests of the foraminifera species *Globigerina bulloides* and *Neogloboquadrina pachyderma* (Manoj et al., 2013; Manoj and Thamban, 2015). The radiocarbon ages were corrected and converted to calendar years using CALIB 5.0.2 program (Stuiver et al., 2005). Δ-R correction value of 800 years was used for calibration (Bard, 1988). The age model for the sedimentary sequence of the piston sediment core SK200/22a has been published previously by Manoj et al. (2011, 2013). In the present study, the top 3 m section of the core corresponding to 41,500 years before present (41.5 ka BP) was utilized for coccolith analysis.

2.2.4. Sediment sample processing for the coccoliths

Permanent slides were prepared from the surface sediments and sediment core. Samples from the sediment core were processed at 2 cm intervals. In some sections of the core, the interval was increased to 4 cm due to the limitation of the samples. Samples were processed following the technique described by Flores and Sierro (1997). This method allows uniform distribution of coccoliths on a coverslip. A small quantity of the sediment sample was oven-dried at 50 °C for 48 hours. Exactly 50 mg of this dried sediment was weighed on a

microbalance, transferred into a clean prewashed 15 mL glass tube and 10 mL of buffered water was added. The suspension was mixed well and sonicated for 30 seconds to eliminate aggregated particles. A total of 100 µL of this well-mixed suspension was then transferred into a 60 mm Petri dish containing a coverslip at the bottom and filled with 10 mL gelatin solution (pH >8). The water-containing sample in the Petri dish was mixed several times using a micropipette to ensure uniform distribution of coccoliths. The Petri dish was left undisturbed on a flat surface for 12 hours at 20 °C. The water in the Petri dish was then gently removed by placing a lint-free tissue paper strip at the edge of the Petri dish while not disturbing the coverslip containing the sample. Once the water was drained, the coverslip containing the sample was allowed to air dry and mounted on a glass slide using Canada balsam (refractive index 1.5) as a fixative. The slides were observed under Zeiss Axioscope A1 circular polarizing microscope at 1,000 × magnification. A minimum of 400 coccoliths in each sample were counted. The identification of coccoliths was carried out using Nannotax3 (www.mikrotax.org) and previously published literature (Young et al., 2003; Cros and Fortuño, 2002).

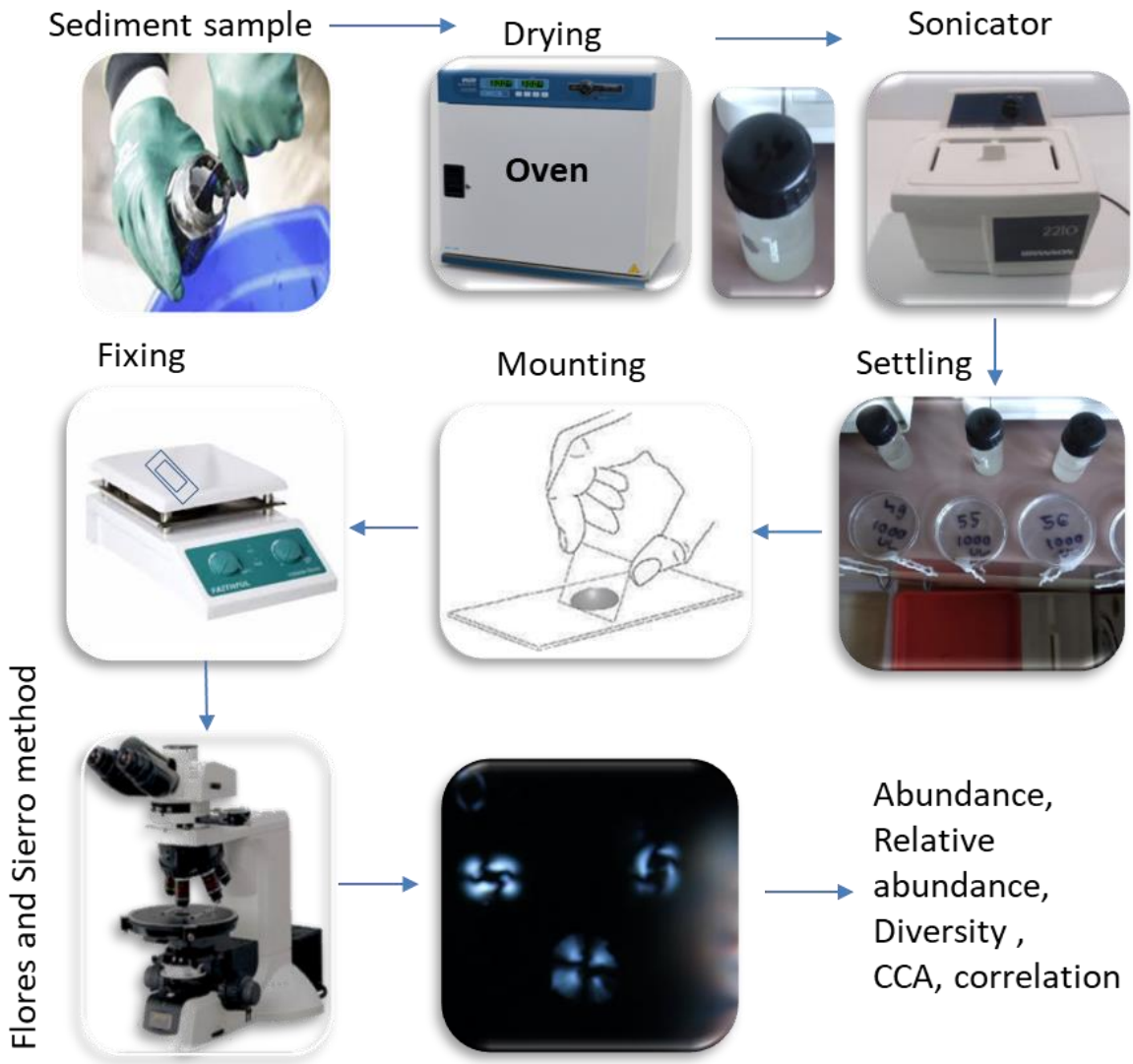

Figure 3. Steps carried out for sediment sample processing and analysis

2.3. Calculation and statistical analysis of coccospheres and coccoliths

2.3.1. Coccosphere analysis in water samples

The quantification of the coccospheres was carried out using the following formula:

$$\text{No. of coccospheres/L} = (F \times C)/(V \times A)$$

Where F is the effective filtration area (mm^2), C is the number of specimens counted, V is the filtration volume (in L), and A is the investigated filter area (mm^2).

2.3.2. Coccolith analysis in sediment samples

For absolute abundance, the number of coccoliths per gram of dry sediment was estimated using the following formula:

$$N = n \times (V / V_p) \times (P_a / A_o) \times 1/W$$

Where N is the total number of coccoliths; n is the number of coccoliths counted per field of view; V is the volume of water added to the dry sediment; V_p is the volume of suspension withdrawn from the micropipette; P_a is the area of the Petri dish; A_o is the area of the field of view; W is the weight of the sediment used.

2.3.3. Canonical correspondence analysis

Canonical correspondence analysis is a multivariate method to interpret the relationships between species assemblages and their environment variables (Ter Braak, and Verdonschot., 1995). To assess the relationship between coccolithophore distribution and known environmental parameters, a CCA was carried out using PAST 4.03.exe software (Hammer et al., 2001). It is essentially a constrained reciprocal averaging ordination, a hybrid technique of ordination and multiple regression. This ordination analysis offers information on how the coccolithophore structure is constrained by the environmental factors in frontal regions, helping

to understand the spatial distribution of coccolithophores. The species whose abundance was more than 0.5×10^4 coccospheres/L were used for analysis. In the ordination, the importance of the explanatory variables is associated with the length of the arrow and the direction of the arrow indicates positive and negative correlations (Jasprica et al., 2012, Laskar and Gupta, 2013).

2.3.4. Pearson's correlation

Pearson's correlation analysis was applied to evaluate interactions between coccolithophore abundance and environmental variables.

2.3.5. Bray–Curtis similarity index

Similarity between species was calculated using the Bray–Curtis similarity index (1957). Bray–Curtis similarity calculation was carried out after square root transformation of the original data, an approach recommended by Clarke and Warwick (2001) using Primer (V6), and cluster/dendrogram was created.

2.3.6. Diversity index

The Shannon–Wiener diversity index (H') was determined for coccolithophores using PRIMER-version 5 (PRIMER-E Limited, UK).

$$H' = -\sum_{i=1}^{S} pi \ln pi$$

Where S is the number of taxa; p_i is the proportion of individuals belonging to the i^{th} species.

2.4. Coccolith dissolution index (CEX)

To analyse the effect of carbonate dissolution on the coccolith assemblages, the ratio of two abundant species with differential preservation was adapted from Dittert et al. (1999). Carbonate dissolution has greater impacts on *E. huxleyi*, which produces fragile coccoliths, than on *C. leptoporus* which produces robust calcified coccoliths. Thus, the ratio of these two species will change with increasing carbonate dissolution. Coccolith Dissolution Index (CEX') was calculated for surface sediment samples and core samples.

The equation taken from Dittert et al. (1999) is as follows:

$$\frac{\textit{E. huxleyi}\ (\%)}{\textit{E. huxleyi}\ (\%) + \textit{C. leptoporus}\ (\%)}$$

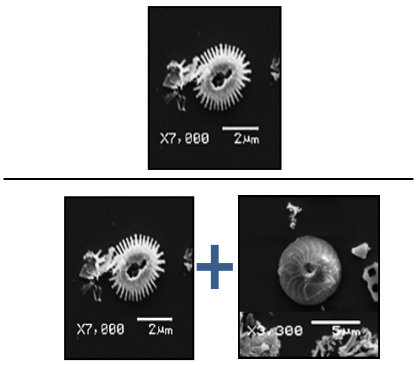

2.5. Coccolith carbonate mass calculation

The calcite content of the coccoliths was estimated using the equation proposed by Young and Ziveri (2000), and lengths of the coccoliths and ks (shape factor) factors were used as estimated by Rigual-Hernández et al. (2020) for coccoliths from the subantarctic zone.

Coccolith calcite (in picograms) = $2.7 \times ks \times l^3$

Where 2.7 is the calcite density, ks is the shape factor, l^3 is the length of the coccolith

2.6 *Coccolithus pelagicus* subsp. *braarudii* morphometry and analysis

Morphometric changes in *Coccolithus pelagicus* subsp. *braarudii* for the past 41.5 Ka BP was studied using the sediment core SK200/22a. A total of 120 permanent slides were prepared following the method described by Flores and Sierro (1997) (Fig. 3).

In each of the 120 samples, morphometric measurements of 60 coccoliths of *C. pelagicus* subsp. *braarudii* were carried out using an Olympus polarizing microscope (Olympus BX51) at 1000 × magnification connected to (Olympus 0733 camera) and CellSens microscope imaging software. The morphometric measurements taken included the length of the distal shield (DL), width of the distal shield (DW), length of the central area (CL), and width of the central area (CW) (Fig. 4).

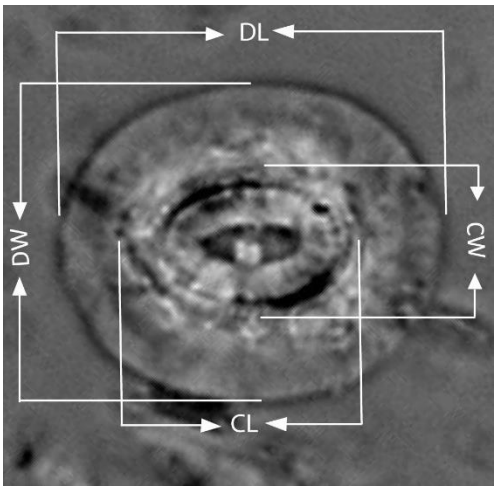

Figure 4. Morphometric measurements of *C. pelagicus* subsp. *braarudii*. DL, Distal shield length; DW, Distal shield width; CL, Central length; CW, Central width.

Chapter 3

Key coccolithophore species

3.1. Introduction

In this chapter, terminology of key coccolithophores those form higher abundance in the water and sediment samples is presented. Along with the terminology, their scanning electron microscope images and light microscopic images are provided for identification and correlation.

The terminology described in the chapter is followed after "Guidelines for Coccolith and Calcareous Nannofossil terminology", by Young et al. (1997). The additional details on coccolithophore terminology is available at the INA website (http://ina.tmsoc.org/terminology/index.htm). The identification of living coccolithophores and fossil coccoliths is followed after Young et al. (2003), www.mikrotax.org, and previously published literature.

Some essential aspects of coccolithophores with regard to identification are: coccolith structure and morphology which are highly variable during diploid or haploid phases of their life cycle. During the diploid stage, coccolithophores produce heterococcoliths which are formed of a radial array of crystal units, whereas, during their haploid stage of life cycle, they produce holococcoliths which are formed of numerous minute euhedral crystallites of <1 micron in the diameter. Each heterococcolith can be subdivided into the rim and central areas (Fig. 1a), made of a hierarchy of three components: (1) elements- which are superficial discrete units on the surface of a coccolith; (2) crystal units- composed of numerous interconnected superficial discrete elements; and 3) a segment- which consists of crystal units constituting one radially repeated portion of a heterococcolith. Furthermore, based on their discrete shapes, heterococcoliths are further divided into three different types, viz. placoliths, muroliths, and nannoliths (Fig. 1a).

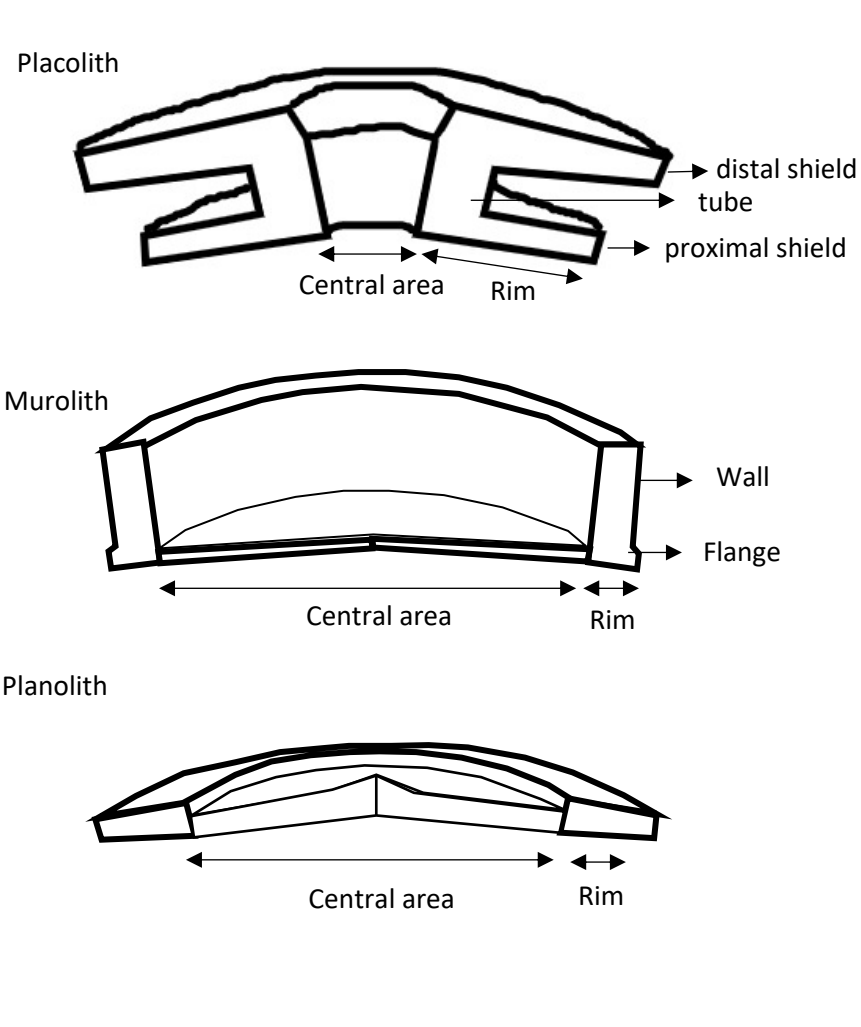

Examples

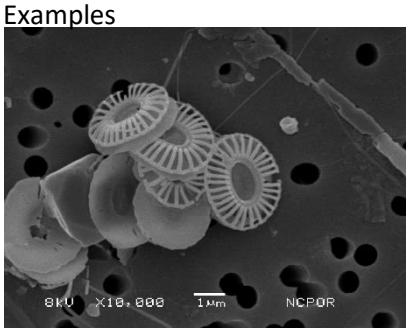

Emiliania huxleyi

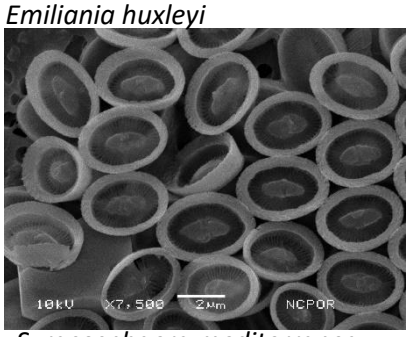

Syracosphaera mediterranea

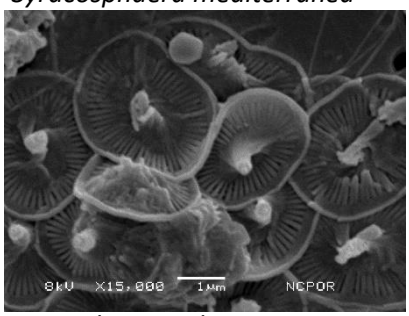

Cyrtosphaera cidaris

* These are commonly occurring shapes of coccoliths and are purely descriptive and hold no taxonomic meaning.

(a)

(b)

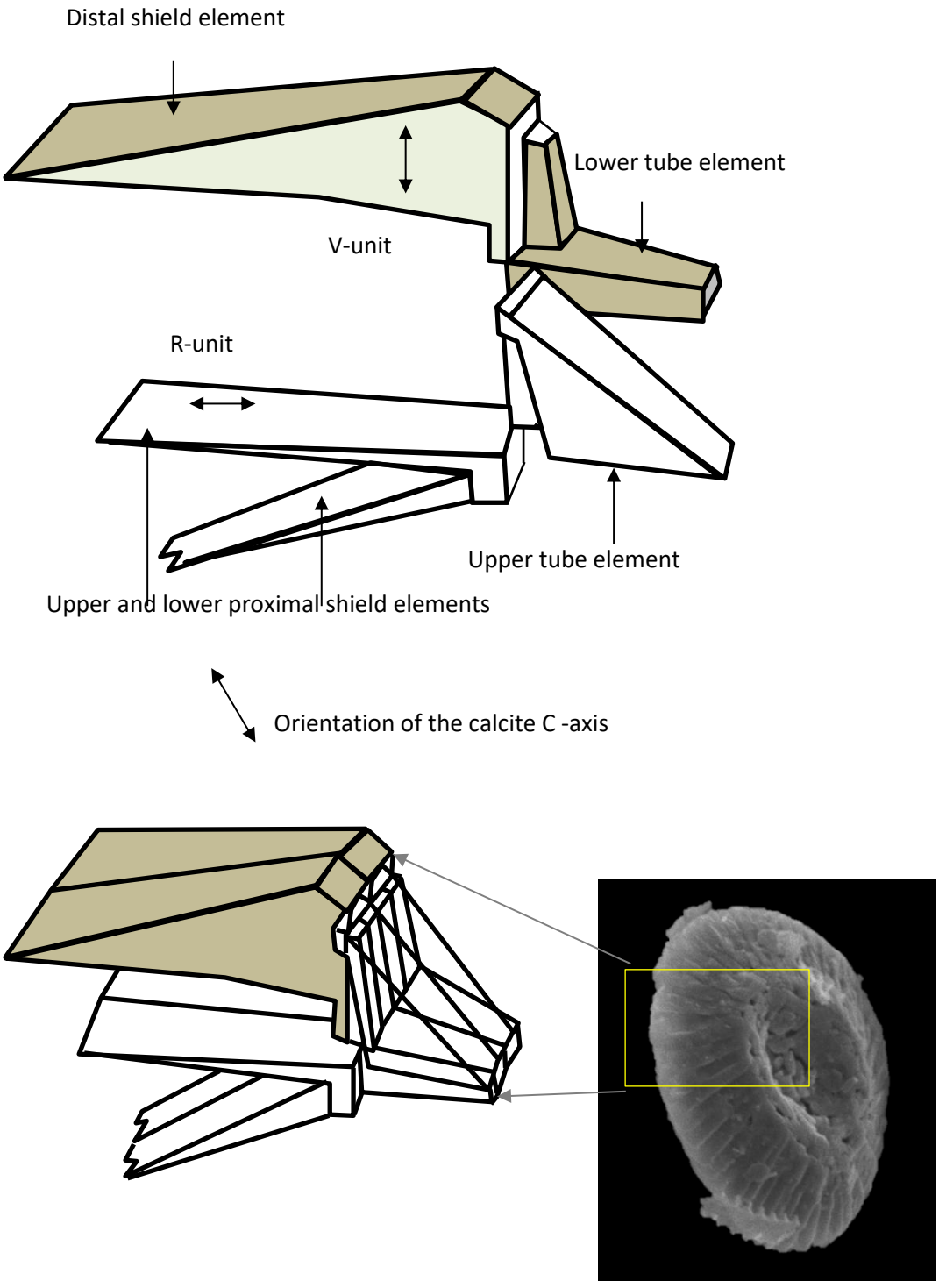

Figure 1. (a) Heterococcolith shape types b) heterococcolith structure: Typical V/R Rim structure, superficially discrete numerous elements interconnect to form two cycles of crystal units; each radial segment thus consists of a V-unit and an R-unit. Example shown is a coccolith of *Coccolithus pelagicus*

Conventions and abbreviations used

HOL: Holococcolithophore

HET: Heterococcolithophore

BC: Body Coccolith

CFC: Circum- flagellar coccolith

XC: Exothecal coccoliths

Lith: Coccolith

LM: Light Microscope

SEM: Scanning Electron Microscope

STZ: Subtropical Zone

SAZ: Subantarctic Zone

PFZ: Polar Frontal Zone

3.2. Major heterococcolithophores documented in this study

3.2.1. Order: Isochrysidales (Pascher 1910)

Family: Noelaerhabdaceae (Jerkovic 1970 emend. Young & Bown 1997)

***Emiliania huxleyi* (Lohmann 1902) Hay & Mohler, in Hay et al. 1967**

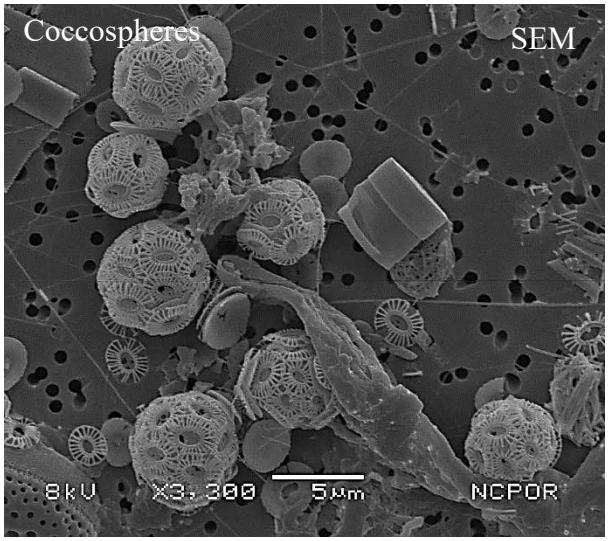

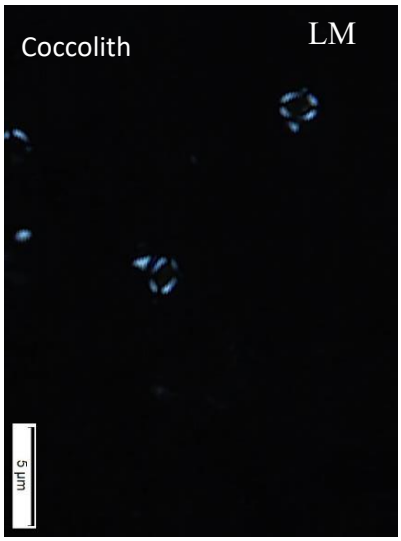

Emiliania huxleyi is a ubiquitous and abundant species, often forms blooms. Coccospheres with multiple layers of coccoliths is often documented. *Emiliania huxleyi* is distinguished into Seven morphotypes (A, B, C, B/C, var. corona, type O, R) (Young and Westbroek, 1991, Young et al., 2003, Okada and McIntyre, 1977, Hagino et al., (2011), out of which Morhptypes A, B, B/C and C are common in the Southern Indian Ocean.

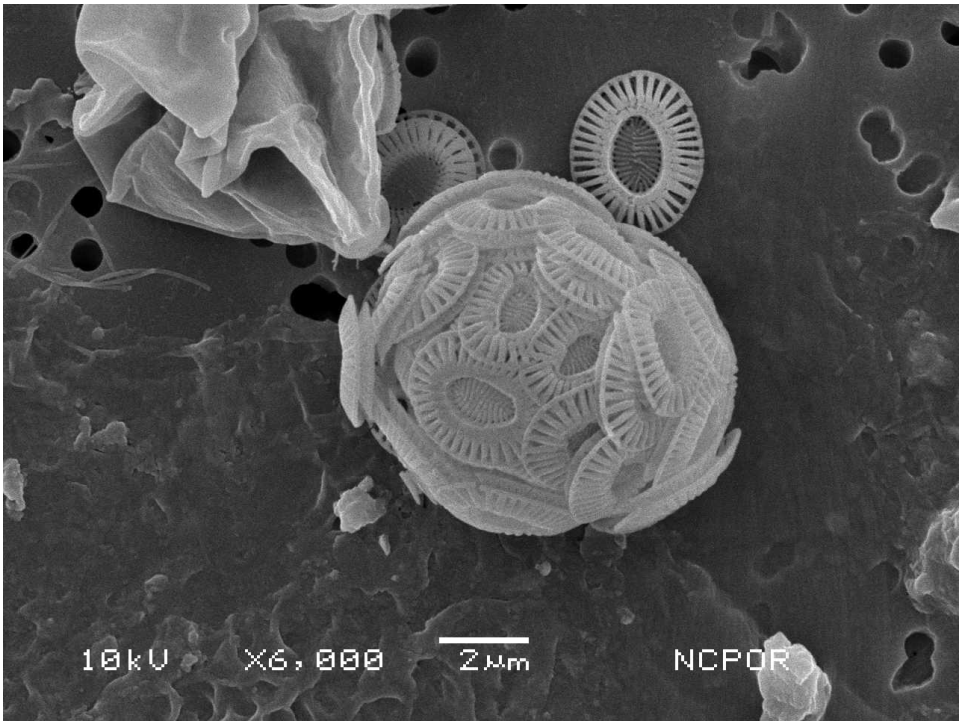

***Emiliania huxleyi* type A sensu Young & Westbroek, 1991**

Distinguishing features: Elliptical, placolith with robust distal shield elements. Central area conjunct, grill, or vacant.

Liths: Medium sized (2.5–4 µm)

Coccosphere size: 5–8 µm

Occurrence extent: STZ-PFZ

Latitude: 31.5°S – 48°S

Abundance in the present study: STZ

Station No: Surface stn 10

Temperature range: 3.3–20 ℃

Salinity range: 33.5–35.7 psu

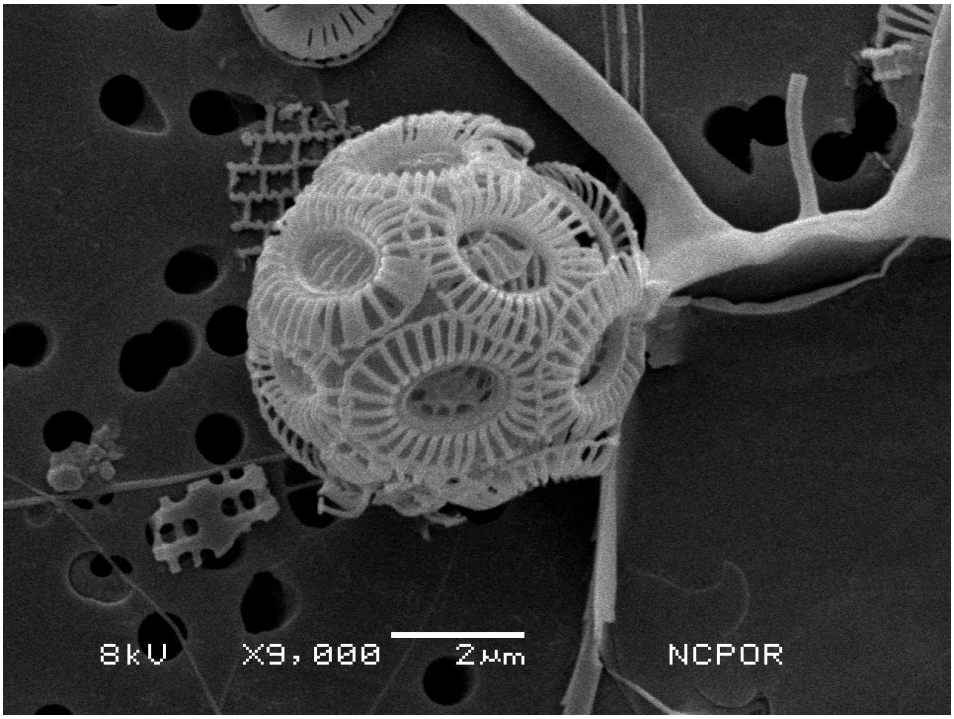

***Emiliania huxleyi* type B sensu Young & Westbroek, 1991**

Distinguishing features: Distal shield is curved and smaller than proximal shield; consists of narrow tube; central area could be open or with plate or irregular laths; delicate distal shield elements

Lith: large size (3–5 µm)

Coccosphere size: 6–10 µm

Occurrence extent: STZ

Latitude: 31.5 °S – 44°S

Abundance in the present study: STZ

Station No: Surface stn 10

Temperature range: 15–20 °C

Salinity range: 34.3–35.7 psu

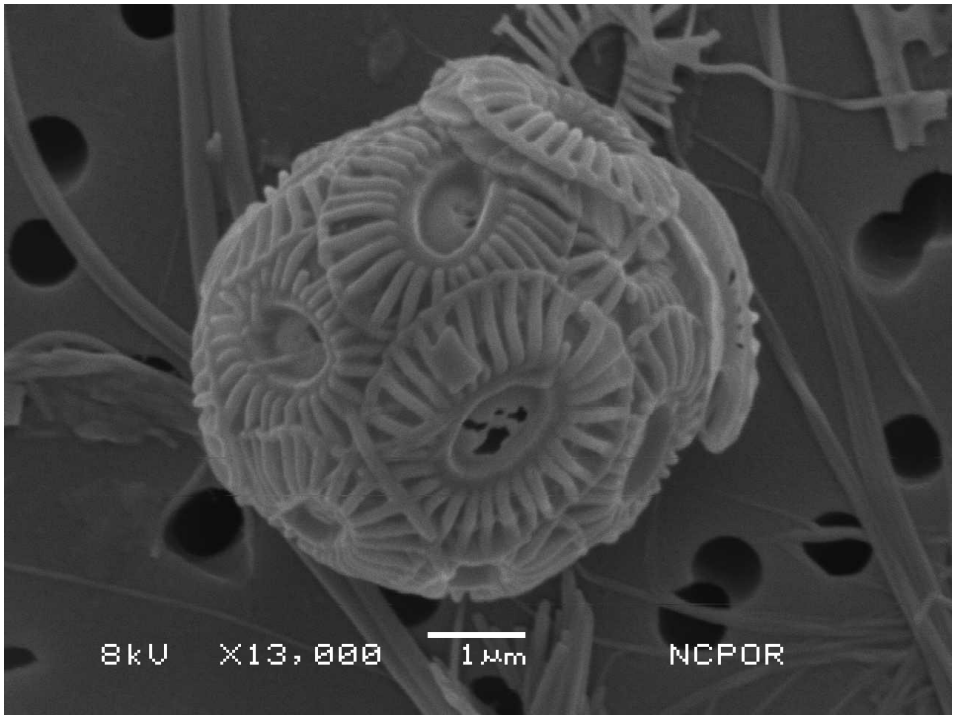

***Emiliania huxleyi* type B/C sensu Young et al., 2003**

Distinguishing features: Distal shield is curved and consists of narrow tube; central area could be open or with plate or irregular laths; delicate distal shield elements; the morphology is like type B and C however, liths are intermediate in size, thick collar present.

Lith: medium in size (3–4 µm) **Coccosphere size:** 6–8 µm

Occurrence extent: STZ-AZ **Latitude:** 39.17°S – 58°S

Abundance in the present study: STZ **Station No:** Surface stn 10

Temperature range: 1.1–20 ℃ **Salinity range:** 33.5–35.7 psu

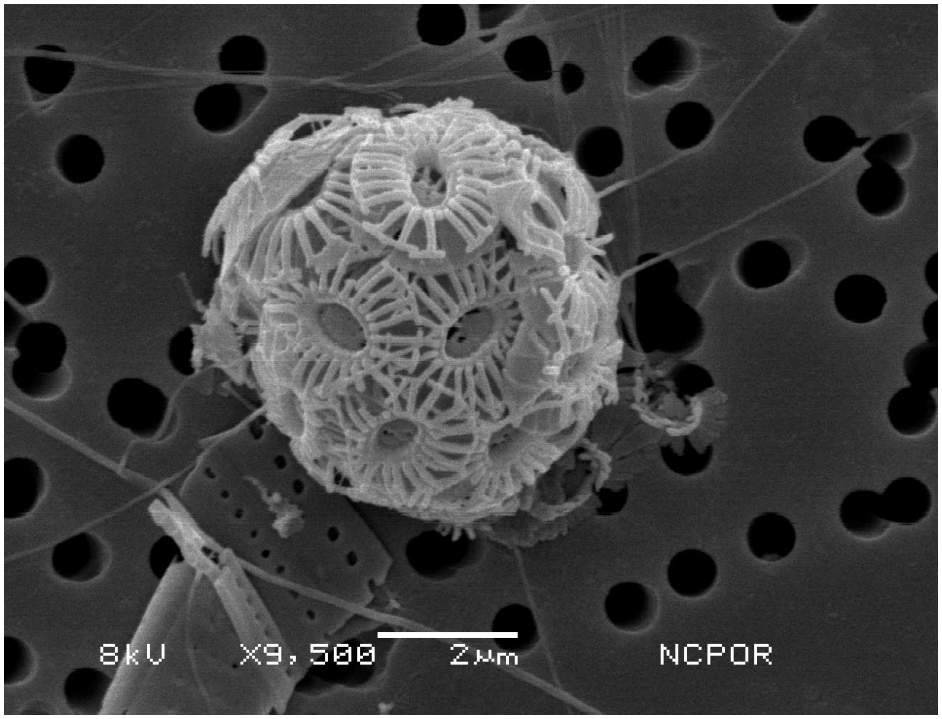

***Emiliania huxleyi* type C sensu Young & Westbroek, 1991**

Distinguishing features: distal shield consists of delicate elements; central area is open or covered by thin membrane or might have laths like in type B, but smaller in size.

Lith: small size (2–3 µm)

Coccosphere size: 4–8 µm

Occurrence extent: STZ-AZ

Latitude: 31.5°S – 58°S

Abundance in the present study: PFZ

Station No: Profile stn 2

Temperature range: 0.5–20 ℃

Salinity range: 33.5–35.7 psu

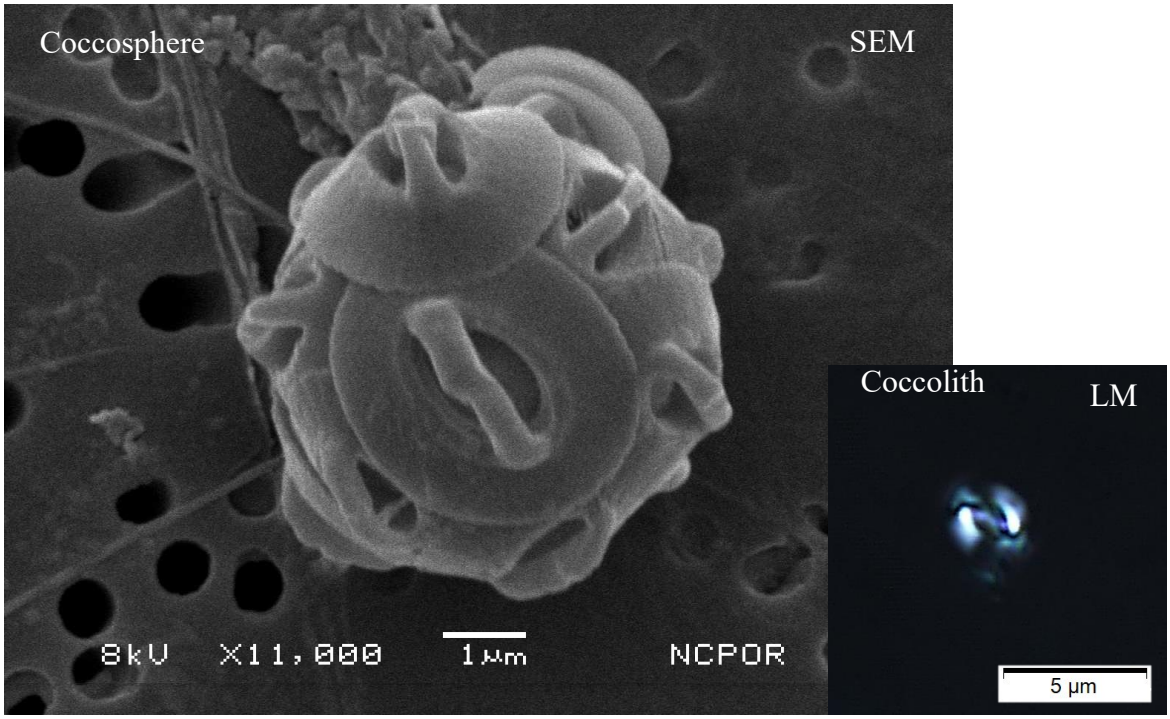

***Gephyrocapsa muellerae* Bréhéret, 1978**

Distinguishing features: Central area small and consists bridge, the bridge is often from long axis to low angle. *G. muellerae* was formerly referred to as *G. caribbeanica.*

Lith size: 3–4 µm

Coccosphere size: 5–8 µm

Occurrence extent: STZ-NSAZ

Latitude: 33.51°S – 45.03°S

Abundance in the present study: STZ

Station No: Surface stn 10

Temperature range: 8–20 ℃

Salinity range: 33.7–35.7 psu

Note: *G muellerae* has an affinity for cold waters and it occurs in great abundance, even as dominant taxon (Winter and Siesser, 1994; Findlay and Giraudeau, 2000; Ziveri et al., 2004)

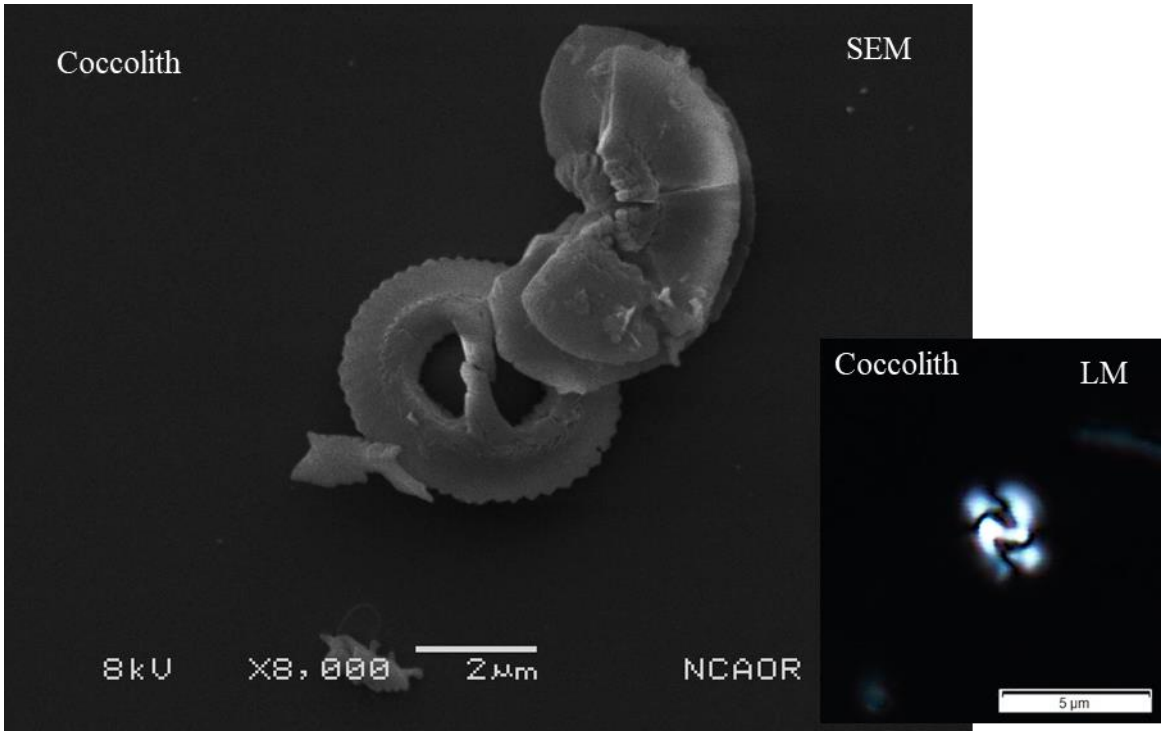

***Gephyrocapsa oceanica* Kamptner, 1943**

Distinguishing features: wide central area consists of bridge; the bridge is often from low to intermediate angle to short axis.

Lith size: 3.5–6 µm; **Coccosphere size:** 6–10 µm;

Number of liths per sphere: 9–35

Occurrence extent: Recorded only in the sediment samples.

Note: *Gephyrocapsa oceanica* is a low-latitude eutrophic species and is a tropical-subtropical species (Okada and McIntyre, 1979). This species was found only in sediment samples

3.2.2. Order: Coccolithales Schwarz, 1932

Family: Calcidiscaceae Young & Bown, 1997

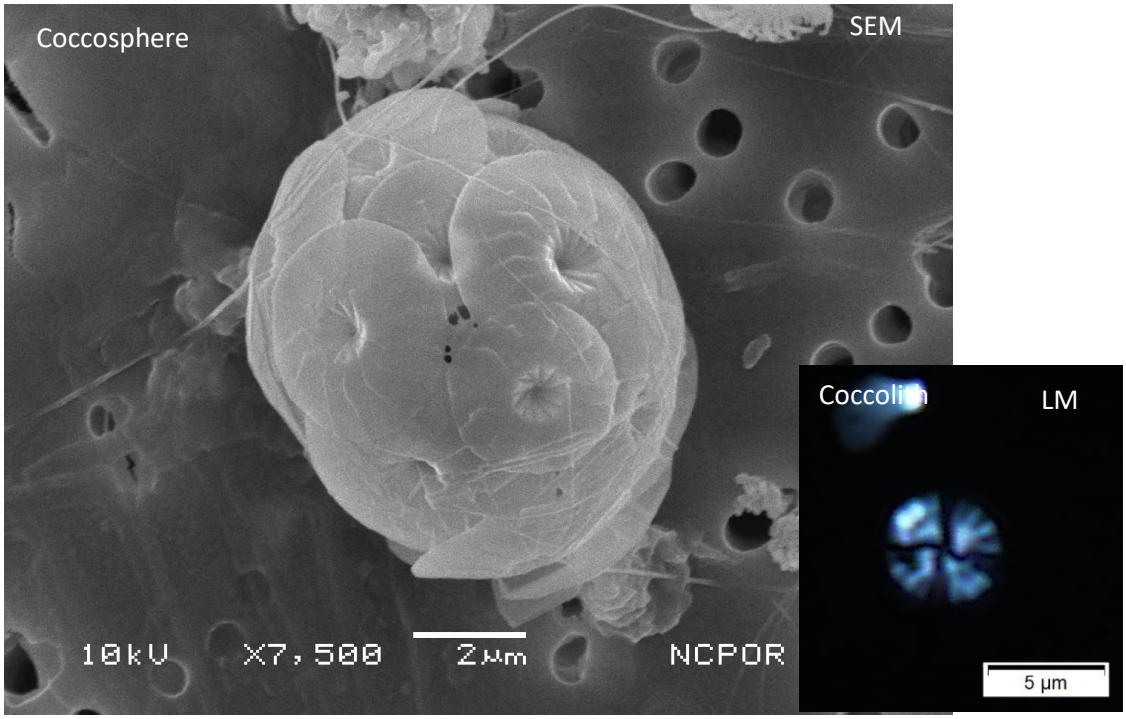

***Calcidiscus leptoporus* subsp. *small sensu* Young et al., 2003**

Distinguishing features: coccoliths circular to subcircular in shape, distal shield consists of complex angular and serrated sutures, 10–12 elements closed central area

Lith size: 3–5 µm

Coccosphere size: 5–12 µm;

Occurrence extent: STZ-SAZ

Latitude: 39.17°S – 48°S

Abundance in the present study: SAZ

Station No: Surface stn 12

Temperature range: 5–17 ℃

Salinity range: 33.5–35.5 psu

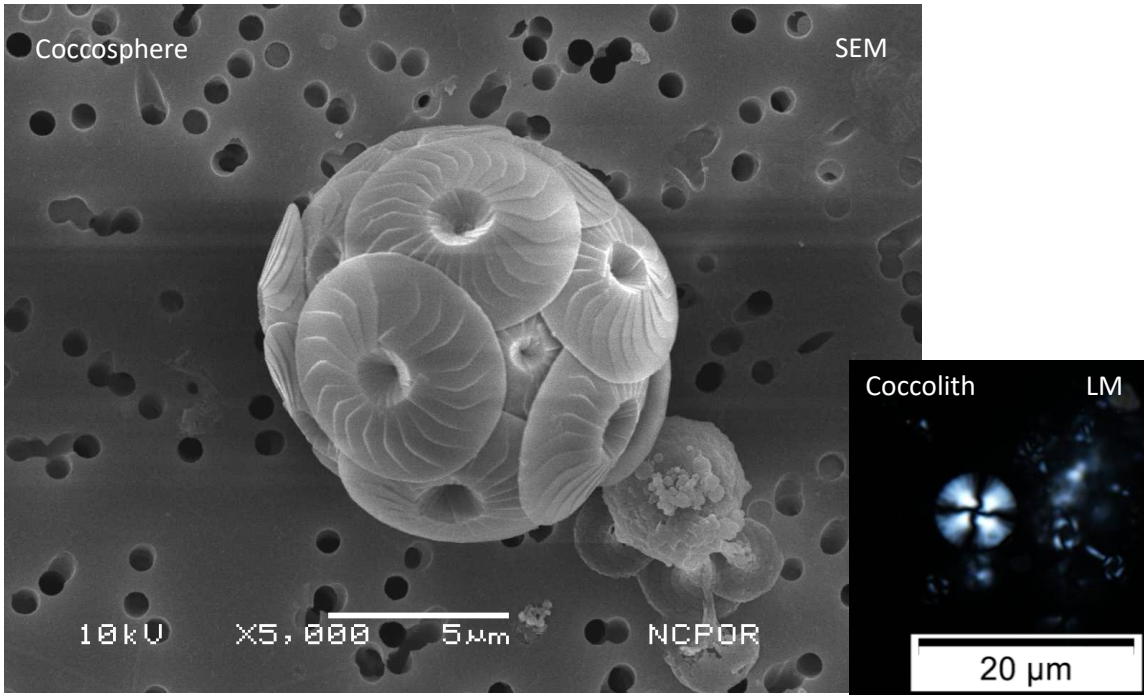

***Calcidiscus leptoporus* subsp. *leptoporus* (Murray & Blackman 1898) Loeblich & Tappan, 1978**

Distinguishing features: Elliptical, sharp sutures around closed central area

Lith size: 5–8 µm

Coccosphere size: 10–18 µm;

Occurrence extent: STZ-NSAZ

Latitude: 31.5°S – 47.02°S

Abundance in the present study: SAZ

Station No: Surface stn 15

Temperature range: 5–20 ℃;

Salinity range: 33.5–35.7 psu

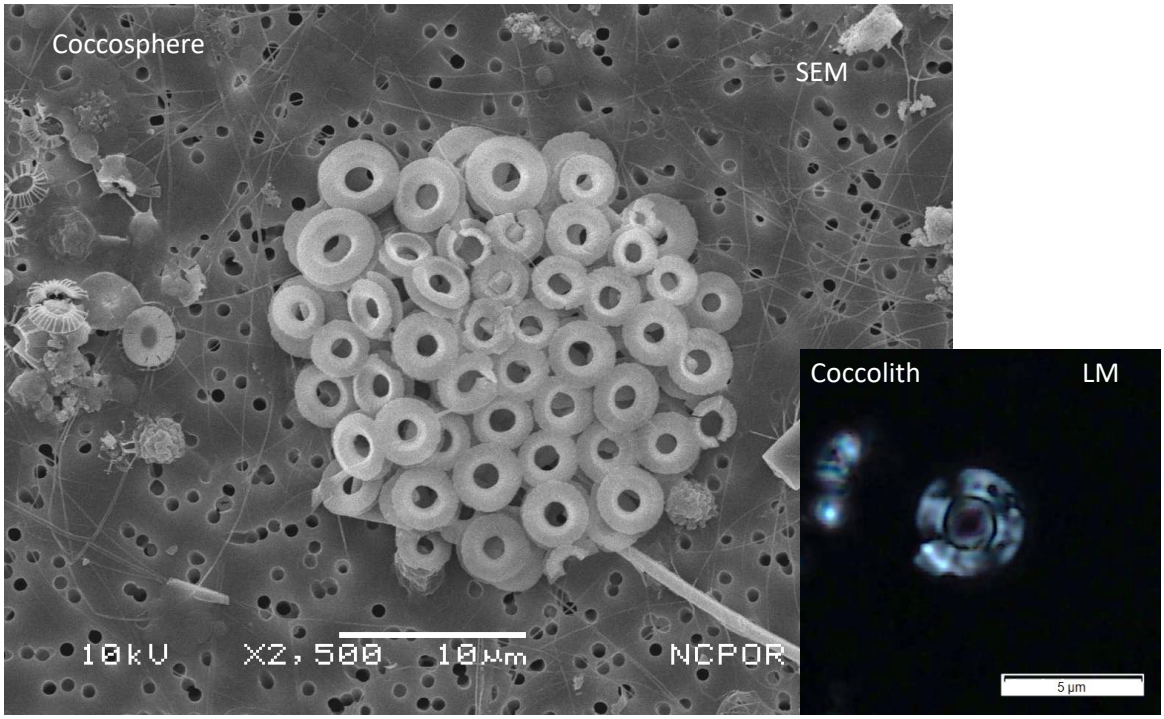

***Umbilicosphaera sibogae* (Weber van Bosse 1901) Gaarder, 1970**

Distinguishing features: wide central area; proximal shield unicyclic and larger than distal shield

Lith size: 3–6 µm

Number of liths per sphere: 40–200

Coccosphere size: 20–30 µm;

Occurrence extent: STZ

Latitude: 31.5°S – 44°S

Abundance in the present study: STZ

Station No: Surface stn 13

Temperature range: 10.5–20 ℃

Salinity range: 33.9–35.7 psu

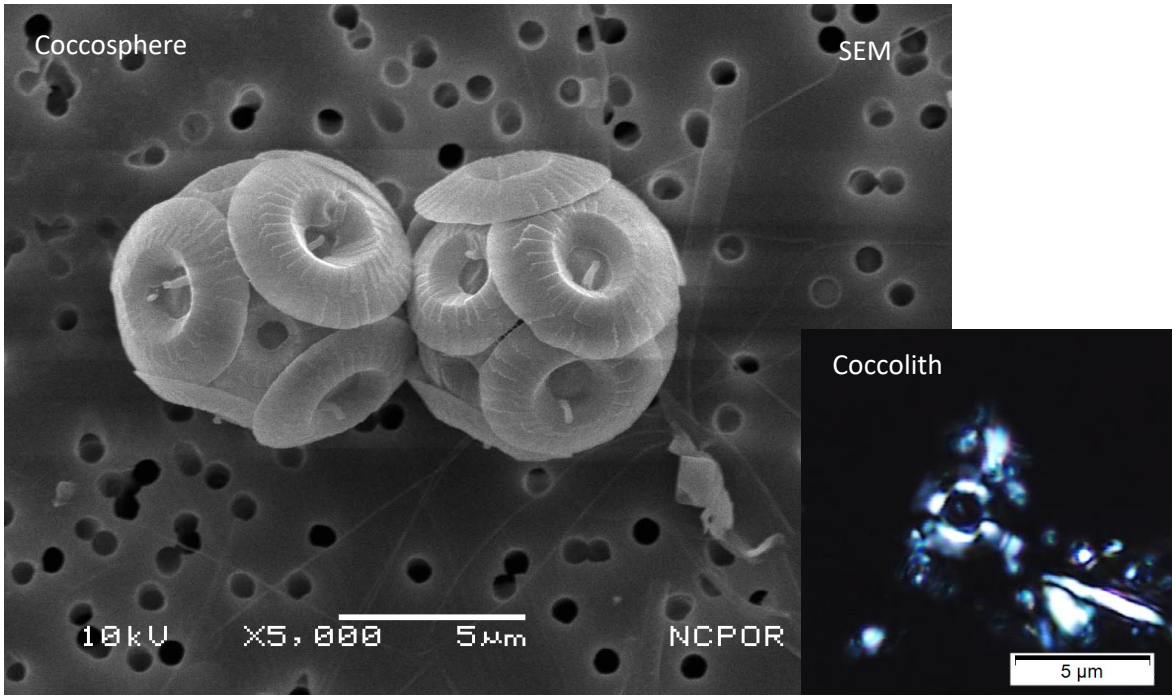

***Umbilicosphaera foliosa* (Kamptner 1963) Geisen in Sáez et al., 2003**

Distinguishing features: Narrow central area, bicyclic proximal shield larger than distal shield

Lith size: 4.5–7 µm

Number of liths per sphere: 10–30 **Coccosphere size:** 12–13 µm

Occurrence extent: STZ **Latitude:** 39°S

Abundance in the present study: STZ **Station No**: Profile stn 1

Temperature range: 10.5–20 ℃ **Salinity range:** 33.9–35.7 psu

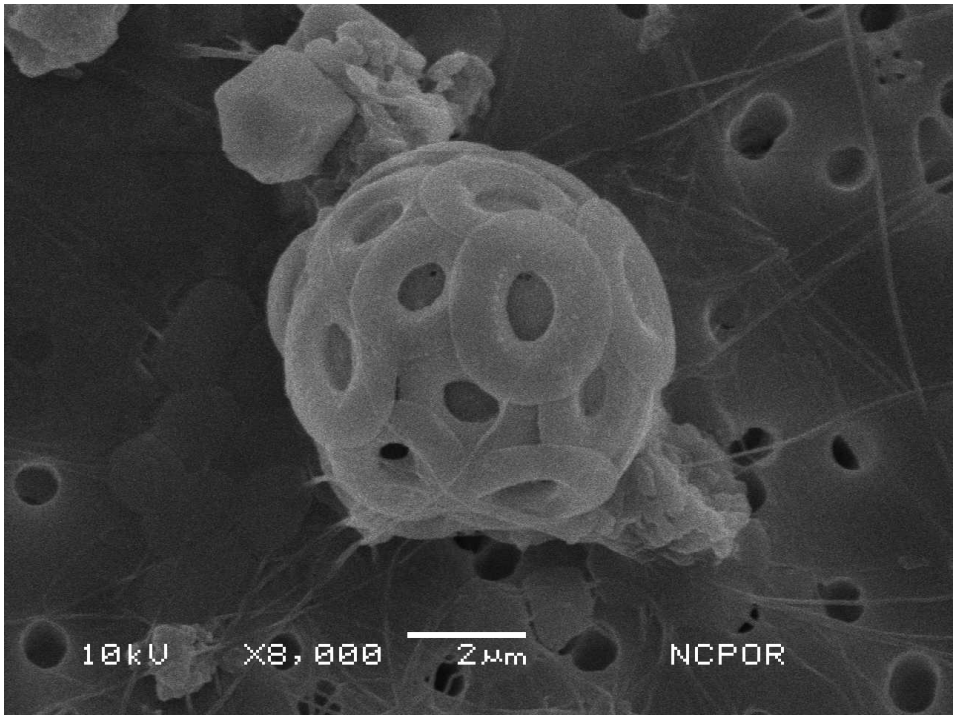

***Umbilicosphaera hulburtiana* Gaarder, 1970**

Distinguishing features: Similar to *U. foliosa*, however, coccoliths are elliptical.

Lith size: 4–6 µm

Number of liths per sphere: 14–30 **Coccosphere size:** 8–10 µm

Occurrence extent: STZ-SAZ **Latitude:** 39.17°S– 45.03°S

Abundance in the present study: STZ **Station No:** Surface stn 44

Temperature range: 10.5–20 ℃ **Salinity range:** 33.9–35.7 psu

3.2.3. Order: Syracosphaerales Hay, 1977 emend. Young et al., 2003

Family: Calciosoleniaceae Kamptner, 1927

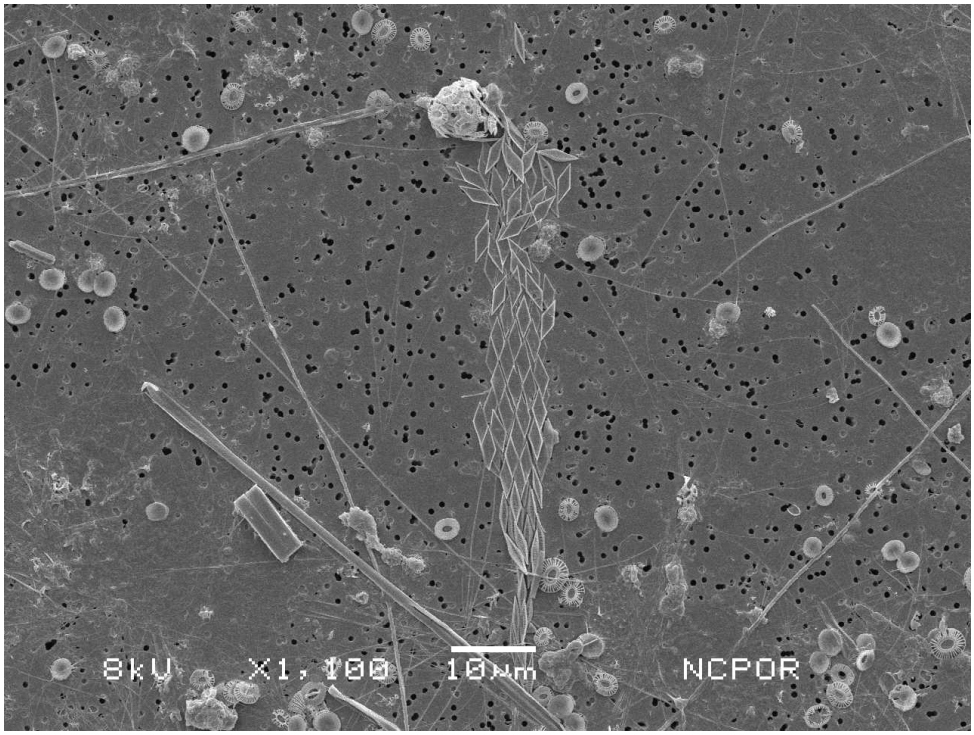

***Calciosolenia brasiliensis* (Lohmann, 1919) Young** in Young et al., (2003)

Distinguishing features: Muroliths are rhombic, Central area floored by transverse laths, coccosphere without spines.

Lith size: 5–7 µm

Number of liths per sphere: 80–190 **Coccosphere size:** 45–95 µm

Occurrence extent: STZ **Latitude:** 39. 59°S

Abundance in the present study: STZ **Station No:** Profile stn 1

Temperature range: 10.5–20 ℃ **Salinity range:** 33.9–35.7 psu

Family: Rhabdosphaeraceae Haeckel, 1894

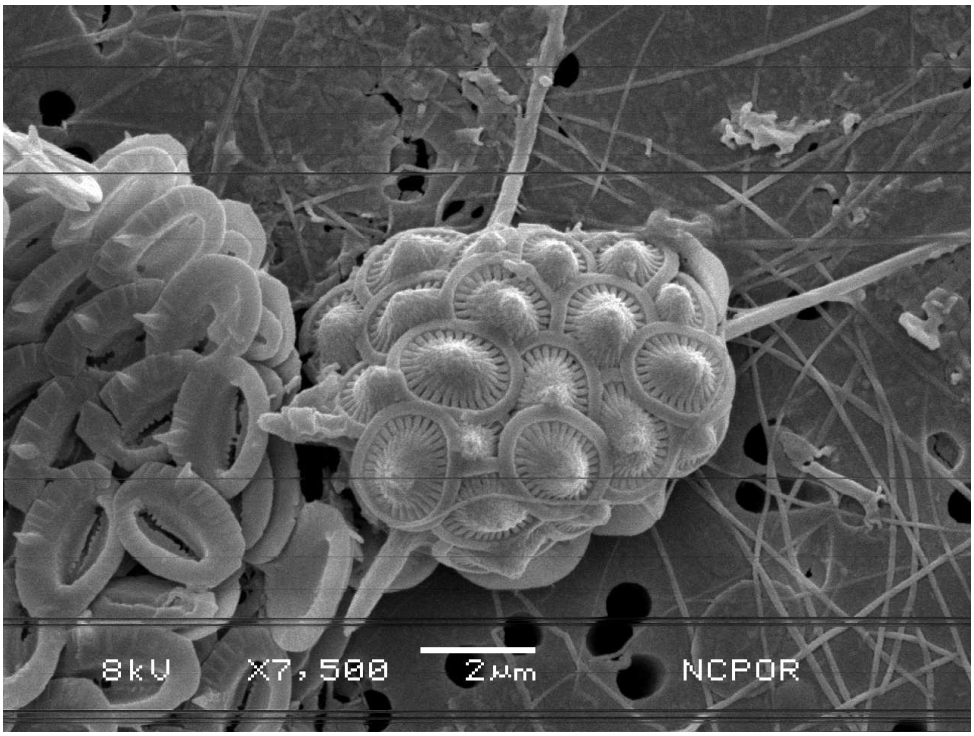

***Acanthoica quattrospina* Lohmann, 1903**

Distinguishing features: Coccosphere polymorphic body coccoliths sub-circular consists of slit between radial cycle elements, low cones are made by lamellar cycle usually polar coccoliths are with well-developed long spines.

Lith size: 1.5–2.5 µm

Number of liths per sphere: 45–105

Coccosphere size: 6–12 µm

Occurrence extent: STZ -SAZ

Latitude: 33.51°S– 48°S

Abundance in the present study: STZ

Station No: Profile stn 1

Temperatur range: 8–20 ℃

Salinity range: 33.7–35.7 psu

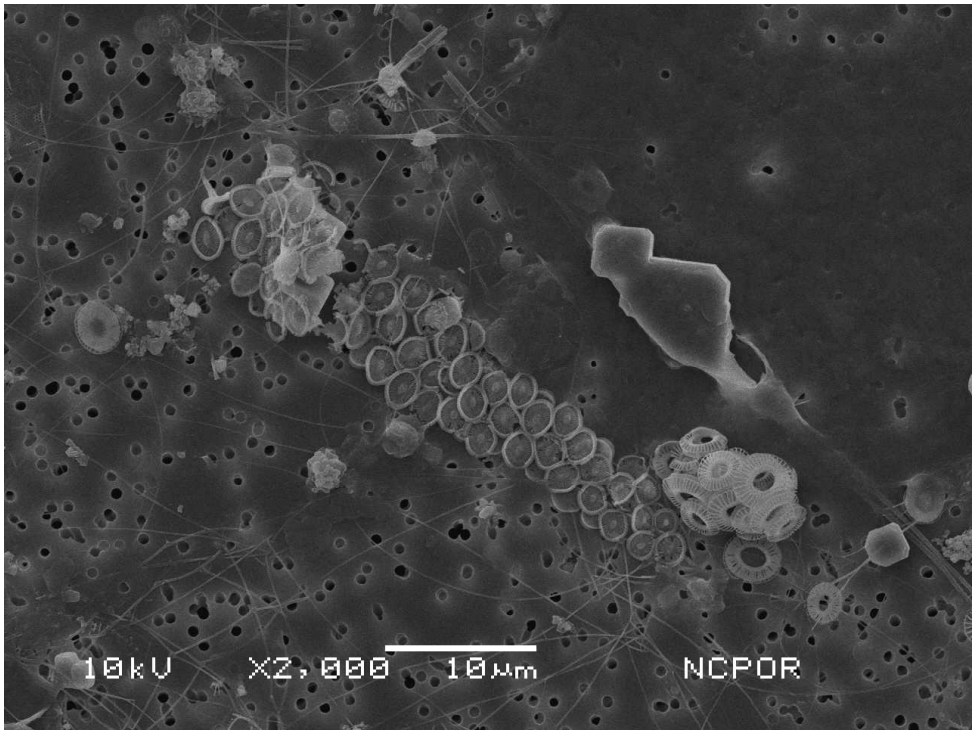

***Syracosphaera prolongata* Gran 1912 ex Lohmann, 1913**

Distinguishing features: Coccosphere shape varies it could be spherical, pyriform or spectacularly elongate. XCs - sub-circular muroliths. BCs - small (1.5-2.5 µm), elliptical to lenticular, CFCs - spines with bifurcate tips

Lith size: 1.5–3 µm

Number of liths per sphere: 40–120 **Coccosphere size:** 10–70 µm

Occurrence extent: STZ -SAZ **Latitude:** 39.17°S– 45.03°S

Abundance in the present study: STZ **Station No:** Profile stn 1

Temperature range: 8–20 ℃ **Salinity range:** 33.7–35.7 psu

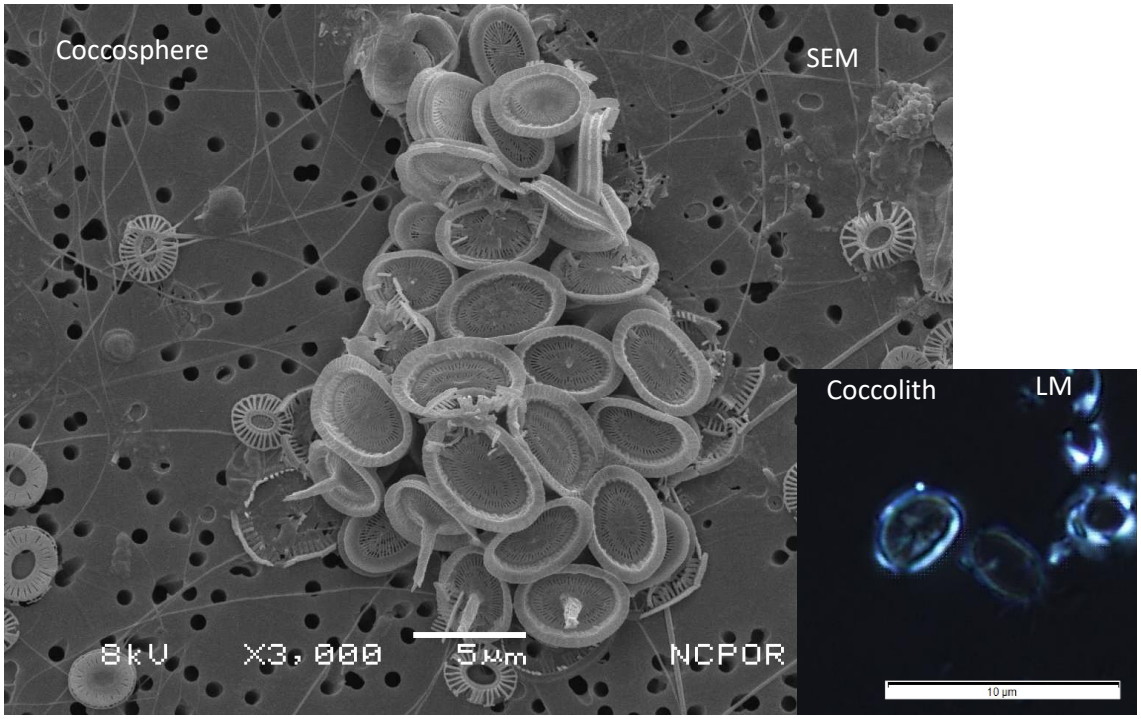

***Syracosphaera pulchra* Lohmann**

Distinguishing features: BCs lack spines, large (4.5–8 µm); XCs are dome-shaped and with central depression, thin radial laths form three concentric cycles in the central area; CFCs – consist of robust bifurcate-tipped spine.

Lith size: 4–8 µm

Number of liths per sphere: 20–60

Coccosphere size: 15–25 µm

Occurrence extent: STZ-NSAZ

Latitude: 33.51 °S– 45.03 °S

Abundance in the present study: STZ

Station No: Surface stn 10

Temperature range: 8–20 ℃

Salinity range: 33.7–35.7 psu

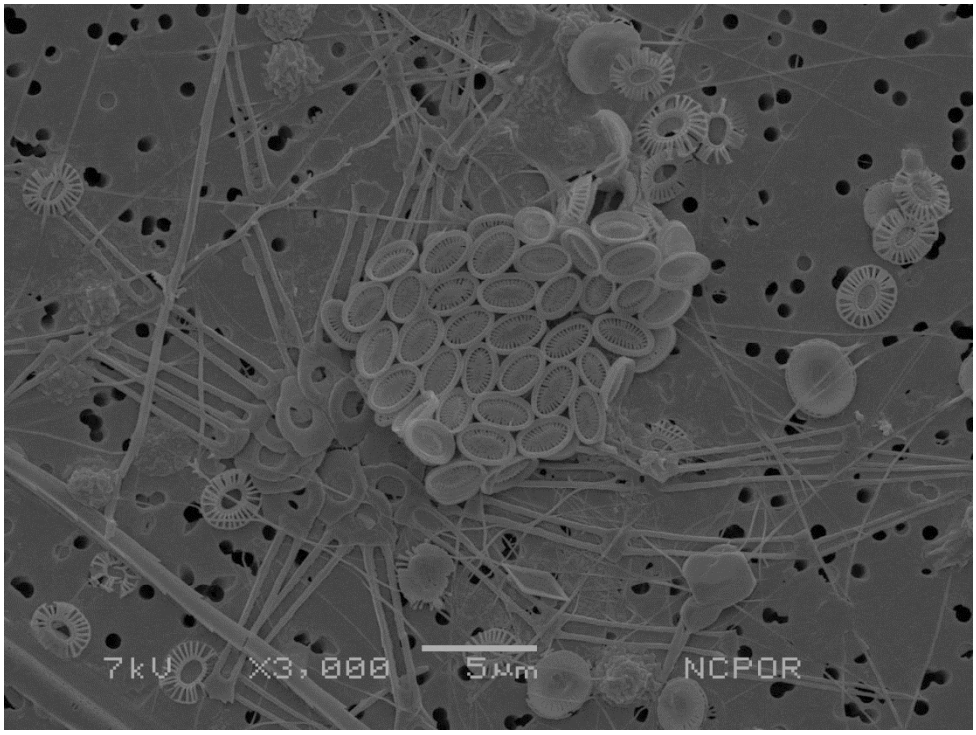

***Michaelsarsia elegans* Gran, 1912**

Distinguishing features: BCs are well calcified with broad rims with proximal flange; axial structure is disjunct and formed of numerous small elements; laths are bipartite. CFCs are small and lenticular with low spines. Whorl coccoliths are planoliths with circular central opening and asymmetric rim. Link coccoliths (osteoliths) are elongate, symmetrical, and convex sided with spoon-shaped ends.

Lith size: 1.8–2.5 µm

Coccosphere size: 10–20 µm

Occurrence extent: STZ–SAZ

Latitude: 33.51°S – 45.03°S

Abundance in the present study: STZ

Station No: Profile stn 1

Temperature range: 8–20 ℃

Salinity range: 33.7–35.7 psu

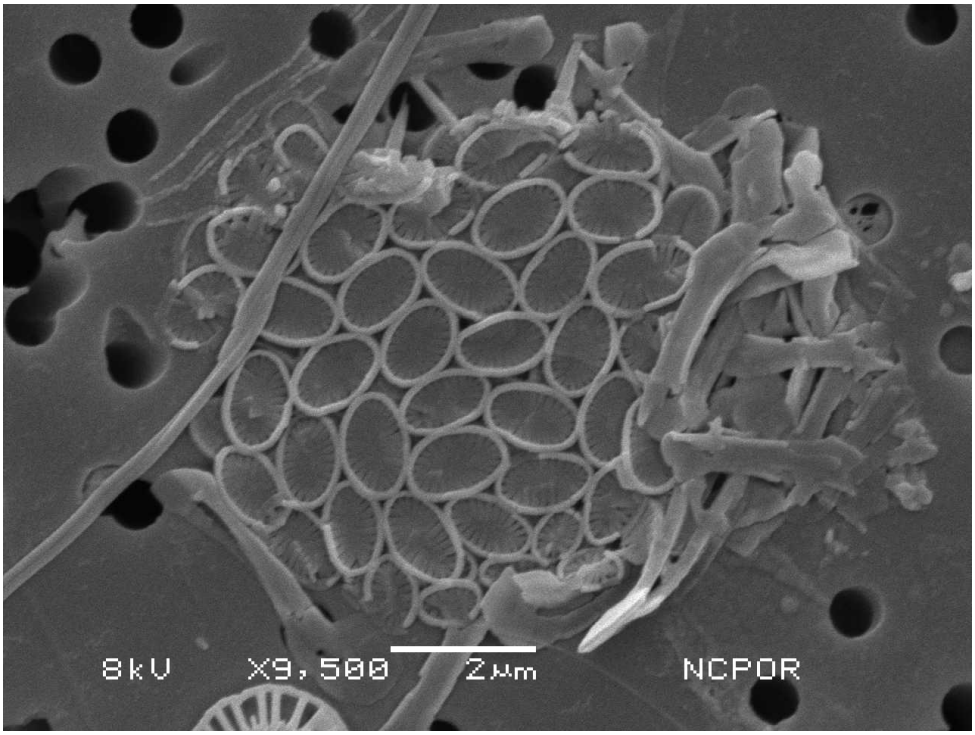

***Ophiaster hydroideus* (Lohmann 1903) Lohmann, 1913**

Distinguishing features: Appendages are made of strings that are highly modified antapical coccoliths, lack whorl coccoliths

Lith size: 0.8–1.5 µm

Number of liths per sphere: 50–100 **Coccosphere size:** 5–7 µm

Occurrence extent: STZ–SAZ **Latitude:** -39.59°S – 47.3°S

Abundance in the present study: STZ **Station No:** Profile stn 1

Temperature range: 8–16 ℃ **Salinity range:** 33.7–35.7 psu

3.3. Holococolithophores

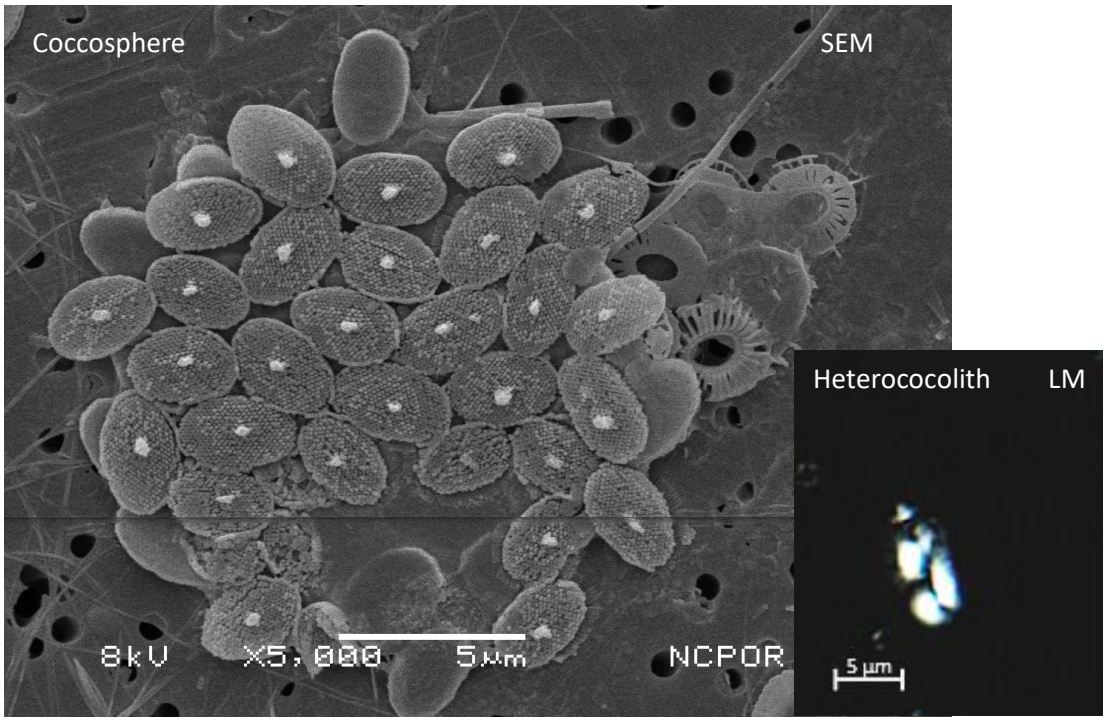

***Helicosphaera* HOL catilliferus type**

Distinguishing features: Liths with flat-top lacking perforations which results in the rhombohedral array structure; pyramidal boss near centre; rim is high by 5-6 crystallites; on proximal side central opening is either small or absent.

Lith size: 2–3.5 µm;;

Number of liths per sphere: 50–100

Size of coccosphere: 12–15.5 µm

Occurrence extent: STZ-NSAZ

Latitude: - 33.51°S – -45.03°S

Abundance in the present study: STZ

Station No: Profile stn 1

Temperature range: 8–20 ℃

Salinity range: 33.7–35.7 psu

Note: Only coccosphere of holococcolith of this species was observed and single heterococcolith was found in plankton sample. However, heterococcoliths were relatively abundant in sediment sample

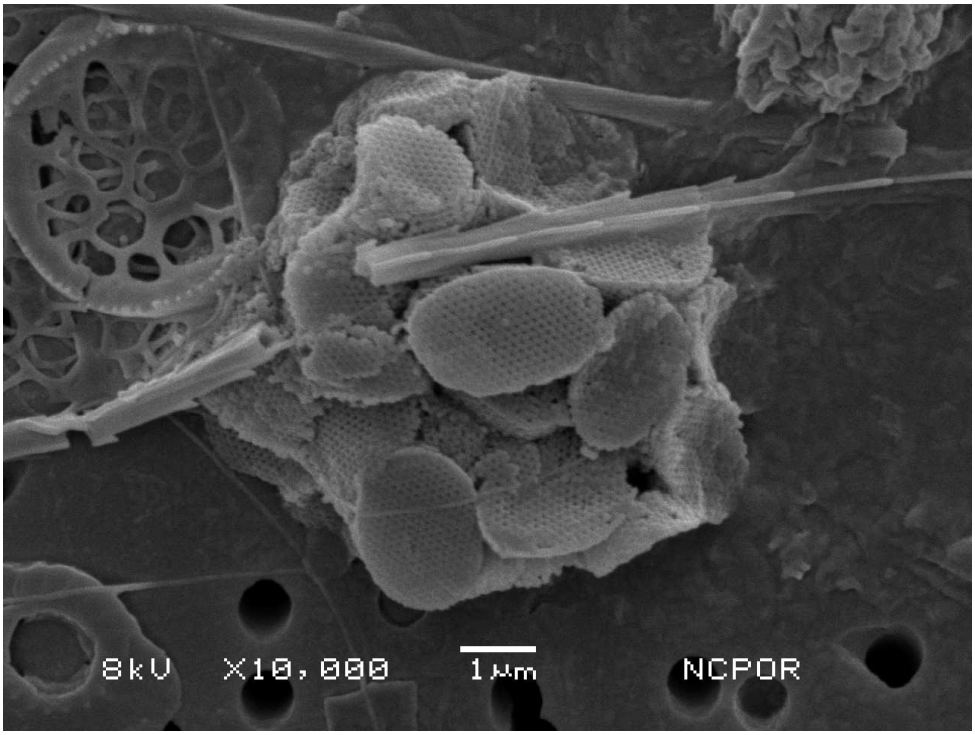

***Syracosphaera histrica* Kamptner, 1941 HOL**

Distinguishing features: BCs tube is 9 crystallites high, flange is absent; flat distal surface flat; tube and distal cover have hexagonal mesh fabric. CFCs are vaulted with flat hexagonal mesh plates sloping towards the centre from each end. An irregular area of parallel strings of crystallites occurs between these plates.

Liths ca.: 2 µm long.

Occurrence extent: STZ **Latitude:** - 39.59°S

Abundance in the present study: STZ **Station No:** Profile stn 1

Temperature range: 10–20 ℃ **Salinity range:** 34–35.7 psu

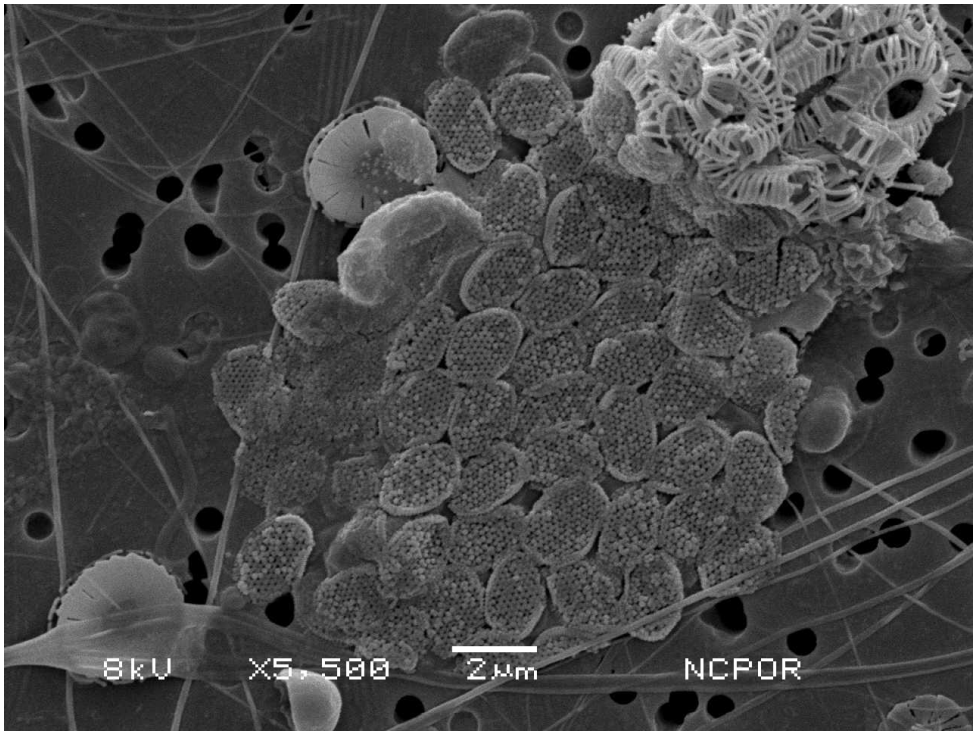

***Calcidiscus leptoporus* subsp. *leptoporus* (Murray & Blackman 1898) Loeblich & Tappan, 1978 HOL**

Distinguishing features: Liths consist of hexagonal meshwork array made of double layer of crystallites, incomplete rim 3 crystallites high.

Lith size: 1.6–2.4 µm

Number of liths per sphere: 50–200 **Coccosphere size:** 8–15 µm

Occurrence extent: STZ–SAZ **Latitude:** - 33.51°S –-47.3°S

Abundance in the present study: STZ **Station No:** Profile stn 21

Temperature range: 8–20 ℃; **Salinity range:** 34–35.7 psu

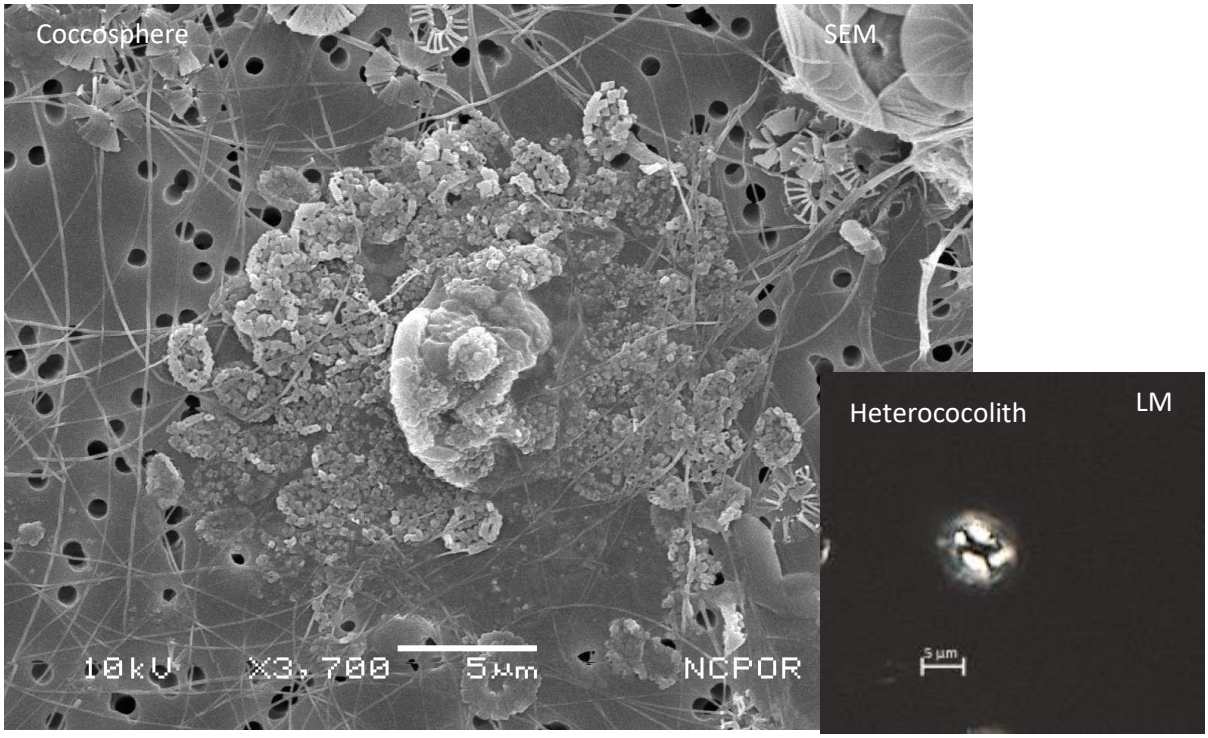

***Coccolithus pelagicus* subsp. *braarudii* HOL (Gaarder 1962) Geisen et al., 2002 HOL**

Distinguishing features: Disk consists of single layer of crystallites arranged in radial strings

Lith size: 2–3 µm

Coccosphere size: 13–20 µm;

Occurrence extent: SAZ

Latitude: - 47.3°S

Abundance in the present study: SAZ

Station No: Profile stn 21

Temperature range: 5–8 °C

Salinity range: 34–35.7 psu

3.4. Tintinnid tests bearing coccoliths

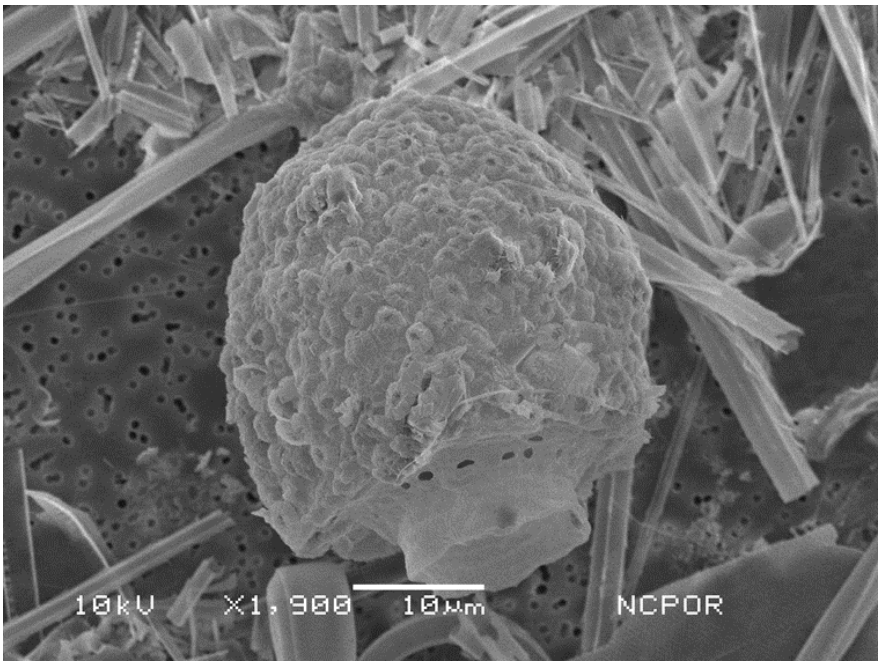

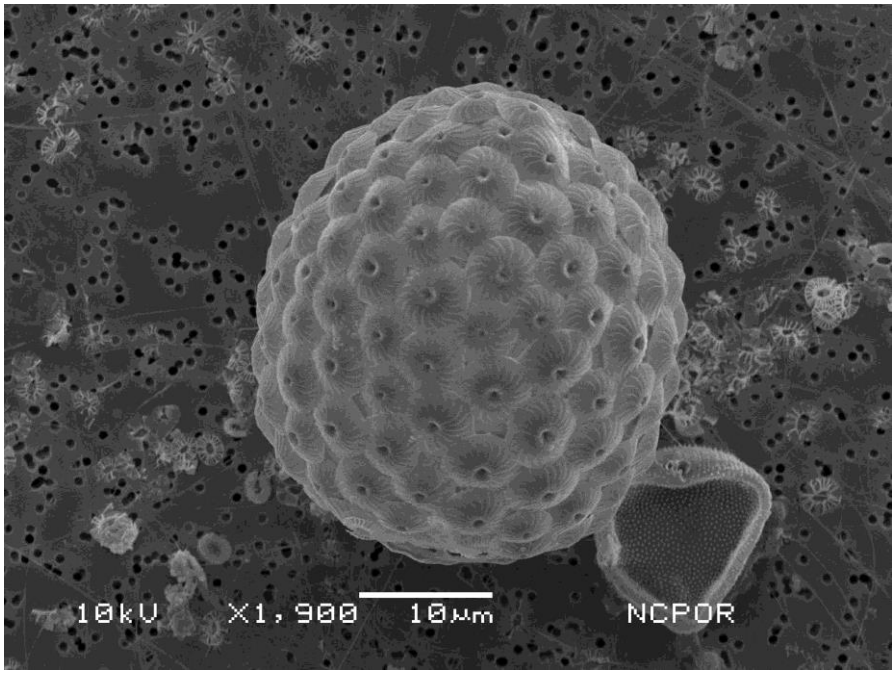

Occurrence extent: SAZ–PFZ

Note: Tintinnids are microzooplanktons that graze on coccolithophores and while doing so incorporate coccoliths into their shells. However, the coccoliths eventually dissolve or sink to the seafloor (Tyrrell and Young, 2009).

Chapter 4

Ecology and biogeography of extant coccolithophores in the Southern Indian Ocean

4.1. Background

The Southern Ocean is a major high nutrient low chlorophyll (HNLC) zone where low iron availability limits phytoplankton productivity in nutrient-replenished surface waters (De Baar, 1994). The Subtropical Zone (STZ) and sub-Antarctic Zone (SAZ) are nutrient depleted, and the productivity is mainly contributed by calcareous organisms like coccolithophores (Ragueneau et al., 2000). However, south of 50°S, the Polar Frontal Zone (PFZ) is inhabited by a monospecific assemblage of the coccolithophore *Emiliania huxleyi*, whereas the Antarctic zone is devoid of coccolithophores (Mohan et al., 2008; Saavedra-Pellitero et al., 2014; Patil et al., 2017). In these two zones, water masses are relatively nutrient-rich and support siliceous productivity contributed by diatoms and radiolarians (Balch et al., 2016; Nissen et al., 2018).

Coccolithophores are single-celled calcifying phytoplankton responsible for forming the Great Calcite Belt along the Southern Ocean fronts during the austral summers (Balch et al., 2016). They play a crucial role in influencing the biological carbon pump by drawing down CO_2 through photosynthesis. Furthermore, they influence the carbonate pump by the formation of calcite plates and their subsequent sinking to depths alters the alkalinity of the upper ocean, affecting air/sea exchanges of CO_2 (Rost and Riebesell 2004). Pelagic carbonate production, primarily contributed by foraminifera and coccolithophores, governs the alkalinity burial from the ocean through its impact on carbonate compensation depth (CCD; depth at which no carbonate is preserved) thus influencing the deep ocean [CO_3^{2-}] and the atmospheric pCO_2 (Sigman and Boyle, 2000; Rickaby et al., 2007).

Coccolithophore biogeography and distribution is controlled by the combined effect of the physical and biogeochemical environment, which is imprinted on the coccoliths that are transported to bottom sediments to become a part of microfossils. The fluctuation of coccolith assemblages and abundances in the sediment core is used as a tool to reconstruct

paleoenvironmental conditions, such as the position of the oceanic fronts in the Southern Ocean (Flores et al., 1999; Findlay and Flores, 2000; Fenner and Di Stefano, 2004; Tangunan et al., 2021).

In recent decades in-situ investigations of the latitudinal distribution of coccolithophores in relation to the frontal positions and the factors affecting them have been carried out in the Atlantic sector (Boeckel and Baumann, 2008), Pacific sector (Gravalosa et al. 2008; Saavedra-Pellitero et al., 2014) Indian Sector (Mohan et al. 2008; Patil et al., 2017; 2020), Drake Passage (Charalampopoulou et al., 2016), and the Southern Ocean (Balch et al., 2016). These studies indicate a latitudinal biogeographic distribution of a majority of coccolithophore species inhabiting a specific ecological niche, which can vary regionally due to local hydrographic changes, terrigenous influences due to islands, nutrient sources, and alkalinity changes. For example, the ubiquitous species *E. huxleyi* is well known for producing large phytoplankton blooms at temperate to subpolar latitudes (Holligan et al., 1993; Brown and Yoder, 1994), but has never been recorded in comparable numbers in waters at low latitudes such as the Arabian Sea (Andruleit et al., 2000; Zeltner, 2000). *Gephyrocapsa oceanica,* a tropical-subtropical species (Okada and McIntyre, 1979; Findlay and Giraudeau 2002) has been recorded in low abundance equatorward of the STF in the Australian sector of the Southern Ocean (Findlay and Giraudeau 2000). In the Pacific sector of the Southern Ocean, occasional occurrence of *G. oceanica* and *G. ericsoni* in surface sediment of the SAZ was recorded whereas it was absent in plankton samples from this zone. It has been suggested that these species might have lived sporadically in the warm waters of SAZ and/or partly drifted into the study area (Saavedra-Pellitero et al., 2014, Saavedra-Pellitero and Baumann 2015; Vollmar et al., 2021). This suggests that variations in the distribution and the ecology of coccolithophore assemblages in the surface ocean may also alter the palaeoceanographic signals of coccolith assemblages preserved in these locations. These signals can vary from those seen in other regions. Regional

studies of extant coccolithophores, and species-specific local ecological affinities, tolerances, and seasonal variations are necessary to assess their potential for local paleoenvironmental reconstructions. Thus, this study aims to gain a detailed understanding of the latitudinal distribution of coccolithophore species along the fronts in the Southern Indian Ocean, factors controlling the distribution, diversity, and effects on fossilizing groups of extant coccolithophore species.

4.2. Methodology

For the study of extant coccolithophores water samples along with associated parameters were collected from 31°S–66°S from the Southern Indian Ocean using a CTD rosette. Approximately 0.5–2.5 L water was filtered through a 0.8 µm pore size, 47 mm diameter membrane filter. The filter papers with the samples were dried and kept in a sterile Petri dish for SEM analysis. A 5 mm^2 piece of this filter paper was attached to an aluminium stub and sputter coated with platinum. In each sample, ~400 coccospheres were counted in the range of 500–3000 fields of view. Coccolithophore identification was carried out following Young et al. (2003), Jordan et al. (2004), and the Nannotax3 online guide to the biodiversity and taxonomy of coccolithophores (https://www.mikrotax.org/Nannotax3/). Further details regarding the methodology and study area are contained in Chapter 2.

4.3. Results

The spatial distribution of coccolithophores (Fig. 1) and physical and chemical parameters, namely, temperature, salinity, pH, chlorophyll a, and nutrients (NO_3, NO_2, SiO_4, PO_4) (Fig. 2), exhibited zonal patterns in the Southern Indian Ocean.

4.3.1. Coccolithophore total abundance and diversity

Coccolithophores are consistently present from the STZ to the north of the Antarctic Zone, ranging between 3–400 × 10^4 coccospheres/L, and utterly absent in the south of the AZ (Fig.1a, c). Coccolithophore absolute abundance (CAA) was highest in the STZ, varying between 3–400 × 10^4 coccospheres/L; where the temperature ranged from 11–20 ℃; salinity, 34–35.7 PSU; pH, 7.8–8.1; NO_3, 0.1– 7.1 µm; NO_2, 0.035–0.2 µm; SiO_4, 0.2–1.4 µm; PO_4, 0.1–2 µm. Furthermore, in the PFZ, CAA ranged between 5–308 × 10^4 coccospheres/L, and the temperature, 2–5 ℃; salinity, 33.7–33.9 PSU; pH, 7.6–8.0; NO_3, 5.1–27.8 µm; NO_2, 0.03–0.3 µm; SiO_4, 0.5–16.4 µm, PO_4; 1.0–1.9 µm (Fig. 1a, c, and Fig. 2).

However, in the SAZ the CAA ranged between 5–194 × 10^4 coccospheres/L; where the temperature ranged from 5–9 ℃; salinity, 33.5–33.8 PSU; pH,7.7–8.1; NO_3, 3.9–14.1 µm; NO_2, 0.1–0.2µm; SiO_4, 0.1–2.2 µm, PO_4; 0.6–1.3 µm. The lowest total coccolithophore abundance of 3 × 10^4 coccospheres/L was recorded in the north of STZ and 2.5 × 10^4 coccospheres/L, south of APF (Fig. 1a, c and Fig. 2).

A total of 55 coccolithophore species and 8 holococcolithophores were recorded from the Agulhas Return Front (ARF) to AZ. The diversity index of coccolithophores varied from 0.02–2. The coccolithophore diversity is highest (2) in STZ at 0–10 m depths (Fig. 1b) and decreases towards the south exhibiting a decreasing trend from north to south. The lowest diversity is observed in the PFZ (0.02) at depths of 10 m, 50 m, and 75 m (Fig. 1b, d).

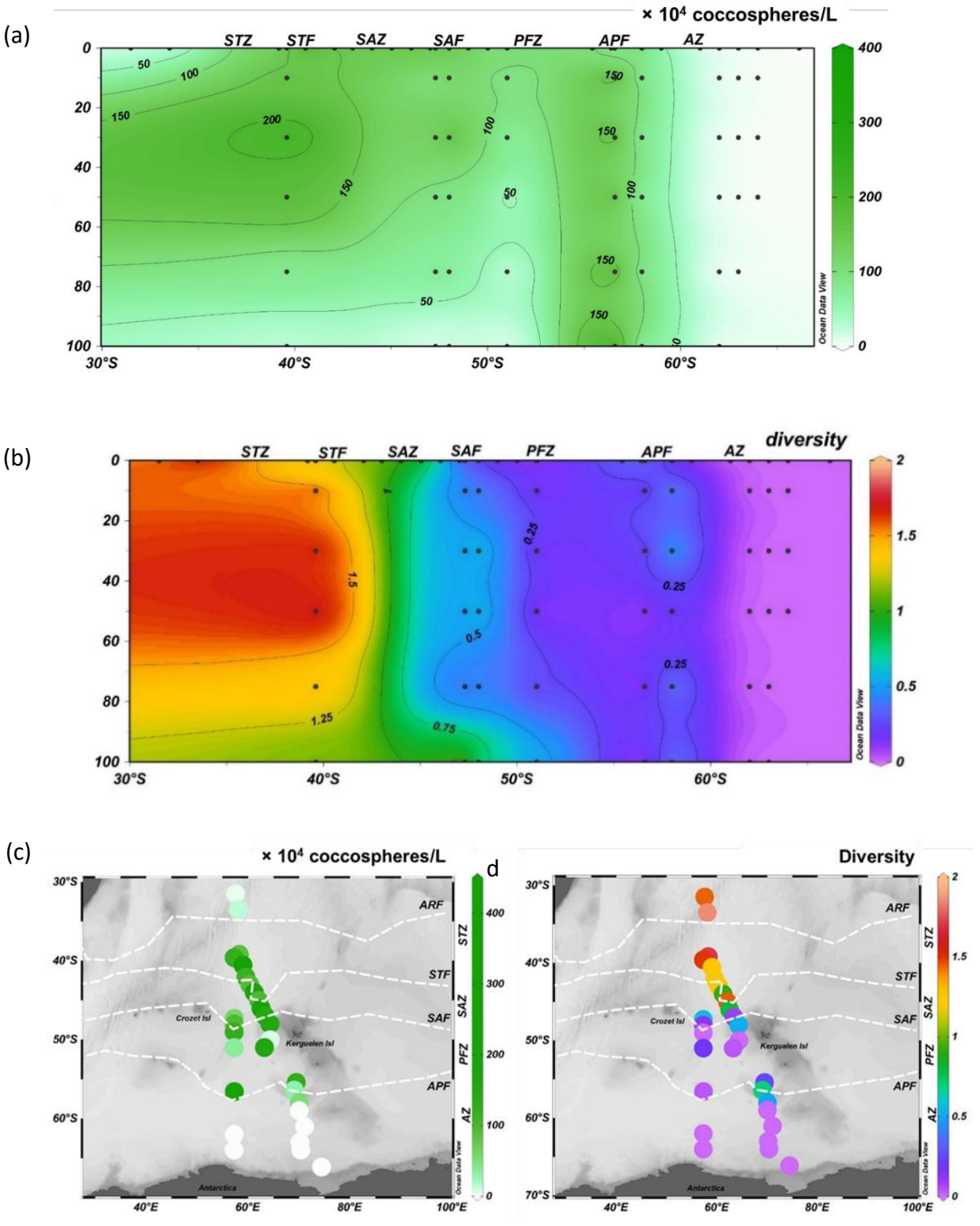

Figure 1. (a) Total abundance of Coccolithophores (0–100 m depth) along the north-south transect (b) Shannon–Wiener Diversity index (0–100 m depth) (c) Total abundance of coccolithophores lateral view (d) diversity index lateral view.

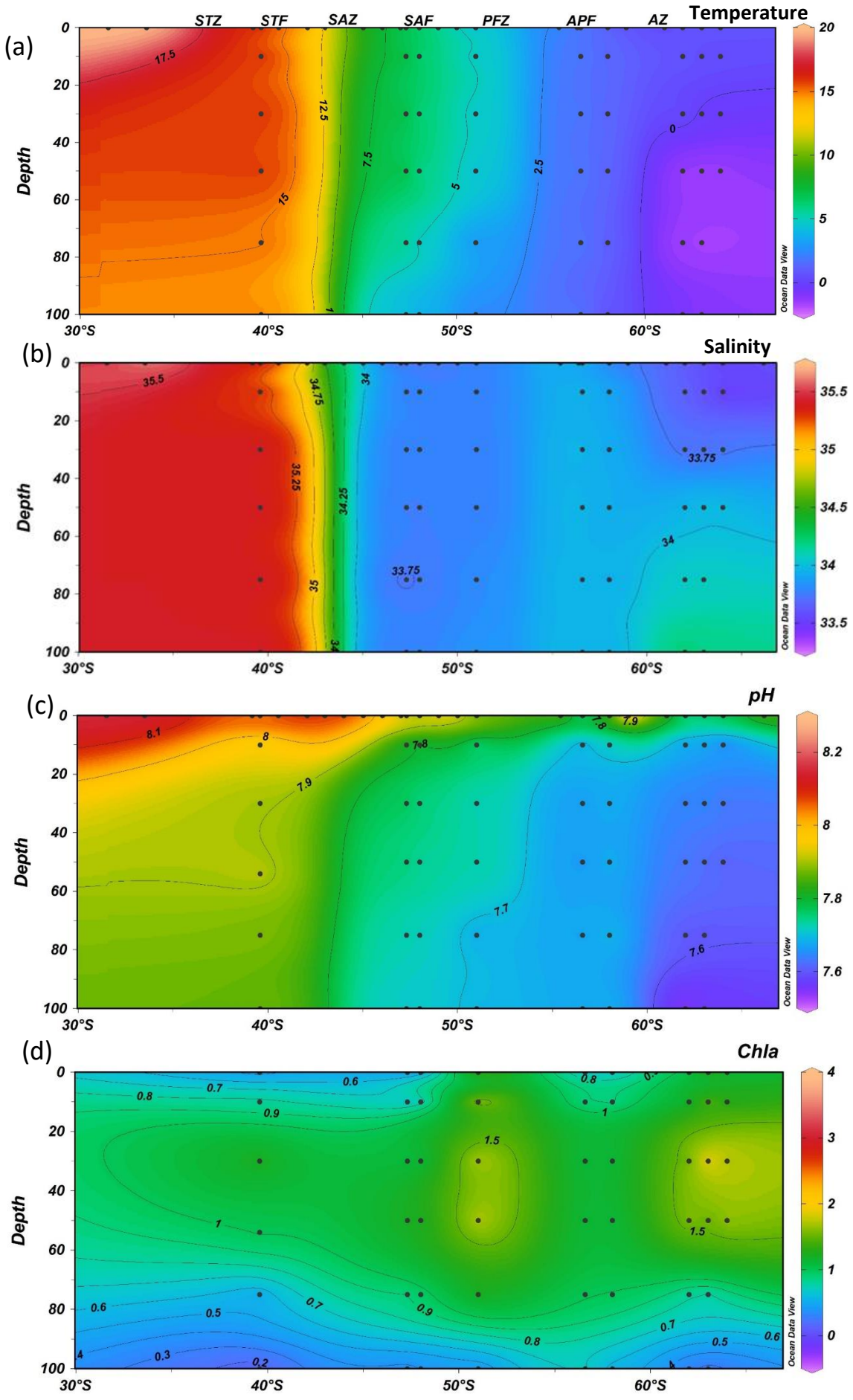
(a)
Temperature
STZ
STF
SAZ
SAF
PFZ
APF
AZ
Depth
30°S
40°S
50°S
60°S
Ocean Data View
(b)
Salinity
(c)
pH
(d)
Chla

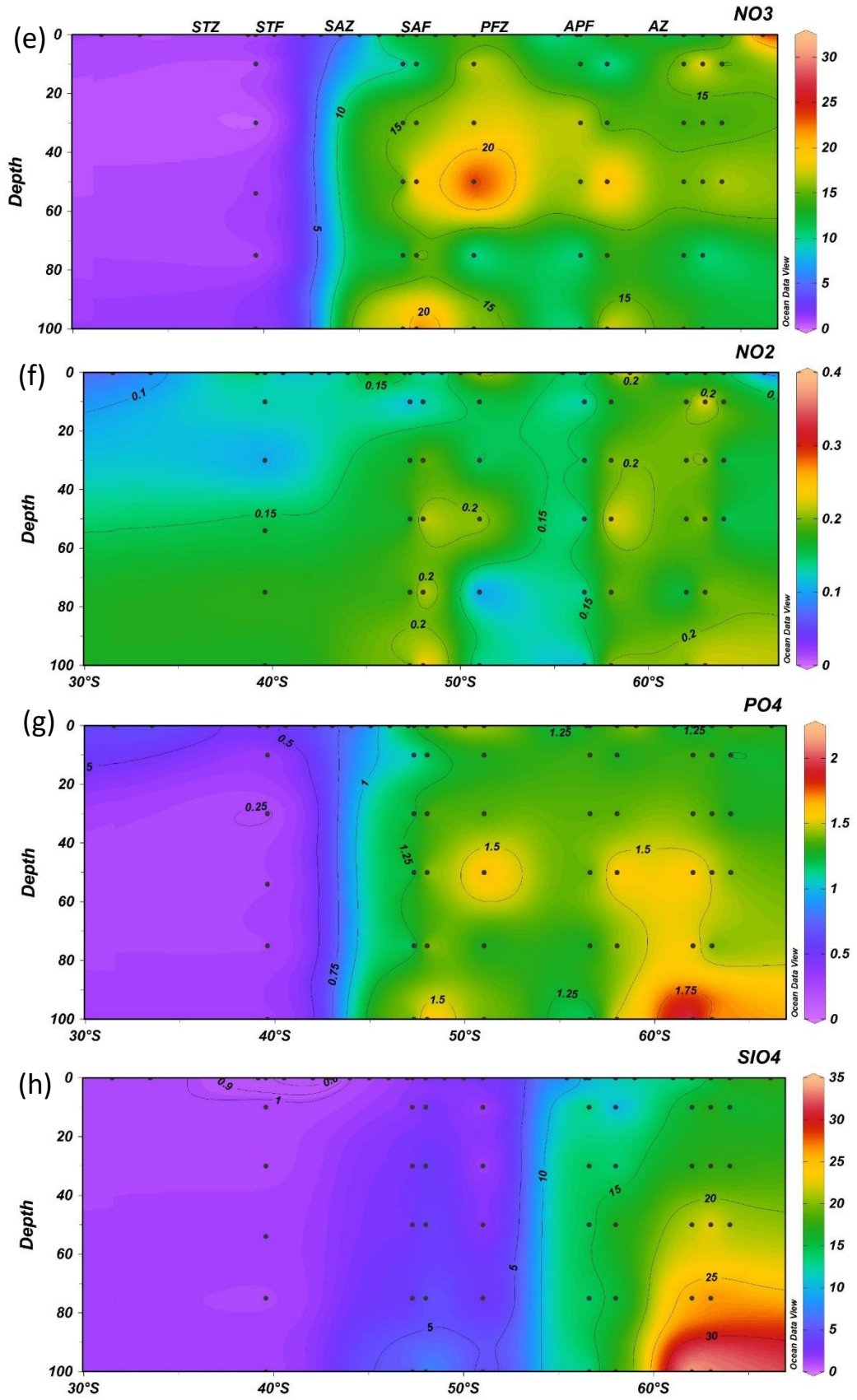

Figure 2. Physicochemical parameters recorded by CTD during the sample collection (a) Temperature (°C), (b) Salinity (PSU), (c) pH, (d) Fluorescence (Chlorophyll), (e) Nitrate (µM), (f) Nitrite (µM), (g) Phosphate (µM), (h) Silicate (µM)

4.3.2. Distribution of coccolithophore species

The most abundant species in surface and profile samples distributed across the Southern Ocean is *E. huxleyi* (92%) (consisting of four morphotypes *E. huxleyi* type A, *E. huxleyi* type B, *E. huxleyi* type B/C, *E. huxleyi* type C). Apart from *E. huxleyi*, other species were *Calcidiscus leptoporus* (2%), *Umbellosphaeraceae tenuis* (2%) *Syracosphaera* spp. (1.4%) *Michaelsarsia elegans* (1%), *Gephyrocapsa muellerae* (0.4%), *Acanthoica quattrospina* (0.2%), holococcoliths (0.4%), and other cumulative minor species across the Southern Ocean fronts (Table 1 and Table 2).

4.3.3. Distribution of *Emiliania huxleyi* morphotypes

Emiliania huxleyi is the most abundant coccolithophore species and contributed the most to the coccolithophore composition from 31.5°S to 59°S throughout the transect. The most common morphotype of this species is *E. huxleyi* type C, which is most abundant in the PFZ (0.2–297.2 × 10^4 coccospheres/L) and the STZ (0–256 × 10^4 coccospheres/L), whereas their abundance is reduced in the SAZ (0–154 × 10^4 coccospheres/L) and the AZ (0.5–168 × 10^4 coccospheres/L). In addition, deformed *E. huxleyi* was recorded throughout the transect, largely consisting of *E. huxleyi* type C. The highest abundance of this morphotype was recorded in the PFZ (0–65.1 × 10^4 coccospheres/L) followed by AZ (0–9.6 × 10^4 coccospheres/L), STZ (0–3.6 × 10^4 coccospheres/L), and the lowest was recorded in the SAZ (0–1.78 × 10^4 coccospheres/L).

Similar to *E. huxleyi* type C, *E. huxleyi* type B/C is present in all the zones, with the maximum abundance recorded in STZ (58 × 10^4 coccospheres/L) and the PFZ (0–36 × 10^4 coccospheres/L). Their abundance was lower in the AZ (0–12.2 × 10^4 coccospheres/L) and lowest in SAZ (0–5.2 × 10^4 coccospheres/L). *Emiliania huxleyi* type B was present mainly in

STZ (0–4.9 × 10^4 coccospheres/L) (Fig. 3). This morphotype is absent in the SAZ with sporadic occurrence in the south of SAF (0.4 × 10^4 coccospheres/L).

Emiliania huxleyi type A is largely restricted to the STZ (0.7–50 × 10^4 coccospheres/L). The occurrence of this species extended south of STF (1.8–4.1 × 10^4 coccospheres/L), with a sporadic presence in PFZ (0.2–4.2 × 10^4 coccospheres/L) (Fig. 3). The coccospheres of all the morphotypes were intact and morphotype A, especially compared to other morphotypes, was the most robust.

4.3.4. Distribution of coccolithophore assemblages other than *E. huxleyi* across the frontal zones

The coccolithophore assemblages based on their lateral surface and vertical depth distribution (0–100 m) are described across the different oceanic zones (Fig. 3). In the STZ, 54 heterococcolithophores species and 8 holococcolithophore species were recorded with an average total abundance of 128 × 10^4 coccospheres/L. The most common coccolithophore species in this zone were *Gephyrocapsa muellerae* (0–6.8× 10^4 coccospheres/L); *U. tenuis (U. tenuis* type I, type IIIb, type IV*)* (0–3.3 × 10^4 coccospheres/L); *M. elegans* (0–7.8× 10^4 coccospheres/L); *C. leptoporus*, including both *C. leptoporus* subsp. *leptoporus* and *C. leptoporus* subsp. small (0–3.9 × 10^4 coccospheres/L); *K. baumannii* (0–12.6 × 10^4 coccospheres/L); *S. pulchra* (0–2.9 × 10^4 coccospheres/L); *A. quattrospina* (0–5.5 × 10^4 coccospheres/L); and *Ophiaster hydroideus* (0–6.9 × 10^4 coccospheres/L). Sporadic occurrence of *Helicosphaera carteri* and *Rhabdosphaera clavigera* coccoliths was also observed.

Holococcolithophore abundance in the STZ ranged from 0.1–6.4 × 10^4 coccospheres/L, with *S. histrica* HOL making up the majority (0–6.4 × 10^4 coccospheres/L), followed by *H. carteri* HOL *catilliferus* type (0–2.2 coccospheres/L). Other holococcolithophores observed in

this zone were *Zygosphaera hellenica*, *H. carteri* HOL perforate, *C. leptoporus* subsp. *leptoporus* HOL, and *C. gracilis*.

In the SAZ, 19 species were recorded, with an average abundance of 88.1 × 10^4 coccospheres/L. The most common species were *C. leptoporus* subsp. small (0–22 × 10^4 coccospheres/L), *C. leptoporus* subsp. *leptoporus* (0–20.8 × 10^4 coccospheres/L), *S. halldalii* (0–2.5 × 10^4 coccospheres/L), and *M. elegans* (0–4.7 × 10^4 coccospheres/L). The assemblage in the SAZ also included *C. leptoporus* subsp. *leptoporus* HOL, *Syracosphaera* sp. HOL, and *C. pelagicus* subsp. *braarudii* HOL holococcolithophores.

In the PFZ, the average total abundance was 125 × 10^4 coccospheres/L, of which the most abundant was *E. huxleyi* type B/C, C, and deformed *E. huxleyi*. Other than *E. huxleyi*, *C. leptoporus* subsp. small, *Balaniger virgulosa*, and *K. baumanii* were distributed sporadically in the north of the PFZ. The AZ consisted only of *E. huxleyi* type B/C, C, and deformed with no other species present with an average total abundance of 52 × 10^4 coccospheres/L.

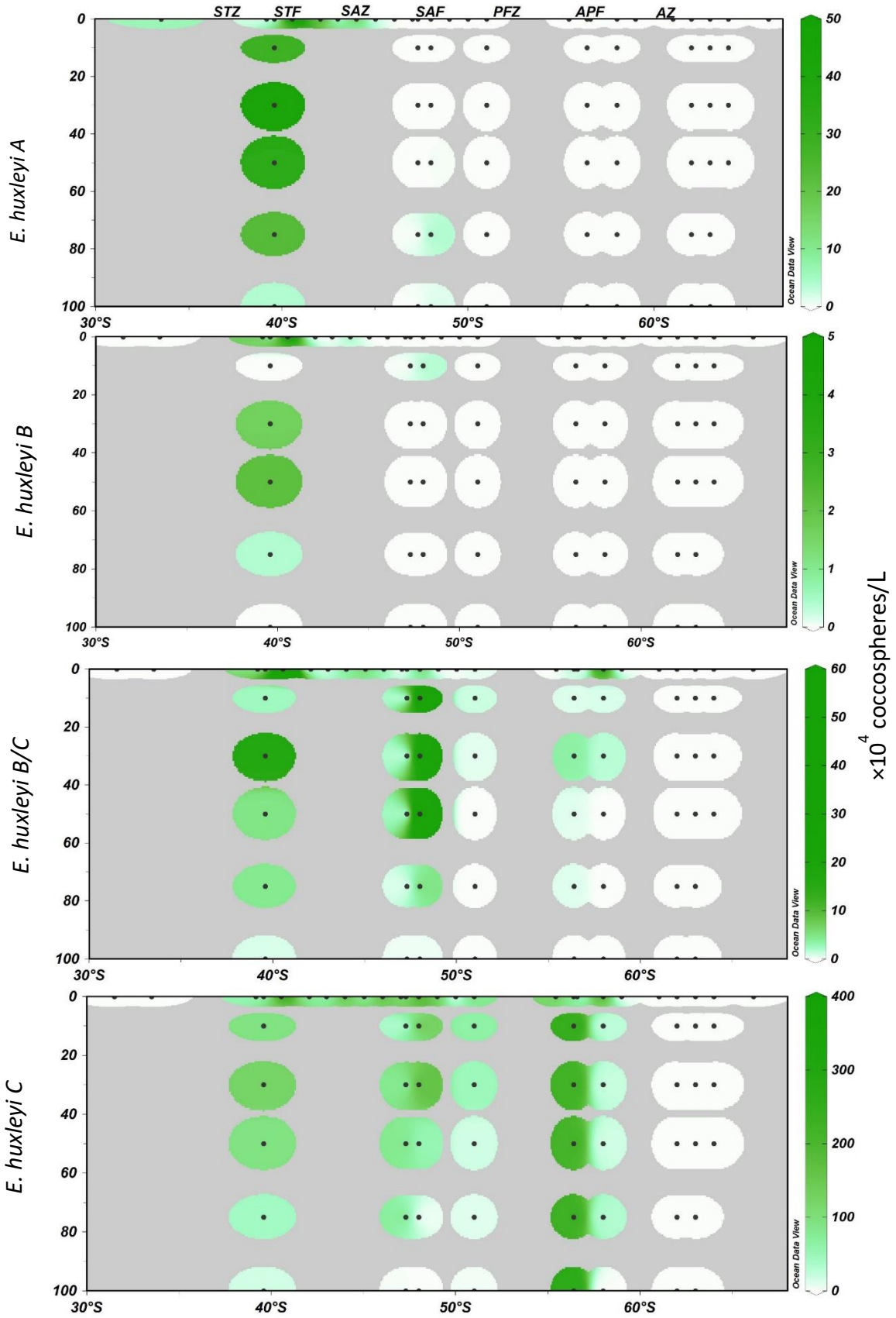
STZ
STF
SAZ
SAF
PFZ
APF
AZ
E. huxleyi A
E. huxleyi B
E. huxleyi B/C
E. huxleyi C
30°S
40°S
50°S
60°S
Ocean Data View
×10^4 coccospheres/L

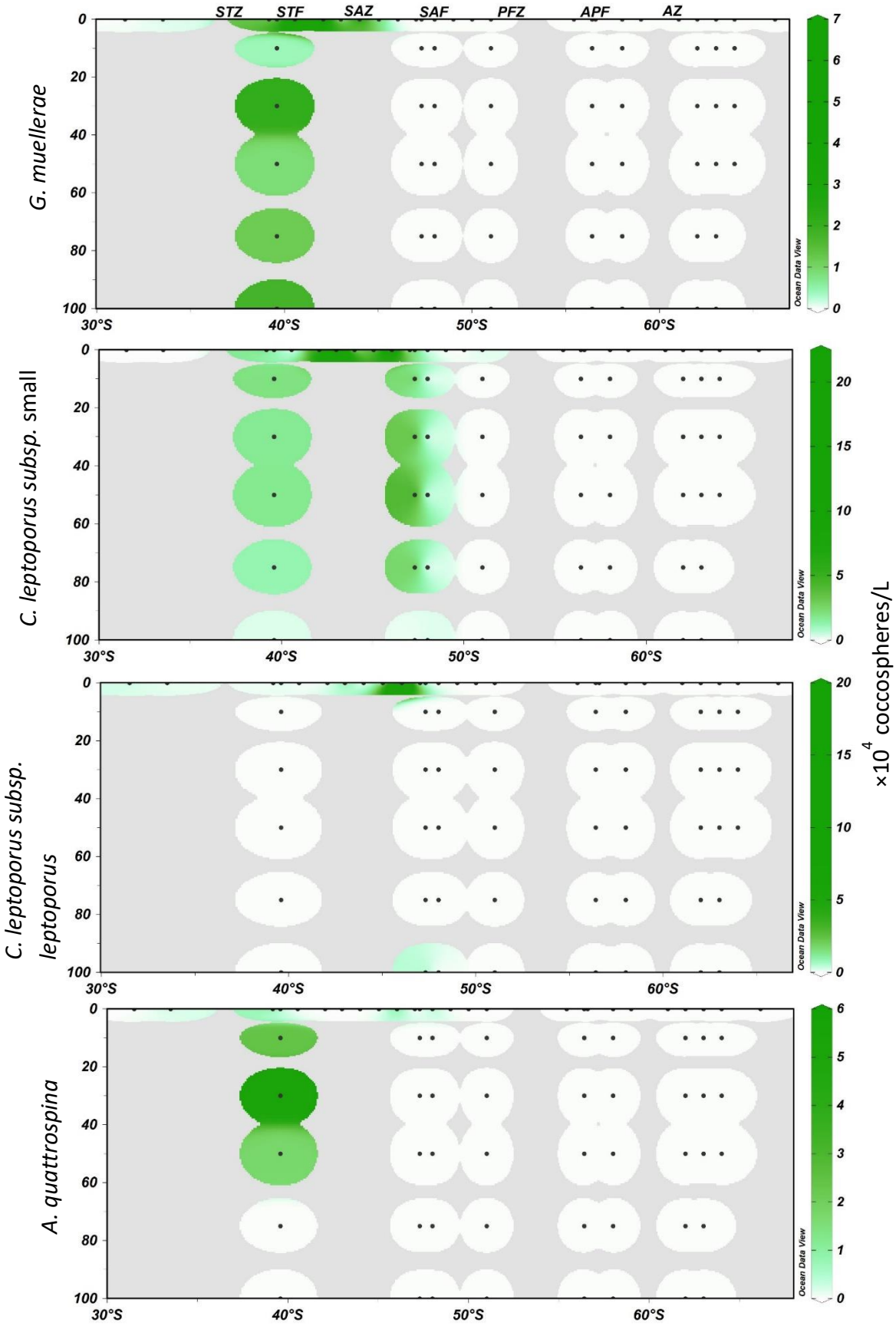
STZ
STF
SAZ
SAF
PFZ
APF
AZ
G. muellerae
C. leptoporus subsp. small
C. leptoporus subsp. leptoporus
A. quattrospina
30°S
40°S
50°S
60°S
Ocean Data View
×10^4 coccospheres/L

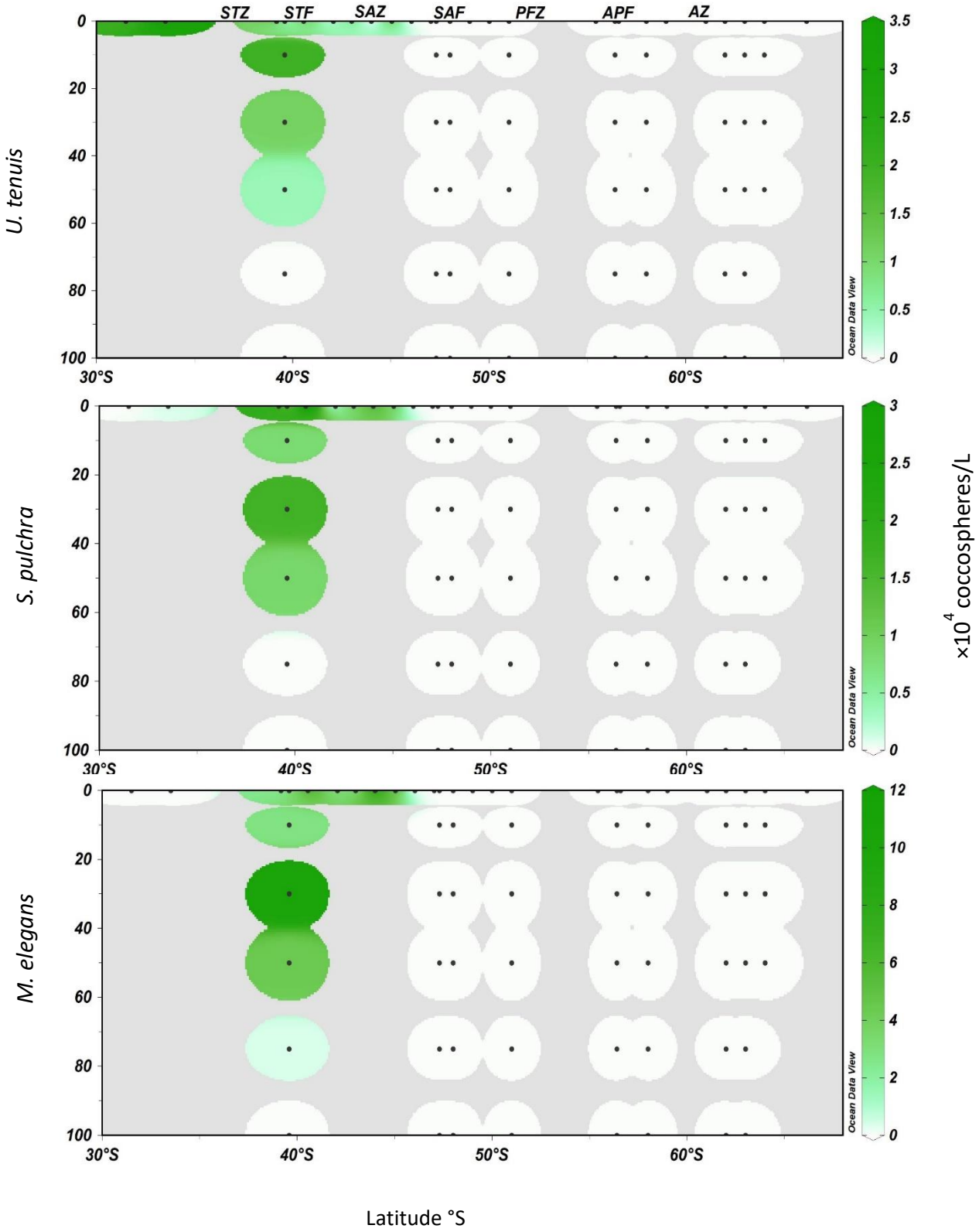
STZ
STF
SAZ
SAF
PFZ
APF
AZ
U. tenuis
S. pulchra
M. elegans
0
20
40
60
80
100
30°S
40°S
50°S
60°S
3.5
3
2.5
2
1.5
1
0.5
0
12
10
8
6
4
Ocean Data View
×10^4 coccospheres/L
Latitude °S

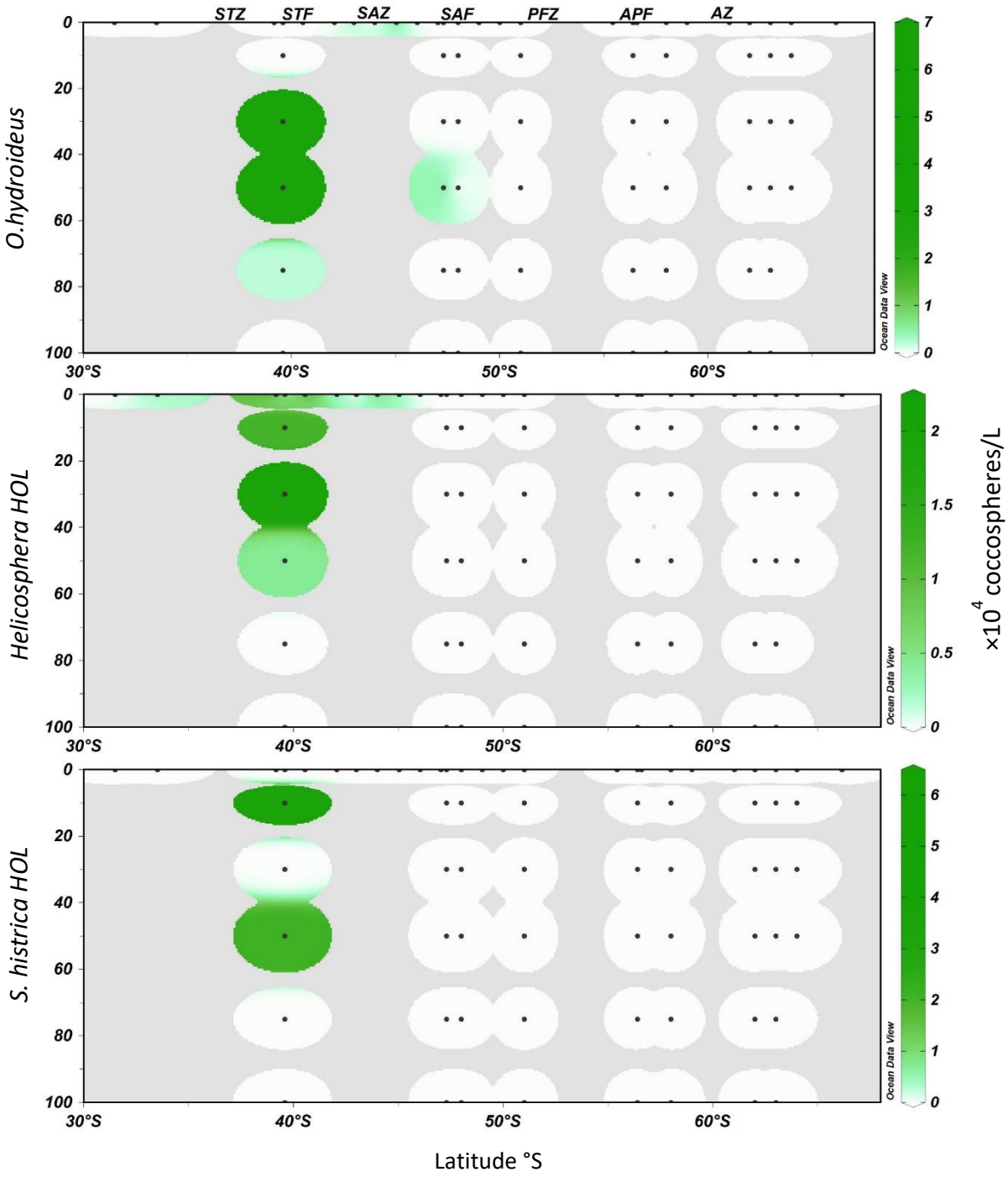

Figure 3. Abundance and distribution of major coccolithophore species recorded between surface and 100 m water depth along the transect.

Table 1. Location of water samples collected and total coccolithophore abundance

Stations and total abundance				
Station	**Depth (m)**	**Latitude (°S)**	**Longitude (°E)**	**Coccospheres × 10^4/L**
Surface 50	0	-31.5	57.56	3
Surface 4	0	-33.51	58.09	13
Surface 44	0	-39.17	58.27	86
Profile 1	0	-39.59	57.29	50
	10			167
	30			229
	50			178
	75			78
	100			25
Surface 10	0	-40.55	59.02	400
Surface 11	0	-42.06	59.57	115
Surface 12	0	-43	60.35	92
Surface 13	0	-44	61.23	191
Surface 14	0	-45.03	62.09	96
Surface 15	0	-46.04	62.55	195
Profile 21	0	-47.3	57.3	62
	10			31
	30			80
	50			92
	75			79
	100			5.0
Surface 16	0	-47.02	63.41	144
Surface 37	0	-48	57.3	95
Profile 2	0	-48	64.28	308

	10			166
	30			236
	50			90
	75			73
	100			22
Surface 36	0	-49	57.3	123
Surface 17	0	-50	64.37	6
Profile 20	0	-51	57.3	69
	10			64
	30			48
	50			17
	75			11
	100			5
Surface 18	0	-51	63.22	161
Surface 22	0	-55.42	69.45	127
Profile 19	0	-56.59	57.32	113
	10			254
	30			228
	50			216
	75			231
	100			277
Surface 23	0	-56.4	69.06	30
Profile 4	0	-58	70.04	182
	10			35
	30			32
	50			18
	75			41
	100			3
Surface 24	0	-59	70.04	0
Surface 26	0	-61.02	71.08	0

Profile 18	0	-62	57.3	0
	10			0
	30			0
	50			0
	75			0
	100			0
Profile 5	0	-63	70.19	0
	10			0
	30			0
	50			0
	75			0
	100			0
Profile 17	0	-64	57.3	0
	10			0
	30			0
	50			0
Surface 28	0	-64	70.35	0
Surface 30	0	-66.15	74.43	0

4.3.5. Coccolithophore and its relation with the environmental parameters

To elucidate the relationship between coccolithophore assemblages and environmental parameters, canonical correspondence analysis (CCA) (Fig. 4a, b) and Pearson correlation (Fig. 5, 6) were carried out using Past version 4.03 (Hammer et al., 2001) and RStudio version 4.2 (RStudio Team, 2020) respectively.

Based on coccolithophore abundance data, the CCA explained 75.54% and 91.2% of the variance within the Surface and Profile sample dataset (cumulative percentage variance of species data, first two CCA axes), respectively (Fig. 4).

In surface water *E. huxleyi* type A, B, and B/C, *Gephyrocapsa muellerae*, *Umbellosphaeraceae tenuis* type II, *Umbilicosphaera foliosa*, *Umbilicosphaera sibogae*, *Umbilicosphaera hulburtiana*, *Syracosphaera azureaplaneta*, *Syracosphaera prolongata*, *Syracosphaera anthos*, *Syracosphaera ossa*, *Syracosphaera pulchra*, *Syracosphaera tumularis*, *Syracosphaera bannocki*, *Syracosphaera histrica*, *Syracosphaera nana*, *Syracosphaera mediterranea*, *Oolithotus fragilis*, *Alisphaera spatula*, *Alisphaera unicornis*, *Alisphaera biscayensis*, *Alisphaera ordinate*, *Acanthoica quattrospina*, *Michaelsarsia elegans*, *Calciosolenia corsellii*, *Discosphaera tubifera*, *Kataspinifera baumanii*, Holococcolithophore *Calcidiscus leptoporus* subsp. *leptoporus* HOL showed affinity towards elevated temperature, salinity, pH, and low nutrient (NO_2, PO_4, NO_3, and SiO_4) concentrations. However, *E. huxleyi* type C, *Ophiaster hydroideus*, *Calcidiscus leptoporus* subsp. *leptoporus*, *Syracosphaera noroitica*, *Algirosphaera cucullata*, *Algirosphaera robusta*, and Holococcolithophore *Coccolithus pelagicus* subsp. *braarudii* HOL showed affinity towards higher concentrations of NO_2, PO_4, NO_3, and SiO_4. Whereas, no relation was observed between *E. huxleyi* deformed, *Umbellosphaera tenuis* type IIIb, type IV, and *Syracosphaera molischii* III, IV, and the environmental parameters.

In the Profile samples, *E. huxleyi* morphotype type A and B, *C. leptoporus*, *G. muellerae*, *G. ericsonii*, *Calcidiscus leptoporus* subsp. small, *C. leptoporus* subsp. *leptoporus*, *U. tenuis* type II, *U. foliosa*, *U. sibogae*, *U. hulburtiana*, *S. ossa*, *S. anthos*, *S. tumularis*, *Syracosphaera nodosa*, *S. molischii*, *Syracosphaera carolla*, *S. azureaplaneta*, *S. histrica*, *S. nana*, *S. pulchra*, *Syracosphaera pemmadiscus*, *S. bannocki*, *O. hydroideus*, *M. elegans*,

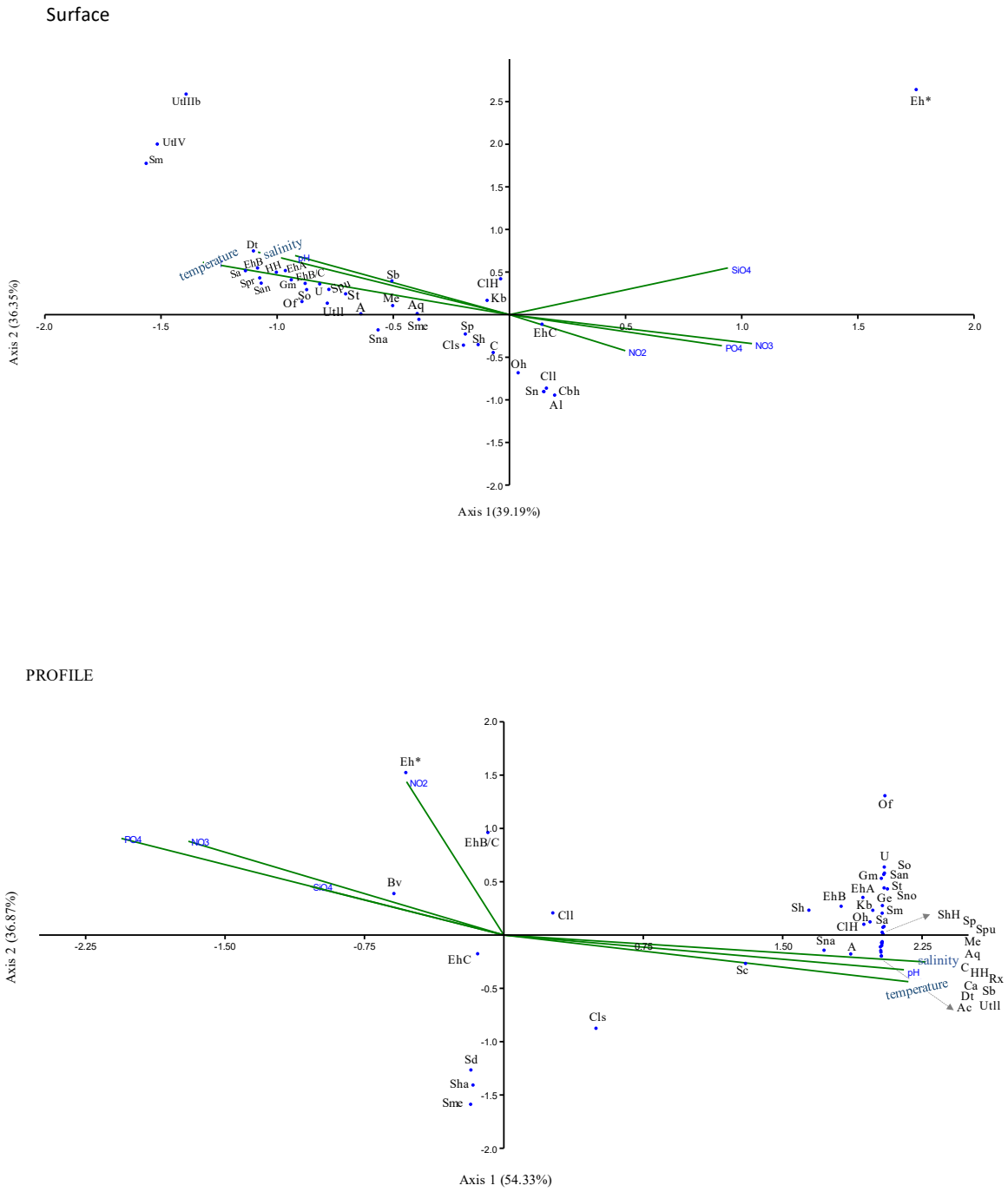

Figure 4. Canonical corresponding analysis (CCA) ordination diagram for coccolithophore community structure and environmental variables (temperature, salinity, NO_2, NO_3, PO_4, SIO_4) (a) surface samples (b) profile samples (0–100 m depth). Abbreviations for each group are provided in Table 2.

A. quattrospina, *Acanthoica cidaris*, *Calciosolenia brasiliensis*, *Calciosolenia subtropicus*, *C. corsellii*, *Cyrtosphaera aculeata*, *D. tubifera*, *R. xiphos*, *K. baumanii*, and

holococcolithophores such as *C. leptoporus* subsp. *leptoporus* HOL, *S. histrica* HOL, *H. carteri* HOL perforate, *H. carteri* HOL perforate, *H.* HOL *catilliferus* type, showed affinity towards increased temperature, pH, salinity, and low nutrient conditions. However, *E. huxleyi* type C, *E. huxleyi* type B/C, and deformed species showed a preference towards PO_4 and NO_2 respectively. *Balaniger virgulosa* showed an affinity towards NO_3. *Syracosphaera dilatata*, *Syracosphaera halldalii*, and *Syracosphaera mediterranea* did not exhibit any association with the parameters.

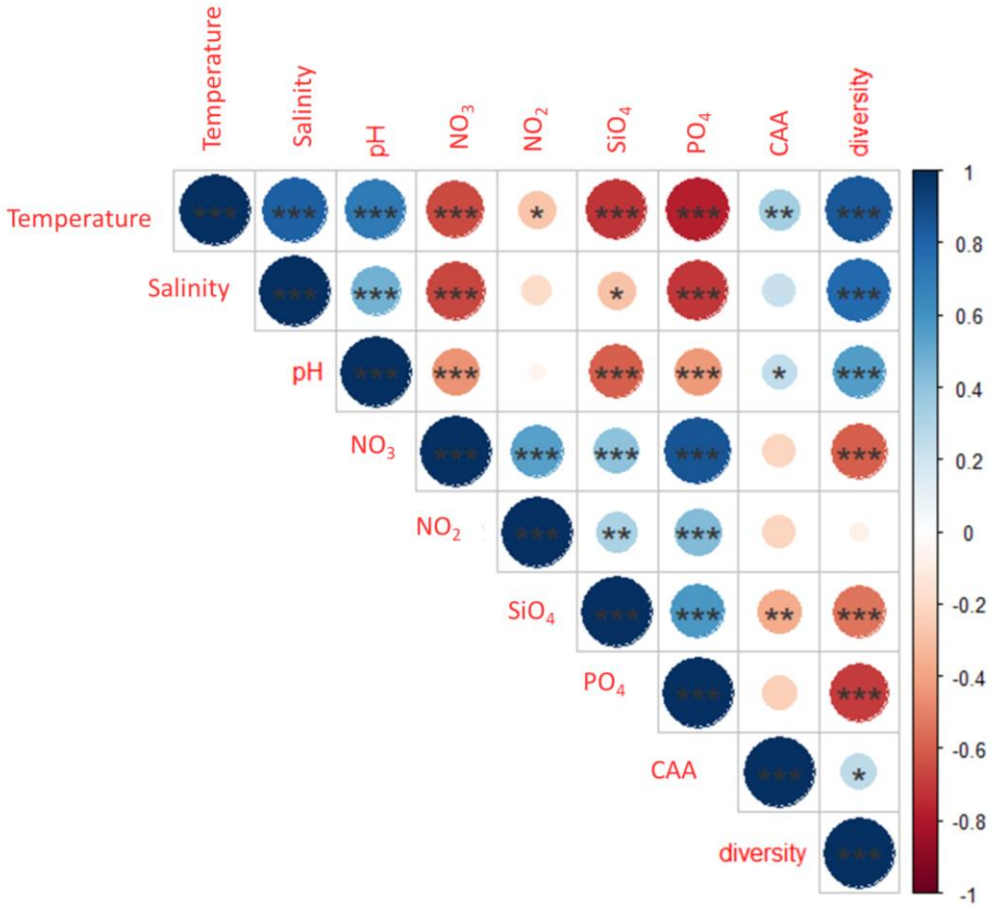

Figure 5. Correlation matrix diagram (Pearson's Correlation analysis). Parameters used are environmental variables, Coccolithophore absolute abundance (CAA), and diversity. The colored bar indicates blue as positive correlations and red as negative correlations. The size of the dots in the diagram indicates the strength of the correlation. Correlations with $p > 0.05$ were left blank.

Pearson correlation analysis revealed a positive correlation between diversity and temperature ($r = 0.85$, $p < 0.001$), Salinity ($r = 0.78$, $p < 0.001$), and pH ($r = 0.56$, $p < 0.001$),

respectively. However, total coccolithophore absolute abundance (CAA) showed a weak correlation with temperature ($r = 0.33$, $p < 0.01$), salinity ($r = 0.22$, $p = 0$), and pH ($r = 0.25$, $p < 0.05$). In contrast, an inverse correlation was observed between diversity and nutrients, specifically, NO_3 ($r = -0.06$, $p < 0.001$), NO_2 ($r = -0.08$, $p = 0$), SiO_4 ($r = -0.54$, $p < 0.001$), and PO_4 ($r = -0.69$, $p < 0.001$). The CAA exhibited a weak correlation with nutrients NO_3 ($r = -0.22$, $p = 0$), NO_2 ($r = -0.21$, $p = 0$), SiO_4 ($r = -0.36$, $p < 0.01$), PO_4 ($r = -0.23$, $p < 0.001$) (Fig. 5). It is evident that most of the species (Fig. 6, 7a, b) are positively correlated to elevated temperature, salinity, and pH; and inversely correlated to nutrients. This indicates the preference of coccolithophores for high temperatures and low nutrients. Based on the Bray–Curtis similarity index and heat map between the species (Fig. 7a, b, c), the coccolithophore species can be divided into four assemblage groups, namely, the STZ, SAZ, PFZ, and STZ-PFZ. The STZ-PFZ group shows the formation of a cluster with 25% similarity. The STZ group shows the cluster among the species most abundant only in STZ forming 30% similarity, SAZ group shows 20% similarity. Besides, *E. huxleyi* type C shows very low similarity with other species, and this species exclusively inhabits the PFZ.

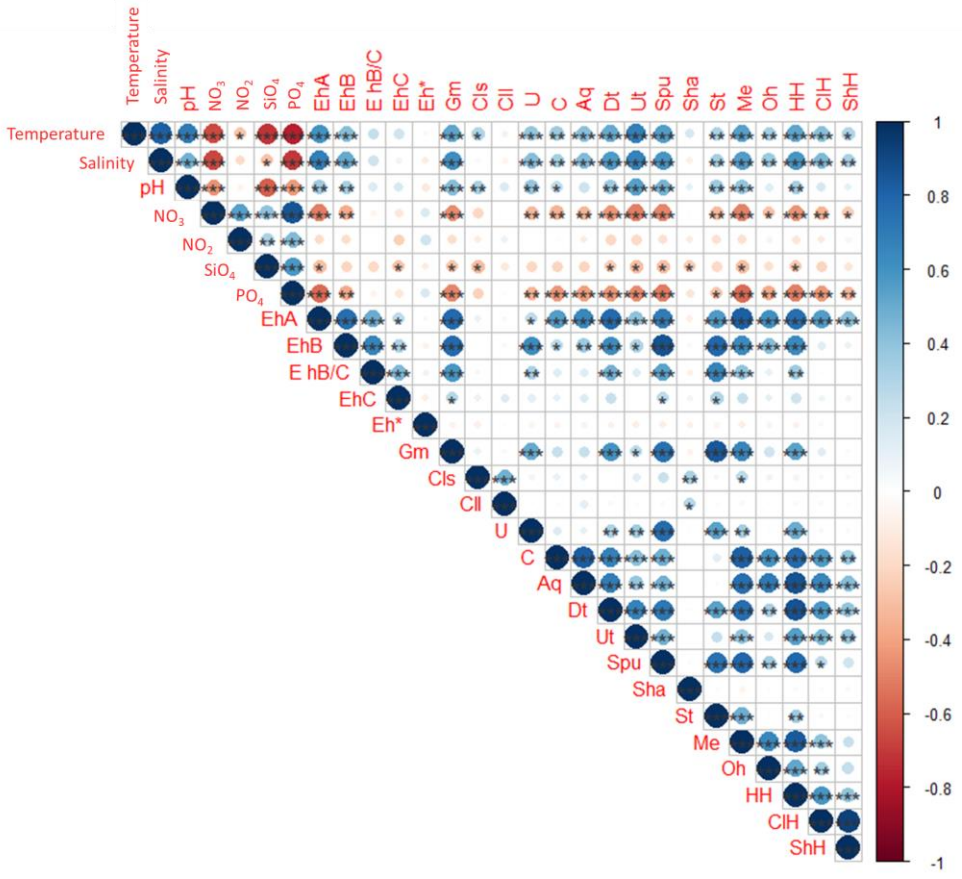

Figure 6. Correlation matrix diagram (Pearson's correlation analysis). Parameters used are environmental variables and major coccolithophore species abundance. The colored bar indicates blue as positive correlations and red as negative correlations. The size of the dots in the diagram indicates the strength of the correlation. Correlations with $p > 0.05$ were left blank. Abbreviations for each group are provided in Table 2.

Table 2. Coccolithophore species distribution and abbreviation used in the study

Species	Abbreviation	STZ	STF-SAZ	SAF-PFZ	APF-AZ
Emiliania huxleyi A	EhA	+	-	+	-
Emiliania huxleyi B	EhB	+	-	+	-
Emiliania huxleyi B/C	EhB/C	+	+	+	+
Emiliania huxleyi C	EhC	+	+	+	+
Emiliania huxleyi deformed	Eh*	+	+	+	+
Gephyrocapsa ericsonii	Ge	+	-	-	-

Gephyrocapsa muellerae	Gm	+	+	-	-
Calcidiscus leptoporus small	Cls	+	+	+	-
Calcidiscus leptoporus subsp. *leptoporus*	Cll	+	+	-	-
Oolithotus fragilis	Of	+	+	-	-
Umbilicosphaera foliosa	U	+	-	-	-
Umbilicosphaera sibogae		+	-	-	-
Umbilicosphaera hulburtiana		+	+	-	-
Calciosolenia brasiliensis	C	+	-	-	-
Calciosolenia subtropicus		+	-	-	-
Calciosolenia corsellii		+	+	-	-
Acanthoica quattrospina	Aq	+	+	-	-
Acanthoica cidaris	Ac	+	-	-	-
Acanthoica acanthos^{+}	Aa	+	-	-	-
Algirosphaera cucullate	Al	-	+	-	-
Algirosphaera robusta		-	+	-	-
Discosphaera tubifera	Dt	+	+	-	-
Rhabdosphaera xiphos	Rx	+	-	-	-
Alisphaera spatula	A	+	+	-	-
Alisphaera unicornis		+	+	-	-
Alisphaera biscayensis		+	-	-	-
Alisphaera ordinata		+	-	-	-
Alisphaera gaudii		-	+	-	-
Canistrolithus valliformis Pol^{+}	Cav	-	+	-	-
Umbellosphaera tenuis type II	UtII	+	+	-	-

Umbellosphaera tenuis type IIIb	UtIIIb	+	-	-	-
Umbellosphaeraceae tenuis type IV	UtIV	+	-	-	-
Syracosphaera pemmadiscus	Sp	+	-	-	-
Syracosphaera dilatata	Sd	-	+	-	-
Syracosphaera azureaplaneta	Sa	+	-	-	-
Syracosphaera carolla^{+}	Sc	+	+	-	-
Syracosphaera noroitica	Sn	-	+	-	-
Syracosphaera prolongata	Spr	+	+	-	-
Syracosphaera histrica	Sh	+	+	-	-
Syracosphaera pulchra	Spu	+	+	-	-
Syracosphaera halldalii	Sha	+	+	-	-
Syracosphaera molischii type I	Sm	+	-	-	-
Syracosphaera molischii type III		+	-	-	-
Syracosphaera molischii type IV		+	-	-	-
Syracosphaera rotula^{+}	Sr	+	-	-	-
Syracosphaera ossa type I	So	+	-	-	-
Syracosphaera ossa type II		+	+	-	-
Syracosphaera anthos	San	+	-	-	-
Syracosphaera tumularis	St	+	+	-	-
Syracosphaera nana	Sna	+	+	-	-
Syracosphaera nodosa type A^{+}	SnA	-	+	-	-
Syracosphaera nodosa	Sno	+	-	-	-
Syracosphaera bannocki	Sb	+	+	-	-

Syracosphaera mediterranea	Sme	+	+	-	-
Syracosphaera didyma^{+}	Sdi	-	+	-	-
Syracosphaera sp. ui^{+}	Sui	+	-	-	-
Michaelsarsia elegans	Me	+	+	-	-
Ophiaster hydroideus	Oh	+	+	-	-
Reticulofenestra parvula	Rp	+	-	-	-
Cyrtosphaera aculeata	Ca	+	-	-	-
C. cristatus CER *rostratus* type+hoops^{+}	Crh	+	-	-	-
Papposphaera sagittifera^{+}	Ps	+	-	-	-
Papposphaera sp. like^{+}	Pa	+	-	-	-
Balaniger virgulosa	Bv	-	-	+	-
Kataspinifera baumanii	Kb	+	+	+	-
*Polycrate*r sp. ladle like^{+}	P	-	+	-	-
Zygosphaera hellenica	Zh	+	-	-	-
Helicosphera carteri HOL *perforate*	HH	+	-	-	-
Helicosphaera HOL *catilliferus* type		+	+	-	-
Calcidiscus leptoporus subsp. *leptoporus* HOL	ClH	+	+	-	-
Syracosphera histrica HOL	ShH	+	-	-	-
Corisphaera gracilis^{+}	Cg	+	+	-	-
Syracosphaera sp. HOL	SH	-	+	-	-
Coccolithus pelagicus spp *braarudii* HOL	CbH	-	+	-	-
Holoccolith Ui^{+}	Hui	+	-	-	-

Superscripted + in the species column indicates that a species was not included in the CCA and Pearson correlation analysis.

4.4. Discussion

4.4.1. Coccolithophore abundance and diversity in the southern Indian Ocean and comparison with other sectors of the Southern Ocean

The diversity and distribution pattern of coccolithophore species varies across the fronts enclosing the different zones. From the STZ to the AZ, coccolithophore diversity decreased from a maximum in the STZ (temperature, 15–20 ℃) to a minimum in the northern AZ (temperature, 0.4–1.5 ℃) which consisted of a monospecific assemblage of *E. huxleyi*. In the south of the AZ (temperature, −1.6–1 ℃), there is a complete absence of coccolithophores. A similar trend was observed in the Southern Indian Ocean (Mohan et al., 2008; Patil et al., 2017), South Atlantic (Eynaud et al., 1999), and Pacific sector of the Southern Ocean (Saavedra-Pellitero et al., 2014; Malinverno et al., 2015). A previous study has suggested that coccolithophore production is inhibited at temperatures lower than 2 °C (Findlay and Giraudeau, 2000).

Like in other sectors of the Southern Ocean, along the transect observed in this study, coccolithophore abundance and composition were dominated by *E. huxleyi* (Verbeek, 1989; Eynaud et al., 1999; Saavedra-Pellitero et al., 2014; Malinverno et al., 2015). In this study, the coccolithophore absolute abundance (CAA) was highest in the surface waters of the STZ (400 $\times 10^4$ cells/L) and the PFZ (308 $\times$ 10^4 cells/L) from December 2017–February 2018 (early to mid-austral summer. Likewise, Mohan et al. (2008) also recorded higher coccolithophore abundance in the north of the STF (~450 $\times$ 10^4 cells/L) during January–March 2004 (mid-late austral summer), Higher abundance in SAZ during mid-austral summer (742 $\times$ 10^3 coccospheres/L) and early- to mid-austral summer (2203 $\times$ 10^3 coccospheres/L) was recorded and attributed to the elevated abundance of *E. huxleyi* which is regulated by environmental factors such as an increase in nutrients (Patil et al., 2020). Findlay and Giraudeau (2000)

recorded the highest abundance in the north of the SAF (~500 × 10^3 cells/L) and the STF (208 × 10^3 cells/L) in January 1994 and February 1995, respectively (from early to mid-austral summer).

In the Pacific sector, higher abundances were found at the STF (552 × 10^3 cells/L), followed by SAF (493 × 10^3 cells/L), and the PF (312 × 10^3 cells/L) by Gravalosa et al. (2008) in February–April (late austral summer). Malinverno et al. (2015) recorded the highest abundance (~137 × 10^3 cells/L) in the STF and lower values in the SAZ from 1–5th January (early austral summer). Saavedra-Pellitero et al. (2014) recorded a higher abundance of coccolithophores at 20 m depth (642 × 10^3 cells/L) close to STF from 27th November 2009–27th January 2010 (early austral summer). In the Atlantic sector, Eynaud et al. (1999) recorded the highest abundance (493 × 10^3 cells/L) south of the PF in February (Late austral summer).

According to these studies, factors affecting the coccolithophore distribution and diversity showed a positive correlation between temperature, salinity, and inverse correlation with nutrients (Fig. 7c). Higher diversity and abundance were observed under the conditions of high temperatures and low nutrient concentrations in the STZ and SAZ. Higher abundance was also recorded in the high nutrient zones south of SAZ and PFZ mainly consisting of single species *E. huxleyi* type C. It appears that coccolithophore total abundance was recorded highest in STZ in most studies however, Patil et al., (2020) recorded coccolithophore abundance highest in SAZ during early to mid-austral summer. One possible explanation of this discrepancy could be due to variations in availability of micronutrients as a result of seasonal changes in the depth of mixed layer depth in the frontal zones. Deepening of mixed layered depth in the winter brings micronutrients into the euphotic zone which are not utilised during winter as a result of low light levels (Tagliabue et al., 2014). Additionally, these nutrients help in the summer blooms (Prakash et al., 2020).

However, in this study, higher temperatures, salinity, pH, moderate concentration of NO_2 and PO_4, and low concentrations of NO_3 and SIO_4 were responsible for higher abundance and diversity in the STZ (Mohan et al., 2008; Patil et al 2017,2020). In the PFZ, low temperatures, salinity, pH, high concentrations of NO_2 and PO_4, and moderate concentrations of NO_3 and SIO_4 were responsible for high abundance and low diversity. In general, the trend of coccolithophore density diversity and distribution in the Southern Indian Ocean correlated with latitudinal gradients in temperature, salinity, pH, and light levels across the calcite belt (40–60°S) and anti-correlated with nutrient concentrations and silicate belt (below 60°S) (Paasche, 2002; Boyd et al., 2010; Charalampopoulou et al., 2011; Balch et al., 2016; Nissen et al., 2018). Grazing pressure could be a possible explanation for low coccolithophore abundance in the SAZ in this study though zooplankton data was not quantified in this study, the occurrence of tintinnids with agglutinated *C. leptoporus* coccoliths in SAZ and *E. huxleyi* coccoliths in PFZ (Chapter 3, Section 3.4) indicates the possibility of grazing pressure in regulating the coccolithophore abundance (Malinverno et al., 2015).

Temporal variation of coccolithophores is primarily governed by changes in light intensity, physicochemical properties, and nutrients. High coccolithophore abundance and diversity during early to mid-austral summer was attributed to enriched nutrient conditions, high light intensity, moderate temperature, salinity, and reduced silicate concentrations (Patil et al., 2020). Decreased coccolithophore diversity and abundance during the late summer was attributed to possible uneven nutrient ratios, unavailability of trace elements, and increased heterotrophs grazing pressure (Patil et al., 2013). During the mid -to late austral summer, in the Indian sector of the Southern Ocean, based on trophic efficiency, grazing pressure on the phytoplankton communities was reported (Kerkar et al., 2022) In late summer, grazing rates by mesozooplankton exhibited significant impact on phytoplankton primary production in the Indian sector of Southern Ocean (Mayzaud et al., 2002). Based on particulate organic carbon,

and pigment analysis high grazing exertion on phytoplankton was reported in the eastern Weddell Sea during the transition from late autumn to winter (Krell et al., 2005).

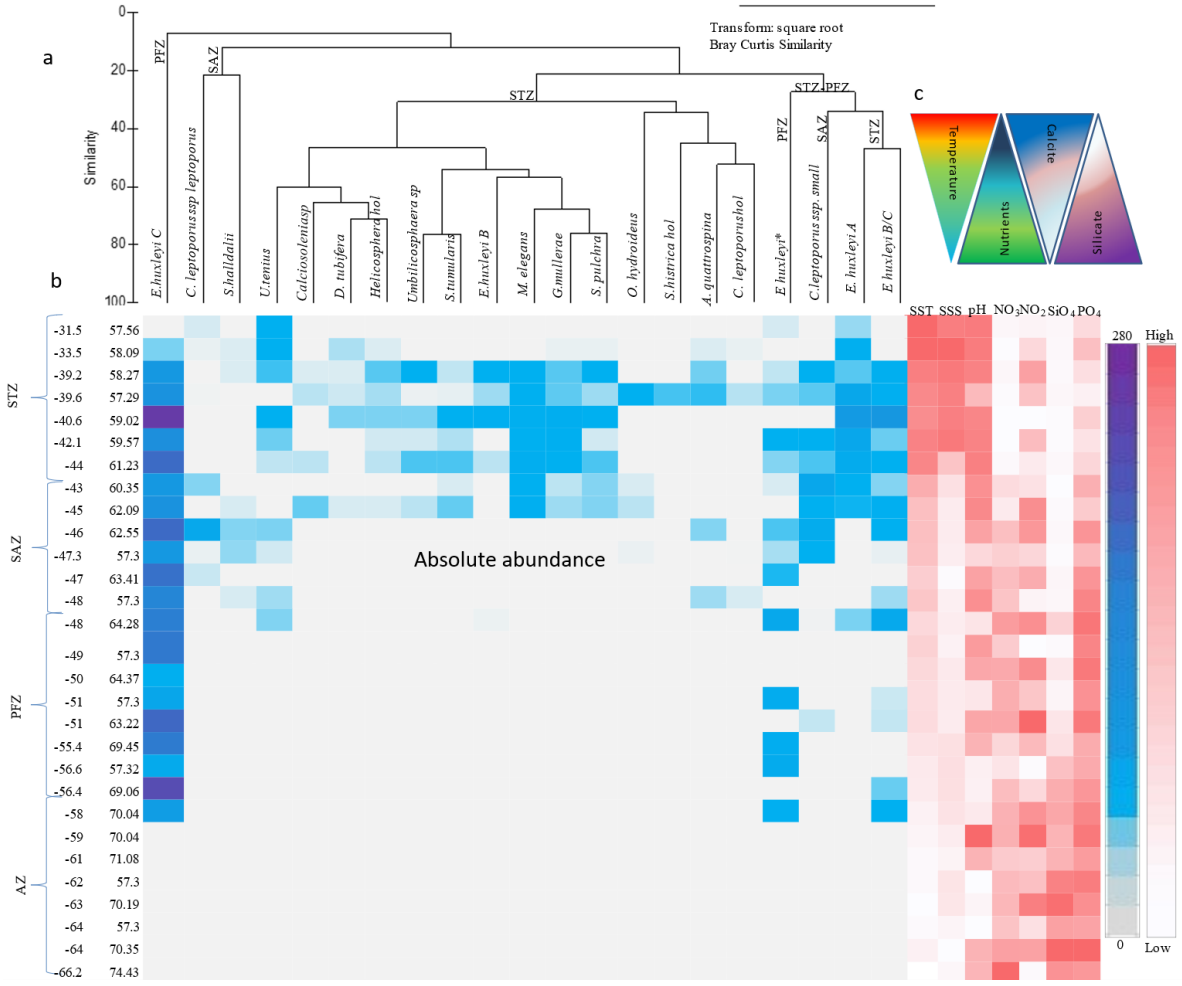

Figure 7. (a) Dendrogram produced by cluster analysis based on Bray–Curtis similarity index. (b) Heat map with latitude and longitude at the left, blue shade indicates the abundance of the species ($\times 10^4$ coccospheres/L) in the respective zones, red shade represents physicochemical parameters (c) general representation of temperature, nutrients, calcite, and silicate distribution in the Southern Ocean.

4.4.2. Factors affecting the coccolithophore species distribution across the frontal zones

The coccolithophore species distribution and composition suggest that the highest diversity is observed in the STZ, whereas the AZ had the lowest diversity and is characterized by the monospecific assemblage of coccolithophores. Based on the similarity index and correlation

with physicochemical parameters of frontal zones coccolithophores distribution can be classified into different assemblages.

Subtropical Zone assemblage

The subtropical composition exhibited the maximum coccolithophore diversity between ARF and STF, showing affinity to the region with warm, relatively saline, low nutrient, and higher alkaline waters. The most abundant species was *E. huxleyi*, comprising different morphotypes viz. *E. huxleyi* morphotype A, B, C, B/C, var. corona, morphotype 'O' (Young et al., 2003; Hagino et al., 2011). However, the distribution of morphotypes varies with the frontal zones (Okada and Honjo, 1973; Findlay and Giraudeau, 2000; Gravalosa et al., 2008; Mohan et al., 2008; Beaufort et al., 2011; Hagino et al., 2011; Henderiks et al., 2012; Saavedra-Pellitero et al., 2014; Patil et al., 2017, 2020: Malinverno et al., 2015).

The *E. huxleyi* type C and B/C morphotypes were consistently present throughout the transect, exhibiting tolerance to a wide range of environmental conditions. These morphotypes were most abundant in the STZ and SAZ. *Emiliania huxleyi* type B and A were also abundant, and primarily restricted to STZ and north of SAZ, thriving in warm, high saline, low nutrient conditions (Fig 7a, b). This agrees with the findings of previous studies by Hiramatsu and De Deckker (1996), Findlay and Giraudeau (2000), Mohan et al. (2008), and Patil et al. (2017, 2020). Likewise, in the Pacific sector of the Southern Ocean, *E. huxleyi* type A was observed to be restricted to the west and north of the SAZ (Saavedra-Pellitero et al., 2014; Malinverno et al., 2015, 2016). While, the deformed *E. huxleyi* (mostly belonging to type B/C and C) were highly abundant in the polar frontal waters (Malinverno et al., 2005; Mohan et al., 2008).

Gephyrocapsa muellerae was abundant in the STZ and north of the SAZ within a temperature range of 8–20 ℃ and was absent beyond 45°S, exhibiting a preference towards low nutrient concentrations and elevated temperatures relative to the south of the SAZ and PFZ (Fig. 3, 6). Similar observations were made in the Southern Indian Ocean (Patil et al. 2017, 2020) and the

Australian sector of the Southern Ocean (Findlay and Giraudeau, 2000). However, low abundance at the STF and relatively higher abundance in plankton and surface sediment of SAZ and PFZ were recorded in the Pacific sector of the Southern Ocean (Saavedra-Pellitero et al., 2014; Saavedra-Pellitero and Baumann, 2015). The studies by Vollmar et al. (2021) recorded this species south of the PF as far as 62°S, however, sediment records reflect data pertaining to long periods of time as opposed to a single season. This indicates that the species prefer cold and nutrient-rich water and is being used as a cold-water proxy for palaeoceanographic studies (Winter and Siesser, 1994; Winter et al., 1999; Findlay and Flores, 2000; Ziveriet al., 2004). The discrepancy in the distribution of this species between the Indian sector and other sectors of the Southern Ocean could be a combination of the wider temperature tolerance of the species and differences in the regional settings of these studies.

Calcidiscus leptoporus subsp. *leptoporus* was abundant in SAZ and rarely present in the STZ whereas *C. leptoporus subsp.* small was abundant in the SAZ and STZ. In previous studies, the presence of *C. leptoporus* was recorded south of the SAF (PFZ) in the Indian sector of the Southern Ocean (Mohan et al., 2008) and dominant poleward to the STF (SAZ) in the Australian sector of the Southern Ocean (Nishida, 1986; Findlay and Giraudeau, 2000). Further Higher abundance of *C. leptoporus* in the surface sediment of SAZ in the Drake Passage was recorded (Vollmar et al., 2021). In the Pacific sector of the Southern Ocean, *C. leptoporus* subsp. *leptoporus* was abundant in the SAZ and was also recorded in PF regions (Gravalosa et al., 2008; Saavedra-Pellitero et al., 2014; Malinverno et al., 2015). The occurrence of *C. leptoporus/ C. leptoporus subsp. leptoporus* in higher abundance south of STF confirms the affinity of this species to cooler waters of the Southern Ocean (Nishida, 1986; McIntyre and Bé, 1967). However, higher abundance for both subspecies was recorded in the STZ and as far south as SAZ (Patil et al., 2017) indicating a preference for warmer waters (Hiramatsu and De Deckker, 1996). It should be noted that studies from the Pacific sector of the Southern Ocean

lack STZ as the stations covered were only from SAZ to PFZ. However, in this study the occurrence of *C. leptoporus* subsp. small and *C. leptoporus* subsp. *leptoporus* was abundant in SAZ and showed no clear correlation with any parameter (Fig. 6, 7).

Syracosphaera spp. was the most diverse genus, and 23 species were recorded in this study. *S. pulchra* was most abundant in the STZ, followed by *S. prolongata*, *S. tumularis*, and other minor species showing a preference for high temperature, salinity, and low nutrient conditions. These findings agree with the results of previous studies in the Southern Indian Ocean (Patil et al. (2017, 2020). However, the occurrence of this genus was rare in the Indian sector of the Southern Ocean (Mohan et al., 2008). The abundance of *Syracosphaera* spp. in the STZ indicates a preference for warmer waters and low nutrient conditions which is also exhibited in the Australian (Findlay and Giraudeau 2000), Pacific (Malinverno et al., 2015; Saavedra-Pellitero et al., 2014), and Atlantic sectors of the Southern Ocean (Boeckel and Baumann, 2008).

Other abundant species recorded in the warm waters of STZ were *A. quattrospina, U. tenuis, M. elegans, O. hydroideus, O. fragilis, G. ericsonii*, and *D. tubifera*. These species were low in abundance or not observed in previous studies (Mohan et al., 2008; Patil et al., 2017). *Umbilicosphaera* spp., *Calciosolenia* spp., *Acanthoica* spp., and *Kataspinifera baumanii* were some of the other species recorded in the STZ. Apart from these, holococcoliths *Syracosphaera histrica* HOL, *Helicosphaera* HOL, and *Calcidiscus leptoporus* subsp. *leptoporus* HOL were abundant in the STZ, indicating a preference for warmer waters. Data collected in this study also recorded rare occurrences of *R. purvula*, *C. aculeata*, *C. cristatus* CER rostratus type+hoops, *Papposphaera sagittifera*, and *Z. hellenica*.

Subantarctic Zone assemblage

The SAZ assemblage was dominated by *E. huxleyi* type C. *Emiliana huxleyi* type B/C with low abundances of deformed type, however, *E. huxleyi* type A was restricted to north of the SAZ. This agrees with previous studies (Findlay and Giraudeau, 2000; Gravalosa et al., 2008; Mohan et al., 2008; Charalampopoulou et al., 2011; Patil et al., 2013, 2017; Malinverno et al., 2015). *Calcidiscus leptoporus* subsp. small and *C. leptoporus* subsp. *leptoporus* were abundant in the SAZ, which agrees with the findings of a study of the Pacific sector (Saavedra-Pellitero et al., 2014). Mohan et al. (2008) recorded the rare occurrence of these species in the south of the SAZ and the PFZ of the Indian sector of the Southern Ocean. On the other hand, Patil et al. (2017) did not record these species south of the PFZ. These species have been previously described as a tropical species, inhabiting temperature ranges of 20–30 ℃, and recorded in colder waters, as low as 6 ℃ (McIntyre et al., 1970). Preference of *C. leptoporus* subsp. *leptoporus* to cold nutrient-poor waters and *C. leptoporus* subsp. small to warm nutrient-rich stratified water was observed in the samples from the north Atlantic (Renaud et al., 2002) however in the southern Indian ocean these species showed no clear preference regarding temperature or nutrients (Fig. 6, 7). Which indicates other factors are influencing these species.

Gephyrocapsa muellerae, M. elegans, O. hydroideus, Umbellosphaera sp., *Algirosphaera* sp., *Acanthoica* sp., *D. tubifera,* and most members of *Syracosphaera* spp. were present in low abundance and restricted to north of SAZ (Patil et al 2017; Saavedra-Pellitero et al. 2014). *Syracosphaera pemmadiscus*, *S. noroitica, S. didyma,* and *S. nodosa* type A occurred only in the SAZ. *S. dilatata, S. halldalii,* and *S. mediterranea* were abundant and present throughout SAZ. The occurrence of *Gephyrocapsa oceanica* in the southernmost Atlantic and Indian Oceans has been recorded in previous studies (Verbeek, 1989; Eynaud et al., 1999; Mohan et al., 2008). However, *G. oceanica* was not observed in this study. Similar observations were made by Saavedra-Pellitero (2014) in the Pacific sector of the SO and Patil

et al., (2017) in the Indian sector of the SO. A rare occurrence of holococcolithophores *Calcidiscus leptoporus* subsp. *leptoporus* HOL, *C. pelagicus* subsp. *braarudii* HOL was recorded in the SAZ zone. In previous studies, *C. pelagicus* subsp. *braarudii* was never recorded in water samples from the Indian sector of the SO (Mohan et al., 2008; Patil et al., 2017, 2020). In contrast, in this study, holococcoliths were recorded in the surface samples, similar to observations made by Saavedra-Pellitero and Baumann (2015) in the Pacific sector. Low abundance in sediment trap studies was observed in the Australian sector of the Southern Ocean (Hernández et al., 2019). The occurrence of holococcolithophore *C. pelagicus* subsp. *braarudii* in the Indian sector of the Southern Ocean indicates that this species generally occurs in very low abundance and is scarce in the Southern Ocean, in contrast to the dominance of this species in sub-Arctic regions (Andruleit 1997; Baumann et al., 2000). Furthermore, Langer et al. (2022) postulated that the heterococcoliths of *C. pelagicus* subsp. *braarudii* have a low tolerance to light compared to holococcolithophores and are more prevalent in winter and at greater depths.

Polar Frontal Zone and Antarctic Zone assemblages

The coccolithophore assemblage in this region is primarily dominated by *E. huxleyi* type B/C and *E. huxleyi* type C, which occur as far as 58°S. Similar observations were recorded in other sectors of the Southern Ocean (Findlay and Giraudeau, 2000; Cubillos et al., 2007; Gravalosa et al., 2008; Mohan et al., 2008; Charalampopoulou et al., 2011; Patil et al., 2013, 2017; Malinverno et al., 2015). In this study, sporadic occurrence of *E. huxleyi* type A was observed in the PFZ. Similar observations were made in surface sediments by Saavedra-Pellitero and Baumann (2015), and Cubillos et al. (2007). In this study, sporadic occurrences of *C. leptoporus* small, *K. baumanii*, and *B. virgulosa* were observed, but below temperatures of 1 ℃, no coccospheres were recorded, which is consistent with observations made by Patil et al.

(2017). However, this contradicts a previous study by Winter et al. (2014), which suggests an increasing southward expansion of *E. huxleyi*.

Malinverno et al. (2016) described how coccolithophores represent most hard-shelled phytoplankton in the SAZ and make an important contribution to total fossilizable phytoplankton groups throughout the SAZ and PFZ. Though coccolithophores represent one of the groups used in palaeoceanographic reconstructions, their efficacy might vary based on their differing responses to the physicochemical properties of different sectors of the Southern Ocean, as well as the time of sampling. Here it is essential to conduct year-round studies of the current coccolithophore composition and the factors affecting this composition in important regions of the Southern Ocean, using ship-based sampling or sediment traps. This long-term approach might help elucidate the differences in the coccolithophore ecology distribution and factors regulating the seasonal variation in composition in different sectors of the Southern Ocean.

4.5. Conclusions

The distribution and number of coccolithophores along the transect of the Southern Indian Ocean varied significantly in different frontal zones

In total, 54 species of coccolithophore, including 8 holococcolithophores were recorded. *E. huxleyi* was consistently dominant along the transect. Species diversity showed a decreasing trend from north to south.

Higher abundance and diversity were recorded in the STZ, but a highly abundant monospecific assemblage of *E. huxleyi* was observed in the PFZ furthermore AZ was completely devoid of coccolithophores. Temperature and nutrient concentration significantly regulated the abundance and distribution pattern in the Southern Indian Ocean.

The present study essentially agrees with the findings of previous studies in the Southern Indian Ocean, however, certain variations are also present, likely due to seasonal variation and time of sampling. Though the distribution of coccolithophore is comparable to that seen in other sectors of the Southern Ocean certain species such as *G. muellerae* however are abundant in the STZ of the Southern Indian Ocean. However, these species are found abundant in the SAZ in different sectors of the Southern Ocean, which could be due to differences in oceanographic settings.

Holoccolithophores of *C. pelagicus* subsp. *braarudii* were observed, whereas heterococcoliths were absent due to the difference in the temporal and spatial distribution of different life cycle phases.

Calcidiscus leptoporus showed no clear association with any of the parameters recorded in this study, suggesting that other factors, such as grazing, might affect their distribution.

To better understand the difference in the biogeographic distribution of coccolithophore species for palaeoceanographic implications it is necessary to conduct year-round observation using ship-based sampling or sediment trap studies.

Chapter 5

Distribution of coccoliths in surface sediments of the Southern Indian Ocean: Biogeography, preservation, and carbonate contribution

5.1. Background

The Southern Indian Ocean consists of unique oceanographic features. Owing to highly varied bottom topography, the intensity of fronts varies, fronts merge, split and steer (Kostianoy et al., 2004; Sokolov and Rintoul, 2007a, 2009a) in the Crozet (Park et al., 1993) and Kerguelen regions (Belkin and Gordon, 1996). The Southern Indian Ocean consists of the Agulhas Return Front (ARF) which merges with the Subtropical Front (STF) (Lutjeharms and Ansorge, 2001). The frontal system further south consists of the Subantarctic Front (SAF), Polar front (PF), and the Antarctic zone (AZ), which consists of the southern ACC front (SACCF) and Southern boundary (SB) of the ACC (Sokolov and Rintoul 2009a.).The fronts and zones in the Southern Ocean vary in the physicochemical parameter as well as biological features (Jasmine et al., 2009). The properties of surface waters of the Southern Ocean such as stability of water column, variation in sea ice extent, light availability, temperature, salinity, density, and nutrient concentrations (Tsuchiya et al., 1994; Orsi et al., 1995; Belkin and Gordon, 1996; Park et al., 2001; Lutjeharms, 2006) play important role in regulating primary production and the potential of Southern Ocean to sink CO_2 by the means of a biological pump and carbonate pump.

In the modern ocean along with other groups of phytoplankton, coccolithophore plays an important role in the climate system via dimethyl sulphide formation, and the carbon cycle. Satellite studies revealed that coccolithophores are abundant south of STZ and north of the PF, forming the Great Calcite Belt during the austral summer (Balch et al., 2011, 2016). They contribute up to 16.5% of the total annual net primary production south of 30°S (Nissen et al., 2018) and their distribution is controlled by latitudinal zonation and frontal system dynamics (McIntyre and Bé, 1967; Findlay and Flores, 2000; Ziveri et al., 2004). Coccolithophores play a complicated and vital role in the carbon cycle (Salter et al., 2014). They release CO_2 into the surface water and atmosphere during calcite plate/coccolith formation (Rost and Riebesell,

2004), which reduces its uptake into the surface ocean. Conversely, organic matter produced through photosynthetic activity by coccolithophores enhances carbon sequestration through the biological carbon pump (Volk and Hoffert, 1985). However, owing to their high density and low dissolution rate, coccoliths act as an effective ballast for organic matter as well as inorganic carbon ($CaCO_3$) via marine snow, thereby increasing the sequestration of carbon to the depths (Buitenhuis et al., 2001; Boyd and Trull, 2007; Ziveri et al., 2007). Coccolithophores respond to the changes in surface water masses by varying in distribution, abundance, assemblages/composition, and morphology (McIntyre and Bé, 1967). This information is imprinted in the sediment records of coccoliths which form a major part of deep-sea sediment accumulating into fossil records and providing paleoenvironmental information.

In the current climate change scenario, little is known about the coccolithophore response to environmental changes (Iglesias-Rodriguez et al., 2008). Few studies have shown a southward shift in the coccolithophore species and assemblages (Cubillos et al., 2007; Patil et al 2020). A study by Donahue et al. (2019) exhibited taxon-specific and regional variation in coccolithophores in response to increased pCO_2 and light intensity. Reduced calcification in three morphotypes of *E. huxleyi* from different latitudes under varying ocean acidification conditions was observed by Müller et al. (2015, 2017).

In recent years new information on biogeographic distribution, ecology, and factors affecting extant coccolithophores in the different sectors of the Southern Ocean and in the more restricted areas has come to light (Boeckel and Baumann, 2008; Gravalosa et al., 2008; Mohan et al., 2008; Guerreiro et al., 2013; Malinverno et al., 2015; Saavedra-Pellitero et al., 2014; Patil et al., 2017, 2020). Additionally, information and studies on the transformation of living coccolithophores to surface sediment assemblages and the factors affecting them are very scarce with few exceptions (e.g., Baumann et al., 2000; Andruleit et al., 2004; Boeckel and Baumann, 2008), particularly at high latitudes in the Pacific sector (Saavedra-Pellitero and

Baumann, 2015; Vollmar et al., 2021), Australian sector (Rigual Hernández et al., 2018), Atlantic sector (Boeckel and Baumann, 2004) and Indian sector (Patil, 2015) of the Southern Ocean. The sinking assemblage reaches the sea floor in a highly altered state that varies significantly from the surface water assemblage (Honjo and Okada, 1974; Steinmetz, 1994; Kinkel et al., 2000). The deposition and preservation of coccoliths in the surface sediment is the result of organic matter flux to the ocean floor, its respiration and remineralization., transport of carbonates via currents, and carbonate chemistry (i.e., pH, alkalinity, partial pressure of CO_2, dissolved inorganic carbon) of the water masses in the water column and above the sediment (Hauck et al., 2012; Pörtner and Farrell, 2008; Doney et al., 2012). These factors alter the surface ocean signals recorded by the coccoliths and thus making it challenging to decipher the paleoenvironmental signatures using coccolith records (Gerotto et al., 2022). Apart from studying ecology, biology, and distribution of living coccolithophores in plankton samples, it is essential to also study the taphonomical processes which alter coccolith assemblages during their accumulation on the seafloor (Andruleit et al., 2004).

In this study, the robustness of recent coccolith in the surface sediments in reflecting the distribution of the coccolithophore assemblage in the overlying surface ocean is examined. Surface sediment assemblages are compared with plankton assemblages to gain information on the occurrence of species, their preservation, calcium carbonate contribution, and factors affecting their composition and preservation in the Southern Indian ocean.

5.2. Methodology

Surface sediment samples used in this study were collected during Indian Southern Ocean Expeditions and from the archives of the University of Bordeaux, across the latitude 30°S–70°S and longitude 30°E–100°E. The physicochemical parameter data has been extracted from the European Commission's Copernicus Marine Environment Monitoring Service. For

analysis, samples were processed following the technique described by Flores and Sierro (1997). A minimum of 400 coccoliths in each sample were counted and identification of coccoliths was carried out using Nannotax3 (www.mikrotax.org) and previous literature (Young et al., 2003; Cros and Fortuño, 2002). Further, coccolith absolute abundance, diversity, and dissolution index (CEX) were calculated and further statistical analysis was done. For more details regarding methodology and study area, refer to Chapter 2.

5.3. Results

5.3.1. Changes in the coccolith absolute abundance and diversity across the fronts

Coccolith distribution patterns displayed latitudinal variation in the surface sediment samples taken from the Southern Indian Ocean. A total of 21 coccolithophore species were recorded and coccoliths were consistently present from the STZ to the PFZ at varying oceanic bottom depths. (Table 1, Fig. 1a). Total coccolith absolute abundance (CAA) was highest in the STZ with average values of 11.1×10^9 coccoliths/g of sediment followed by south of SAZ where average values were 9.3×10^9 coccoliths/g of sediment. The CAA was relatively low in PFZ with an average value of 2.5×10^9 coccoliths/g of sediment, whereas, the samples taken south of the PFZ and AZ were devoid of coccoliths.

Coccolith diversity was highest in the STZ (1–2) and PFZ (0.2–1.9) and lower values were recorded in the SAZ (0.4–1.6) (Fig. 1b). Absolute abundance and diversity were highest in the STZ however the decreasing trend in diversity did not extend to the PFZ. Coccolith absolute abundance and diversity showed a strong positive correlation with temperature ($R = 0.74$, $P<0.001$ and $R = 0.65$, $P<0.001$ respectively) and a positive but weak relationship with salinity ($R = 0.30$ and $R = 0.40$, $P<0.05$ respectively). Inverse correlation was observed with nitrate ($R = 0.71$, $P<0.001$ and $R = 0.61$, $P<0.01$) and phosphate ($R = 0.71$, $P<0.001$ and $R = 0.62$, $P<0.01$) (Fig. 4)

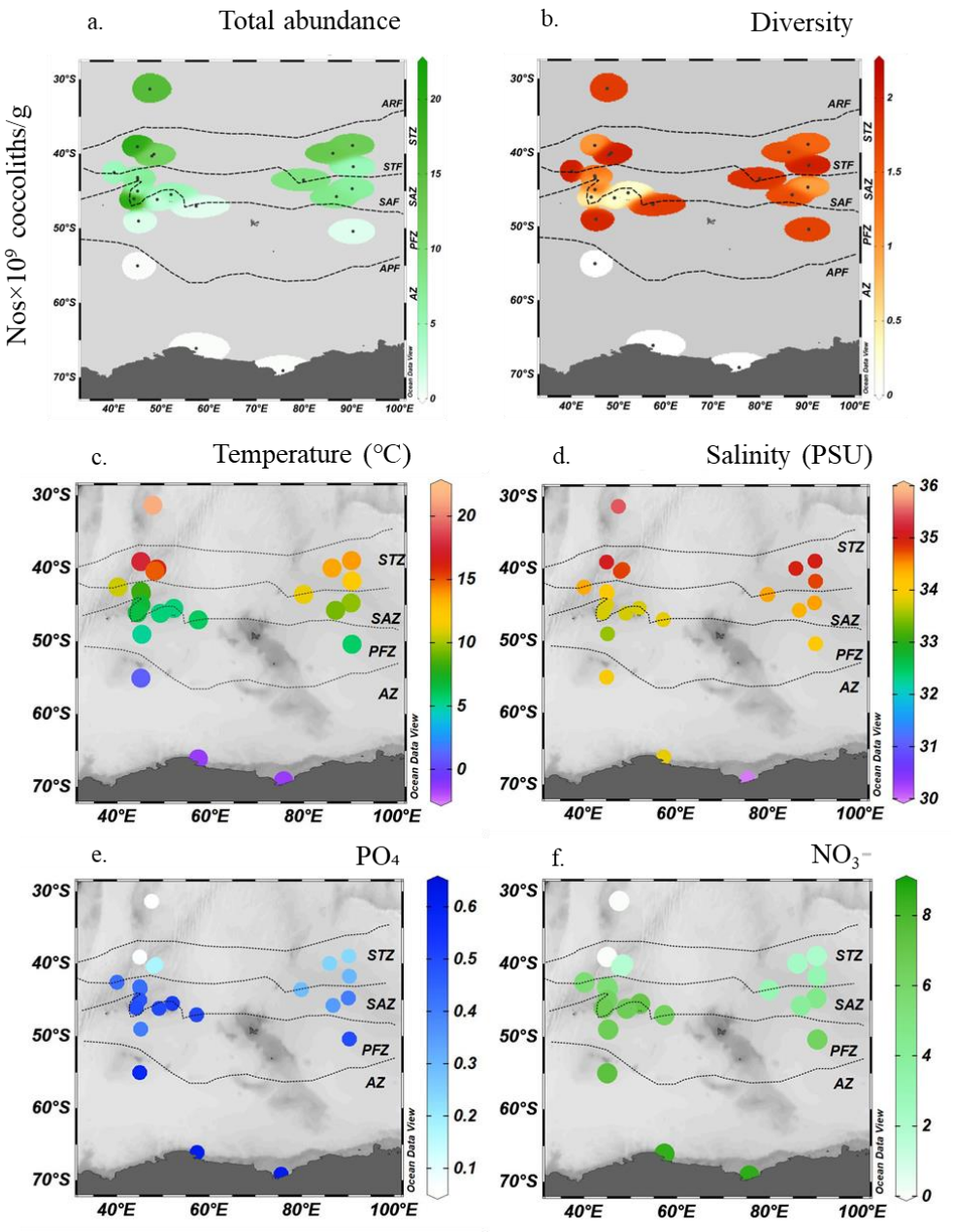

Figure 1. a) Total Coccolith absolute abundance b) diversity c) temperature d) salinity e) phosphate (µM) and f) nitrate (µM) data extracted from European Commissions Copernicus Marine Environment Monitoring Service (https://marine.copernicus.eu/access-data)

5.3.2. Coccolith species distribution across the frontal zones

In the surface sediment samples, a total of 21 coccolithophore species were recorded (Table 1) of which a ubiquitous species *Emiliania huxleyi* was the most abundant species in most of the samples. The highest abundance of *E. huxleyi* was recorded in SAZ (1.7–19.5 × 10^9

coccoliths/g of sediment) and STZ (1.7–14.9 × 10^9 coccoliths/g of sediment) lowest abundance was recorded in the north of PFZ (0.4–4.7 × 10^9 coccoliths/g of sediment) and is completely absent in AZ (Fig. 2a).

A higher abundance of *Gephyrocapsa oceanica* was recorded in STZ (0.3–4.4 × 10^9 coccoliths/g of sediment) followed by SAZ (0.1–0.6 × 10^9 coccoliths/g of sediment) and PFZ (0.04–0.1 × 10^9 coccoliths/g of sediment). A similar pattern was recorded in *Gephyrocapsa muellerae* highest abundance was recorded in STZ (0.1–1.3 × 10^9 coccoliths/g of sediment) whereas abundance was reduced in SAZ (0–0.4 × 10^9 coccoliths/g of sediment) and the lowest was recorded in PFZ (0–0.03 × 10^9 coccoliths/g of sediment) *Reticulofenestra* sp. was present in same concentration in STZ and SAZ (0–0.1 × 10^9 coccoliths/g of sediment) and absent in PFZ. (Fig. 2l).

Calcidiscus leptoporus was the second most abundant species, consisting primarily of C. *leptoporus* subsp. small and *C. leptoporus* subsp. *leptoporus. C. leptoporus* subsp. small was recorded highest in STZ (0.04–0.8 × 10^9 coccoliths/g of sediment) and showed a decreasing trend towards the south (Fig. 2e). *Calcidiscus leptoporus* subsp. *leptoporus* was most abundant in the SAZ (1.1–3 × 10^9 coccoliths/g of sediment), STZ (0–1.7 × 10^9 coccoliths/g of sediment), and PFZ (0–0.3 × 10^9 coccoliths/g of sediment) (Fig. 2f). *Calcidiscus leptoporus* subsp. *quadriperforatus* was present but relatively scarce. *Coccolithus pelagicus* subsp. *braarudii* was present in the STZ, SAZ, and PFZ and ranged between (0.0–0.1 × 10^9 coccoliths/g of sediment) in all three zones (Fig. 2 h).

The decreasing trend from STZ to PFZ was observed in *Umbilicosphaera* sp., STZ (0–0.05 × 10^9 coccoliths/g of sediment), SAZ (0.01–0.1 × 10^9 coccoliths/g of sediment), PFZ (0–0.01 × 10^9 coccoliths/g of sediment) (Fig. 2i), *Helicosphaera carteri* STZ (0–0.03 × 10^9 coccoliths/g of sediment) SAZ (0.01–0.1 × 10^9 coccoliths/g of sediment) PFZ (0–0.02 × 10^9

coccoliths/g of sediment) (Fig. 2 d) and *Florisphaera profunda,* a low photic zone taxa, was abundant in STZ (0–5.9 × 10^9 coccoliths/g of sediment), SAZ (0.02–0.3 × 10^9 coccoliths/g of sediment) and very low abundance in PFZ (0–0.1 × 10^9 coccoliths/g of sediment) (Fig. 2j). The highest abundance of *Umbellosphaera sp.* was recorded in the STZ (0–0.2 × 10^9 coccoliths/g of sediment) followed by SAZ (0–0.3 × 10^9 coccoliths/g of sediment), but it was absent in PFZ (Fig. 2g). *Syracosphaera pulchra* showed a similar trend, with the highest abundance in the STZ (0–0.2 × 10^9 coccoliths/g of sediment) followed by SAZ (0–0.3 × 10^9 coccoliths/g of sediment), and it was absent in the PFZ (Fig. 2k). *Reticulofenestra* sp. was recorded in the north of the PFZ (0.3 × 10^9 coccoliths/g of sediment) with sporadic occurrence in the STZ and SAZ (Fig. 2l). Other minor species included *Rhabdosphaera clavigera*, *Ceratolithus cristatus*, *Calciosolenia* sp, *Pontosphaera* sp, *Oolithotu*s sp., and *Calciopappus* sp.

Based on coccolith abundance, the axes of the canonical correspondence analysis (CCA) explained 85.28% of the variance within the surface sediment dataset (Fig. 3). However, most species were close to the centre of the axis, thus presenting a very vague affinity towards the parameters. *Coccolithus pelagicus* subsp. *braarudii* and *Reticulofenestra* sp showed affinity to NO_3 and PO_4. *Florisphaera profunda* showed affinity to temperature and salinity (Fig. 3). All the species showed a positive correlation with temperature, a weak positive correlation with salinity, and an inverse correlation with NO_3 and PO_4 (Fig. 4). *C. leptoporus* subsp. *leptoporus, Coccolithus pelagicus* subsp. *braarudii, Reticulofenestra* sp. showed very weak correlation with parameters (Fig. 4)

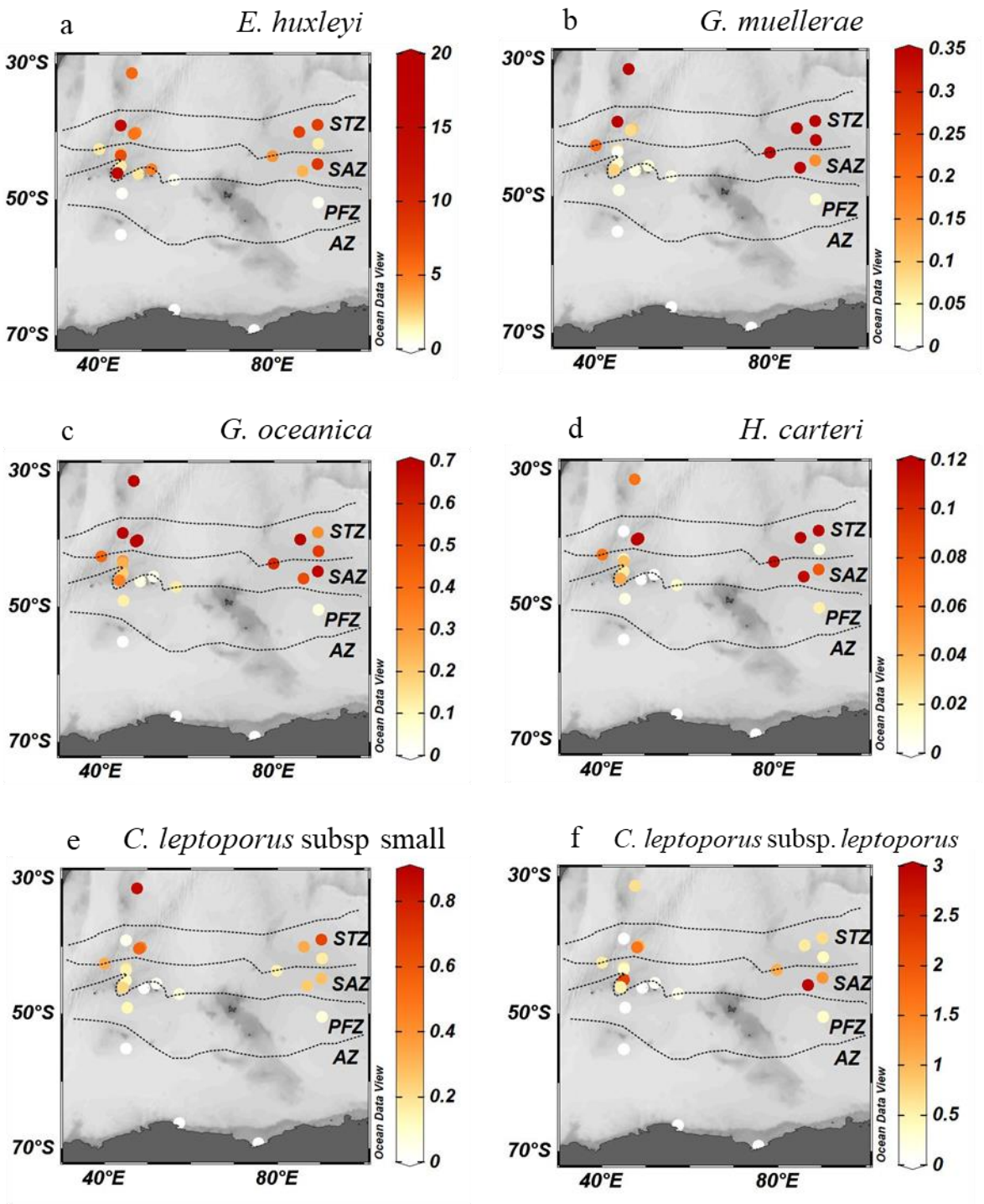
a
E. huxleyi
30°S
50°S
70°S
40°E
80°E
STZ
SAZ
PFZ
AZ
Ocean Data View
20
15
10
5
0
b
G. muellerae
0.35
0.3
0.25
0.2
0.15
0.1
0.05
0
c
G. oceanica
0.7
0.6
0.5
0.4
0.3
0.2
0.1
0
d
H. carteri
0.12
0.1
0.08
0.06
0.04
0.02
0
e
C. leptoporus subsp small
0.8
0.6
0.4
0.2
0
f
C. leptoporus subsp. leptoporus
3
2.5
2
1.5
1
0.5
0

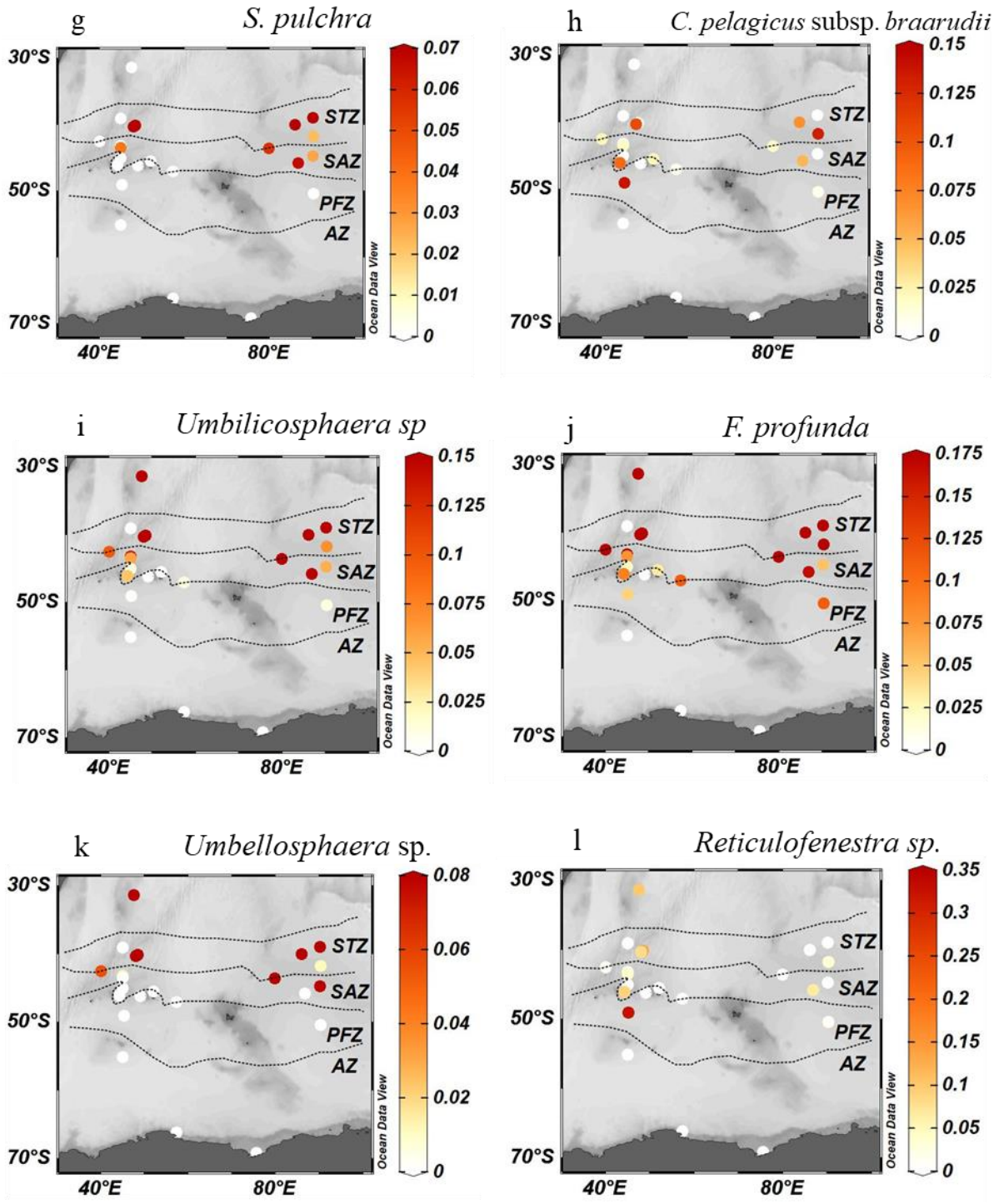

Figure 2. Abundant species ($\times 10^9$ coccoliths per gram of sediment a) *E. huxleyi*, b) *G. muellerae* c) *G. oceanica*, d) *H. carteri*, e) *C. leptoporus* subsp. small f) *C. leptoporus* subsp. *leptoporus*, g) *S. pulchra*, h) *C. pelagicus* subsp. *braarudii*, i) *Umbilicosphaera* sp, j) *F. profunda*, k) *Umbellosphaera* sp. l) *Reticulofenestra* sp.

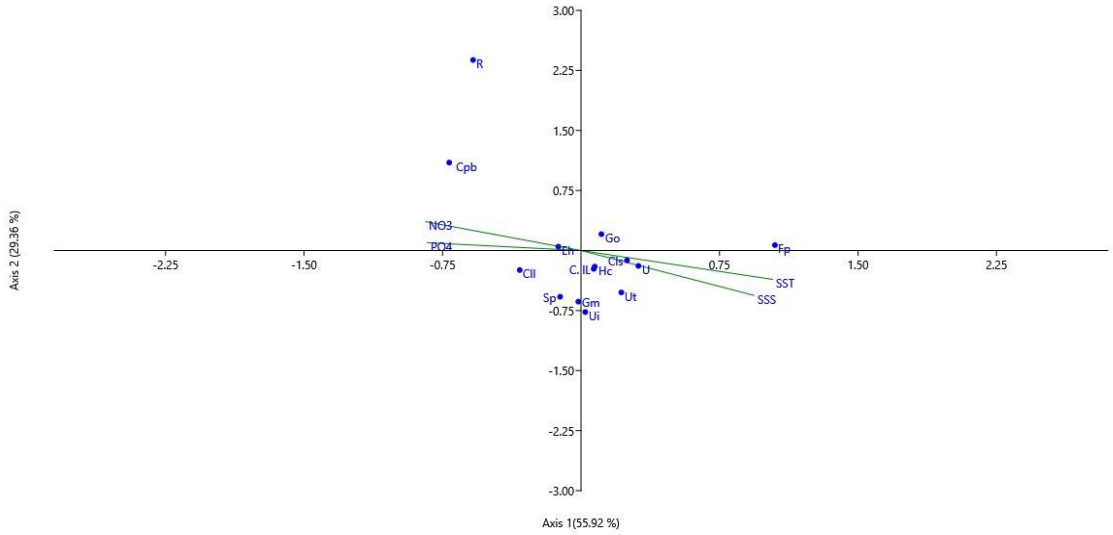

Figure 3. Canonical corresponding analysis (CCA) ordination diagram for coccolith assemblages and environmental variables (temperature, salinity, NO_3, PO_4) Abbreviations for each group are provided in Table 1.

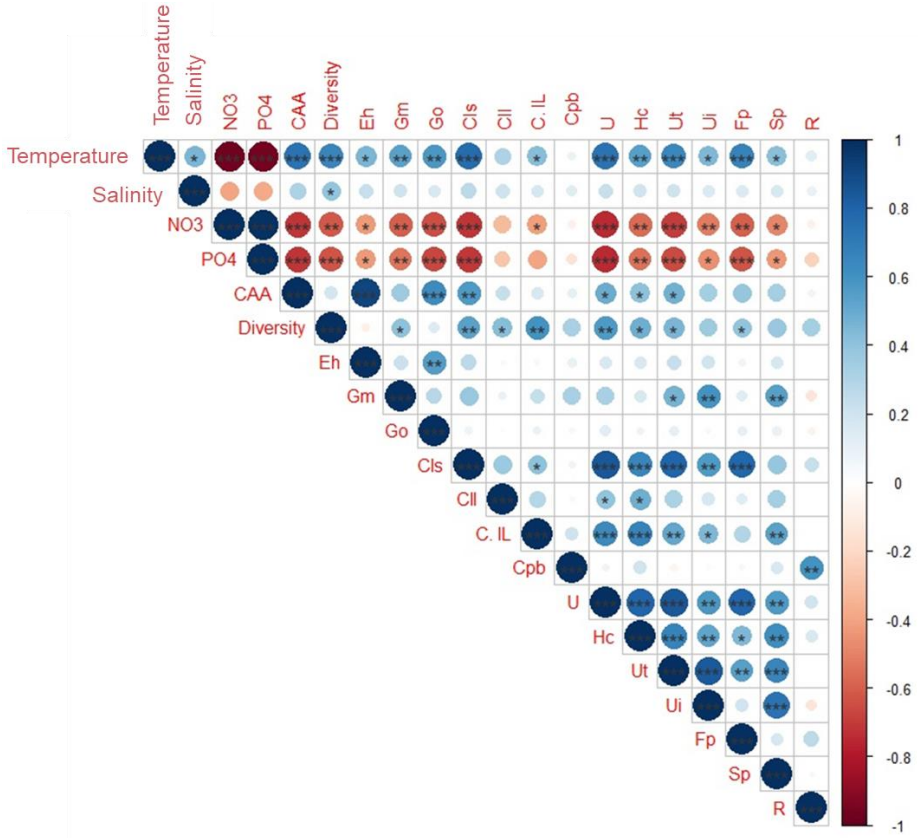

Figure 4. Correlation matrix diagram (Pearson's Correlation analysis. Parameters used are environmental variables Coccolithophore absolute abundance (CAA) and diversity. The color bar indicates blue as positive correlations and

red as negative correlations. The size of the dots in the diagram indicates the strength of the correlation. Correlations with p>0.05 were left blank.

Table 1. Stations and species recorded in surface sediment samples

Station	Depth (m)	Latitude (°S)	Longitude (°E)	× 10^9 coccoliths/ g of sediment	Species	Abbreviation	STZ	SAZ	PFZ	AZ
ABP S6	4065	-31.3	47.58	15.7	*Emiliania huxleyi*	Eh	+	+	+	-
MD94-08BC	3491	-38.86	90.12	12.4	*Gephyrocapsa muellerae*	Gm	+	+	+	-
SK 200/17	4022	-39.03	44.97	19.8	*Gephyrocapsa oceanica*	Go	+	+	+	-
MD97-2102	3440	-39.92	86.01	13.3	*Gephyrocapsa* sp.	G	+	+	-	-
ABP S4	4065	-40.03	48.44	10.9						
ABP S3	3635	-40.29	48	12.4	*Calcidiscus leptoporus* small	Cls	+	+	+	-
MD94-07BC	2768	-41.71	90.28	4.7	*Calcidiscus leptoporus* ssp. *leptoporus*	ClI	+	+	+	-
ABP S1	3182	-42.5	40.08	4.6	*Calcidiscus leptoporus large*	ClL	+	+	-	-
SK 200/21	3210	-43.15	44.98	5.4	*Coccolithus pelagicus* ssp. *braarudii*	Cpb	+	+	+	-
Sk20022a	2723	-43.42	45.04	8.4	*Umbilicosphaera sibogae*	U	+	+	+	-
MD94-102	3205	-43.5	79.83	9.5	*Umbilicosphaera foliosa*		+	+	+	-
MD97-2101G	-	-43.50	79.84	8.1	*Helicosphaera carteri*	Hc	+	+	+	-
MD94-06BC	-	-44.66	90.06	11.4	*Calciosolenia* sp.	C	+	+	-	-
MD94-109	-	-44.67	90.06	6.5	*Rhabdosphaera clavigera*	Rc	+	+	-	-
SK 200/23	1423	-45	45.01	4.5	*Umbellosphaera tenuis*	Ut	+	+	-	-
MD19-3579	-	-45.43	52.01	5.0	*Umbellosphaera irregularis*	Ur	+	+	-	-
MD00-2375G	-	-45.72	86.75	7.99	*Syracosphaera pulchra*	Sp	+	+	-	-
MD19-3575	2400	-46.03	44.22	21.1	*Syracosphaera* spp.	S	+	-	-	-
MD19-3577	800	-46.11	49.11	2.0	*Reticulofenestra* sp.	R	+	+	-	-
SN2	4400	-47	57.3	0.98	*Florisphaera profunda*	Fp	+	+	+	-
MD94-04BC	-	-50.38	90.25	1.07	*Ceratolithus cristatus*	Cc	+	-	-	-
sk200/27	4377	-49	45.22	1.20	*Pontosphaera* sp.		+	-	-	-
sk200/33	4185	-55.01	45.01	0						
st 1	-	-66.1	57.31	0						
ANT 1	-	-69.09	75.53	0						

5.3.3. Variation in coccolith dissolution index and coccolith carbonate

The effect of carbonate dissolution on coccolith assemblage and preservation was determined by the ratio of *E. huxleyi* and *C. leptoporus*. The coccolith dissolution index (CEX) was >0.6 except in a few samples of SAZ and PFZ where the lowest CEX value was 0.4 at depths 1423 m and 3485 m respectively (Fig. 5b, Fig. 6a,b). The CEX values in STZ were highest, at 0.7–0.9, while in the SAZ and PFZ, CEX ranged between 0.4–0.9 indicating the good preservation conditions and low dissolution effect in the southern Indian ocean.

To estimate coccolith $CaCO_3$ contribution, coccolith mass of abundant species was calculated. The highest $CaCO_3$ w% was recorded in STZ (12.0–33.85 w%) followed by SAZ (8–29.5 w%) and the lowest was recorded in PFZ (0.8–7.0 w%). *C. leptoporus* (0.2–21.44 w%), *G. oceanica* (0.1–12.46 w%), *H. carteri* (0–6.73), *E. huxleyi* (0.1–5.4 w%), *U. sibogae* (0–2.62 w%), *C. pelagicus* subsp. *braarudii* (0–5.35 w%) were major contributors to the total $CaCO_3$ w% (Fig. 7).

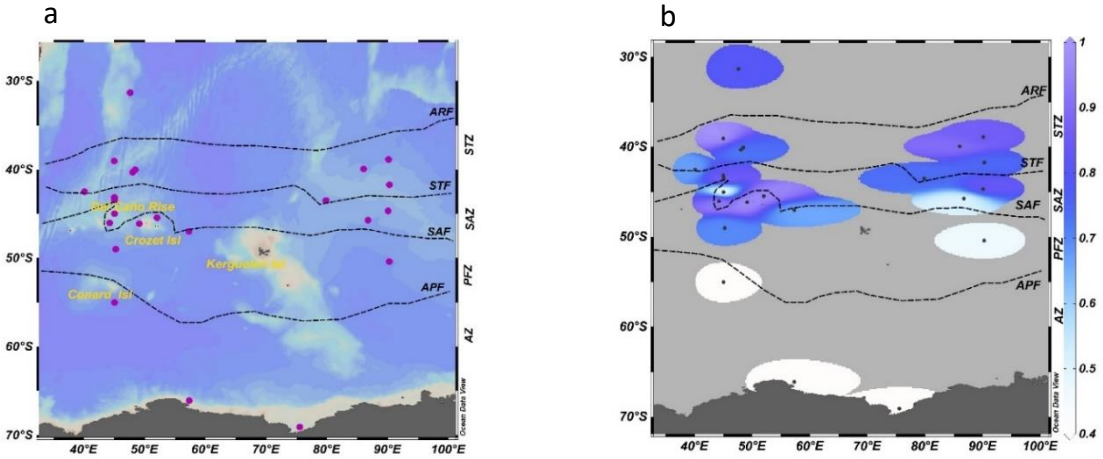

Figure 5. a) Location of surface sediment samples b) Coccolith dissolution index (CEX)

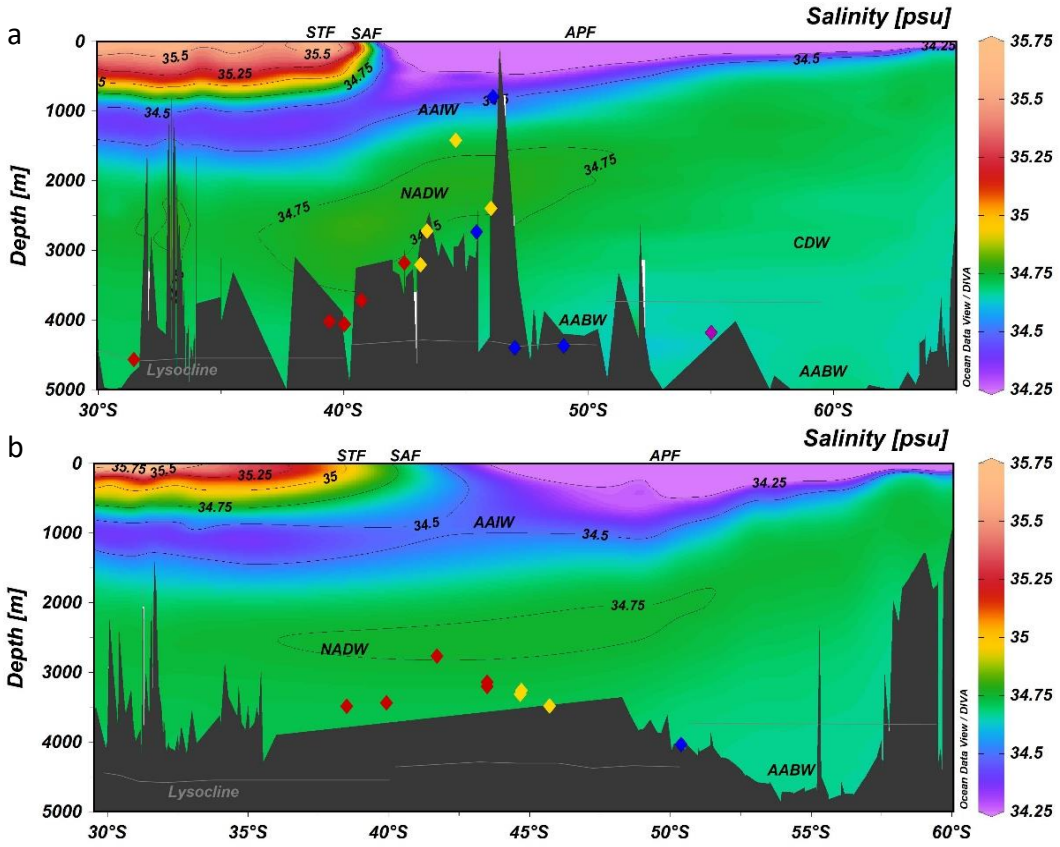

Figure 6. Location of samples in bottom topography, a) Latitudinal (30–60°S) cross-section at 40°E–60°E longitude, b) Latitudinal (30°S–60°S) cross-section at 80°E–100°E longitude background map of annual mean salinity derived from World Ocean Atlas 2018 (Garcia et al., 2019) and gridded with Ocean Data View software (Schlitzer, 2016). Red diamonds indicate STZ samples, yellow diamonds indicate SAZ samples, blue diamonds indicate PFZ samples, and purple diamonds indicate AZ samples.

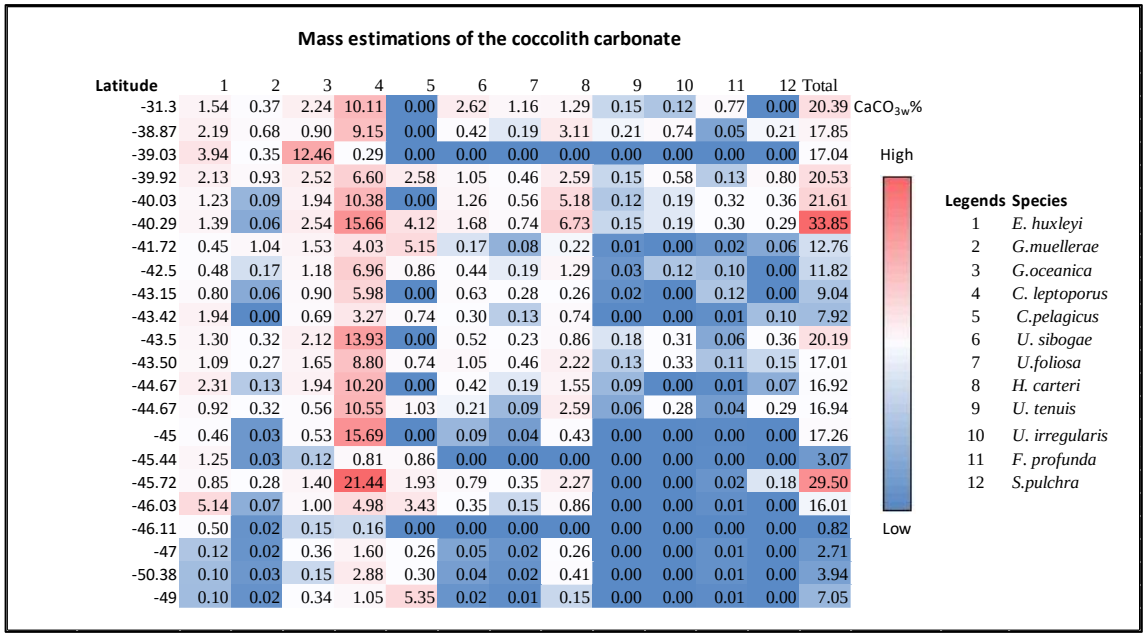

Figure 7. Heat map depicting coccolith carbonate content ($CaCO_3$ w% g^{-1} sediment) of different species in the surface sediment samples

5.4. Discussion

5.4.1. Coccolith distribution in the surface sediment samples

Coccolithophore assemblages and distribution in the plankton sample were not mirrored in the sediment. Species with delicate coccoliths recorded in the plankton community were absent in the surface sediment (e.g., Acanthoica spp., *Algirosphaera* spp., *Alisphaera* spp., *Syracosphaera* spp., *Michaelsarsia* sp., and holoccolithophores). Similar results were obtained in the Pacific sector of the Southern Ocean by Saavedra-Pellitero and Baumann (2015).

Some species e.g., *E. huxleyi, G. muellerae*, and *C. leptoporus* were found in both the surface sediment and plankton samples. *Emiliania huxleyi* was the most abundant species distributed from STZ to PFZ in surface sediment. However, it is restricted to north of PFZ in surface sediment, unlike surface water distribution. In surface waters it is the only species present further south in AZ, as seen in Chapter 4 (Fig. 3) and in previous records (Mohan et al., 2008, Patil et al., 2017). The preservation of *E. huxleyi* to the south of PFZ and AZ is impacted

by low productivity, dilution by siliceous groups, and dissolution (Findlay and Giraudeau, 2000) owing to low calcite saturation (Rigual Hernández et al., 2018).

In surface sediment samples *G. muellerae was* abundant in both the STZ and SAZ, mimicking the distribution in surface waters (see Chapter 4, Fig. 3 and previous records (Patil et al., 2017)) showing affinity to warm and low nutrient waters. However, rare occurrence of this species in the north of PFZ was also recorded (Fig. 2b). Similar distribution was observed in the Australian sector of the Southern Ocean (Findlay and Giraudeau, 2000). In the sinking assemblages of SAZ, this species was recorded as a secondary component of total contributing coccolithophores according to sediment trap studies by Rigual Hernández et al. (2020). This species was largely recorded in SAZ and PFZ in the surface sediment and plankton samples of the Pacific sector of the Southern Ocean (Saavedra-Pellitero and Baumann, 2015; Saavedra-Pellitero et al., 2019). However, previous studies suggest the affinity of *G. muellerae* to cold nutrient-rich waters (Winter and Siesser, 1994; Winter et al., 1999; Boeckel and Baumann, 2004; Saavedra-Pellitero et al., 2010). The discrepancy between the results of these studies and those from the Indian sector of the Southern Ocean suggests that *G. muellerae* in the southern Indian Ocean might have wider temperature range tolerance and flourish in temperate to subtropical waters. Alternatively, this may be due to the difference in regional settings of the Indian sector of the Southern Ocean. Further studies are required to elucidate these differences.

Calcidiscus leptoporus was abundant (0.02–3.2 × 10^9 coccoliths/g of sediment) in the surface sediments and present from the STZ to PFZ. *Calcidiscus leptoporus* subsp. *leptoporus* and *C. leptoporus* subsp. small showed higher abundance in the SAZ and STZ, respectively. However, in the plankton samples, both subspecies were abundant in the SAZ alone. Patil et al. (2017, 2020) observed that this species was abundant in the water samples of the Agulhas zone and STZ followed by SAZ. However. *C. leptoporus*/*C. leptoporus* subsp. *leptoporus* were recorded as abundant south of the STZ and SAZ (Nishida, 1986; McIntyre and Bé, 1967); Australian

sector (Findlay and Giraudeau, 2000); Atlantic sector (Boeckel and Baumann, 2008); Indian sector (Patil et al., 2017); Pacific sector (Malinverno et al., 2015; Saavedra-Pellitero and Baumann, 2015) and in sediment samples taken from the Drake passage (Vollmar et al., 2021). Compared to these observations, previous studies from the Indian sector of the Southern Ocean recorded rare occurrences of this species in the water sample of SAZ and PFZ (Mohan et al., 2008). In contrast, *C. leptoporus* subsp. small has been previously described as a warm water species owing to its high abundance in the STZ (Hiramatsu and De Deckker, 1996; McIntyre et al., 1970); and restricted to subtropical gyre (Boeckel and Baumann, 2008). In this study, *C. leptoporus* subsp. small showed a positive correlation to temperature and an inverse relationship to nutrients. In contrast, *C. leptoporus* subsp. *leptoporus* species did not show any clear affinity to temperature, salinity, and nutrients (Fig. 2e, f, and Fig. 3, 4). The discrepancies in the abundance of different subspecies of *C. leptoporus* may be due to the factors in the water column such as seasonal variations in the subspecies abundances, competition for nutrients, and grazing impact (Renaud and Klaas, 2001; Renaud et al., 2002).

Other minor species were *H. carteri*, *S. pulchra*, *Umbellosphaera* spp. (*U. tenuis* and *U. irregularis)*, and *Umbilicosphaera* spp. (*U. sibogae* and *U. foliosa*). These species were mainly restricted to STZ and SAZ. Owing to the preference for warm and oligotrophic subtropical and tropical waters (Okada and McIntyre, 1979; Ziveri et al., 1995; Boeckel and Baumann, 2004; Mohan et al., 2008). *Umbilicosphaera* spp. were recorded in STZ and SAZ with higher abundance in the open ocean sample compared to samples in proximity to Crozet Island (Fig. 2i). In plankton data both species are restricted to STZ The rich *Syracosphaera* spp. diversity seen in the plankton sample was not observed in the sediment sample - only a single species, *S. pulchra,* was preserved in open ocean regions (Fig. 2g), showing affinity to high temperature, salinity, and low NO_3, PO_4 concentration (Patil et al., 2020) (Fig. 4).

Some species were present exclusively in the surface sediment, namely *G. oceanica*, *C. pelagicus*, *F. profunda*, *R. clavigera*, and *Reticulofenestra* sp.

Gephyrocapsa oceanica is a low-latitude, r-selected species with an affinity toward elevated nutrient and temperature conditions (Boeckel and Baumann, 2004). However, very rare specimens were recorded in conditions below 13 ℃ (McIntyre and Bé, 1967; Eynaud et al., 1999; Hagino et al., 2005). Low abundance of this species was recorded in the subtropical assemblages north of 41°S in the Indian sector of the Southern Ocean (Mohan et al., 2008). Though abundant (0.1–4.4× 10^9 coccoliths/g of sediment) in surface sediment samples, *G. oceanica* was absent in the plankton samples in the present study. A similar discrepancy was observed in previous studies conducted in the Southern Indian Ocean (Patil et al., 2017, 2020) and in the Pacific sector of the Southern Ocean (Saavedra-Pellitero et al., 2014; Saavedra-Pellitero and Baumann, 2015). The sporadic distribution of this species in the surface sediments of the Pacific sector could be due to the occasional warmer conditions in the SAZ or through drifting into the study area as a result of ocean currents (Saavedra-Pellitero and Baumann, 2015). This may hold true also for its pattern of occurrence in the southern Indian Ocean, considering the presence of this species in the surface sediments in the PFZ.

Reticulofenestra sp. is sporadically distributed in the surface sediments and was not recorded in the plankton samples. Vollmar et al. (2021) observed similar distribution in the drake passage. However, this species was not recorded in the plankton samples (Mohan et al., 2008, Patil et al., 2017).

A decreasing trend of *Florisphaera profunda* was observed from STZ to PFZ. This species is a lower photic zone subtropical-temperate species abundant between 30°N–30°S and rarely occurs in high abundance in the higher latitudes (Hernández-Almeida et al., 2019). This species occurred sporadically and was absent at latitudes greater than 40°S in plankton samples

(Mohan et al., 2008). However, in the present study, atypical abundance was observed in the surface sediments of the PFZ. Similar observations were made in plankton samples by Winter et al. (1999) and in surface sediment samples by Vollmar et al. (2021) in the Drake Passage. Previous reports recorded only a few numbers of this species in the sediment near New Zealand and suggested that this specimen might be transported by currents (Saavedra-Pellitero and Baumann, 2015).

The occurrence of warm water species such as *G. oceanica*, *F. profunda*, *Umbellosphaera* sp. *Umbilicosphaera* sp. in the south of the SAZ and the PFZ could be the result of physical transport via warm water eddies shed from Agulhas return current as these mechanisms transport large amounts of heat, salt, and organisms towards poles (Winter et al., 1999; Chacko et al., 2014).

Higher abundances of these species in the eastern transect compared to the western transect suggests a strong influence of warm water currents flowing from the eastern part of the Southern Ocean, such as the Indonesian throughflow and east Australian current, combined with the progressive shallowing of the Agulhas Return Current which loses its strength and warmth beyond 60°E (Kostianoy et al., 2004; Lutjeharms, 2006). Similar observations were recorded in radiolarian assemblages in the Indian and Pacific sectors of the Southern Ocean (Civel-Mazens et al., 2023).

Coccolithus pelagicus subsp. *braarudii*, a temperate water species (Ziveri et al., 2004) was present from south of the STZ to north of the PFZ in the surface sediment, and only holococcoliths in the SAZ were recorded in the plankton sample in the present study. This species has not been previously recorded in the surface waters of the southern Indian Ocean (Mohan et al., 2008; Patil et al., 2017, 2020) and the Pacific sector of the Southern Ocean (Saavedra-Pellitero and Baumann 2015). A possible explanation could be that this species

exists in surface water in low abundance, and only in the austral winter. Their presence in the surface sediments might be a result of the differential dissolution of individual coccolith taxa. Large, heavily calcified, robust coccoliths of *C. pelagicus* can weigh as much as 150 pg whereas those of smaller species such as *E. huxleyi* weigh 2–5 pg (Giraudeau and Beaufort, 2007). This stark variation can result in comparatively better preservation of large, heavily calcified, coccoliths (Findlay and Giraudeau, 2002; Choudhari et al., 2023).

Overall, all coccolithophore species (from the western and eastern transect) decline in abundance from the SAZ to the PFZ, and are entirely absent in AZ. This is mainly due to the N-S decline in calcite saturation in surface waters and surface sediments south of 45 S are below the calcite saturation horizon. STZ and SAZ showed no clear pattern of assemblages and most species were abundant in these zones.

Unlike in the plankton samples, no clear biogeographic distribution of coccolith assemblages according to frontal zones was observed in the sediment samples. Possible explanations for this are the varying dissolution rates in different coccolithophore species, (Boeckel and Baumann, 2004) and varying carbonate saturation of water masses (Samtleben and Schröder, 1992), resulting in the preservation of only robust and heavily calcified species.

5.4.2. Factors responsible for the variation of coccoliths in the surface sediments

Details regarding factors affecting the distribution and concentration of coccoliths on the underlying sediments are relatively scarce. Surface water communities are affected by seasonal variations in oceanographic conditions (Andruleit, 1997), and the response of coccolithophores to these conditions is observed in the productivity, composition, ploidy, and type and morphology of coccoliths. Though coccoliths in the sediment should reflect these conditions (Deuser et al., 1990; Baumann et al., 2005) the interaction of factors such as selective dissolution and the dilution effect (Howard and Prell, 1994; Baumann et al., 2000;

Andruleit et al., 2004), sinking rates (Fischer and Karakaş, 2009), and physical forces alter and weaken their use as proxies in paleoenvironmental reconstructions.

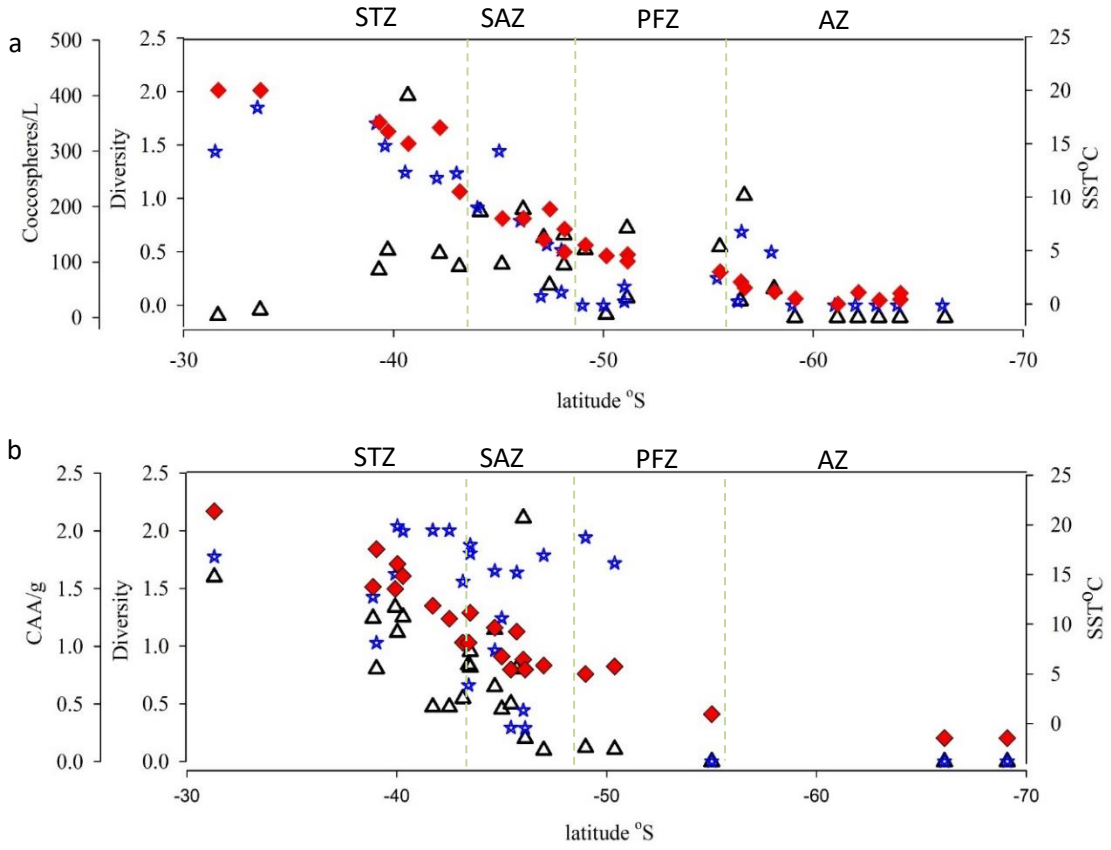

Figure 8. Comparison between plankton (×10^4 coccospheres/L) and surface sediment (×10^4 coccoliths/g) absolute abundance of coccolithophore (triangle), diversity (blue star), temperature (red diamond) a) surface water data b) surface sediment data.

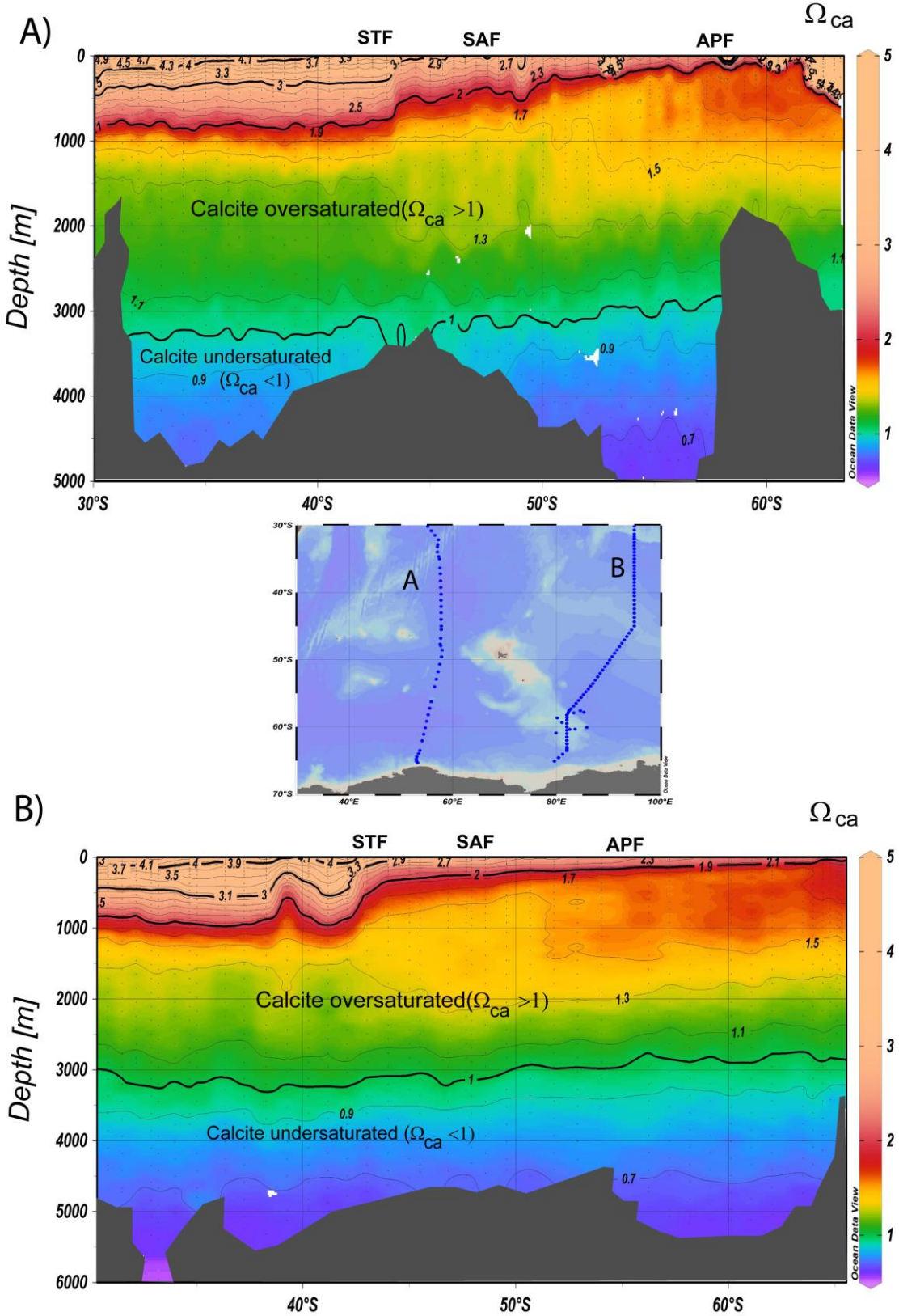

Figure 9. The vertical distribution of the calcite saturation, Ω_{ca}. The Global Ocean Data Analysis Project (GLODAPv2.2021; Lauvset et al., 2021) dataset was used to compute Ω_{ca} using CO2sys.xls (Lewis and Wallace, 1998). Transect A and B are the closest (to the study region) available samples from the GLODAPv2.2021 dataset.

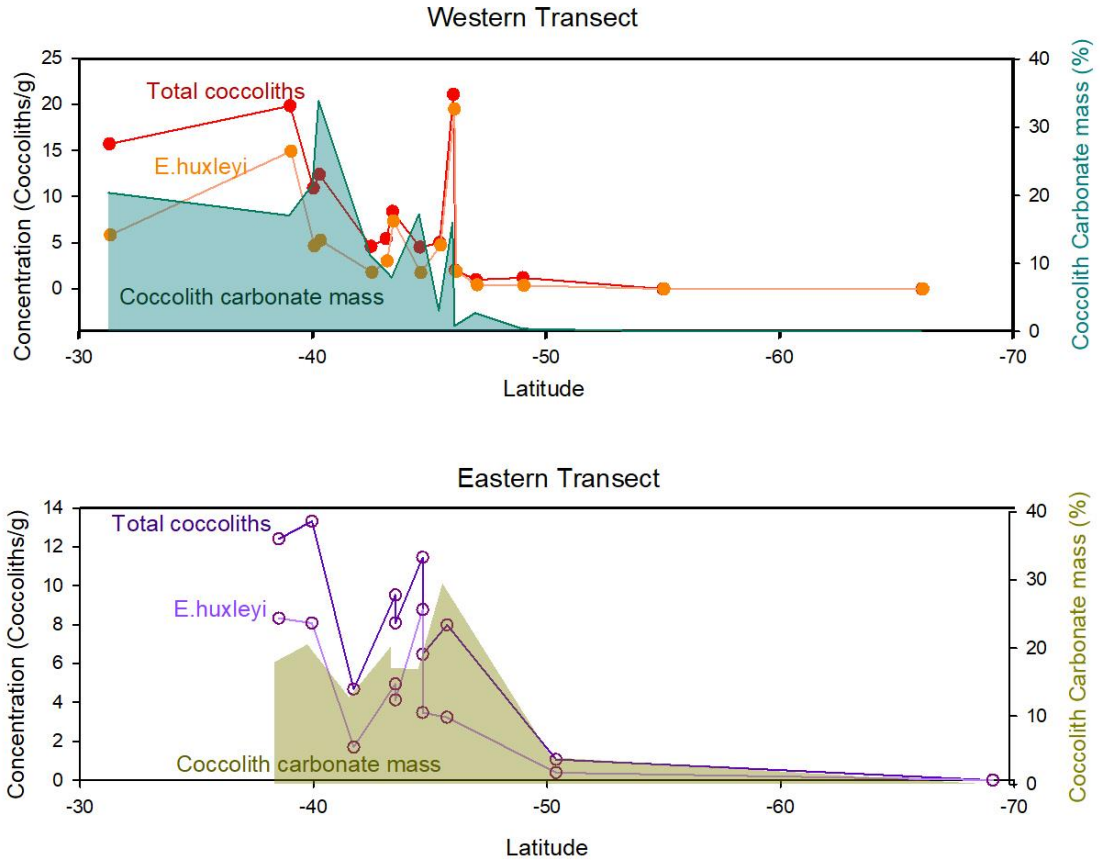

Figure 10. Latitudinal variation in the total coccoliths, *Emiliania huxleyi*, and coccolith carbonate mass from surface sediments of the western (40°E–60°E longitude) and eastern (80°E–100°E) transect of the study region.

In this study, the absolute abundance and diversity of coccoliths in sediment samples was compared with that of coccolithophores in plankton samples. In plankton samples, diversity of living coccolithophores varied with temperature from the STZ to the AZ (Fig. 8a, b). However, the diversity in the surface sediment sample did not show a clear trend from the STZ to the AZ indicating that regional factors affect their composition and preservation. Coccolithophore and coccolith absolute abundance in water and sediment samples varied from high to low concentrations from the STZ to the PFZ A similar trend was recorded in the Pacific sector of the Southern Ocean (Saavedra-Pellitero and Baumann, 2015). However, south of PFZ, where the living assemblage consisted of only *E. huxleyi* type C, the surface sediment was devoid of coccoliths owing to calcite dissolution that occurs at low temperatures and increased pressure (Sulpis et al., 2018) (Fig. 8). Calcite saturation states Ω_{ca} in the surface waters of the

study region display values >1, which generally indicate waters oversaturated with respect to calcite (Feeley et al., 2009). However, the calcite saturation values decrease from STF (Ω_{ca} >3) to APF (Ω_{ca} ~ 2) in surface waters (Fig. 9), which may be responsible for the north-south decline in the coccolithophore abundance in the plankton samples. Values lower than calcite saturation (Ω_{ca} <1) are located below 3200 m at STZ and SAZ, whereas the PFZ and AZ waters are calcite undersaturated below 3000 m depth (Fig. 9). The deeper location of the sediment samples (below calcite saturation depths; <3000–3200 m) and north-south decline in calcite saturation values of the surface waters, together contributed towards the decline in the coccolith abundance from STZ to PFZ sediments and absence of coccoliths in AZ sediments (Fig. 9, 10).

Varying calcium carbonate dissolution rates in deeper waters may alter the taxonomic composition of recent planktonic microfossil assemblages in the surface sediment (Thierstein, 1980). To utilize coccolith assemblages in paleoenvironmental interpretations it is necessary to identify the dissolution effect on the coccolith assemblages. Various coccolith dissolution indices (CEX) are proposed (Matsuoka and Okada, 1991; Dittert et al., 1999; Boeckel and Baumann, 2004). However, in this study, the method prescribed by Dittert et al. (1999), which is based on the differential dissolution between larger robust species *C. leptoporus* and delicate small species *E. huxleyi,* was followed. Most of the samples in STZ, SAZ, and northern PFZ showed good preservation (>0.6), while the southern PFZ and AZ displayed values <0.6 indicating poor coccolith preservation (Fig. 5b). The CEX values lower than 0.6 in the southern PFZ and AZ can be attributed to calcite undersaturation (Ω_{ca} <1) at greater depths (>3000 m) and decreasing values of calcite saturation (Ω_{ca} ~2) in PFZ and AZ waters lowering the abundance *of E. huxleyi* significantly and thereby reducing the CEX (Fig. 9). Earlier studies from in and around Crozet Island (Smith et al., 2017) have reported reduced dissolution indices in the surface sediment samples which may be due to the influence of water masses such as Antarctic bottom waters (Fig. 5b, Fig. 6a, b). However, the application of the coccolith

dissolution index can give an approximation of the extent of dissolution. To obtain more precise results, applying a combination of multiple dissolution proxies, such as *Globigerina bulloides* dissolution index (BDX), foraminiferal fragmentation indices, and carbon rain ratio is required (Boeckel and Baumann, 2004).

Coccolith mass variation in the different species of coccolithophore was estimated. Though *E. huxleyi* makes up the majority of the sinking assemblage in the Southern Ocean, it contributed relatively less to coccolith $CaCO_3$. The major contribution and export of $CaCO_3$ came from less abundant but larger, more heavily calcified species such as *G. oceanica*, *C. leptoporus*, *C. pelagicus*, *H. carteri*, and *U. sibogae* (Fig. 7). This agrees with the results of sediment trap studies in the Australian-New Zealand sector of the Southern Ocean (Boeckel and Baumann, 2004; Rigual Hernández et al., 2020). *Calcidiscus leptoporus* was the major contributor to $CaCO_3$ w%, followed by *G. oceanica*, *H carteri*, *C. pelagicus*, and *U. sibogae*. Total coccolith $CaCO_3$ w% showed a high to low trend from the STZ to the PFZ. However, at a few stations in the SAZ, lower concentrations were recorded. Total coccolith $CaCO_3$ w% follows a north-south trend similar to the calcite saturation states (Fig. 9, 10) indicating that the declining calcite saturation values in the surface waters and undersaturated deeper ocean can lead to lower coccolith carbonate mass in the PFZ. The $CaCO_3$ w% calculated here does not project the total contribution in its entirety as seasonal variations in the morphotypes and different degrees of calcification of coccoliths (Poulton et al., 2011) cannot be determined in the sediment. Typically, only complete coccoliths are taken into consideration for the calculation of coccolith mass and detrital coccoliths are overlooked (Boeckel and Baumann, 2004). Coccolith mass of individual species also differs based on the method used. For example, the mass estimation by morphometric approach shows two-fold higher values than with the birefringence approach (Charalampopoulou et al., 2016; Saavedra-Pellitero et al., 2019, Rigual Hernández et al., 2020).

5.4.3. Factors affecting paleoceanographic implications

The balance between $CaCO_3$ production in supersaturated surface waters and dissolution in under-saturated deep water regulates $CaCO_3$ production (Farrell and Prell, 1989). Coccolithophore production in surface water and dissolution and dilution in the surface sediment of the ocean floor controls the accumulation of coccoliths (Flores et al., 2003). Understanding the nature of present and past carbonate chemistry is essential as the sedimentary records of coccoliths are applied for paleoenvironmental reconstructions (Barbosa, 2009; Baumann et al., 2005). However, the interpretation of coccolith fossil records could be challenging owing to their ecological and physiological response to the environmental conditions during their lifecycle and preservation in the ocean sediments. The coccolithophore productivity in the surface waters shows seasonal variations, which is a likely cause for the significant differences in species composition between the sampling periods (Friedinger and Winter, 1987). Seasonal changes in the position, temperature, and alkalinity of the oceanic fronts (e.g., Kostianoy et al., 2004; Bakker et al., 2014; Freeman et al., 2016; Balch et al., 2016; Pauthenet et al., 2018), intensity and extent of ocean currents such as the Agulhas current (Lutjeharms, 2006; Krug and Tournadre, 2012) which transfers excess equatorial heat to mid and high latitudes (Colling, 2001; Imawaki et al., 2013). Recurring eddy formations and meandering of water masses and associated plankton activity as a result of the interaction of the Antarctic Circumpolar Current with islands and complex dynamics of fronts and bathymetry (Durgadoo et al., 2010) play a crucial role in the variation of coccolithophore composition in the surface waters. Apart from abiotic factors biological factors such as competition, grazing pressure, and viral lysis also alter the coccolithophore composition in the surface waters (Nissen et al., 2018). According to Margalef's mandala, a seasonal succession from diatoms to coccolithophores occurs when nutrient levels decrease and light levels increase (Margalef, 1978). Microzooplankton exert grazing pressure on phytoplankton and control the total

phytoplankton biomass and composition (Le Quéré et al., 2016). Major groups like tintinnid ciliates and dinoflagellates significantly control pico- and nanophytoplankton stocks in the Southern Ocean (Fronemann, 2004; Mayers et al., 2019).

On one hand, zooplankton grazing impacts coccolithophore assemblage in surface water causing variation in the coccolithophore composition due to selective grazing. On the other hand, aggregated coccoliths and coccospheres in zooplankton faecal pellets generally aid in the rapid transport through the undersaturated waters to the sea floor resulting in good preservation (Honjo, 1976; Honjo and Roman, 1978). However, in the upper 500 m, reduced coccolith and coccosphere abundance due to consumption and acid gut dissolution, defecation, and aggregation, has also been observed (Sherrell et al., 1998; Thomalla et al., 2008).

In the sediment samples coccolith assemblages are prone to differential dissolution due to the varying carbonate saturation state of overlaying bottom water masses (Gottschalk et al., 2018; González-Dávila et al., 2011), dilution by siliceous phytoplankton like diatoms, and various inputs from other sediment components (Boeckel et al., 2006). Erosion and reworked sediment also affect the coccolith assemblages (Findlay and Giraudeau, 2002).

All these factors influence the diversity pattern and abundance of coccolithophore assemblages in the sediment. As the surface sediment coccolith composition is the representation of accumulation over time, it is essential to take these factors into consideration for the application of the coccolith record in paleoenvironmental reconstruction. To obtain a clearer idea of factors regulating coccolithophore abundance and diversity in the southern Indian ocean year-round sediment trap studies are required to understand the influence of abiotic (such as effects of water masses, seasonal variations, and dissolution) and biotic factors (such as grazing pressure, dilution by other groups) on coccolithophore assemblages.

5.5 Conclusion

From 25 surface sediment samples analysed from the southern Indian Ocean, a total of 21 coccolithophore species were recorded. Total coccolith absolute abundance showed decreasing pattern from STZ to PFZ like that in the plankton samples. However, a clear pattern in the coccolith assemblage was not observed.

In the further south in the PFZ and north of the AZ, samples are barren of coccolith as a result of dissolution due to the calcite under-saturated bottom water masses.

Diversity along the frontal zones showed no clear pattern, number of species in surface sediment was less compared to plankton samples. Species that form delicate coccoliths (*Acanthoica* spp., *Algirosphaera* spp., *Alisphaera* spp., *Syracosphaera* spp., *Michaelsarsia* sp.) were absent in the surface sediment. However, some species recorded in the surface sediment sample (*G. oceanica, C. pelagicus* subsp. *braarudii*, *F. profunda*, *R. clavigera*, *Reticulofenestra* sp.) were not found in the plankton samples.

Warm water species such as *G. oceanica* and *F. profunda* were found in the PFZ, Additionally, abundance of warmer water species was higher in the eastern transect compared to the western transect, indicating influence and transport of the species via warm water currents such as the Agulhas Return Currents, and the Indonesian throughflow and associated eddies. This suggests regional factors affecting the coccolithophore production in surface water and accumulation on the sea floor and selective dissolution over time.

CEX values indicate that coccoliths were well preserved in STZ, SAZ, and northern PFZ. However, lower than 0.6 values in the southern PFZ and AZ suggest poor coccolith preservation. For precise results on calcite dissolution applying a combination of multiple dissolution proxies is required.

Total coccolith carbonate mass decreases from the STZ to the PFZ, owing to decreased calcite saturation states in the surface and calcite undersaturated (Ω_{ca} <1) deeper waters. Less abundant, larger species such as *C. leptoporus* and *C. pelagicus* subsp. *braarudii* contributed more to coccolith mass than more abundant species such as *E. huxleyi*.

To understand the factors affecting the diversity of fossil coccolith assemblages in the surface sediments long-term studies involving sediment traps are essential.

Chapter 6

Variations in the Southern Ocean carbonate production, preservation, and hydrography for the past 41, 500 years: Evidence from coccolith and $CaCO_3$ records

6.1. Background and rationale

The elevated levels of carbon dioxide (CO_2) in the atmosphere due to anthropogenic industrial activities since the beginning of the industrial era have impacted the marine ecosystem in diverse ways, including increasing sea surface temperature, decrease in carbonate ions [CO_3^{2-}], and surface ocean pH (ocean acidification) (Rost and Riebesell, 2004; IPCC, 2013). It has been suggested that these changes will have a major bearing on calcifying organisms such as corals, pteropods, planktonic foraminifera, and coccolithophores, with reductions in their rate of calcification under the future ocean acidification circumstances (Bijma et al., 2002; Langdon and Atkinson, 2005; Orr et al., 2005; Bach et al., 2015; Meyer and Riebesell, 2015). Due to its low temperature and moderate alkalinity, the Southern Ocean will likely become undersaturated with aragonite and calcite by 2040 and 2100, respectively (Cao and Caldeira, 2008; McNeil and Matear, 2008; Shadwick et al., 2013). This will lead to the dissolution of aragonite and calcite shells, thus making it difficult for calcifiers inhabiting the Southern Ocean to biologically precipitate carbonate (Gattuso and Hansson, 2011). Since ocean acidification occurs faster in polar oceans, the Southern Ocean is expected to be an early indicator of the ocean acidification imprints on the marine ecosystem at the mid and low latitudes (Fabry et al., 2009; Krumhardt et al., 2020).

The Southern Ocean has received much attention in palaeoceanographic research, precisely for its role in the reduction of CO_2 during glacial periods (Moore et al., 2000; Sigman et al., 2010; Martínez-Garcia et al., 2011; Watson et al., 2015). Studies explaining the glacial drawdown of atmospheric CO_2 invoke a reduction in Southern Ocean surface CO_2 driven by increased productivity, ocean circulation changes, and global ocean alkalinity (Boyle, 1988; Boyle, 1989; Broecker and Peng, 1989). Ocean alkalinity is mainly regulated by a balance between carbonate fluxes from river inflow and carbonate removal through burial flux (Boyle, 1988; Toggweiler, 1999; Rickaby et al., 2010; Sigman et al., 2010; Kobayashi and Oka, 2018;

Kobayashi et al., 2021). Carbonate burial flux is determined by carbonate flux reaching the deep sea and deep ocean carbonate saturation. During the glacial conditions, the increased accumulation of dissolved CO_2 led to acidic conditions in the deep ocean, causing the dissolution of carbonates. This has led to the imbalance between riverine input and burial removal of carbonates (i.e., riverine input exceeds the burial removal of carbonates) and resulted in the increase in ocean alkalinity, which partly explains glacial atmospheric CO_2 drawdown (Sigman et al., 2010; Kobayashi et al., 2021).

Coccolithophores, with the maximum abundance and diversity, are the most significant carbonate-producing phytoplankton group in the subantarctic region of the Southern Ocean and play a complex role in the carbon cycle (Trull et al., 2018; Rigual Hernandez et al., 2020). They are known to decrease surface ocean alkalinity through calcite production and reduce the uptake of atmospheric CO_2 by the ocean. On the other hand, the organic matter production via photosynthesis and its burial in an ocean and the long-term preservation of carbon in the form of $CaCO_3$ in coccoliths in the ocean sediments enhance carbon sequestration (Volk and Hoffert, 1985; Baumann et al., 2005). However, the role of carbonate production, by coccolithophores, as a source of pCO_2 depends on the ratio of calcification to photosynthesis (Frankignoulle et al., 1994; Delille et al., 2005). The response of coccolithophores to the changing environmental conditions is recorded by coccolith abundance in the sediment; thus, they serve as a robust proxy for paleoceanographic reconstruction (Baumann et al., 1999; Ziveri et al., 2004; Boeckel et al., 2006). Through their abundance and distribution, coccolithophores have a substantial role in Southern Ocean carbonate chemistry and act as indicators of surface ocean changes.

In this study, we aim to understand the factors responsible for the coccoliths and $CaCO_3$ burial in the subantarctic sediments of the Indian sector of the Southern Ocean during the span of 41,500 years before the present (41.5 ka BP). Our study also focuses on paleoceanographic changes in the Agulhas region and the Agulhas Return Current, recorded by the warmer

coccolithophore assemblage from the subtropical South Indian Ocean and present study area. To achieve the objectives of the study we used coccolith abundance records, sizes of *Coccolithus pelagicus* subsp. *braarudii*, coccolith carbonate masses, dissolution and diversity indices.

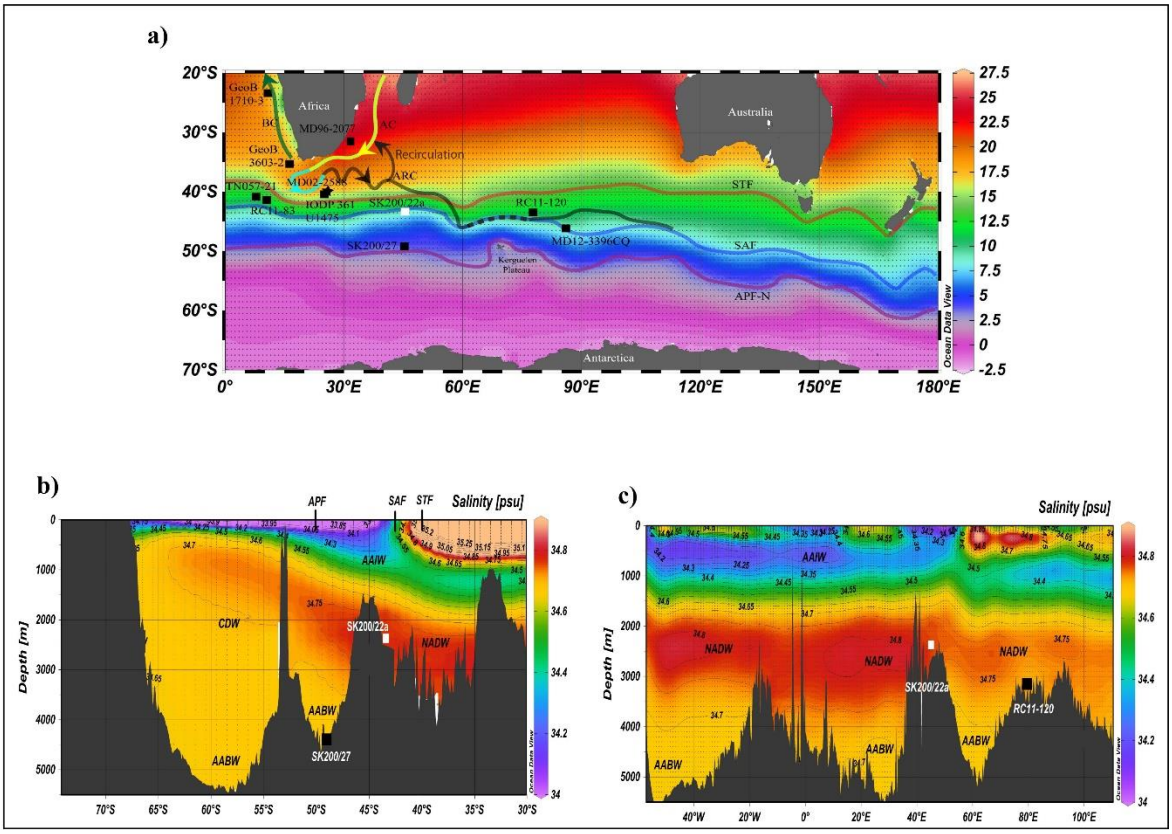

Figure 1. Location of core SK200/22a (white square) and supporting data (black square) shown on a (a) background map of annual mean sea surface temperature derived from World Ocean Atlas 2018 (Garcia et al., 2019) and gridded with Ocean Data View software (Schlitzer, 2021), (b) 45◦E longitudinal hydrographic section of annual mean salinity (Garcia et al., 2019) and (c) 43.5◦S latitudinal hydrographic section of annual mean salinity (Garcia et al., 2019). Positions of the Subtropical front (STF; red line) and Subantarctic front (SAF; blue line) is shown after Orsi et al. (1995). The Agulhas Current (AC; yellow line), Agulhas Return Current (ARC; black line) is marked based on Graham and De Boer (2013) and Benguela Current (BC; dark green line) is shown after Wedepohl et al. (2000). The Antarctic Polar Front (APF; pink line) is located based on Sokolov and Rintoul (2009b). The North Atlantic Deep Water (NADW), Circumpolar Deep Water (CDW), Antarctic Intermediate Water (AAIW) and Antarctic Bottom Water (AABW) are marked after Emery (2001).

6.2. Materials and methods

A marine sediment core, SK200/22a, 7.54 m long, was recovered onboard ORV Sagar Kanya from north of the Del Ca˜no Rise, just south of the SAF (43°42′ S, 45° 04′ E; 2730 m water depth) in the Indian Sector of Southern Ocean during the Indian Southern Ocean Expedition (Fig. 1a). For the present study, only the top 3 m section of the core was utilized. Core lithology varied significantly and was comprised of calcareous white to light grey sandy silt/clay at the top 115 cm (Thamban et al., 2005; Manoj et al., 2012). A dark greyish band dominated by silty-clay was present between depths of 130 and 148 cm. Below this depth, the sediments were dominated by light grey clays. The chronology of the sediment core section was determined by accelerator mass spectrometry (AMS) ^{14}C dating of handpicked tests of the foraminiferal taxa, *Globigerina bulloides* and *Neogloboquadrina pachyderma* (Manoj et al., 2012; Manoj and Thamban, 2015). The age model for the sedimentary sequence of the core has been described previously by Manoj and Thamban (2015). The youngest sediment date is 2.764 ka, and the oldest is 41.5 ka (Manoj and Thamban, 2015; Nair et al., 2015). The sedimentation rate varied significantly for the top 3 m section, with values ranging from 8 to 17 cm/kyr during the Holocene, 3–10 cm/kyr during the deglacial, and 1–55 cm/kyr during the glacial period. The sample resolution ranged from 56 to 112 years/cm during the Holocene, 97–264 years/cm during the deglacial, and 18–1000 years/cm during the glacial.

6.2.1 Sample preparation and identification of coccoliths

Permanent slides were prepared at every 2 cm interval and at times at 4 cm intervals of the sediment cores following the technique described by Flores and Sierro (1997). The slides were observed under a polarizing microscope (Axio Scope A1, Zeiss Microscopes) at 1000× magnification. A minimum of 400 coccoliths in each sample were counted. The identification of coccoliths was carried out according to identification keys on

https://www.mikrotax.org/Nannotax3/index.html (Young et al., 2017) and previously published literature (Young et al., 2003; Frada et al., 2010). The coccolith absolute abundance (CAA) per gram of sediment, Coccolith diversity, Coccolith dissolution index was calculated. further coccolith morphometric measurements were also taken using an Olympus polarizing microscope (Olympus BX51) at 1000 × magnification connected to (Olympus 0733 camera) and CellSens microscope imaging software. Additional details of methodology are provided in Chapter 2.

6.3 Results

6.3.1. Down core variation of coccolith absolute abundance and diversity

The coccolith records from the core SK200/22a displayed a distinct glacial-Holocene trend for the last 41.5 ka (Fig. 2). A contrasting pattern was observed between coccolith diversity and CAA variations from glacial to Holocene (Fig. 2a; b). During glacial periods, coccolith diversity was the highest, with a diversity index of approximately 2, whereas the CAA was the lowest, with values ranging from 0 to 2 × 10^9 coccoliths/g of sediments. In contrast, the deglacial recorded a gentle drop in the coccolith diversity (2–1.5) and a steady increase in the CAA (0–4 × 10^9 coccoliths/g). This was followed by a rapid decrease in coccolith diversity (from 1.5 to 0.5) and an immediate rise in the CAA (from 4 to 12 × 10^9 coccoliths/g) during the Holocene.

6.3.2 Glacial-Holocene changes in abundances of coccolith assemblages

The coccolith assemblages in the core SK200/22a are comprised of a warm tropical-subtropical group, a relatively colder Subantarctic Zone (SAZ) group, and species such as *E. huxleyi* with a broader ecological range. The tropical-subtropical assemblage— *Florisphaera profunda, Gephyrocapsa oceanica, Umbilicosphaera sibogae*— (Flores et al., 1999) had

distinctly higher (10–13%; 0.4–1.8 × 10^9 coccoliths/g) average abundance during the glacial and deglacial periods as compared to the Holocene (Fig. 2d–f), whereas the Holocene recorded an average relative abundance of <4% (and absolute abundance of approximately 1 × 10^9 coccoliths/g) of tropical-subtropical assemblage. *G. oceanica* was a dominant species in this assemblage with an average relative abundance of 5% compared to *F. profunda* (average 2.5%) and *U. sibogae* (average 1.3%) for the entire 41.5 ka BP period. Unlike tropical-subtropical assemblage, within the SAZ group, species such as *Calcidiscus leptoporus* and *G. muellerae* (Saavedra-Pellitero et al., 2014) rarely displayed a glacial-Holocene trend, except for the species *C. pelagicus* subsp. *braarudii* (Fig. 2c; g; h).

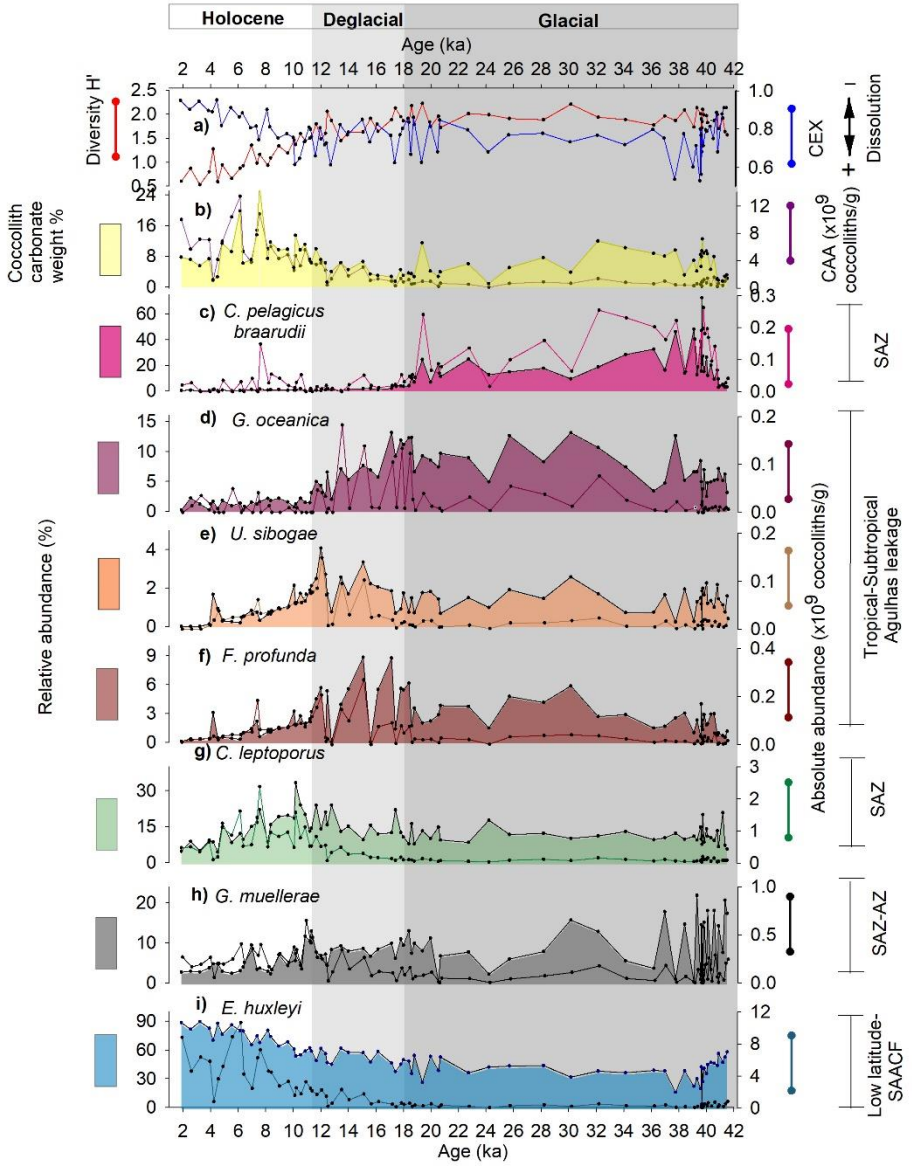

Figure 2. Coccolith records from Sk200/22a sediment core. (a) Shannon–Wiener diversity index and coccolith dissolution index (CEX) (b) Total Coccolith Absolute Abundance (CAA) per gram of sediment and coccolith carbonate weight percent, relative abundance (%) and CAA (per gram of sediment) of coccolith assemblages (c) *C. pelagicus* ssp. *braarudii*, (d) *G. oceanica*, (e) *U. sibogae*, (f) *F. profunda*, (g) *C. leptoporus* , (h) *G. muellerae* and (i) *E. huxleyi*. Dark grey, light grey and white band indicate glacial period, deglacial phase, and Holocene respectively.

A highly calcified and large coccolith species, *C. pelagicus* subsp. *braarudii* (Rigual Hernandez et al., 2020), had the highest occurrences during the glacial period (5–72%; 0–0.24 × 10^9 coccoliths/g) and were nearly absent (< 1%; < 0.1 × 10^9 coccoliths/g) during the deglacial and Holocene phases (Fig. 2c). The variation in the relative abundance of *G.*

muellerae generally was higher during the glacial period (0–20%) and more stable during the deglacial period (approximately 10%), whereas the Holocene exhibited intermediate variation (3–10%) in the abundance of this species (Fig. 2h). The relative abundance of *C. leptoporus* displayed minimal variation between the glacial and deglacial periods, whereas the highest variation (5–34%) was recorded during the Holocene (Fig. 2g). *E. huxleyi* is a species with ubiquitous distribution and a broad ecological range in the modern ocean, from low latitudes to the southern boundary of the Antarctic Circumpolar Current (Boeckel, 2002; Charalampopoulou, 2011; Vollmar et al., 2021), was the dominant species throughout the core SK200/ 22a, with relative abundance ranging from 20 to 90% (Fig. 2i). The absolute abundance of *E. huxleyi* varied like the CAA which suggests that this species contributes significantly to total coccolith variation in the sediment core (Fig. 2 b, i). In contrast to *C. pelagicus* subsp. *braarudii*, *E. huxleyi* is a smaller and weakly calcified coccolith species (Boeckel, 2002; Rigual Hernandez et al., 2020) and displayed a trend opposite to that exhibited by *C. pelagicus subsp. braarudii*, with lower abundance during the glacial (20–40%; $< 1 \times 10^9$ coccoliths/g) than during Holocene (60–90%; $2–11 \times 10^9$ coccoliths/g).

6.3.3 Coccolith carbonate mass variation

The coccolith carbonate mass (%) varied between 0 and 10% from glacial to Holocene (Fig. 2b). Major contribution to the coccolith carbonate was by *C. leptoporus* (~ 60%) and *C. pelagicus subsp. braarudii* (~80%) during the Holocene and glacial period, respectively (Fig. 3). The contribution of coccoliths to the total carbonate fraction is minimal (<30%) throughout the sediment core, with occasionally >30% contribution during the glacial period (Fig. 3a). During the glacial period, the highest contribution to total $CaCO_3$ by coccoliths was 49% and 58% at 32 ka and 30 ka respectively.

6.3.4 Changes in *Coccolithus pelagicus* subsp. *braarudii* size

The size parameters viz. distal length (DL), distal width (DW), central length (CL), and central width (CW) of the *C. pelagicus* subsp. *braarudii* displayed significant glacial-Holocene variation for the last 41.5 ka (Fig. 3d-e). During the glacial period, the values of the distal parameters of this coccolith species were the lowest (DL ~ 12.5 µm; DW ~ 10.5 µm), whereas the last deglaciation and Holocene exhibited the highest values of the DL and DW (DL > 12.5 µm; DW > 10.5 µm). Similarly, the parameters (CL and CW) of the central part of this species showed lower (CL < 5.5 µm; CW < 3.5 µm) and higher (CL > 5.5 µm; CW > 3.5 µm) values during the glacial and Holocene, respectively. The only difference between the variation in the distal (DL and DW) and central (CL and CW) size parameters of the coccolith is that the distal parameters increased at the beginning of the last deglaciation. In contrast, the central area grew at the start of the Holocene (Fig. 3).

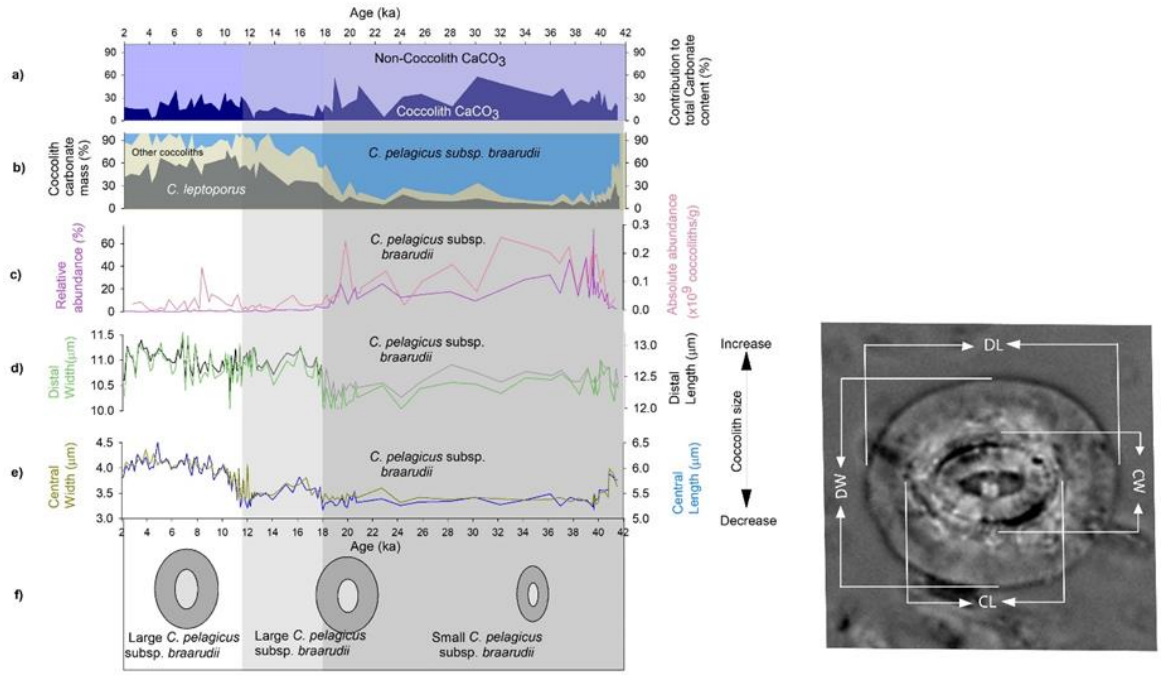

Figure 3. a) Coccolith contribution to the total $CaCO_3$ content (%), b) Coccolith Carbonate mass (%) of *C. leptoporus*, *C. pelagicus* subsp. *braarudi*, and other coccoliths, c) *C. pelagicus* subsp. *braarudi* abundance, d) *C. pelagicus* subsp. *braarudi* distal width and length, e) *C. pelagicus* subsp. *braarudi* central width and length and f) Schematic changes in the sizes of *C. pelagicus* subsp. *braarudi*. The figure on the lower right is the light

microscope image of *C. pelagicus* subsp. *braarudi* with different size parameter indicated. Dark grey, light grey and white band indicate glacial period, deglacial phase, and Holocene respectively.

6.4 Discussion

The coccolith records from the Subantarctic Zone (SAZ)/northern Polar Frontal Zone (PFZ) core SK200/22a displayed a clear glacial to Holocene variability (Fig. 2). The most significant aspect was the increased diversity of the coccoliths accompanied by low CAA during the glacial period when the APF was at its northerly position. This was followed by a drop in the coccolith diversity as the CAA, characterized by a nearly monospecific assemblage dominated by *E. huxleyi*, rose to higher values during the Holocene subantarctic conditions (Fig. 2a). This contrasts with earlier studies (Mohan et al., 2008; Saavedra- Pellitero et al., 2014; Patil et al., 2017; Rigual Hernandez et al., 2018, 2020) which reported a higher coccolith diversity in SAZ and *E. huxleyi*-monospecific assemblage south of APF. The increased coccolith diversity in the glacial sediments could primarily be a consequence of the low relative abundance of the *E. huxleyi* and the high relative abundance of warm tropical-subtropical coccolith species (*G. oceanica*, *F. profunda* and *U. sibogae*) during the glacial period as compared to the Holocene (Fig. 2d–f; i). The low relative abundance of *E. huxleyi* in the glacial sediments could result from poor $CaCO_3$ preservation due to the dissolution effect (Howard and Prell, 1994: Sigman et al., 2010; Gottschalk et al., 2018; Kobayashi et al., 2021). As far as the glacial rise in the proportion of tropical-subtropical assemblage is concerned, it could be related to the strength of Agulhas Return Current (Civel-Mazens et al., 2021) and will be discussed in detail in a later section. The low absolute abundance of *E. huxleyi* and total coccolith concentrations in the glacial sediments could be related to the decreased coccolithophore productivity (Quere et al., 2005; Sinha et al., 2010; Rigual Hernandez et al., 2020), dilution by biogenic silica in the glacial sediments (Howard and Prell, 1994) and dissolution (Howard and Prell, 1994: Sigman et al., 2010; Gottschalk et al., 2018; Kobayashi et al., 2021). In addition,

the low *E. huxleyi* and total coccolith concentrations coincide with the enrichment of heavily calcified taxa, *C. pelagicus* subsp. *braarudii*, in the glacial sediments, which underscores the role of dissolution-related changes in the coccolith assemblages.

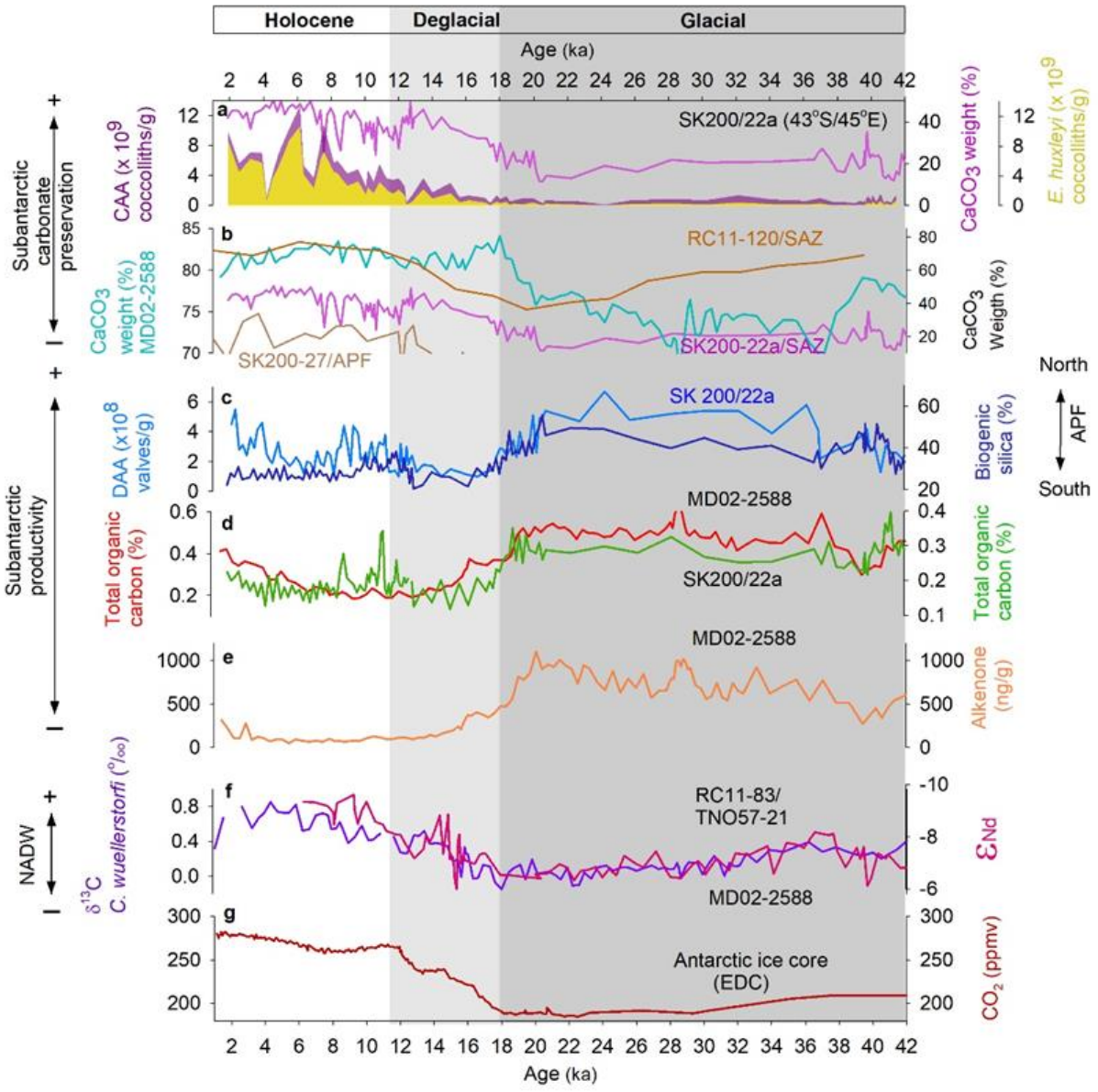

Figure 4. a) Glacial-Holocene changes in E. huxleyi absolute abundance(coccoliths per gram of sediment), total coccolith absolute abundance (CAA) (per gram of sediment) and $CaCO_3$ weight (%) (Manoj and Thamban, 2015) at SK200/22a site, (b) Calcium Carbonate weight (%) from SK200/22a (Manoj and Thamban, 2015), RC11–120 (Kent, 1982; Howard and Prell, 1994), SK200/27 (Manoj and Thamban, 2015) and MD02–2588 (Romero et al., 2018a, 2018b), (c) Diatom absolute abundance (DAA) (Nair et al., 2015) and biogenic silica (Manoj and Thamban, 2015), (d) Total organic carbon (%) (Romero et al., 2018a, 2018b; Manoj and Thamban, 2015) (e)

Alkenone (ng/g) (Romero et al., 2018a, 2018b). (f) *C. wuellerstofi* δ13C (Starr et al., 2020) and water mass source indicator εNd (Piotrowski et al., 2008), (g) Atmospheric CO_2 from Antarctic EDC ice core (Petit et al., 1999; Monnin et al., 2001; Pepin et al., 2001; Raynaud et al., 2005). Dark grey, light grey and white bands indicate glacial period, deglacial phase, and Holocene respectively, while the horizontal bands indicate SST for SAF (red band) and APF-N (blue band).

As mentioned in section 4.3, the contribution of coccoliths to the total carbonate fraction is minimal (<30%) throughout the sediment core, with occasionally higher than 30% contribution during the glacial periods (Fig. 3a). So, throughout the core SK200/22a, heterotrophic calcifiers (i.e., foraminifera and pteropods) are major contributors to the total $CaCO_3$. The contribution of coccolith to the total carbonate decreases from glacial (average 30%) to Holocene (average 18%), which could result from the decline in the abundance of heavier and larger coccolith species, *C. pelagicus* subsp. *braarudii*, from the glacial to Holocene period (Fig. 3c). Additionally, the coccolith carbonate do not covary with the CAA in the core since different coccolith species contribute to these two parameters. The CAA variation is primarily a result of changes in the *E. huxleyi* population, whereas *C. leptoporus* and *C. pelagicus* subsp. *braarudii* mainly make up the coccolith carbonate content (Fig. 3). The non-carbonate and non-biogenic opal fractions vary between 20 and 50% and are more likely to be representing the silt content in the sediments (Manoj et al., 2012). Here we focus on understanding the role of carbonate productivity, preservation, dissolution, and dilution in the downcore variation of coccolith abundance, sizes, and $CaCO_3$ concentrations in the Indian Sector of the Southern Ocean. We also focus on the glacial-Holocene changes in ARC strength based on the abundance of tropical-subtropical coccolith assemblage.

6.4.1. Glacial-Holocene changes in coccolithophore and carbonate production and preservation

The fate of coccoliths and carbonate content (carbonate burial) in the deep-sea sediments are mainly decided by the factors such as dilution by non-carbonate material like

diatoms, surface water carbonate productivity (carbonate flux reaching the ocean bottom) and dissolution (via changes in carbonate saturation) in the deep waters, water column and pore waters (Gottschalk et al., 2018). The low concentration of coccoliths and $CaCO_3$ in the glacial sediments of the core site SK200/22a could result from these factors. The sediment trap studies from the Subantarctic, Polar Frontal, and Antarctic Zones by Rigual-Hernandez et al. (2015); Rigual-Hernandez et al. (2015); Rigual Hernandez et al. (2018, 2020) suggest the decline in the coccolith and carbonate export fluxes from SAZ to Antarctic Zone is due to the decrease in their production. Likewise, during the glacial period, when the APF was shifted northward (Manoj and Thamban, 2015; Nair et al., 2019), the present core site resembled the modern-day APF thereby recording lower coccolith and $CaCO_3$ content. The proxies of subantarctic export production indicated high diatom export production owing to the increased dust flux and northward shift of APF along with nutrient replete southern sourced waters during the glacial period (Anderson et al., 2014; Jaccard et al., 2013 Chase et al., 2014; Romero et al., 2015; Fig. 4). We speculate that increased diatom population in SAZ waters, could have led to the reduced coccolithophore biomass through competition for light and nutrients (Quere et al., 2005; Sinha et al., 2010; Rigual Hernandez et al., 2020) despite high nutrient stock during glacial times (Robinson et al., 2005; Sigman et al., 2010). Additionally, the increase in biogenic silica content in the glacial sediments introduces a dilution effect which could be responsible for the lower coccolith and $CaCO_3$ concentrations in the glacial sediments compared to the Holocene (Howard and Prell, 1994).

The similarity between the variation of carbonate records from the present study site and core sites from the Atlantic sector (Gottschalk et al., 2018) hints toward an association of sedimentary carbonate dissolution with the water masses dynamics (AMOC variability) and changes in the carbonate saturation state of the bottom waters (Gottschalk et al., 2018). The study site is currently bathed by North Atlantic Deep Water (NADW) which has high carbonate

ion [CO_3^{2-}] concentration along with a calcite oversaturation state (Ω = 1.4) (Gonzalez-Davila et al., 2011). During the peak glacial condition (19–30 kyr) the weaker Atlantic Meridional Overturning Circulation possibly led to the shallowing of NADW (Fig. 4f) and occupation of the present core site by southern sourced water masses such as Lower Circumpolar Deep Waters (CDW) and Antarctic Bottom Waters (AABW) (Fig. 5b). The southern sourced water masses with the typical low [CO_3^{2-}] and undersaturated calcite (Gonzalez-Davila et al., 2011; Gottschalk et al., 2018) might have promoted the carbonate dissolution leading to decreased carbonate burial at the present core site during the peak glacial (Fig. 5b). In contrast, during the Holocene, strengthened AMOC conditions and the presence of carbonate saturated northern sourced water (NADW) (Bohm et al., 2015) in Southern Ocean have been posited as an explanation for the better preservation of $CaCO_3$, leading to the higher values of carbonate weight percentage and coccoliths (CAA) at SAZ (Fig. 5a). Thus, coccolith and $CaCO_3$ records reveals a strong association of carbonate burial with AMOC strength via changes in NADW flux in Southern Ocean (Howard and Prell, 1994; Rickaby et al., 2010).

The carbonate saturation state of bottom waters is also affected by the dissolution (decomposition) of organic carbon (C_{org}), which is transferred to the deep ocean through the sinking-biological pump (Sigman et al., 2010; Kobayashi et al., 2021). During the peak glacial conditions, a stronger biological pump in the SAZ (Fig. 4c–e) resulted in the reduced concentration of CO_2 and higher alkalinity in the surface waters, which could have partly contributed to the glacial drawdown of atmospheric CO_2 (Fig. 4g; 5b). But the increased decomposition of C_{org} led to the rise in the concentration of respired CO_2 in deep waters. This combined with the strong stratification in the glacial Antarctic Zone probably resulted in the increased storage of CO_2 in the deep Southern Ocean accounting for the reduced carbonate saturation of deep ocean and the shoaling of the lysocline (Sigman et al., 2010; Sigman et al., 2021; Kobayashi et al., 2021). Carbonate undersaturated deep ocean contributed to reduced

carbonate burial resulting in lower values of carbonate weight percentages and coccolith abundance in the glacial sediments, as evident from our core site. During the peak glacial, the decreased burial of $CaCO_3$ in SAZ had far-reaching consequences on ocean alkalinity and atmospheric CO_2 drawdown. Ocean alkalinity is determined by the balance between riverine carbonate input and carbonate burial, where the former increases the ocean alkalinity and the latter decreases the alkalinity (Sigman et al., 2010; Kobayashi et al., 2021). Since the carbonate burial is the primary mechanism through which the ocean loses alkalinity, the reduction in carbonate burial during the glacial period caused excess input of carbonates to the ocean through riverine inflow, which led to the rise in ocean alkalinity (Sigman et al., 2010; Kobayashi et al., 2021). During the Holocene, a state of equilibrium was reached gradually as the increased whole ocean alkalinity relaxed the imbalance between riverine flow and burial removal of carbonate. This was achieved by restoring the deep ocean CO_3^{2-} (carbonate saturation) and increasing the carbonate burial (a process known as carbonate compensation) after a 10,000-year scale of adjustment since LGM, but by that time, the atmospheric pCO_2 was already reduced (Kobayashi et al., 2021). So, during the glacial period, the stronger biological pump reduces the atmospheric pCO_2 by 1) decreasing the CO_2 concentration in the surface ocean and 2) increasing whole ocean alkalinity (Sigman et al., 2010).

Our observation indicates that the glacial-interglacial changes in the carbonate content in the Atlantic (Hodell et al., 2003) and Indian SAZ (Howard and Prell, 1994; Manoj and Thamban, 2015) were primarily governed by variation in the deep ocean carbonate saturation via changes in AMOC and C_{org} dissolution. However, not all the SAZ sites of the Southern Ocean follow the same ocean processes. The deeper (>4000 m) Atlantic northern SAZ sites, such as ODP 1089, recorded high $CaCO_3$ content during the glacial periods (Rickaby et al., 2010), which was linked to two factors. Firstly, increased coccolithophore and carbonate productivity owing to the northward shift of Antarctic divergence (upwelling zone) (Flores et

al., 2012). Secondly, better preservation due to the higher alkalinity Weddell Sea water (AABW) replacing the lower alkalinity CDW during the glacial periods (Rickaby et al., 2010). Likewise, shallow (<1000 m) SAZ site from the southeast Pacific recorded increased fluxes of organic carbon, opal, $CaCO_3$, and coccoliths indicating high export production as a result of increased supply of nutrients from the northward displacement of ACC (Saavedra-Pellitero et al., 2011; Chase et al., 2014). Unlike the site SK200/22a, the southeast Pacific did not record the glacial decline in the carbonate content due to respiratory calcite dissolution despite the high export production. This might be due to the shallower depth of the Southeast Pacific core site, well above the carbonate lysocline depth (~3500 m), that might have promoted better carbonate and coccolith preservation (Broecker and Broecker, 1974; Berger et al., 1976).

The carbonate records in the northern Antarctic zone and APF mainly signal changes in carbonate productivity rather than preservation (Howard and Prell, 1994; Manoj and Thamban, 2015). This is evident in the carbonate records from APF site SK200/27 (>4000 m) (Manoj and Thamban, 2015). During the glacial period, despite the influence of high alkaline AABW (compared to CDW) (Fig. 1b) (Rickaby et al., 2010), this site recorded low $CaCO_3$ concentration (Fig. 4) (Manoj and Thamban, 2015). While during the Holocene, the site was influenced by the relatively less alkaline lower CDW and recorded higher $CaCO_3$ concentration (Fig. 5; 45°E longitudinal transect) (Rickaby et al., 2010). This suggests that the changes in carbonate production were the dominant factor, rather than deep ocean carbonate saturation changes, that led to the low $CaCO_3$ content despite the glacial increase in ocean alkalinity (Sigman et al., 2010; Kobayashi et al., 2021). Similarly, the sites south of present-day APF recorded low $CaCO_3$ accumulation combined with low biogenic silica flux during glacial periods because of low carbonate and opal productivity (Charles et al., 1991; Howard and Prell, 1994; Ghadi et al., 2020). Such low productivity is linked to increased winter sea ice (spatially and temporally) and a northward shift of the circumpolar upwelling belt (away from the core

sites) associated with the northward displacement of Southern Hemisphere Westerlies (Charles et al., 1991; Ghadi et al., 2020). The sedimentary $CaCO_3$ and coccolith records in these regions are more likely to signal carbonate productivity changes than preservation or deep-water carbonate chemistry changes.

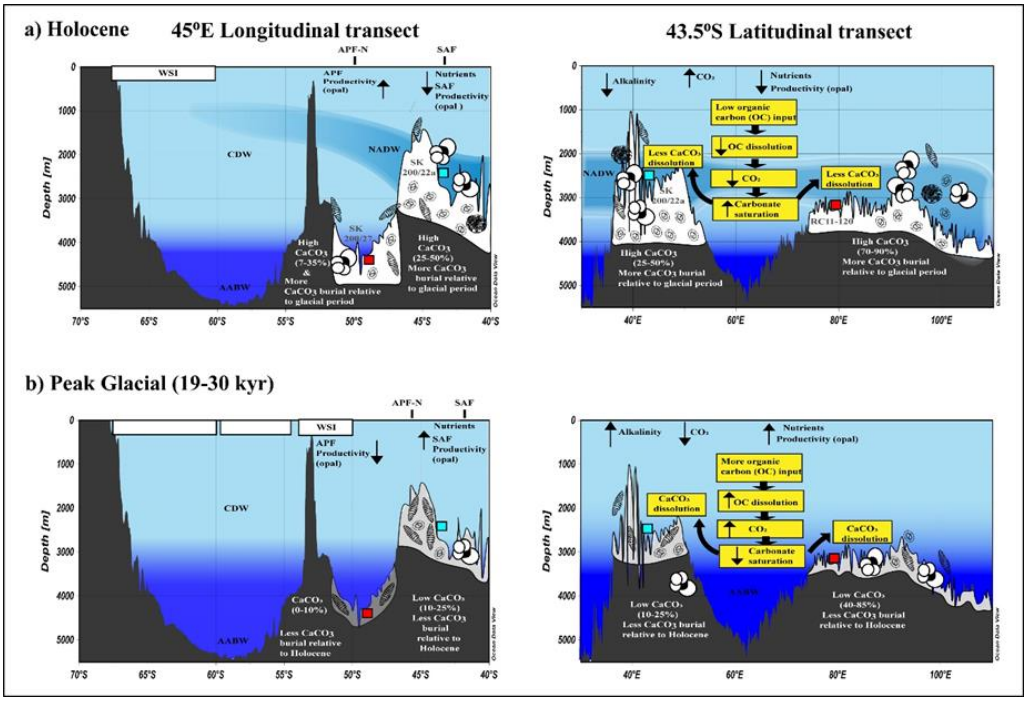

Figure 5. Schematic representation of variation in calcium carbonate ($CaCO_3$) preservation at 45◦E longitudinal and 43.5◦S latitudinal section. (a) Holocene changes and (b) glacial changes. North Atlantic Deep Waters (NADW), Antarctic Bottom Water (AABW) and Circumpolar Deep Water (CDW) were identified based on Emery (2001). Glacial AABW, and CDW were marked as per Govin et al. (2009).

6.4.2 Glacial enrichment of heavily calcified taxa *Coccolithus pelagicus* subsp. *braarudii*

Coccolithus pelagicus is known to produce the largest coccoliths and has the highest carbonate mass ranging from 170 to 399 pg (Boeckel, 2002; Rigual Hernandez et al., 2020). The extant *C. pelagicus* has two subspecies, a sub-Arctic species, *C. pelagicus* subsp. *pelagicus*, with sizes <10 µm, and a larger temperate subspecies, *C. pelagicus* subsp. *braarudii*, with sizes >10 µm (Baumann et al., 2000; Geisen et al., 2002; Saez et al., 2003; Geisen et al., 2004). This species is highly abundant in the Northern Atlantic (Ziveri et al., 2004), but it

shows very low abundance in the Southern Ocean (Saavedra-Pellitero et al., 2014; Rigual Hernandez et al., 2020; Vollmar et al., 2021; Wilks et al., 2021). Despite the very low abundance of this species in the present-day Southern Ocean, the glacial sediments of the site SK200/22a recorded higher average absolute (approximately 0.1×10^9 coccoliths/g) and relative (about 18%) abundances (Fig. 2c; 3). Such glacial rise in the abundance of this species was also recorded in the subantarctic region of the Atlantic Sector of the Southern Ocean (Flores et al., 2003).

The rise in the absolute and relative abundance of *C. pelagicus* subsp. *braarudii* during the glacial period in the Southern Ocean could reflect two possibilities. Firstly, the production of this species could have increased relative to other species in the surface waters during the glacial period and contributed to their higher abundance in the glacial sediments. Secondly, the glacial production of *C. pelagicus* subsp. *braarudii* might have been low, like the Holocene. Still, the dissolution of relatively smaller but major species like *E. huxleyi*, *G. muellerae,* and *C. leptoporus* in the deep waters, water column, and pore waters may have resulted in the enrichment of the most heavily calcified species, *C. pelagicus* subsp. *braarudii*, in the glacial sediments (Fig. 2f–i). The second scenario is likely due to extremely low and scattered *C. pelagicus* subsp. *braarudii* production in the modern Southern Ocean having no specific ecological preference to justify their glacial rise in abundance (Saavedra-Pellitero et al., 2014; Rigual Hernandez et al., 2020; Vollmar et al., 2021). Also, given the higher diatom production and increased competition for light and nutrients in the glacial SAZ (Anderson et al., 2014; Nair et al., 2015), the increase in the production of larger coccolithophore such as *C. pelagicus* subsp. *braarudii* is very unlikely. This is also evident from the reduced sizes of *C. pelagicus* subsp. *braarudii* during the glacial periods (Fig. 3d-e). Coccolithophore size is governed by factors such as nutrients, light, temperature, and CO_3^{2-} concentration (Beaufort et al., 2011; Guiti´an et al., 2020). We speculate that despite the increased surface ocean alkalinity (Sigman

et al., 2010; Kobayashi et al., 2021) and nutrient replete conditions (Robinson et al., 2005; Sigman et al., 2010), the competition for light and nutrients from diatoms might have induced unfavorable conditions for *C. pelagicus* subsp. *braarudii* leading to their reduced sizes during the glacial period. Furthermore, the increased dissolution during the glacial period is also supported by low CEX index indicating higher dissolution. During the glacial periods, the low carbonate saturation in the deep waters of the SAZ sites (including site SK200/22a) enhances $CaCO_3$ dissolution and decreases its burial (Sigman et al., 2010; Gottschalk et al., 2018; Kobayashi et al., 2021). This could have affected the large proportion of the coccolith species with less impact on *C. pelagicus* subsp. *braarudii*.

Coccolithus pelagicus subsp. *braarudii,* with its enrichment and high carbonate mass, is the highest contributor to the total coccolith carbonate mass (80%) in the glacial sediments (Fig. 3). Whereas, in the Holocene sediments, despite the higher abundances of *E. huxleyi*, the major contribution to the total coccolith mass is by *C. leptoporus* (Fig. 3). This resembles the typical SAZ conditions, where greater contribution to the $CaCO_3$ production and export is by larger coccolithophore species rather than the more abundant species (Rigual Hernandez et al., 2020). It can therefore be assumed that the anomalously higher abundance of this robust species in Southern Ocean sediment cores is a good indicator of coccolith dissolution.

6.4.3 Evidence of strengthened Agulhas Return Current during the glacial period

The core site SK200/22a is close to the Agulhas Return Current (ARC) and has recorded the glacial–Holocene changes in the strength of the ARC through the variation in tropical–subtropical coccolithophore assemblages. The Agulhas Current (AC), which travels southwards and leaks into the South Atlantic, has characteristic tropical-subtropical coccolithophore (also known as AC assemblage) comprising of *G. oceanica*, *F. profunda* and *U. sibogae* (Flores et al., 1999), like the foraminifera Agulhas leakage fauna (ALF) described

in Peeters et al. (2004). In this study, we attempted to understand the glacial-Holocene variation in ARC strength and its association with Agulhas Leakage (AL) intensity and surface ocean circulation. To understand the changes in ARC strength, we considered the relative abundance of AC assemblage (*G. oceanica* + *F. profunda* + *U. sibogae*) from the present study and the Indian STF site (site IODP 361/U1475) (Tangunan et al., 2021). However, we refrained from using their absolute abundance as ARC proxies because at these sites, the total coccolith concentrations in the glacial sediments were likely diluted by high biogenic silica (Romero et al., 2015; Manoj and Thamban, 2015; Nair et al., 2015), which is reflected in the low glacial absolute abundance of AC assemblage. In addition, the Δ temperature (difference in surface and subsurface temperature) record from the Kerguelen Plateau region was used as a proxy for ARC strength (Civel-Mazens et al., 2021) (Fig. 6a–c). The ARC records were compared with the AL proxies such as ALF and AC assemblage abundance off South Africa (site GeoB 3603–2) (Peeters et al., 2004; Boeckel, 2002) and AC assemblage records off south-west Africa (site GeoB1710–3) (Baumann, 2005) (Fig. 6d–f). Additionally, the AC assemblage records from within the main flow of AC (site MD96–2077) (Tangunan et al., 2020) were used to understand whether there were any changes in the upstream of AC that could account for the variability in the AL and ARC records.

The overall comparison revealed an increase in the values of ARC records (Fig. 6a–c) and lower values of AL proxies (Fig. 6d–f) during the glacial period compared to the Holocene. This does support the notion of reduced Agulhas Leakage (due to the northward shift of STF) and stronger Agulhas retroflection causing the increased flow of ARC during the glacial period (Peeters et al., 2004; Civel-Mazens et al., 2021). The strengthened ARC may have transported greater numbers of AC assemblage along its path toward the Indian sector (U 1475 and SK 200/ 22a), while the reduced AL decreased the transport of this assemblage to the South Atlantic sites (GeoB 1710–3; GeoB 3603–2) (Fig. 7b). Contrastingly, during the Holocene, the

southward shift of STF combined with broader Agulhas passage may have enhanced Agulhas Leakage. This likely led to the increased transport of AC assemblage in the South Atlantic and weaker ARC carrying lower numbers of AC assemblage to the Indian sector (Fig. 7a).

However, as per Simon et al. (2013), the glacial-interglacial changes in ALF at the AL corridor may not necessarily be linked to the leakage itself. Instead, these changes partly reflect the upstream variation in the hydrography of AC and ALF production, which is controlled by the dynamics of the Southwest Indian Ocean sub-gyre (SWIOSG), ARC, and Southern Hemisphere Westerly winds. As per this notion, the changes observed in the AC assemblages at the AL corridor (GeoB 3603–2; Fig. 6d) may not be linked to leakage. Instead, it may reflect the variation in their production upstream of AC. However, the dissimilarity in the variation of AC assemblage from the upstream region (MD96–2077) and the AL corridor (Fig. 6e and g) may not suggest the same. The reasons for such discrepancies are unclear, and the notion that the downstream changes are linked to the upstream conditions of the AC system may be debatable. Nevertheless, the strengthened SWIOSG and ARC, along with the increased cross-frontal mixing along the STF (Simon et al., 2013), can be held accountable for the increased proportion of AC assemblage at the site STF and SAZ (U 1475 and SK 200/22a) during the glacial period (Fig. 7b).

So, be it the interplay of hydrological fronts and AL (Peeters et al., 2004; Civel-Mazens et al., 2021) or the changes in the dynamics of SWIOSG (Simon et al., 2013), both cases recorded a variation in the ARC strength during the glacial-Holocene period. We propose that during the glacial period, despite its strengthened transport, the ARC was still located north of the core site, SK200/22a, and ARC did not have to be at the core site to transport the tropical–subtropical coccolith assemblage. Earlier studies (Manoj et al., 2013; Manoj and Thamban, 2015; Nair et al., 2015, 2019) from the same site could not capture the changes in ARC strength, as the proxies (biogenic silica, ice-rafted debris, diatoms, and sea ice) involved were

essentially indicative of the process occurring south of the SAF and APF. Our results suggest that site SK200/22a captures the oceanographic changes in the subtropical southern Indian Ocean (ARC strength) as well as the latitudinal shifts in APF (Manoj and Thamban, 2015; Nair et al., 2019).

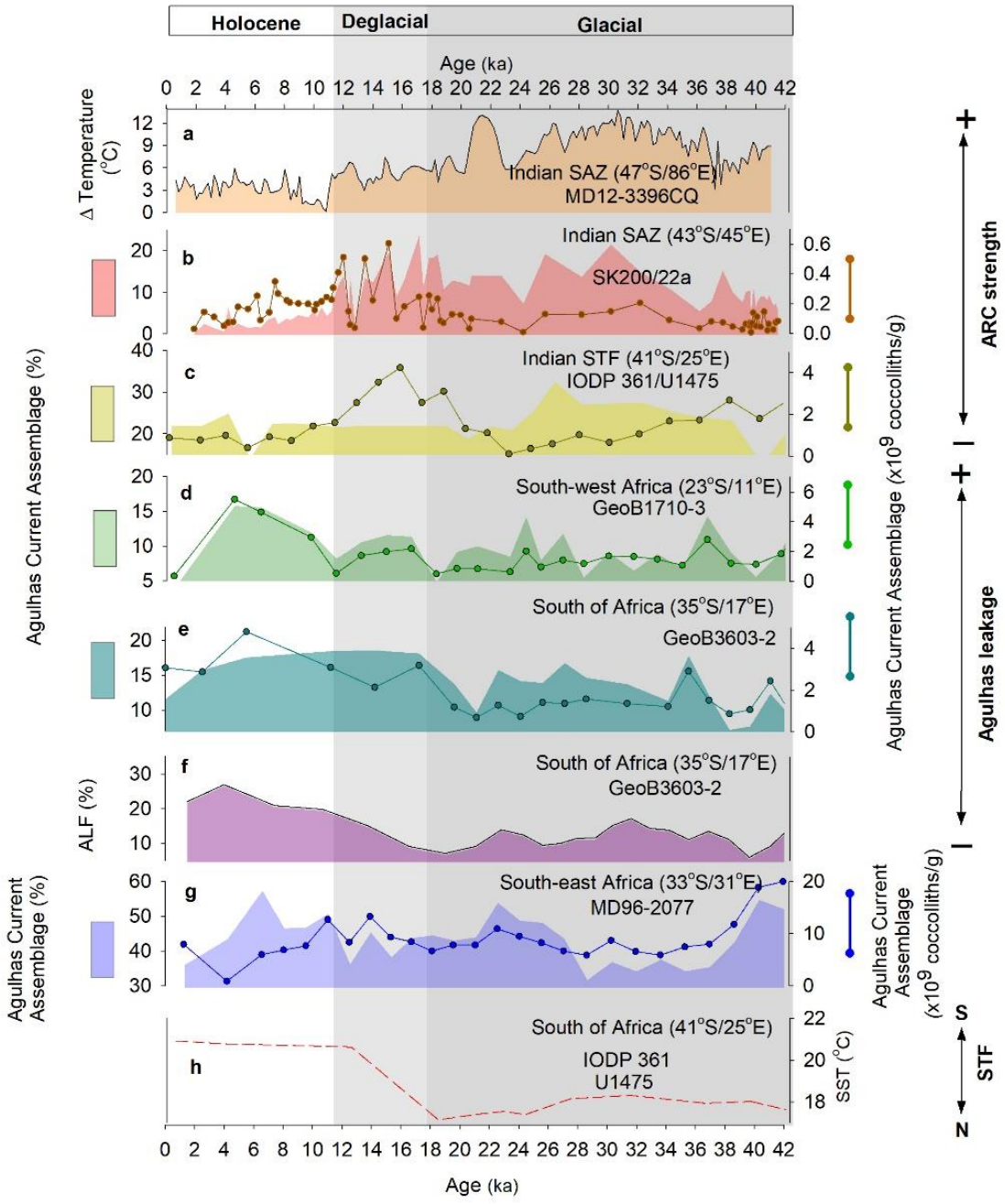

Figure 6. Multi proxy reconstruction of Agulhas Return Current in Indian Sector. (a) Δ Temperature-Difference between SST and subsurface temperature from core MD12–3396CQ (Civel-Mazens et al., 2021), Agulhas Current assemblage relative and absolute abundances from (b) present study, (c) Indian STF (core IODP 361/u 1475)

(Tangunan et al., 2021), (d) South-west Africa (core GeoB 1710–3) (Baumann, 2005), (e) South of Africa, Cape Basin (core GeoB 3603–2) (Boeckel, 2002), (f) Agulhas leakage fauna (ALF) abundance from South of Africa, Cape Basin (core GeoB 3603–2) (Peeters et al., 2004), (g) Agulhas Current assemblage relative and absolute abundances from south-east Africa (MD96–2077) (Tangunan et al., 2020) and (h) sea surface temperature (◦C) (Tangunan et al., 2021). Dark grey, light grey and white bands indicate glacial period, deglacial phase, and Holocene respectively.

6.5. Conclusion

The down core coccolith records from the site SK200/22a exhibits glacial-Holocene variation in coccolith production, dilution of $CaCO_3$ sediments, dissolution related changes in coccolith, and the strength of Agulhas Return Current (ARC). The glacial subantarctic zone (SAZ) was characterized by low coccolith production owing to the increased competition from diatoms for light and nutrients which is reflected in the lower coccolith concentration and smaller sizes of coccolith (*C. pelagicus* subsp. *braarudii*). Additionally, the high diatom production during the glacial periods increased the biogenic silica content in glacial sediments, thereby diluting the carbonate sediments and coccolith concentrations. The other vital factors that contributed to low coccolith concentration in glacial sediments was the reduced carbonate burial (preservation). During the glacial period, the weak Atlantic Meridional Overturning Circulation resulted in the replacement of carbonate saturated, North Atlantic Deep Waters by the undersaturated southern sourced water masses leading to the reduced carbonate burial at the site SK 200/22a. The additional factor that contributed to the glacial reduction in carbonate saturation was the increased storage of dissolved CO_2 in the deep glacial Southern Ocean. This is primarily a result of strong biological pump and associated increase in organic carbon respiration in the deep ocean.

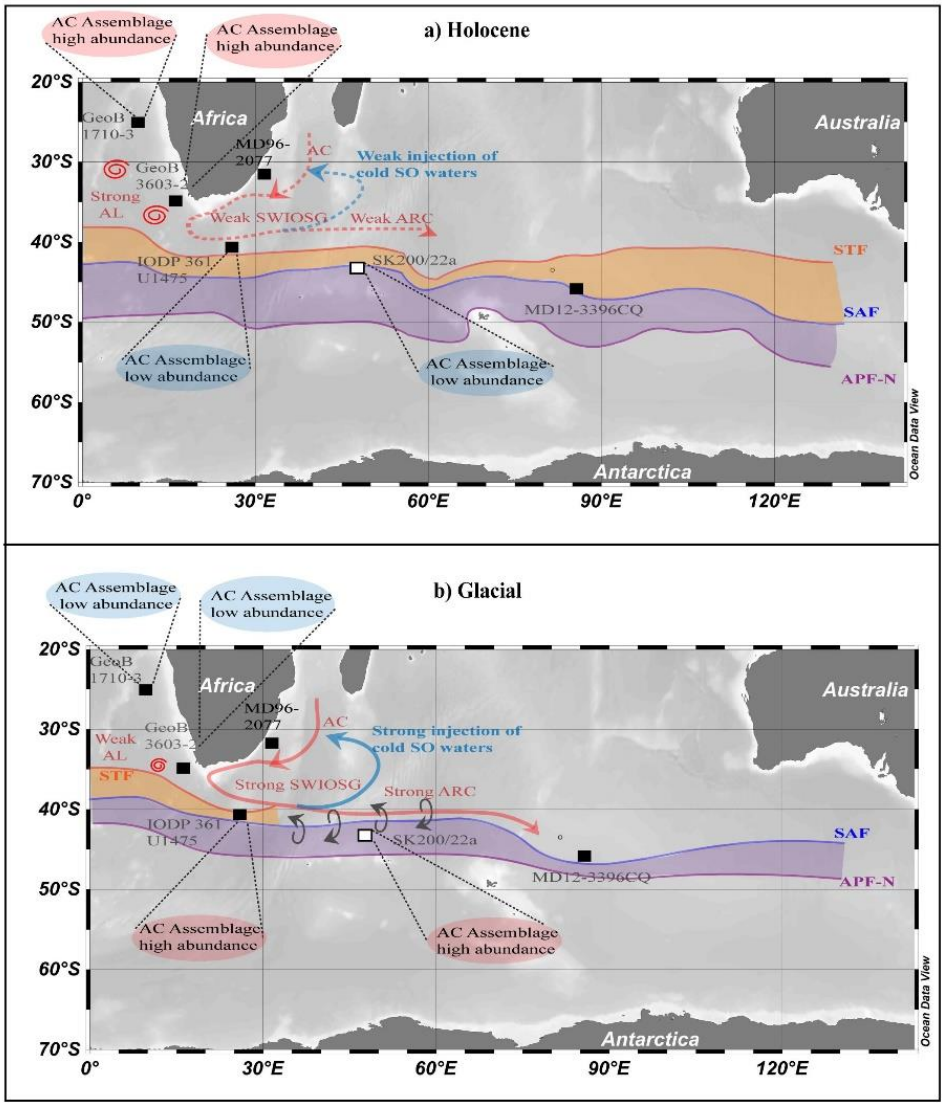

Figure 7. Schematic representation of Fig. 6. (a) Holocene position of Subtropical Front (STF; orange line), Subantarctic Front (SAF; blue line), Antarctic Polar Front-northern branch (APF-N; dark pink line), Agulhas leakage (AL; red spirals) and Agulhas Return Current (ARC; red line), (b) Glacial location of STF, SAF, APF-N and ARC. The location of fronts and ARC during Holocene and glacial were marked based on Civel-Mazens et al. (2021) and the position of Benguela Current (BC; dark green line) during Holocene is according to Wedepohl et al. (2000). Orange and purple shaded areas represent the Subantarctic Zone (SAZ) and Polar Frontal Zone (PFZ) respectively. White squares indicate location of present study site. Black squares indicate location of sediment cores used for supporting data.

The glacial reduction in the carbonate saturation is well supported by the enrichment of larger, heavily calcified, dissolution-resistant species such as *C. pelagicus* subsp. *braarudii* in the glacial sediments as compared to the Holocene sediments. The pelagic carbonate production and degree of deep ocean carbonate saturation govern the coccolith and $CaCO_3$ burial in the

subantarctic Southern Ocean sediments. The anomalously high abundance of tropical–subtropical species or Agulhas Current assemblage (*G. oceanica*, *F. profunda,* and *U. sibogae*) in the SAZ during the glacial period, relative to Holocene signifies the stronger transport of the Agulhas Return Current. However, further coccolithophore based sediment core studies are needed from the upstream region of the AC and along the subtropical front in the south-west Indian Sector of the Southern Ocean to delineate the mechanism governing the stronger glacial transport of Agulhas Return Current.

Chapter 7

Summary and Conclusion

This thesis contributes to the existing knowledge of extant coccolithophore distribution, ecology in association with oceanic fronts in the Southern Indian Ocean (Chapter 4), distribution and factors affecting the preservation in the immediate past utilizing coccoliths data from surface sediments (Chapter 5), and their implications in the reconstruction of past carbonate production and hydrography of the Southern Indian Ocean with the carbonate and coccolith records from sediment core (Chapter 6).

Coccolithophores are single-celled calcifying phytoplankton and are one of the most important primary producers and fossilizing groups. Before utilizing them as proxies in paleoenvironmental studies it is necessary to understand the present distribution, ecology, and response of coccolithophores to existing environmental conditions and the factors affecting them. In this study coccolithophore abundance and diversity varied with the southern ocean fronts and showed decreasing diversity from the STZ to the PFZ. However, high abundance in the STZ and PFZ, and the assemblage mainly consisted of a single species, *Emiliania huxleyi*. Temperature and nutrients regulate coccolithophore assemblages in the southern Indian ocean. Discrepancies in the distribution of some species compared to that in other sectors of the Southern Ocean were observed, implying differences arising from the regional settings and time of sampling (Chapter 4).

Further preservation conditions and distribution of coccoliths in the surface sediments of the Southern Ocean revealed that coccolith abundance showed a decreasing trend from STZ to PFZ and samples south of PFZ and AZ were completely barren of coccoliths. However, diversity was highest in the STZ and PFZ unlike in plankton samples. Coccolith assemblages in the sediment samples did not clearly represent the coccolithophore assemblages in the surface water column. The plausible reasons are the variation in the dissolution of large and robust coccoliths and small weakly calcified coccoliths, physical transport of coccoliths via ocean currents and associated eddies (Chapter 5). Sediment core data of coccoliths and carbonate for

the past 41.5 kyrs further shows the variation in coccolith abundance, dilution of $CaCO_3$ sediments, changes related to dissolution in coccolith, and the strength of Agulhas return current during the glacial-Holocene. Low coccolith abundance and $CaCO_3$ in the SAZ sediment during the glacial is attributed to dilution due to increased production and preservation of diatom (biogenic silica). Another factor influencing carbonate preservation was the replacement of carbonate-saturated North Atlantic deep waters with the undersaturated southern sourced water masses. This glacial reduction of carbonate saturation is also observed in the decreased size of *Coccolithus pelagicus* subsp. *braarudii* compared to the Holocene sediments. Pelagic carbonate production and the degree of carbonate saturation in the deep ocean regulate the coccolith and $CaCO_3$ burial in the subantarctic Southern Ocean sediments. During the glacial period high abundance of warm water species (*Gephyrocapsa oceanica*, *Florisphaera profunda*, and *Umbilicosphaera sibogae*) in the SAZ, compared to Holocene signifies the stronger transport of the Agulhas return current (Chapter 6). In totality, the multivariate statistical analysis identifies that a combination of surface water nutrient availability and carbonate chemistry in the surface and bottom waters covarying with temperature are the dominant drivers of coccolithophores in the Southern Ocean.

For better applicability of coccoliths as a proxy it is necessary to consider the effects of conditions of surface water and the water column above the sea floor. Further long-term inter- and intra-annual studies are required to understand factors affecting coccolithophore composition such as environmental parameters, competition, grazing pressure, change in the life cycle phases, and their response to the environmental changes at different seasons in the southern Indian ocean. Detailed studies on the response of coccolithophores to local and regional settings of different sectors of the Southern Ocean are required to better understand the variations in these responses.

References

Armstrong, R. A., Lee, C., Hedges, J. I., Honjo, S., & Wakeham, S. G. (2001). A new, mechanistic model for organic carbon fluxes in the ocean based on the quantitative association of POC with ballast minerals. Deep Sea Research Part II: Topical Studies in Oceanography, 49(1-3), 219–236.

Anderson, R. F., Barker, S., Fleisher, M., Gersonde, R., Goldstein, S. L., Kuhn, G., ... & Sachs, J. P. (2014). Biological response to millennial variability of dust and nutrient supply in the Subantarctic South Atlantic Ocean. Philosophical Transactions of the Royal Society A: Mathematical, Physical and Engineering Sciences, 372(2019), 20130054.

Andruleit, H. (1997). Coccolithophore fluxes in the Norwegian-Greenland Sea: seasonality and assemblage alterations. Marine Micropaleontology, 31(1-2), 45-64.

Andruleit, H. A., von Rad, U., Brans, A., & Ittekkot, V. (2000). Coccolithophore fluxes from sediment traps in the northeastern Arabian Sea off Pakistan. Marine Micropaleontology, 38(3-4), 285-308.

Andruleit, H., Stäger, S., Rogalla, U., & Čepek, P. (2003). Living coccolithophores in the northern Arabian Sea: ecological tolerances and environmental control. Marine Micropaleontology, 49(1-2), 157–181.

Andruleit, H., Rogalla, U., & Stäger, S. (2004). From living communities to fossil assemblages: origin and fate of coccolithophores in the northern Arabian Sea. Micropaleontology, 50(Suppl_1), 5–21.

Anilkumar, N., Luis, A. J., Somayajulu, Y. K., Babu, V. R., Dash, M. K., Pednekar, S. M., ... & Pandey, P. C. (2006). Fronts, water masses and heat content variability in the Western Indian sector of the Southern Ocean during austral summer 2004. Journal of Marine Systems, 63(1-2), 20-34.

Bach, L. T., Riebesell, U., Gutowska, M. A., Federwisch, L., & Schulz, K. G. (2015). A unifying concept of coccolithophore sensitivity to changing carbonate chemistry embedded in an ecological framework. Progress in Oceanography, 135, 125-138.

Bakker, P., Masson-Delmotte, V., Martrat, B., Charbit, S., Renssen, H., Gröger, M., ... & Varma, V. (2014). Temperature trends during the Present and Last Interglacial periods–a multi-model-data comparison. Quaternary Science Reviews, 99, 224-243.

Balch, W., Drapeau, D., Bowler, B., & Booth, E. (2007). Prediction of pelagic calcification rates using satellite measurements. Deep Sea Research Part II: Topical Studies in Oceanography, 54(5-7), 478-495.

Balch, W.M., Drapeau, D.T., Bowler, B.C., Lyczskowski, E., Booth, E.S. and Alley, D. (2011). The contribution of coccolithophores to the optical and inorganic carbon budgets during the Southern Ocean Gas Exchange Experiment: New evidence in support of the "Great Calcite Belt" hypothesis. Journal of Geophysical Research: Oceans, 116(C4).

Balch, W.M., Bates, N.R., Lam, P.J., Twining, B.S., Rosengard, S.Z., Bowler, B.C., Drapeau, D.T., Garley, R., Lubelczyk, L.C., Mitchell, C. and Rauschenberg, S., (2016). Factors regulating the Great Calcite Belt in the Southern Ocean and its biogeochemical significance. Global Biogeochemical Cycles, 30(8), 1124–1144.

Balch, W. M., Bowler, B. C., Drapeau, D. T., Lubelczyk, L. C., Lyczkowski, E., Mitchell, C., & Wyeth, A. (2019). Coccolithophore distributions of the north and South Atlantic ocean. Deep Sea Research Part I: Oceanographic Research Papers, 151, 103066.

Barbosa, A. B. (2009). Dynamics of living phytoplankton: implications for paleoenvironmental reconstructions. In IOP Conference Series: Earth and Environmental Science (Vol. 5, No. 1, p. 012001). IOP Publishing.

Baumann, K. H., Čepek, M., & Kinkel, H. (1999). Coccolithophores as indicators of ocean water masses, surface-water temperature, and paleoproductivity—examples from the South Atlantic. Use of proxies in paleoceanography: Examples from the South Atlantic, 117-144.

Baumann, K. H., Andruleit, H., & Samtleben, C. (2000). Coccolithophores in the Nordic Seas: comparison of living communities with surface sediment assemblages. Deep Sea Research Part II: Topical Studies in Oceanography, 47(9-11), 1743-1772.

Baumann, K.H., Böckel, B., Donner, B., Gerhardt, S., Henrich, R., Vink, A., Volbers, A., Willems, H. and Zonneveld, K.A.F. (2004). Contribution of calcareous plankton groups to the carbonate budget of South Atlantic surface sediments. The South Atlantic in the Late Quaternary: Reconstruction of Material Budgets and Current Systems, pp.81–99.

Baumann, K. H., Böckel, B., & Frenz, M. (2004). Coccolith contribution to South Atlantic carbonate sedimentation. Coccolithophores: from molecular processes to global impact, 367–402.

Baumann, K. H., Andruleit, H., Böckel, B., Geisen, M., & Kinkel, H. (2005). The significance of extant coccolithophores as indicators of ocean water masses, surface water temperature, and palaeoproductivity: a review. Paläontologische Zeitschrift, 79(1), 93–112.

Baumann, K. H., Boeckel, B., & Čepek, M. (2008). Spatial distribution of living coccolithophores along an east-west transect in the subtropical South Atlantic. J. Nannoplankt. Res, 30(1), 9-21.

Beaufort, L., Probert, I., de Garidel-Thoron, T., Bendif, E. M., Ruiz-Pino, D., Metzl, N., ... & De Vargas, C. (2011). Sensitivity of coccolithophores to carbonate chemistry and ocean acidification. Nature, 476(7358), 80-83.

Belkin, I.M., Gordon, A.L. (1996). Southern Ocean fronts from the Greenwich meridian to Tasmania. Journal of Geophysical Research 101, 3675–3696.

Berger, W. H., Adelseck Jr, C. G., & Mayer, L. A. (1976). Distribution of carbonate in surface sediments of the Pacific Ocean. Journal of Geophysical Research, 81(15), 2617-2627.

Bijma, J., Hönisch, B., & Zeebe, R. (2002). Impact of the ocean carbonate chemistry on living foraminiferal shell weight: Comment on" Carbonate ion concentration in glacial-age deep waters of the Caribbean Sea" by WS Broecker and E. Clark. Geochemistry geophysics geosystems, 3 (11), 1064.

Billard, C., & Inouye, I. (2004). What is new in coccolithophore biology?. Coccolithophores: from molecular processes to global impact, 1-29.

Bodas-Salcedo, A., Williams, K.D., Ringer, M.A., Beau, I., Cole, J.N., Dufresne, J.L., Koshiro, T., Stevens, B., Wang, Z. and Yokohata, T. (2014). Origins of the solar radiation biases over the Southern Ocean in CFMIP2 models. Journal of Climate, 27(1), 41–56.

Boeckel, B. (2003). Present and past coccolith assemblages in the South Atlantic: implications for species ecology, carbonate contribution and palaeoceanographic applicability.

Boeckel, B., & Baumann, K. H. (2004). Distribution of coccoliths in surface sediments of the south-eastern South Atlantic Ocean: ecology, preservation and carbonate contribution. Marine Micropaleontology, 51(3-4), 301–320.

Boeckel, B., Baumann, K. H., Henrich, R., & Kinkel, H. (2006). Coccolith distribution patterns in South Atlantic and Southern Ocean surface sediments in relation to environmental gradients. Deep Sea Research Part I: Oceanographic Research Papers, 53(6), 1073–1099.

Boeckel, B., & Baumann, K. H. (2008). Vertical and lateral variations in coccolithophore community structure across the subtropical frontal zone in the South Atlantic Ocean. Marine micropaleontology, 67(3-4), 255–273.

Böhm, E., Lippold, J., Gutjahr, M., Frank, M., Blaser, P., Antz, B., ... & Deininger, M. (2015). Strong and deep Atlantic meridional overturning circulation during the last glacial cycle. Nature, 517(7532), 73-76.

Bollmann, J. (1997). Morphology and biogeography of Gephyrocapsa coccoliths in Holocene sediments. Marine Micropaleontology, 29(3-4), 319–350.

Bollmann, J., Baumann, K. H., & Thierstein, H. R. (1998). Global dominance of Gephyrocapsa coccoliths in the late Pleistocene: selective dissolution, evolution, or global environmental change? Paleoceanography, 13(5), 517–529.

Bown, P.R., 1998. Calcareous Nannofossil Biostratigraphy. British Micropalaeontological Society Publication Series, London: Chapman & Hall, pp. 315.

Boyd, P. W., Watson, A. J., Law, C. S., Abraham, E. R., Trull, T., Murdoch, R., ... & Zeldis, J. (2000). A mesoscale phytoplankton bloom in the polar Southern Ocean stimulated by iron fertilization. Nature, 407(6805), 695-702.

Boyd, P. W., & Trull, T. W. (2007). Understanding the export of biogenic particles in oceanic waters: Is there consensus? Progress in Oceanography, 72(4), 276–312.

Boyd, P. W., Strzepek, R., Fu, F., & Hutchins, D. A. (2010). Environmental control of open-ocean phytoplankton groups: Now and in the future. Limnology and oceanography, 55(3), 1353-1376.

Boyle, E. A. (1988). The role of vertical chemical fractionation in controlling late Quaternary atmospheric carbon dioxide. Journal of Geophysical Research: Oceans, 93(C12), 15701-15714.

Boyle, E. A. (1989). Effect of high latitude processes on glacial chemical profiles and atmospheric CO2. Eos. Trans. AGU, 70, 1143.

Bray JR & Curtis JT. (1957). An ordination of the upland forest communities of Southern Wisconsin. Ecol. Monogr. 27, 325–349

Bralower, T. J., Bown, P. R., & Siesser, W. G. (1991). Significance of upper Triassic nannofossils from the southern hemisphere (ODP Leg 122, Wombat Plateau, NW Australia). Marine Micropaleontology, 17(1-2), 119-154.

Broecker, W. S., & Broecker, S. (1974). Carbonate dissolution on the western flank of the East Pacific Rise.

Broecker, W. S., & Peng, T. H. (1989). The cause of the glacial to interglacial atmospheric CO2 change: A polar alkalinity hypothesis. Global Biogeochemical Cycles, 3(3), 215-239.

Brownlee, C., & Taylor, A. (2004). Calcification in coccolithophores: a cellular perspective. Coccolithophores: from molecular processes to global impact, 31-49.

Buitenhuis, E. T., van der Wal, P., & de Baar, H. J. (2001). Blooms of Emiliania huxleyi are sinks of atmospheric carbon dioxide: A field and mesocosm study derived simulation. Global Biogeochemical Cycles, 15(3), 577-587.

Buitenhuis, E. T., Pangerc, T., Franklin, D. J., Le Quéré, C., & Malin, G. (2008). Growth rates of six coccolithophorid strains as a function of temperature. Limnology and Oceanography, 53(3), 1181–1185.

Cachao, M., & Moita, M. T. (2000). Coccolithus pelagicus, a productivity proxy related to moderate fronts off Western Iberia. Marine Micropaleontology, 39(1-4), 131–155.

Cao, L., & Caldeira, K. (2008). Atmospheric CO2 stabilization and ocean acidification. Geophysical Research Letters, 35(19).

Cavender-Bares, K. K., Karl, D. M., & Chisholm, S. W. (2001). Nutrient gradients in the western North Atlantic Ocean: Relationship to microbial community structure and comparison to patterns in the Pacific Ocean. Deep Sea Research Part I: Oceanographic Research Papers, 48(11), 2373–2395.

Chacko, R., Murukesh, N., George, J. V., & Anilkumar, N. (2014). Observational evidence of the southward transport of water masses in the Indian sector of the Southern Ocean. Current Science, 1573-1581.

Chapman, M. R., Shackleton, N. J., Zhao, M., & Eglinton, G. (1996). Faunal and alkenone reconstructions of subtropical North Atlantic surface hydrography and paleotemperature over the last 28 kyr. Paleoceanography, 11(3), 343-357.

Charalampopoulou, A. (2011). Coccolithophores in high latitude and polar regions: relationships between community composition, calcification and environmental factors (Doctoral dissertation, University of Southampton).

Charalampopoulou, A., Poulton, A.J., Bakker, D.C., Lucas, M.I., Stinchcombe, M.C., Tyrrell, T. (2016). Environmental drivers of coccolithophore abundance and calcification across Drake Passage (Southern Ocean). Biogeosciences, 13(21), 5917–5935.

Charles, C. D., Froelich, P. N., Zibello, M. A., Mortlock, R. A., & Morley, J. J. (1991). Biogenic opal in Southern Ocean sediments over the last 450,000 years: Implications for surface water chemistry and circulation. Paleoceanography, 6(6), 697-728.

Chase, Z., McManus, J., Mix, A. C., & Muratli, J. (2014). Southern-ocean and glaciogenic nutrients control diatom export production on the Chile margin. Quaternary Science Reviews, 99, 135-145.

Choudhari, P., Nair, A., Mohan, R., & Patil, S. (2023). Variations in the Southern Ocean carbonate production, preservation, and hydrography for the past 41, 500 years: Evidence from coccolith and CaCO3 records. Palaeogeography, Palaeoclimatology, Palaeoecology, 614, 111425.

Choudhury, D., Menviel, L., Meissner, K.J., Yeung, N.K., Chamberlain, M. and Ziehn, T. (2022). Marine carbon cycle response to a warmer Southern Ocean: the case of the last interglacial. Climate of the Past, 18(3), 507–523.

Civel-Mazens, M., Crosta, X., Cortese, G., Michel, E., Mazaud, A., Ther, O., ... & Itaki, T. (2021). Impact of the Agulhas Return Current on the oceanography of the Kerguelen Plateau region, Southern Ocean, over the last 40 kyrs. Quaternary Science Reviews, 251, 106711.

Civel-Mazens, M., Cortese, G., Crosta, X., Lawler, K. A., Lowe, V., Ikehara, M., & Itaki, T. (2023). New Southern Ocean transfer function for subsurface temperature prediction using radiolarian assemblages. Marine Micropaleontology, 178, 102198.

Clarke, K. R., & Warwick, R. M. (2001). Change in marine communities. An approach to statistical analysis and interpretation, 2, 1–68.

Colling, A. (2001). Ocean circulation (Vol. 3). Butterworth-Heinemann.

Cros, L., & Fortuño, J. M. (2002). Atlas of northwestern Mediterranean coccolithophores. Scientia Marina, 66(S1), 1-182.

Cubillos, J. C., Wright, S. W., Nash, G., De Salas, M. F., Griffiths, B., Tilbrook, B., ... & Hallegraeff, G. M. (2007). Calcification morphotypes of the coccolithophorid Emiliania huxleyi in the Southern Ocean: changes in 2001 to 2006 compared to historical data. Marine Ecology Progress Series, 348, 47–54.

De Baar, H. J. W. (1994). von Liebig's law of the minimum and plankton ecology (1899–1991). Progress in oceanography, 33(4), 347-386.

De Baar, H. J., Boyd, P. W., Coale, K. H., Landry, M. R., Tsuda, A., Assmy, P., ... & Wong, C. S. (2005). Synthesis of iron fertilization experiments: from the iron age in the age of enlightenment. Journal of Geophysical Research: Oceans, 110(C9).

Delille, B., Harlay, J., Zondervan, I., Jacquet, S., Chou, L., Wollast, R., ... & Gattuso, J. P. (2005). Response of primary production and calcification to changes of pCO2 during experimental blooms of the coccolithophorid Emiliania huxleyi. Global Biogeochemical Cycles, 19(2).

Deppeler, S.L. and Davidson, A.T. (2017). Southern Ocean phytoplankton in a changing climate. Frontiers in Marine Science, 4, 40.

Deuser, W. G., Muller-Karger, F. E., Evans, R. H., Brown, O. B., Esaias, W. E., & Feldman, G. C. (1990). Surface-ocean color and deep-ocean carbon flux: how close a connection? Deep Sea Research Part A. Oceanographic Research Papers, 37(8), 1331–1343.

Dezileau, L., Bareille, G., Reyss, J.L. and Lemoine, F., 2000. Evidence for strong sediment redistribution by bottom currents along the southeast Indian ridge. Deep Sea Research Part I: Oceanographic Research Papers, 47(10), 1899–1936.

de Vargas, C., Aubry, M. P., Probert, I. A. N., & Young, J. (2007). Origin and evolution of coccolithophores: from coastal hunters to oceanic farmers. In Evolution of primary producers in the sea (pp. 251-285). Academic Press.

Dittert, N., Baumann, K. H., Bickert, T., Henrich, R., Huber, R., Kinkel, H., & Meggers, H. (1999). Carbonate dissolution in the deep-sea: methods, quantification and paleoceanographic application. In Use of proxies in paleoceanography (pp. 255-284). Springer, Berlin, Heidelberg.

Donahue, K., Klaas, C., Dillingham, P. W., & Hoffmann, L. J. (2019). Combined effects of ocean acidification and increased light intensity on natural phytoplankton communities from two Southern Ocean water masses. Journal of Plankton Research, 41(1), 30-45.

Doney, S. C., Ruckelshaus, M., Emmett Duffy, J., Barry, J. P., Chan, F., English, C. A., Galindo, H. M., Grebmeier, J. M., Hollowed, A. B., Knowlton, N., Polovina, J., Rabalais, N. N., Sydeman, W. J., & Talley, L. D. (2012). Climate Change Impacts on Marine Ecosystems. Annual Review of Marine Science, 4(1), 11–37.

Durgadoo, J. V., Ansorge, I. J., & Lutjeharms, J. R. (2010). Oceanographic observations of eddies impacting the Prince Edward Islands, South Africa. Antarctic Science, 22(3), 211–219.

Edvardsen, B., Eikrem, W., Green, J. C., Andersen, R. A., Moon-van der Staay, S. Y., & Medlin, L. K. (2000). Phylogenetic reconstructions of the Haptophyta inferred from 18S ribosomal DNA sequences and available morphological data. Phycologia, 39(1), 19-35.

Emery, W. J. (2001). Water types and water masses. Encyclopedia of ocean sciences, 6, 3179-3187.

Eynaud, F., Giraudeau, J., Pichon, J. J., & Pudsey, C. J. (1999). Sea-surface distribution of coccolithophores, diatoms, silicoflagellates and dinoflagellates in the South Atlantic Ocean during the late austral summer 1995. Deep Sea Research Part I: Oceanographic Research Papers, 46(3), 451-482.Fabry, V. J., McClintock, J. B., Mathis, J. T., & Grebmeier, J. M. (2009). Ocean acidification at high latitudes: the bellwether. Oceanography, 22(4), 160-171.

Fabry, V. J., McClintock, J. B., Mathis, J. T., & Grebmeier, J. M. (2009). Ocean acidification at high latitudes: the bellwether. Oceanography, 22(4), 160-171.

Farrell, J.W. and Prell, W.L. (1989). Climatic change and CaCO3 preservation: An 800,000 year bathymetric reconstruction from the central equatorial Pacific Ocean. Paleoceanography, 4(4), 447–466.

Findlay, C.S. and Flores, J.A. (2000). Subtropical front fluctuations south of Australia (45 09′ S, 146 17′ E) for the last 130 ka years based on calcareous nannoplankton. Marine Micropaleontology, 40(4), 403–416.

Findlay, C. S., & Giraudeau, J. (2000). Extant calcareous nannoplankton in the Australian Sector of the Southern Ocean (austral summers 1994 and 1995). Marine Micropaleontology, 40(4), 417-439.

Findlay, C. S., & Giraudeau, J. (2002). Movement of oceanic fronts south of Australia during the last 10 ka: interpretation of calcareous nannoplankton in surface sediments from the Southern Ocean. Marine Micropaleontology, 46(3-4), 431-444.

Fischer, G., & Karakaş, G. (2009). Sinking rates and ballast composition of particles in the Atlantic Ocean: implications for the organic carbon fluxes to the deep ocean. Biogeosciences, 6(1), 85–102. https://doi.org/10.5194/bg-6-85-2009.

Firing, Y. L., Chereskin, T. K., and Mazloff, M. R., 2011.Vertical structure and transport of the Antarctic Circumpolar Current in Drake Passage from direct velocity observations. Journal of Geophysical Research: Oceans, 116(C8).

Flores, J. A., & Sierro, F. J. (1997). Revised technique for calculation of calcareous nannofossil accumulation rates. Micropaleontology, 321-324.

Flores, J. A., Gersonde, R., & Sierro, F. J. (1999). Pleistocene fluctuations in the Agulhas Current Retroflection based on the calcareous plankton record. Marine Micropaleontology, 37(1), 1-22.

Flores, J.A., Marino, M., Sierro, F.J., Hodell, D.A., Charles, C.D. (2003). Calcareous

plankton dissolution pattern and coccolithophore assemblages during the last 600 kyr at ODP Site 1089 (Cape Basin, South Atlantic): paleoceanographic implications. Palaeogeogr. Palaeoclimatol. Palaeoecol. 196 (3–4), 409–426.

Flores, J. A., Filippelli, G. M., Sierro, F. J., & Latimer, J. (2012). The “White Ocean” hypothesis: a late Pleistocene Southern Ocean governed by coccolithophores and driven by phosphorus. Frontiers in microbiology, 3, 233.

Frada, M., Young, J., Cachão, M., Lino, A. M. S., Narciso, Á., & Probert, C. D. V. I. (2010). A guide to extant coccolithophores (Calcihaptophycidae, Haptophyta) using light microscopy. Journal of Nannoplankton Research, 31(2), 58-112.

Frankignoulle, M., Canon, C., & Gattuso, J. P. (1994). Marine calcification as a source of carbon dioxide: Positive feedback of increasing atmospheric CO2. Limnology and Oceanography, 39(2), 458-462.

Freeman, N. M., N. S. Lovenduski, and P. R. Gent (2016), Temporal variability in the Antarctic Polar Front (2002–2014), J. Geophys. Res. Oceans, 121,7263–7276, doi:10.1002/2016JC012145

Froneman, P. W. (2004). Protozooplankton community structure and grazing impact in the eastern Atlantic sector of the Southern Ocean in austral summer 1998. Deep Sea Research Part II: Topical Studies in Oceanography, 51(22-24), 2633–2643.

Friedinger, P. J., & Winter, A. (1987). Distribution of modern coccolithophore assemblages in the southwest Indian Ocean off southern Africa. Journal of Micropalaeontology, 6(1), 5.

Garcia H.E., T.P. Boyer, O.K. Baranova, R.A. Locarnini, A.V. Mishonov, A. Grodsky, C.R. Paver, K.W. Weathers, I.V. Smolyar, J.R. Reagan, D. Seidov, M.M. Zweng (2019). World Ocean Atlas 2018: Product Documentation. A. Mishonov, Technical Editor.

Gattuso, J. P., Frankignoulle, M., Bourge, I., Romaine, S., & Buddemeier, R. W. (1998). Effect of calcium carbonate saturation of seawater on coral calcification. Global and Planetary Change, 18(1-2), 37–46.

Gattuso, J.P., Hansson, L., 2011. Ocean acidification: background and history. Ocean Acidific. 1–20.

Geisen, M., Billard, C., Broerse, A. T., Cros, L., Probert, I., & Young, J. R. (2002). Life-cycle associations involving pairs of holococcolithophorid species: intraspecific variation or cryptic speciation?. European Journal of Phycology, 37(4), 531-550.

Geisen, M., Young, J.R., Probert, I., Saez, A.G., Baumann, A., Sprengel, C., Bollmann, J., Cros, L., De Vargas, C., Medlin, L.K. (2004). Species level variation in coccolithophores. In: Thierstein, H.R., Young, J.R. (Eds.), Coccolithophores – From Molecular Processes to Global Impact. Springer, Berlin, pp. 313–352.

Geitzenauer, K.R., Roche, M.B., McIntyre, A., 1976. Modern pacific coccolithophore assemblages: derivation and application to Late Pleistocene paleotemperature analysis. In: Cline, R.M., Hays, J.D. (Eds.), Investigation of Late Quaternary Paleoceanography and Paleoclimatology. Geological Society of America (GSA), vol. 145, pp. 423– 428.

Gerotto, A., Zhang, H., Nagai, R.H., Stoll, H.M., Figueira, R.C.L., Liu, C. and Hernández-Almeida, I., (2022). Responses of fossil coccolith morphology to preservation conditions in the deep ocean. *EGUsphere*, 1-29.

Ghadi, P., Nair, A., Crosta, X., Mohan, R., Manoj, M. C., & Meloth, T. (2020). Antarctic sea-ice and palaeoproductivity variation over the last 156,000 years in the Indian sector of Southern Ocean. Marine Micropaleontology, 160, 101894.

Gille, S. T. (1994). Mean sea surface height of the Antarctic Circumpolar Current from Geosat data: Method and application. Journal of Geophysical Research: Oceans, 99(C9), 18255-18273.

Gille, S. T. (2002). Warming of the Southern Ocean since the 1950s. Science, 295(5558), 1275-1277.

Giraudeau, J. and Beaufort, L. (2007). Coccolithophores: from extant populations to fossil assemblages, Proxies in Late Cenozoic paleoceanography–Developments in Marine Geology, edited by: Hillaire-Marcel, C. and De Vernal, A., Elsevier, 409–439.

González-Dávila, M., Santana-Casiano, J. M., Fine, R. A., Happell, J., Delille, B., & Speich, S. (2011). Carbonate system in the water masses of the Southeast Atlantic sector of the Southern Ocean during February and March 2008. Biogeosciences, 8(5), 1401-1413.

Govin, A., Michel, E., Labeyrie, L., Waelbroeck, C., Dewilde, F., & Jansen, E. (2009). Evidence for northward expansion of Antarctic Bottom Water mass in the Southern Ocean during the last glacial inception. Paleoceanography, 24(1).

Gottschalk, J., Hodell, D. A., Skinner, L. C., Crowhurst, S. J., Jaccard, S. L., & Charles, C. (2018). Past carbonate preservation events in the deep Southeast Atlantic Ocean (Cape Basin) and their implications for Atlantic overturning dynamics and marine carbon cycling. Paleoceanography and paleoclimatology, 33(6), 643-663.

Gravalosa, J. M., Flores, J. A., Sierro, F. J., & Gersonde, R. (2008). Sea surface distribution of coccolithophores in the eastern Pacific sector of the Southern Ocean (Bellingshausen and Amundsen Seas) during the late austral summer of 2001. Marine Micropaleontology, 69(1), 16-25.

Graham, R. M., & De Boer, A. M. (2013). The dynamical subtropical front. Journal of Geophysical Research: Oceans, 118(10), 5676-5685.

Guerreiro, C., Oliveira, A., De Stigter, H., Cachão, M., Sá, C., Borges, C., ... & Rodrigues, A. (2013). Late winter coccolithophore bloom off central Portugal in response to river discharge and upwelling. Continental Shelf Research, 59, 65–83.

Guitián, J., Dunkley Jones, T., Hernández-Almeida, I., Löffel, T., & Stoll, H. M. (2020). Adaptations of coccolithophore size to selective pressures during the Oligocene to Early Miocene high CO2 world. Paleoceanography and Paleoclimatology, 35(12), e2020PA003918.

Hagino, K., Okada, H., & Matsuoka, H. (2005). Coccolithophore assemblages and morphotypes of Emiliania huxleyi in the boundary zone between the cold Oyashio and warm Kuroshio currents off the coast of Japan. Marine Micropaleontology, 55(1-2), 19-47.

Hagino, K., Bendif, E. M., Young, J. R., Kogame, K., Probert, I., Takano, Y., ... & Okada, H. (2011). New evidence for morphological and genetic variation in the cosmopolitan coccolithophore Emiliania huxleyi (prymnesiophyceae) from the COX1b-ATP4 genes 1. Journal of phycology, 47(5), 1164-1176.

Haidar, A. T., & Thierstein, H. R. (2001). Coccolithophore dynamics off Bermuda (N. Atlantic). Deep Sea Research Part II: Topical Studies in Oceanography, 48(8-9), 1925-1956.

Hammer, Ø., Harper, D.A. and Ryan, P.D., 2001. PAST: Paleontological statistics software package for education and data analysis. Palaeontologia electronica, 4(1), 9.

Hasle, G. R. (1969). An analysis of the phytoplankton of the Pacific Southern Ocean: abundance, composition, and distribution during the Brategg Expedition, 1947-1948. Hvalradets skrifter, 52, 1-168.

Hauck, J., Gerdes, D., Hillenbrand, C.-D., Hoppema, M., Kuhn, G., Nehrke, G., et al. (2012). Distribution and mineralogy of carbonate sediments on Antarctic shelves. J. Mar. Syst. 90, 77–87. doi: 10.1016/j.jmarsys.2011.09.005

Hernández-Almeida, I., Ausín, B., Saavedra-Pellitero, M., Baumann, K. H., & Stoll, H. M. (2019). Quantitative reconstruction of primary productivity in low latitudes during the last glacial maximum and the mid-to-late Holocene from a global Florisphaera profunda calibration dataset. Quaternary Science Reviews, 205, 166-181.

Hodell, D. A., Venz, K. A., Charles, C. D., & Ninnemann, U. S. (2003). Pleistocene vertical carbon isotope and carbonate gradients in the South Atlantic sector of the Southern Ocean. Geochemistry, Geophysics, Geosystems, 4(1), 1-19.

Holliday, N. P., & Read, J. F. (1998). Surface oceanic fronts between Africa and Antarctica. Deep Sea Research Part I: Oceanographic Research Papers, 45(2-3), 217-238.

Honjo, S., 1975. Dissolution of suspended coccoliths in the deepsea water column and sedimentation of coccolith ooze. In: Sliter, W.V., Be´, A.W.H., Berger, W.H. (Eds.), Dissolution of Deep-Sea Carbonates. Special Publication-Cushman Foundation for Foraminiferal Research, vol. 13, pp. 114–128.

Hiramatsu, C. and De Deckker, P. (1996). Distribution of calcareous nannoplankton near the Subtropical Convergence, south of Tasmania, Australia. Marine and Freshwater Research, 47(5),707–713.

Honjo, S. (1976). Coccoliths: production, transportation and sedimentation. Marine Micropaleontology, 1, 65–79.

Honjo, S., & Okada, H. (1974). Community structure of coccolithophores in the photic layer of the mid-Pacific. Micropaleontology, 209-230.

Honjo, S., & Roman, M. R. (1978). Marine copepod fecal pellets: production, preservation and sedimentation. J. mar. Res, 36(1), 45–57.

Howard, W. R., & Prell, W. L. (1994). Late Quaternary CaCO3 production and preservation in the Southern Ocean: Implications for oceanic and atmospheric carbon cycling. Paleoceanography, 9(3), 453-482.

IPCC. (2013). Climate change 2013: the physical science basis. Contribution of working group I to the fifth assessment report of the intergovernmental panel on climate change (AR5). IPCC, New York.

IPCC, 2019: Climate Change and Land: an IPCC special report on climate change, desertification, land degradation, sustainable land management, food security, and greenhouse gas fluxes in terrestrial ecosystems [P.R. Shukla, J. Skea, E. Calvo Buendia, V. Masson-Delmotte, H.-O. Pörtner, D. C. Roberts, P. Zhai, R. Slade, S. Connors, R. van Diemen, M. Ferrat, E. Haughey, S. Luz, S. Neogi, M. Pathak, J. Petzold, J. Portugal Pereira, P. Vyas, E. Huntley, K. Kissick, M. Belkacemi, J. Malley, (eds.)]

Irion, S., Christaki, U., Berthelot, H., L'Helguen, S. and Jardillier, L. (2021). Small phytoplankton contribute greatly to CO_2-fixation after the diatom bloom in the Southern Ocean. The ISME journal, 15(9), 2509–2522.

Iglesias-Rodriguez, M. D., Halloran, P. R., Rickaby, R. E., Hall, I. R., Colmenero-Hidalgo, E., Gittins, J. R., ... & Boessenkool, K. P. (2008). Phytoplankton calcification in a high-CO2 world. science, 320(5874), 336–340.

Imawaki, S., Bower, A.S., Beal, L., Qiu, B. (2013). Western boundary currents. In: International Geophysics, vol. 103. Elsevier, pp. 305e338.

Jaccard, S.L., Hayes, C.T., Martinez-Garcia, A., Hodell, D.A., Anderson, R.F., Sigman, D.

M., Haug, G.H. (2013). Two modes of change in Southern Ocean productivity over the past million years. Science 339 (6126), 1419–1423

Jafar, S. A. (1983). Significance of Late Triassic calcareous nannoplankton from Austria and southern Germany. Neues Jahrbuch fur Geologie und Palaontologie. Abhandlungen, 166, 218-259.

Jasmine, P., Muraleedharan, K. R., Madhu, N. V., Devi, C. A., Alagarsamy, R., Achuthankutty, C. T., Jayan, Z., Sanjeevan V.N., Sahayak, S. (2009). Hydrographic and productivity characteristics along 45 °E longitude in the southwestern Indian Ocean and Southern Ocean during Austral summer 2004. Marine Ecology Progress Series, 389, 97–116.

Jasprica, N., Carić, M., Kršinić, F., Kapetanović, T., Batistić, M., & Njire, J. (2012). Planktonic diatoms and their environment in the lower Neretva River estuary (Eastern Adriatic Sea, NE Mediterranean). Nova Hedwigia, 141, 405–430.

Jordan, R.W., Zhao, M., Eglington, G., Weaver, P.P.E., 1996. Coccolith and alkenone stratigraphy and palaeoceanography at an upwelling site o¡ NW Africa (ODP 658C) during the last 130,000 years. In: Moguilesky, J.A., Whatley, R. (Eds.), Microfossils and Oceanic Environments. University of Wales, Aberystwyth-Press, pp. 112–130

Jordan RW, Cros L, Young JR (2004) A revised classification scheme for living haptophytes. Micropaleontology 50 (Suppl 1):55–79

Käse, L., & Geuer, J. K. (2018). Phytoplankton responses to marine climate change–an introduction. In YOUMARES 8–Oceans Across Boundaries: Learning from each other: Proceedings of the 2017 conference for YOUng MARine RESearchers in Kiel, Germany (pp. 55-71). Springer International Publishing.

Kent, D. V. (1982). Apparent correlation of palaeomagnetic intensity and climatic records in deep-sea sediments.

Kerkar, A.U., Venkataramana, V. and Tripathy, S.C. (2022) Assessing the trophic link between primary and secondary producers in the Southern Ocean: A carbon-biomass based approach. Polar Science, 31, 100734.

Kinkel, H., Baumann, K.-H., Cepek, M. (2000). Coccolithophores in the equatorial Atlantic Ocean: response to seasonal and Late Quaternary surface water variability. Marine Micropaleontology 39, 87– 112.

Kobayashi, H., Oka, A. (2018). Response of atmospheric pCO2 to glacial changes in the Southern Ocean amplified by carbonate compensation. Paleoceanogr. Paleoclimatol. 33 (11), 1206–1229.

Kobayashi, H., Oka, A., Yamamoto, A., & Abe-Ouchi, A. (2021). Glacial carbon cycle changes by Southern Ocean processes with sedimentary amplification. Science Advances, 7(35), eabg7723.

Kolla, V., Bé, A.W. and Biscaye, P.E. (1976). Calcium carbonate distribution in the surface sediments of the Indian Ocean. Journal of Geophysical Research, 81(15), 2605–2616.

Kolla, V., Henderson, L., Sullivan, L., & Biscaye, P. E. (1978). Recent sedimentation in the southeast Indian Ocean with special reference to the effects of Antarctic Bottom Water circulation. Marine Geology, 27(1–2), 1–17. https://doi.org/10.1016/0025-3227(78)90071-3

Kostianoy, A. G., Ginzburg, A. I., Frankignoulle, M., & Delille, B. (2004). Fronts in the Southern Indian Ocean as inferred from satellite sea surface temperature data. Journal of Marine Systems, 45(1-2), 55–73.

Krell, A., Schnack-Schiel, S.B., Thomas, D.N., Kattner, G., Zipan, W. and Dieckmann, G.S., 2005. Phytoplankton dynamics in relation to hydrography, nutrients and zooplankton at the onset of sea ice formation in the eastern Weddell Sea (Antarctica). Polar Biology, 28(9), 700–713.

Krug, M., & Tournadre, J. (2012). Satellite observations of an annual cycle in the Agulhas Current. Geophysical Research Letters, 39(15).

Krumhardt, K. M., Lovenduski, N. S., Long, M. C., Levy, M., Lindsay, K., Moore, J. K., & Nissen, C. (2019). Coccolithophore growth and calcification in an acidified ocean: Insights from community Earth system model simulations. Journal of Advances in Modeling Earth Systems, 11(5), 1418–1437.

Krumhardt, K. M., Long, M. C., Lindsay, K., & Levy, M. N. (2020). Southern Ocean calcification controls the global distribution of alkalinity. Global Biogeochemical Cycles, 34(12), e2020GB006727.

Langdon, C., & Atkinson, M. J. (2005). Effect of elevated pCO2 on photosynthesis and calcification of corals and interactions with seasonal change in temperature/irradiance and nutrient enrichment. Journal of Geophysical Research: Oceans, 110(C9).

Laskar, H. S., & Gupta, S. (2013). Phytoplankton community and limnology of Chatla floodplain wetland of Barak valley, Assam, North-East India. Knowledge and Management of Aquatic Ecosystems, (411), 06.

Lauvset, S.K., Lange, N., Tanhua, T., Bittig, H.C., Olsen, A., Kozyr, A., Álvarez, M., Becker, S., Brown, P.J., Carter, B.R. and Cotrim da Cunha, L. (2021). An updated version of the global interior ocean biogeochemical data product, GLODAPv2. 2021. Earth System Science Data, 13(12), pp.5565–5589.

Le Moigne, M., Daniel, J., Quimbert, E., Montero, M. C., Jack, M. M., Vinci, M., ... & Galgani, F. (2019). Visualization products for Beach and Seafloor Litter data.

Lewis, E., Wallace, D., & Allison, L. J. (1998). Program developed for CO_2 system calculations (No. ORNL/CDIAC-105). Brookhaven National Lab., Dept. of Applied Science, Upton, NY (United States); Oak Ridge National Lab., Carbon Dioxide Information Analysis Center, TN (United States).

Lutjeharms, J., Ansorge, I., Grüdlingh, M., Van Ballegooyen, R., Weeks, S., Machu, E., & Boebel, O. (2004). Comment on "New Global Drifter Data Set available". Eos, Transactions American Geophysical Union, 85(19), 188-188.

Lutjeharms, J.R.E. (2006). The Agulhas Current. Springer, Berlin; New York. https:// doi.org/10.1007/3-540-37212-1

Lutjeharms, J.R.E. and Ansorge, I.J. (2001). The Agulhas return current. Journal of Marine Systems, 30(1-2), 115–138.

Le Quéré, C., Buitenhuis, E. T., Moriarty, R., Alvain, S., Aumont, O., Bopp, L., ... & Vallina, S. M. (2016). Role of zooplankton dynamics for Southern Ocean phytoplankton biomass and global biogeochemical cycles. Biogeosciences, 13(14), 4111–4133.

Malinverno, E., Triantaphyllou, M. V., & Dimiza, M. D. (2015). Coccolithophore assemblage distribution along a temperate to polar gradient in the West Pacific sector of the Southern Ocean (January 2005). Micropaleontology, 489-506.

Manoj, M. C., Thamban, M., Basavaiah, N., & Mohan, R. (2012). Evidence for climatic and oceanographic controls on terrigenous sediment supply to the Indian Ocean sector of the Southern Ocean over the past 63,000 years. Geo-Marine Letters, 32, 251-265.

Manoj, M. C., Thamban, M., Sahana, A., Mohan, R., & Mahender, K. (2013). Provenance and temporal variability of ice rafted debris in the Indian sector of the Southern Ocean during the last 22,000 years. Journal of earth system science, 122, 491-501.

Manoj, M. C., & Thamban, M. (2015). Shifting frontal regimes and its influence on bioproductivity variations during the Late Quaternary in the Indian sector of Southern Ocean. Deep Sea Research Part II: Topical Studies in Oceanography, 118, 261-274.

Mantyla, A.W. and Reid, J.L., 1995. On the origins of deep and bottom waters of the Indian Ocean. Journal of Geophysical Research: Oceans, 100(C2), 2417–2439.

Margalef, R. (1978). Life-forms of phytoplankton as survival alternatives in an unstable environment. Oceanologica acta, 1(4), 493–509.

Martínez-Garcia, A., Rosell-Melé, A., Jaccard, S. L., Geibert, W., Sigman, D. M., & Haug, G. H. (2011). Southern Ocean dust–climate coupling over the past four million years. Nature, 476(7360), 312-315.

Masson-Delmotte, V., Schulz, M., Abe-Ouchi, A., Beer, J., Ganopolski, A., Gonzáles Rouco, J. F., ... & Timmermann, A. (2013). Information from paleoclimate archives.

Matsuoka, H., Okada, H. (1990). Time-progressive morphometric changes of the genus Gephyrocapsa in the Quaternary sequence of the tropical Indian Ocean, Site 709. In Proc. ODP. Sci. Results (Vol. 115, pp. 255-270).

Mayers, K., Poulton, A., Daniels, C., Wells, S., Woodward, E., Tarran, G., Widdicombe, C., Mayor, D., Atkinson, A., & Giering, S. (2019). Growth and mortality of coccolithophores during spring in a temperate Shelf Sea (Celtic Sea, April 2015). Progress in Oceanography, 177, 101928.

Mayzaud, P., Tirelli, V., Errhif, A., Labat, J. P., Razouls, S., & Perissinotto, R. (2002). Carbon intake by zooplankton. Importance and role of zooplankton grazing in the Indian sector of the Southern Ocean. Deep Sea Research Part II: Topical Studies in Oceanography, 49(16), 3169–3187.

McIntyre, A., & Bé, A. W. (1967). Modern coccolithophoridae of the Atlantic Ocean—I. Placoliths and cyrtoliths. In Deep Sea Research and Oceanographic Abstracts (Vol. 14, No. 5, pp. 561-597). Elsevier.

McIntyre, A. (1970). Gephyrocapsa protohuxleyi sp. n. a possible phyletic link and index fossil for the Pleistocene. In Deep Sea Research and Oceanographic Abstracts (Vol. 17, No. 1, pp. 187-190). Elsevier.

McNeil, B. I., & Matear, R. J. (2008). Southern Ocean acidification: A tipping point at 450-ppm atmospheric CO2. Proceedings of the National Academy of Sciences, 105(48), 18860-18864.

van der Meer, M. T., Sangiorgi, F., Baas, M., Brinkhuis, H., Damsté, J. S. S., & Schouten, S. (2008). Molecular isotopic and dinoflagellate evidence for Late Holocene freshening of the Black Sea. Earth and Planetary Science Letters, 267(3-4), 426-434.

Melinte, M. C. (2004). Calcareous nannoplankton, a tool to assign environmental changes. Proceedings of Euro-EcoGeoCentre, Romania, 1-8.

Meyer, J., & Riebesell, U. (2015). Reviews and Syntheses: Responses of coccolithophores to ocean acidification: a meta-analysis. Biogeosciences, 12(6), 1671-1682.

Mix, A. C., Bard, E., & Schneider, R. (2001). Environmental processes of the ice age: land, oceans, glaciers (EPILOG). Quaternary Science Reviews, 20(4), 627-657.

Mohan, R., Mergulhao, L.P., Guptha, M.V.S., Rajakumar, A., Thamban, M., AnilKumar, N., Sudhakar, M. and Ravindra, R. (2008). Ecology of coccolithophores in the Indian sector of the Southern Ocean. Marine Micropaleontology, 67(1-2), pp.30-45.

Monnin, E., Indermuhle, A., Dallenbach, A., Fluckiger, J., Stauffer, B., Stocker, T. F., ... & Barnola, J. M. (2001). Atmospheric CO2 concentrations over the last glacial termination. science, 291(5501), 112-114.

Moore, J. K., Abbott, M. R., Richman, J. G., & Nelson, D. M. (2000). The Southern Ocean at the last glacial maximum: A strong sink for atmospheric carbon dioxide. Global Biogeochemical Cycles, 14(1), 455-475.

Müller, M., Trull, T., and Hallegraeff, G. (2015). Differing responses of three Southern ocean Emiliania huxleyi ecotypes to changing seawater carbonate chemistry. Mar. Ecol. Prog. Ser. 531, 81–90. doi: 10.3354/meps11309 Oceanography, 49(16), 3169–3187.

Müller M.N., Trull, T.W., and Hallegraeff, G.M. (2017). Independence of nutrient limitation and carbon dioxide impacts on the Southern Ocean coccolithophore *Emiliania huxleyi*. ISME J. 11, 1777–1787.

Nair, A., Mohan, R., Manoj, M. C., & Thamban, M. (2015). Glacial-interglacial variability in diatom abundance and valve size: Implications for Southern Ocean paleoceanography. Paleoceanography, 30(10), 1245-1260.

Nair, A., Mohan, R., Crosta, X., Manoj, M. C., Thamban, M., & Marieu, V. (2019). Southern Ocean sea ice and frontal changes during the Late Quaternary and their linkages to Asian summer monsoon. Quaternary Science Reviews, 213, 93-104.

Nanninga, H. J., & Tyrrell, T. (1996). Importance of light for the formation of algal blooms by Emiliania huxleyi. Marine Ecology Progress Series, 136, 195–203.

Nissen, C., Vogt, M., Münnich, M., Gruber, N., & Haumann, F. A. (2018). Factors controlling coccolithophore biogeography in the Southern Ocean. Biogeosciences, 15(22), 6997–7024.

Nishida, S. (1986). Nannoplankton flora in the Southern Ocean, with special reference to siliceous varieties.

Okada, H. and McIntyre, A. (1977). Modern coccolithophores of the Pacific and North Atlantic oceans. Micropaleontology, 23: 1–54.

Okada, H., & McIntyre, A. (1979). Seasonal distribution of modern coccolithophores in the western North Atlantic Ocean. Marine Biology, 54(4), 319–328.

Okada, H., & Wells, P. (1997). Late Quaternary nannofossil indicators of climate change in two deep-sea cores associated with the Leeuwin Current off Western Australia. Palaeogeography, Palaeoclimatology, Palaeoecology, 131(3-4), 413-432.

Olbers, D., Borowski, D., Völker, C., & Wolff, J. O. (2004). The dynamical balance, transport and circulation of the Antarctic Circumpolar Current. Antarctic science, 16(4), 439-470.

Orr, J. C., Fabry, V. J., Aumont, O., Bopp, L., Doney, S. C., Feely, R. A., ... & Yool, A. (2005). Anthropogenic ocean acidification over the twenty-first century and its impact on calcifying organisms. Nature, 437(7059), 681-686.

Orsi, A.H., Whitworth III, T. and Nowlin Jr, W.D. (1995). On the meridional extent and fronts of the Antarctic Circumpolar Current. Deep Sea Research Part I: Oceanographic Research Papers, 42(5), 641–673.

Park, Y.-H., Gamberoni, L., Charriaud, E. (1993). Frontal structure, water masses and circulation in the Crozet Basin. Journal of Geophysical Research 98, 12361–12385.

Park, Y. H., Charriaud, E., Craneguy, P., & Kartavtseff, A. (2001). Fronts, transport, and Weddell Gyre at 30 E between Africa and Antarctica. Journal of Geophysical Research: Oceans, 106(C2), 2857-2879.

Patil, S. M., Mohan, R., Shetye, S. S., Gazi, S., Choudhari, P., & Jafar, S. (2020). Interannual changes of austral summer coccolithophore assemblages and southward expanse in the Southern Indian Ocean. Deep Sea Research Part II: Topical Studies in Oceanography, 178, 104765.

Pauthenet, E., Roquet, F., Madec, G., Guinet, C., Hindell, M., Mcmahon, C.R., Harcourt, R. and Nerini, D. (2018). Seasonal meandering of the Polar Front upstream of the Kerguelen Plateau. Geophysical Research Letters, 45(18), pp.9774–9781.

Peeters, F. J., Acheson, R., Brummer, G. J. A., De Ruijter, W. P., Schneider, R. R., Ganssen, G. M., ... & Kroon, D. (2004). Vigorous exchange between the Indian and Atlantic oceans at the end of the past five glacial periods. Nature, 430(7000), 661-665.

Pépin, L., Raynaud, D., Barnola, J. M., & Loutre, M. F. (2001). Hemispheric roles of climate forcings during glacial-interglacial transitions as deduced from the Vostok record and LLN-2D model experiments. Journal of Geophysical Research: Atmospheres, 106(D23), 31885-31892.

Petit, J. R., Jouzel, J., Raynaud, D., Barkov, N. I., Barnola, J. M., Basile, I., ... & Stievenard, M. (1999). Climate and atmospheric history of the past 420,000 years from the Vostok ice core, Antarctica. Nature, 399(6735), 429-436.

Piotrowski, A. M., Goldstein, S. L., Sidney, R. H., Fairbanks, R. G., & Zylberberg, D. R. (2008). Oscillating glacial northern and southern deep water formation from combined neodymium and carbon isotopes. Earth and Planetary Science Letters, 272(1-2), 394-405.

Pollard, A. M., & Bray, P. (2007). A bicycle made for two? The integration of scientific techniques into archaeological interpretation. Annu. Rev. Anthropol., 36, 245-259.

Pollard, R.T., Read, J.F. (2001). Circulation pathways and transports of the Southern Ocean in the vicinity of the Southwest Indian Ridge. Journal of Geophysical Research 106, 2881–2898

Pollard, R.T., Venables, H.J., Read, J.F., Allen, J.T. (2007). Large-scale circulation around the Crozet Plateau controls an annual phytoplankton bloom in the Crozet Basin. Deep Sea Res., Part II 54, 1915–1929.

Pörtner, H. O., & Farrell, A. P. (2008). Physiology and climate change. Science, 322(5902), 690–692.

Poulton, A. J., Adey, T. R., Balch, W. M., & Holligan, P. M. (2007). Relating coccolithophore calcification rates to phytoplankton community dynamics: Regional differences and implications for carbon export. Deep Sea Research Part II: Topical Studies in Oceanography, 54(5-7), 538-557.

Poulton, A. J., Young, J. R., Bates, N. R., & Balch, W. M. (2011). Biometry of detached Emiliania huxleyi coccoliths along the Patagonian Shelf. Marine Ecology Progress Series, 443, 1-17.

Quere, C. L., Harrison, S. P., Colin Prentice, I., Buitenhuis, E. T., Aumont, O., Bopp, L., ... & Wolf-Gladrow, D. (2005). Ecosystem dynamics based on plankton functional types for global ocean biogeochemistry models. Global Change Biology, 11(11), 2016-2040.

Raynaud, D., Barnola, J. M., Souchez, R., Lorrain, R., Petit, J. R., Duval, P., & Lipenkov, V. Y. (2005). The record for marine isotopic stage 11. Nature, 436(7047), 39-40.

Renaud, S., & Klaas, C. (2001). Seasonal variations in the morphology of the coccolithophore Calcidiscus leptoporus off Bermuda (N. Atlantic). Journal of Plankton Research, 23(8), 779–795.

Renaud, S., Ziveri, P., & Broerse, A. T. (2002). Geographical and seasonal differences in morphology and dynamics of the coccolithophore *Calcidiscus leptoporus*. Marine Micropaleontology, 46(3-4), 363-385.

Rickaby, R.E.M., Elderfield, H., Roberts, N., Hillenbrand, C.D., Mackensen, A. (2010).

Evidence for elevated alkalinity in the glacial Southern Ocean. Paleoceanography 25 (1), p. PA1209.

Riebesell, U., Zondervan, I., Rost, B., Tortell, P. D., Zeebe, R. E., & Morel, F. M. (2000). Reduced calcification of marine plankton in response to increased atmospheric CO2. Nature, 407(6802), 364–367.

Rigual-Hernández, A. S., Trull, T. W., Bray, S. G., Cortina, A., & Armand, L. K. (2015). Latitudinal and temporal distributions of diatom populations in the pelagic waters of the

Subantarctic and Polar Frontal zones of the Southern Ocean and their role in the biological pump. Biogeosciences, 12(18), 5309-5337.

Rigual Hernández, A. S., Flores, J. A., Sierro, F. J., Fuertes, M. A., Cros, L., & Trull, T. W. (2018). Coccolithophore populations and their contribution to carbonate export during an annual cycle in the Australian sector of the Antarctic zone. Biogeosciences, 15(6), 1843-1862.

Rigual-Hernández, A. S., Pilskaln, C. H., Cortina, A., Abrantes, F., & Armand, L. K. (2019). Diatom species fluxes in the seasonally ice-covered Antarctic Zone: New data from offshore Prydz Bay and comparison with other regions from the eastern Antarctic and western Pacific sectors of the Southern Ocean. Deep Sea Research Part II: Topical Studies in Oceanography, 161, 92-104.

Rigual Hernández, A. S., Trull, T. W., Nodder, S. D., Flores, J. A., Bostock, H., Abrantes, F., et al. (2020). Coccolithophore biodiversity controls carbonate export in the Southern Ocean. Biogeosciences, 17(1), 245–263.

Robinson, R. S., Sigman, D. M., DiFiore, P. J., Rohde, M. M., Mashiotta, T. A., & Lea, D. W. (2005). Diatom-bound 15N/14N: New support for enhanced nutrient consumption in the ice age subantarctic. Paleoceanography, 20(3).

Rohling, E. J. and Bigg, G. R. (1998). Paleosalinity and δ 18O: a critical assessment. J. Geophys. Res., 103(C1), 1307–1318

Rohling, E. J., Damsté, J. S. S. and Schouten, S. (2007). Hydrogen isotopic compositions of long-chain alkenones record freshwater flooding of the Eastern Mediterranean at the onset of sapropel deposition. Earth Planet. Sci. Lett., 2007, 262(3–4), 594–600.

Romero, O. E., Kim, J. H., Bárcena, M. A., Hall, I. R., Zahn, R., & Schneider, R. (2015). High-latitude forcing of diatom productivity in the southern Agulhas Plateau during the past 350 kyr. Paleoceanography, 30(2), 118-132.

Romero, O.E., Kim, J.H., Bárcena, M.A., Hall, I.R., Zahn, R., Schneider, R. (2018). Alkenone concentration and sea surface temperature of sediment core MD02-2588. PANGAEA.

Rost, B., Riebesell, U. (2004). Coccolithophores and the biological pump: responses to environmental changes. In: Thierstein, H.R., Young, J.R. (eds) Coccolithophores. Springer, Berlin, Heidelberg.

Roth, P. H. (1994). Distribution of coccolith in oceanic sediments. Coccolithophores, 199-218.

Samtleben, C. and Schröder, A. (1992). Living coccolithophore communities in the Norwegian-Greenland Sea and their record in sediments. Marine Micropaleontology, 19(4), 333–354.

Saavedra-Pellitero, M., Flores, J. A., Baumann, K. H., & Sierro, F. J. (2010). Coccolith distribution patterns in surface sediments of Equatorial and Southeastern Pacific Ocean. Geobios, 43(1), 131–149.

Saavedra-Pellitero, M., Flores, J. A., Lamy, F., Sierro, F. J., & Cortina, A. (2011). Coccolithophore estimates of paleotemperature and paleoproductivity changes in the southeast Pacific over the past~ 27 kyr. Paleoceanography, 26(1).

Saavedra-Pellitero, M., Baumann, K. H., Flores, J. A., & Gersonde, R. (2014). Biogeographic distribution of living coccolithophores in the Pacific sector of the Southern Ocean. Marine Micropaleontology, 109, 1-20.

Saavedra-Pellitero, M. and Baumann, K.H. (2015). Comparison of living and surface sediment coccolithophore assemblages in the Pacific sector of the Southern Ocean. Micropaleontology, 2015, 507–520.

Saavedra-Pellitero, M., Baumann, K.-H., Fuertes, M. Á., Schulz, H., Marcon, Y., Vollmar, N. M., Flores, J.-A., and Lamy, F. (2019). Calcification and Latitudinal Distribution of Extant Coccolithophores across the Drake Passage during Late Austral Summer 2016, Biogeosciences, 16, 3679–3702.

Sáez, A. G., Probert, I., Geisen, M., Quinn, P., Young, J. R., & Medlin, L. K. (2003). Pseudo-cryptic speciation in coccolithophores. Proceedings of the National Academy of Sciences, 100(12), 7163-7168.

Salter, I., Schiebel, R., Ziveri, P., Movellan, A., Lampitt, R., & Wolff, G. A. (2014). Carbonate counter pump stimulated by natural iron fertilization in the Polar Frontal Zone. Nature Geoscience, 7(12), 885-889.

Schlitzer, R. (2016). Ocean Data View http://odv.awi.de

Schlitzer, R. (2021). Ocean Data View. https://odv.awi.de.

Shadwick, E. H., Trull, T. W., Thomas, H., & Gibson, J. A. E. (2013). Vulnerability of polar oceans to anthropogenic acidification: comparison of Arctic and Antarctic seasonal cycles. Scientific reports, 3(1), 2339.

Sherrell, R. M., Field, M. P., & Gao, Y. (1998). Temporal variability of suspended mass and composition in the Northeast Pacific water column: relationships to sinking flux and lateral advection. Deep Sea Research Part II: Topical Studies in Oceanography, 45(4-5), 733-761.

Sikes, E. L., Farrington, J. T., & Keigwin, L. D. (1991). Use of the alkenone unsaturation ratio U37K to determine past sea surface temperatures: core-top SST calibrations and methodology considerations. Earth and Planetary Science Letters, 104(1), 36-47.

Sigman, D. M., & Boyle, E. A. (2000). Glacial/interglacial variations in atmospheric carbon dioxide. Nature, 407(6806), 859-869.

Sigman, D. M., Hain, M. P., & Haug, G. H. (2010). The polar ocean and glacial cycles in atmospheric CO2 concentration. Nature, 466(7302), 47-55.

Sigman, D. M., Fripiat, F., Studer, A. S., Kemeny, P. C., Martínez-García, A., Hain, M. P., ... & Haug, G. H. (2021). The Southern Ocean during the ice ages: A review of the Antarctic surface isolation hypothesis, with comparison to the North Pacific. Quaternary Science Reviews, 254, 106732.

Simon, M. H., Arthur, K. L., Hall, I. R., Peeters, F. J., Loveday, B. R., Barker, S., ... & Zahn, R. (2013). Millennial-scale Agulhas Current variability and its implications for salt-leakage through the Indian–Atlantic Ocean Gateway. Earth and Planetary Science Letters, 383, 101-112.

Sinha, B., Buitenhuis, E. T., Le Quéré, C., & Anderson, T. R. (2010). Comparison of the emergent behavior of a complex ecosystem model in two ocean general circulation models. Progress in Oceanography, 84(3-4), 204-224.

Sokolov, S., Rintoul, S.R. (2007). On the relationship between fronts of the Antarctic Circumpolar Current and surface chlorophyll concentrations in the Southern Ocean, Journal of Geophysical Research. 112(C7), 1–17. doi:10.1029/2006JC004072.

Sokolov, S., and S. R. Rintoul. (2009a). Circumpolar structure and distribution of the Antarctic Circumpolar Current fronts: 1. Mean circumpolar paths, Journal of Geophysical Research., 114, C11018, doi:10.1029/2008JC005108.

Sokolov, S., and S. R. Rintoul. (2009b). Circumpolar structure and distribution of the Antarctic Circumpolar Current fronts: 2. Variability and relationship to sea surface height, Journal of Geophysical Research., 114, C11019, doi:10.1029/2008JC005248.

Smith, H.E., Poulton, A.J., Garley, R., Hopkins, J., Lubelczyk, L.C., Drapeau, D.T., Rauschenberg, S., Twining, B.S., Bates, N.R. and Balch, W.M. (2017). The influence of environmental variability on the biogeography of coccolithophores and diatoms in the Great Calcite Belt. Biogeosciences, 14(21), pp.4905–4925.

Starr, A., Hall, I.R., Ziegler, M. (2020). Pleistocene benthic stable isotopes and ice-rafted debris from the Agulhas Plateau Composite (APcomp). PANGAEA.

Steinmetz, J.C. (1994). Sedimentation of coccolithophores. In: Winter, A., Siesser, W.G. (Eds.), Coccolithophores. Cambridge Univ. Press, Cambridge, pp. 179–197.

Swart, N. C., Gille, S. T., Fyfe, J. C., & Gillett, N. P. (2018). Recent Southern Ocean warming and freshening driven by greenhouse gas emissions and ozone depletion. Nature Geoscience, 11(11), 836–841.

Sulpis, O., Boudreau, B. P., Mucci, A., Jenkins, C., Trossman, D. S., Arbic, B. K., & Key, R. M. (2018). Current CaCO3 dissolution at the seafloor caused by anthropogenic CO2. Proceedings of the National Academy of Sciences, 115(46), 11700–11705.

Sulpis, O., Jeansson, E., Dinauer, A., Lauvset, S. K., & Middelburg, J. J. (2021). Calcium carbonate dissolution patterns in the ocean. Nature Geoscience, 14(6), 423–428.

Talley, L. D. (2013). Closure of the global overturning circulation through the Indian, Pacific, and Southern Oceans: Schematics and transports. Oceanography, 26(1), 80–97.

Tangunan, D., Baumann, K. H., & Fink, C. (2020). Variations in coccolithophore productivity off South Africa over the last 500 kyr. Marine Micropaleontology, 160, 101909.

Tangunan, D., Berke, M. A., Cartagena-Sierra, A., Flores, J. A., Gruetzner, J., Jiménez-Espejo, F., ... & Hall, I. R. (2021). Strong glacial-interglacial variability in upper ocean hydrodynamics, biogeochemistry, and productivity in the southern Indian Ocean. Communications Earth & Environment, 2(1), 80.

Ter Braak, C.J. and Verdonschot, P.F. (1995). Canonical correspondence analysis and related multivariate methods in aquatic ecology. Aquatic Sciences, 57(3), 255–289.

Thamban, M., Naik, S. S., Mohan, R., Rajakumar, A., Basavaiah, N., D'Souza, W., ... & Pandey, P. C. (2005). Changes in the source and transport mechanism of terrigenous input to the Indian sector of Southern Ocean during the late Quaternary and its palaeoceanographic implications. Journal of earth system science, 114, 443-452.

Thierstein, H. R., Geitzenauer, K. R., Molfino, B., & Shackleton, N. J. (1977). Global synchroneity of late Quaternary coccolith datum levels Validation by oxygen isotopes. Geology, 5(7), 400-404.

Thierstein, H. R. (1980). Selective dissolution of Late Cretaceous and earliest Tertiary calcareous nannofossils: experimental evidence. Cretaceous Research, 1(2), 165-176.

Thierstein, H. R., & Young, J. R. (Eds.). (2013). Coccolithophores: from molecular processes to global impact. Springer Science & Business Media.

Thomalla, S. J., Poulton, A. J., Sanders, R., Turnewitsch, R., Holligan, P. M., & Lucas, M. I. (2008). Variable export fluxes and efficiencies for calcite, opal, and organic carbon in the Atlantic Ocean: A ballast effect in action?. Global Biogeochemical Cycles, 22(1).

Toggweiler, J. R. (1999). Variation of atmospheric CO2 by ventilation of the ocean's deepest water. Paleoceanography, 14(5), 571-588.

Trull, T. W., Passmore, A., Davies, D. M., Smit, T., Berry, K., & Tilbrook, B. (2018). Distribution of planktonic biogenic carbonate organisms in the Southern Ocean south of Australia: a baseline for ocean acidification impact assessment. Biogeosciences, 15(1), 31-49.

Tsuchiya, M., Talley, L.D. and McCartney, M.S. (1994). Water-mass distributions in the western South Atlantic; A section from South Georgia Island (54S) northward across the equator. Journal of Marine Research, 52(1), 55–81.

van Sebille, E., Biastoch, A., Van Leeuwen, P. J., & De Ruijter, W. P. M. (2009). A weaker Agulhas Current leads to more Agulhas leakage. Geophysical Research Letters, 36(3).

Vollmar, N.M., Baumann, K.H., Saavedra-Pellitero, M. and Hernández-Almeida, I. (2021). Distribution of coccoliths in surface sediments across the Drake Passage and calcification of *Emiliania huxleyi* morphotypes. Biogeosciences Discussions.

Volk, T., & Hoffert, M. I. (1985). Ocean carbon pumps: Analysis of relative strengths and efficiencies in ocean-driven atmospheric CO2 changes. In: The carbon cycle and atmospheric CO2: natural variations Archean to present, 32, 99-110.

Watson, A. J., Vallis, G. K., & Nikurashin, M. (2015). Southern Ocean buoyancy forcing of ocean ventilation and glacial atmospheric CO2. Nature Geoscience, 8(11), 861-864.

Wedepohl, P. M., Lutjeharms, J. R. E., & Meeuwis, M. (2000). Surface drift in the south-east Atlantic Ocean. South African Journal of Marine Science, 22(1), 71-79.

Westbroek, P., Brown, C. W., van Bleijswijk, J., Brownlee, C., Brummer, G. J., Conte, M., ... & Young, J. (1993). A model system approach to biological climate forcing. The example of Emiliania huxleyi. Global and planetary change, 8(1-2), 27-46.

Whitworth, T. (1983). Monitoring the transport of the Antarctic circumpolar current at Drake Passage. Journal of Physical Oceanography, 13(11), 2045-2057.

Wolf-Gladrow, D. A., Riebesell, U. L. F., Burkhardt, S., & Bijma, J. (1999). Direct effects of CO2 concentration on growth and isotopic composition of marine plankton. Tellus b, 51(2), 461-476.

Winter, A. & Siesser, W.G. (1994). Coccolithophores. Cambridge University Press, Cambridge: 321pp

Winter, A., Siesser, W.G., 1994. Composition and morphology of coccolithophore skeletons. In: Coccolithophores, Winter, A., Siesser, W.G. (Eds.), Cambridge University Press, Cambridge, New York, Melbourne, pp. 39—50.

Winter, A., Elbrächter, M., & Krause, G. (1999). Subtropical coccolithophores in the Weddell Sea. Deep Sea Research Part I: Oceanographic Research Papers, 46(3), 439-449.

Wilks, J. V., Nodder, S. D., & Rigual-Hernandez, A. (2021). Diatom and coccolithophore species fluxes in the Subtropical Frontal Zone, east of New Zealand. Deep Sea Research Part I: Oceanographic Research Papers, 169, 103455.

You, Y., 2000. Implications of the deep circulation and ventilation of the Indian Ocean on the renewal mechanism of North Atlantic Deep Water. Journal of Geophysical Research: Oceans, 105(C10), pp.23895-23926.

Young, J. R. (1994) Functions of Coccoliths. In: Winter, A. and Siesser, W.G., Eds., Coccolithophores, Cambridge University Press, New York, 13-27.

Young, J. R., Bergen, J. A., Bown, P. R., Burnett, J. A., Fiorentino, A., Jordan, R. W., Kleijne, A., Niel, B. E., Romein, A. J., Salis, K. 1997. Guidelines for coccolith and calcareous nannofossil terminology. Palaeontology, 40, 4, 875–912.

Young, J. R., & Ziveri, P. (2000). Calculation of coccolith volume and its use in calibration of carbonate flux estimates. Deep sea research Part II: Topical studies in oceanography, 47(9-11), 1679-1700. https://doi.org/10.1016/S0967-0645(00)00003-5

Young, J. R., Geisen, M., Cros, L., Kleijne, A., Sprengel, C., Probert, I., & Østergaard, J. (2003). A guide to extant coccolithophore taxonomy. Journal of Nannoplankton Research, Special Issue, 1, 1-132.

Young, J. R., Bown, P. R., & Lees, J. A. (2017). Nannotax3 website. International Nannoplankton Association, 21.

Zeltner, A. (2000). Monsoonal influenced changes of coccolithophore communities in the northern Indian Ocean: alteration during sedimentation and record in surface sediments (Doctoral dissertation, Institut und Museum für Geologie und Paläontologie der Universität Tübingen).

Zondervan, I., Rost, B., & Riebesell, U. (2002). Effect of CO2 concentration on the PIC/POC ratio in the coccolithophore Emiliania huxleyi grown under light-limiting conditions

and different daylengths. Journal of Experimental Marine Biology and Ecology, 272(1), 55–70.

Zondervan, I., Zeebe, R. E., Rost, B., & Riebesell, U. (2001). Decreasing marine biogenic calcification: A negative feedback on rising atmospheric pCO2. Global Biogeochemical Cycles, 15(2), 507-516.

Ziveri, P., Thunell, R. C., & Rio, D. (1995). Seasonal changes in coccolithophore densities in the Southern California Bight during 1991–1992. Deep Sea Research Part I: Oceanographic Research Papers, 42(11-12), 1881-1903.

Ziveri, P., Baumann, K. H., Böckel, B., Bollmann, J., & Young, J. R. (2004). Biogeography of selected Holocene coccoliths in the Atlantic Ocean. Coccolithophores: From Molecular processes to global impact, 403-428.

Ziveri, P., de Bernardi, B., Baumann, K. H., Stoll, H. M., & Mortyn, P. G. (2007). Sinking of coccolith carbonate and potential contribution to organic carbon ballasting in the deep ocean. Deep Sea Research Part II: Topical Studies in Oceanography, 54(5-7), 659–675.